Tetrahedrally coordinating ligands

Bates, George Benjamin

Tetrahedrally Coordinating Ligands

By
George Benjamin Bates B.Sc. (Hons.)

University of Durham

Department of Chemistry

A Thesis submitted for the degree of Doctor of Philosophy

October 1995

Statement of copyright

Declaration

The work described in this thesis was carried out in the Department of Chemistry at the University of Durham between October 1992 and September 1995. All the work is my own, unless stated to the contrary and it has not been submitted previously for a degree at this or any other University.

Acknowledgements

First and foremost, I would like to thank my supervisor Prof. David Parker, for his enthusiasm and optimism especially when experiments were not working and for his stimulating exchange of ideas throughout the time I worked with him. I am grateful for my industrial collaborators, Peter Tasker at Zeneca and Derek Thorp for looking after me while I was their guest.

Within the department there are many I would like to thank, who enabled me to complete this work. Julia Say, Alan Kenwright and R. Matthews for running NMR experiments, answering queries and maintaining the machines. Mike Jones and Lara Turner for performing many mass spectra and for teaching me to use the ESMS which has proved to be invaluable. The glass-blowers, Ray and Gordon who have often produced equipment at very short notice. J. Magee, R. Coult, J. Dorstal and Lenny Lauchlin for the elemental, CHN and HPLC departmental services.

Special thanks go to my work colleagues. Those who have helped proof read my thesis and other written work; Steve and Patricia. Again Patricia and Ritu for helping and teaching me all I know about electrochemistry and pH potentiometric titrations and subsequent data analysis. I would have been at a total loss without their guidance. I have had a great time at Durham and wish to thank all those who I have worked with and have not yet mentioned; Gareth, Clive, Tim, both Fiona's, Chris, Mo, Simon B, Matt, Simon P, Stefania, Rachel, Morag and Alvaro, Kanthi, Jim.

Abstract

Tetrahedrally coordinating ligands

Selective ligand coordination of zinc over other metals such as copper (II) and iron (III) is desirable and has potential commercial uses in hydrometallurgy. With this in mind ligands have been synthesised that impart a tetrahedral donor array. Binding to zinc which prefers a tetrahedral binding geometry may achieve selectivity over other non-tetrahedrally coordinating metals.

Di-N-alkylated bisbenzimidazole-4,4'-dicarboxylic acids have been synthesised and shown by proton NMR, ESMS and IR analysis to bind zinc as an $[L_2Zn_2]$ species with selectivity over copper, nickel, lead and cadmium. Hence a reversal of the Irving-Williams sequence is observed. Aqueous extraction tests using a lipophilic N-alkylated derivative indicated that the observed selectivity over copper and iron (III) was not reproduced under these experimental conditions.. The ligand began to extract in the pH 2.3-3.8 region.

2,9-Diphosphinoxymethyl phenanthroline derivatives were synthesised and shown to bind nickel, copper and zinc with similar stability constants, with only marginal enhancement over that of the parent phenanthroline. The 1:1 complexes were produced at acidities below pH 2. Increasing the length of the pendent arm donor groups by using phenylacetic acid moieties did not enhance zinc selectivity. The donor group was not ideal and $[ML_2]$ species were generated (i.e. an N_4 donor set)

Two phenol substituted $12N_3$ ligands were synthesised (N-linked and β-C-linked). Complex stability order followed the Irving-Williams sequence Cu > Zn > Ni. The N-linked derivative formed a six membered chelate on binding and had larger metal-ligand stability constants than for the C-linked derivative which formed an eight membered chelate. The N-linked derivative bound the copper (II) cation in a near tetrahedral arrangement and imparted some copper (I) character to the metal

Abbreviations

2,2,2-TET	1,4,7,10-Tetraazadecane
2,3,2-TET	1,4,8,11-Tetraazaundecane
3,2,3-TET	1,5,8,12-Tetrazadodecane
3,3,3-TET	1,5,9,13-Tetraazatridecane
$12N_3$	1,5,9-Triazacyclododecane
$13N_3$	1,6,10-triazacyclotridecane
Ac	Acetyl
Ar	Aromatic
$BiBzImH_2$	2,2-Bis-1H-benzimidazole
bz	Benzyl
CFSE	Crystal field stabilization energy
CN4	Four coordination
CHN	Carbon, hydrogen, nitrogen combustion analysis
cod	Cycloocta-1,5-diene
cp	Cyclopentadienyl
cych	Cyclohexyl
d	doublet
D2EHPA	Di(2-ethylhexyl)phosphoric acid
DCI	Desorption chemical ionization
dd	doublet of doublets
DMF	N,N-Dimethylformamide
DMSO	Dimethylsulfoxide
EI	Electron impact ionization
en	Ethylenediamine
ESMS	Electrospray mass spectrometry
Et	Ethyl
EtOH	Ethanol
Eqn.	Equation
Fig.	Figure
FTIR	Fourier transform infra-red
HDOP	Di(n-octyl)phosphinic acid
HEH[EHP]	2-Ethylhexylphosphonic acid mono 2-ethylhexyl ester
HPLC	High performance liquid chromatography
HSAB	Hard-soft, acid-base
I.R.	Infra-red
J	Coupling constant
L	Ligand
lit.	Literature

m	Multiplet
M/L	Metal-ligand ratio
m.p.	Melting point
MS	Mass spectrometry
NBS	National Bureau of Standards
n-BuLi	Normal-butyl lithium
NMR	Nuclear magnetic resonance
NOE	Nuclear Overhauser effect
Ph	Phenyl
phen	1,10-Phenanthroline
plc	Preparative thin layer chromatography
ppm	Parts per million
q	Quartet
quint	Quintet
s	Singlet
R_t	Retention time
t	Triplet
td	Triplet of doublets
tosyl	p-Toluenesulphonyl
TfO	Trifluoromethylsulfonate
TFA	Trifluoroacetic acid
THF	Tetrahydrofuran
tlc	Thin layer chromatography
TMA	Tetramethylammonium
tt	Triplet of triplets
U.V.	Ultra-violet

Contents Page

Chapter 1 Introduction

Chapter 2 Bisbenzimidazole based ligands

Chapter 3 Phenanthroline based ligands

Chapter 4 $12N_3$ based ligands

Chapter 5 Experimental

Appendices

Chapter One

Introduction

1.1 Coordination chemistry

The coordination chemistry of ligands has been studied for over a century since Alfred Werner first put forward his ideas on metal coordination[1]. He proposed that the metal had two types of valency. The first, the primary or ionizable valency (i.e. oxidation state) which is satisfied by negative ions. The second (i.e. coordination number) has fixed directions with respect to the central metal and can be satisfied by neutral or anionic donors. Hence complex salts such as $CoCl_3.6NH_3$ were correctly formulated as $[Co(NH_3)_6]^{3+}Cl_3^{3-}$.

Later work by G.N. Lewis and N.V. Sidgwick proposed that a chemical bond required the sharing of an electron pair[2]. A coordination compound or complex is then produced when a ligand (Lewis base, i.e. any molecule or ion that has at least one electron pair to donate) is attached to a metal ion or another electron acceptor (Lewis acid).

1.1.1 Ligand variety and classification

There are many ligands ranging from simple molecules (e.g. NH_3, H_2O) to complex multiatomic structures and hence there is a need to classify them. Ligands can be divided in a number of ways.

One approach is based on the type of bonding interaction between the central atom and the ligand. There are then two groups of ligand. The first are the classical or single donor ligands that form complexes with all types of Lewis acids, metal ions and molecules e.g. H_2O, NH_3. The second group is the non classical ligands, π–bonding or π-acid ligands which mainly interact with transition metals. The metal acceptor has d orbitals that can be used in bonding and the ligand has not only donor capacity but also vacant acceptor orbitals (e.g. 3d), examples include CO, PR_3.

Alternatively ligands can be classified by the number of electrons they contribute to the Lewis acid, as shown in (Fig. 1.1).

$1e^-$ donor : ^-SH, Cl^-

$2e^-$ donor : $:NH_3$, $H_2O:$

$4e^-$ donor : 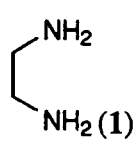 (1) 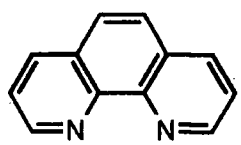 (2)

Fig. 1.1 Ligand classification by electron donor number.

Finally, and most conveniently, ligands may be classified according to the number of donor atoms involved with coordination (Fig. 1.2). A single donor atom

ligand is referred to as a unidentate ligand and there are many polydentate ligands with two to above nine donor atoms.

Unidentate CN^-

Bidentate 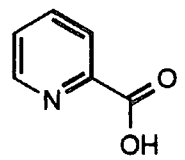 (3)

Tridentate 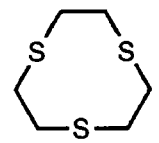 (4)

Tetradentate 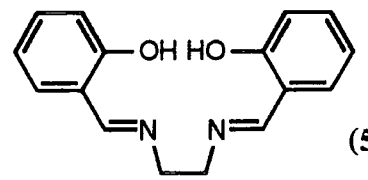 (5)

Fig. 1.2 Ligand classification by number of donor atoms.

1.1.2 Imposing tetrahedral coordination

With many ligands, especially uni and bidentate examples, the geometry of these ligands in the metal complex depends on the nature of the Lewis acid and its preferred coordination number. A good example is the cyanide ligand that binds with many geometries depending on the metal cation (Fig. 1.3).

$[Zn(CN)_4]^{2-}$ tetrahedral

$[Ni(CN)_4]^{2-}$ square planar

$[Ni(CN)_5]^{3-}$ trigonal bipyramidal

$[Fe(CN)_6]^{4-}$ octahedral

Fig. 1.3 Binding geometries of the cyanide ligand.

To achieve a solely tetrahedral arrangement on binding, there are only a certain number of ligand geometries possible. These can be sub-divided into four main types represented in (Fig. 1.4).

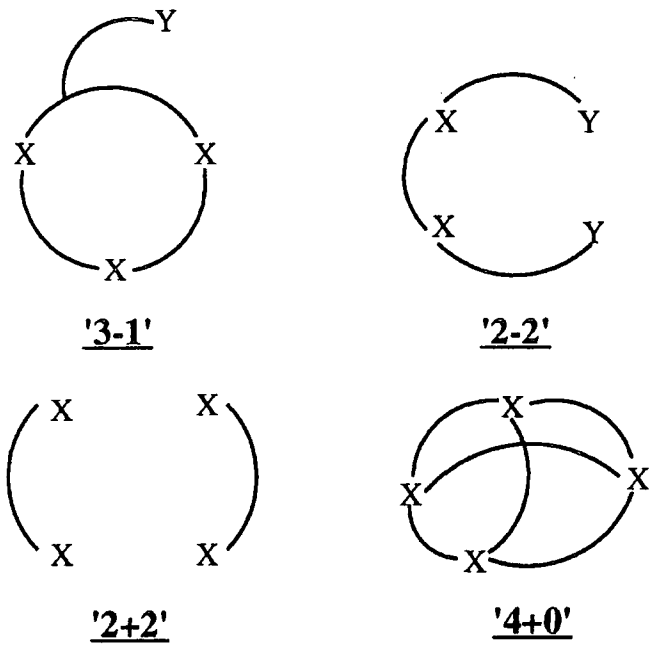

Fig. 1.4 Ligand geometries which may impose tetrahedral coordination.

Each metal is able to take up a coordination number of four with the given ligand or pair of ligands. The ligand must incorporate design features to prevent the adoption of a higher coordination number or of a square planar geometry.

1.1.2.1 '3-1' Ligand arrangement

With this arrangement the three 'X' donor atoms (not necessarily the same) are joined together to form the basal plane. The metal sits above this plane and the fourth donor on the pendent arm binds from above to form the tetrahedron. The pendent arm must be designed to be long enough to reach over the top, but must not be too flexible otherwise increased coordination by other anions binding may be possible. Examples of this geometric arrangement have been sought by E. Kimura[3] and P. Moore[4] and have been based on $12N_3$ macrocycles (Fig. 1.5 and see Chapter 4).

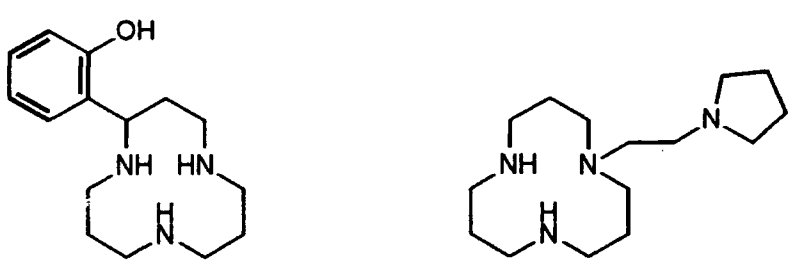

Kimura's ligand (**6**) Moore's ligand (**7**)

Fig. 1.5 Examples of $12N_3$ based tetrahedrally coordinating '3-1' ligands.

Other ligands that possess three linked donors can act as facially coordinating tridentate ligands . However the fourth donor is not specific as it is not attached to the ligand, these ligands are not classified in this group, e.g. tris(pyrazolyl)borate[5] (Fig. 1.6).

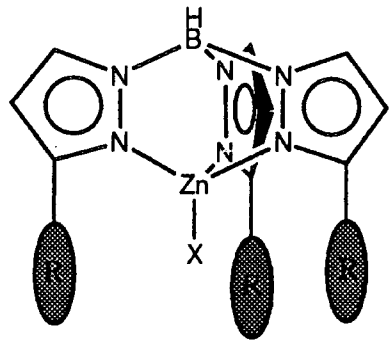

R = Ph, ^{t}Bu

X = Cl, SC_2H_5, H_2O, $SCOCH_3$

Fig. 1.6 Tris(pyrazolyl)borate zinc complex showing tetrahedral binding.

1.1.2.2 '2-2' Ligand arrangement

To limit the number of possible ligand geometries prior to binding the two 'X' donors need to be joined together on a rigid backbone to prevent free rotation. The metal coordinates in the X donor plane, the pendent arms bind from above and below to form the tetrahedron. Again the pendent arms must be long enough but not too flexible. There are a limited number of reported examples, mainly based on a 1,10-phenanthroline backbone[6] (Fig. 1.7 e.g. (**8**) and see Chapter 3). More examples are known where the backbone is the flexible ethylenediamine group such as ethylene-bis(iminomethylene-2-phenol)(N,N'-bis(2-hydroxyl)ethylenediamine)[7] (**9**) (Fig. 1.7).

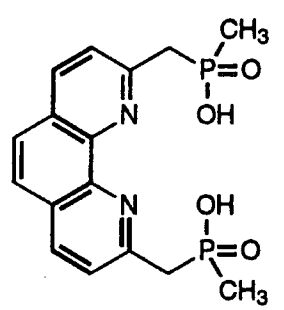

(**8**)

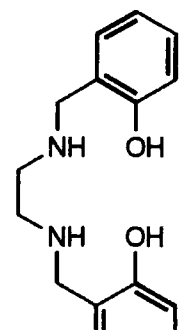

(**9**)

Fig. 1.7 Phenanthroline (**8**) and ethylenediamine (**9**) based '2-2' type ligands.

1.1.2.3 '2+2' Ligand arrangement

There are a vast number of bidentate ligands that in principle are able to bind in a tetrahedral geometry in an $[ML_2]$ complex. However, many are non selective and can also bind in an octahedral or square planar fashion depending on the metal. The ligand requires some steric bulk to prevent such geometries while in the tetrahedral geometry steric repulsion between proximate groups is usually minimised. Imidodiphosphinate ligands (Fig. 1.8) have been shown to bind certain first row transition metals (Fe, Co, Ni, Zn) in a tetrahedral fashion[8]. The preference for tetrahedral binding is probably a result of the steric crowding associated with the substituted phosphorus groups. Changing one of the phosphorus ($-P(=S)R_2$) groups to a thioamide moiety ($-C(=S)NR_2$) resulted in square planar coordination to nickel and copper[9].

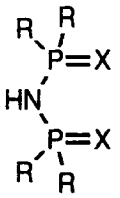

X = S, or O, NH

$R = CH_3, C_6H_5$

(10)

Fig. 1.8 Imidodiphosphinate based '2+2' ligand (**10**).

To increase selectivity and the overall 1:1 stability constant, it may be necessary for the two donors to be held in a rigid fashion and as with '2-2' type ligands functionalized phenanthrolines have been used. Neocuproine (2,9-dimethyl-1,10-phenanthroline)[10] binds copper (I) in a tetrahedral.arrangement to form an $[ML_2]$ complex, this with hydrogen peroxide as a co-oxidant[11] has been used for the sequence-specific scission of DNA. Interlocking '2+2' examples that bind copper (I) in a tetrahedral fashion have been made by Sauvage[12] again based on 1,10-phenanthroline. A linked '2+2' 2,9-disubstituted phenanthroline ligand[13] (**11**) (Fig. 1.9) has also been synthesised that possesses a tetrahedral arrangement of donor atoms prior to complexation. The cavity should be of the correct size to bind many of the smaller metal cations.

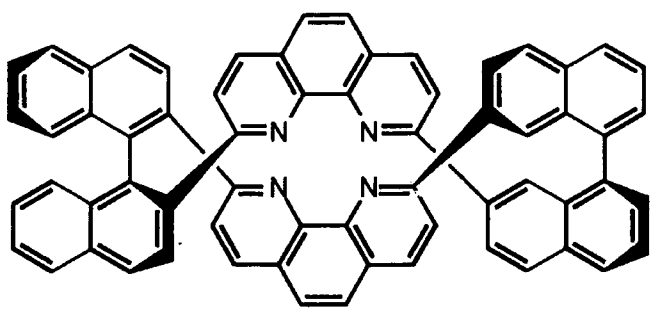

(11)

Fig. 1.9 Linked '2+2' phenanthroline based ligand (**11**).

1.1.2.4 '4+0' Ligand arrangement

With this arrangement all the donor atoms are linked together to form a cage structure. Examples of this geometry have been described[14] (Fig. 1.10), based on tertiary and quaternary amine donors. Even though the ligands present a tetrahedral arrangement of donors they have only been used to investigate halogen anion binding and not cations. Although the nitrogen lone-pairs in the example (**12**) are likely to point inwards, metal complexation may be kinetically slow. Related speherical cryptands have been made by J-M. Lehn[15].

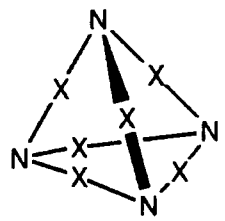

(**12**)

Where X= $(CH_2)_6$ or $(CH_2)_8$

Nitrogens can be methylated

Fig. 1.10 Cage '4+0' based ligand (**12**).

1.1.3 Transition metal complex stability

From many studies of ligands with first row transition metals it was found there was a general trend in the order of stability constants of the complexes irrespective of the ligand involved (Fig. 1.11).

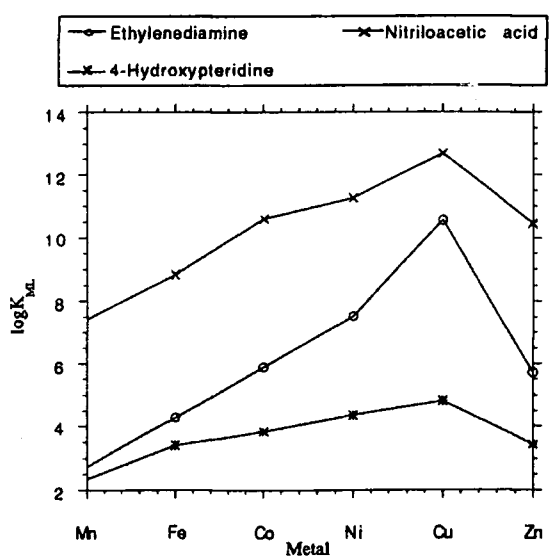

Fig. 1.11 Stability of divalent transition metal complexes with various ligands.

There is an increase in the stability constant of the complexes going across the first row transition metals reaching a maximum at copper. This order is referred to as the Irving-Williams[16] sequence:

$$Mn\ (II) < Fe\ (II) < Co\ (II) < Ni\ (II) < Cu\ (II) > Zn\ (II)$$

This order can be correlated with the electronic structure of the metals, mainly the second ionization potential[17] and is the reverse of the cation radii order. To change this order, the ligand must be able to bind to the required cation more strongly than its neighbouring metals. A possible solution is to synthesise a ligand that binds with a certain preferred geometry, for example a four coordinate tetrahedral donor set. Only cations which favour tetrahedral coordination will bind with high stability constants.

Zinc has a d^{10} electronic configuration in its outer electron shell and as a result is not subject to crystal field effects. Cations such as copper (II) and nickel (II) have an electronically incomplete 3d shell so extra stability can result when these metals bind in certain preferred geometries (Table 1.1). This extra stability can be seen in thermodynamic quantities such as ligation energies, lattice energies and standard reduction potentials. This crystal field stabilization energy (CFSE) increases going from manganese to nickel and falls to zinc. It therefore affords a ready explanation[18] of the empirical Irving-Williams order of stability.

Metal	Preferred geometry
Fe (II)	Octahedral
Co (II)	Octahedral
Ni (II)	Octahedral and Square planar
Cu (II)	Jahn-Teller distorted Square planar
Zn (II)	Tetrahedral

Table 1.1 Preferred binding geometries of various transition metals.

Tetrahedral coordination to zinc can be presented by flexible ligands such as imidazoles and ethylenediamine. However, these ligands also bind to copper (II) and nickel (II) with higher complex stability. To bind zinc selectively in a tetrahedral geometry a structurally demanding ligand needs to be synthesised. It has been suggested[19] that the formation of four coordinate zinc (II) is driven by the Lewis basicity of the donor atoms. If the coordinating ligand is a strong Lewis base[20], the coordination number of zinc is reduced and the bond length shortens. This supports the observation that imidazole groups promote four coordinate zinc (II) formation more effectively than an amine group and even more so than an O-donor.

1.2 Hydrometallurgy

Once zinc selectivity has been achieved, the ligand can be appropriately functionalized to be used in hydrometallurgical recovery of zinc. Traditionally metals are recovered from their ores by pyrometallurgy, i.e. the reduction of relatively concentrated metallic ores at high temperatures (equations 1.1 and 1.2).

Eqn. (1.1) $2ZnS + 3O_2 \longrightarrow 2ZnO + 2SO_2$

Eqn. (1.2) $ZnO + C \longrightarrow Zn + CO$

Hydrometallurgy[21] involves the selective solvent extraction of the metal from an aqueous solution of metal salts (often sulphate or chloride) and its subsequent 'electrowinning' either by electrolysis or electrochemically using a less expensive metal (e.g. scrap iron). One of the major advantages is that the metal can be recovered from complex, low-grade bulk sulphate ores, or from waste residues such as galvanising liquors. There are other advantages[22] which are summarised in Table 1.2.

	Pyrometallurgy	Hydrometallurgy
Energy consumption	High as elevated temps are needed, high percentage is lost.	Low as ambient temperature is often used (electrolysis increases demand).
Dust	Dust problem with ore.	None as materials are wet.
Toxic gases	CO, SO_2 and others often generated need to be contained.	Many processes do not generate gases.
Solid residues	Residue often coarse and harmless can be stored in exposed piles.	Residues are finely divided, potentially dusty and may still contain leachable metals.
Economics	Large scale operation, high capital investment.	Can be small scale, low capital investment.

Table 1.2 Comparison of pyrometallurgy and hydrometallurgy.

1.2.1 Industrial setup

The hydrometallurgical process can be represented schematically (Fig. 1.12). Metal salts are dissolved from the ore using an acidic aqueous chloride medium (ferric chloride and hydrochloric acid). The acidity is maintained below pH 2.5 during the extraction to prevent the problem of ferric hydroxide precipitation. The aqueous solution containing the metals ('feed') is mixed with an organic phase, typically

kerosene based, containing the extractant ligand. The desired metal is selectively extracted into the organic solvent. After phase separation the organic layer is removed and the metal is decomplexed (stripped). This is often achieved using depleted aqueous electrolyte of greater acidity.

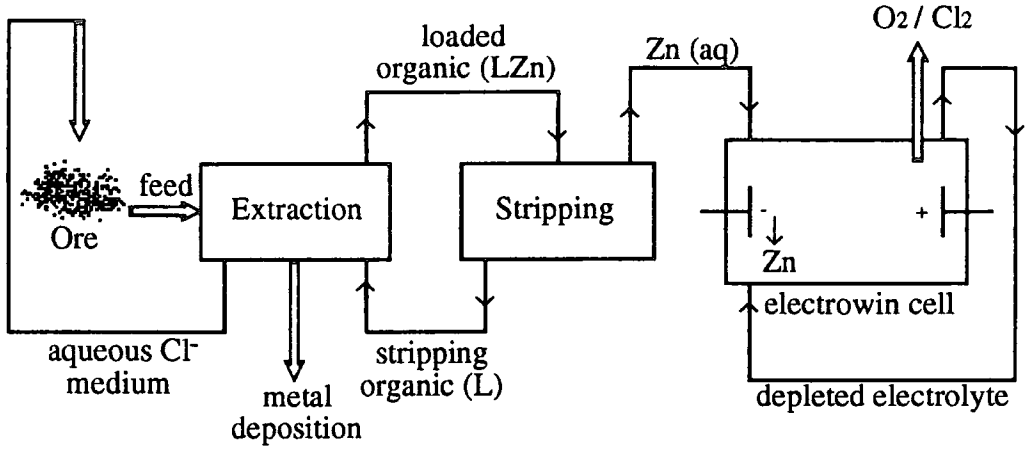

Fig. 1.12 Schematic representation of hydrometallurgical process.

With zinc, metal deposition (electrowinning) can be performed using a simple diaphragm cell. In theory, extraction is a closed circuit with no need for the continuous addition of acid or at any stage the need for base neutralization. In practice there are problems. With continuous recycling of the aqueous chloride medium interferent cations such as copper, cadmium and antimony will build up in concentration. They need to be removed to prevent contamination of the ligand solution and the electrowinning cell. Copper can be readily removed by an alternative hydrometallurgical process. Other metals have to be depleted by other means.

1.2.2 Ligand criteria for the hydrometallurgic extractant

To make extraction efficient and the process viable the chosen ligand needs to fulfil several criteria[23]. It is of primary importance that the ligand must show high selectivity over other metals especially iron (III), copper, cadmium and antimony. Both copper and cadmium will act as competitive cations and cause impure zinc to be deposited. Iron and antimony will have a direct effect on reducing the cell current efficiency. Iron (III) would be reduced at the cathode in preference to zinc and can be readily reoxidized. Complexation and decomplexation should be pH dependent and occur over a small pH range (about 1 pH unit). The ligand must be able to complex under acidic conditions (< pH 2) and decomplex when exposed to stronger acid. This eliminates the need for any neutralization and reacidification of either the ligand or stripping medium. The ligand must show rapid complexation and decomplexation

kinetics to achieve equilibrium in a few minutes (< 5 mins) so a high turn around is possible. Since the ligand is recycled continuously, it must be stable with respect to breakdown to enable thousands of cycles to be completed and make the process economically viable. The ligand must be sufficiently lipophilic to dissolve in the kerosene solvent and show minimal aqueous solubility so that no complex or ligand is lost to the aqueous layer in either extraction or stripping.

Ideally the ligand-metal complex should be charge neutral to avoid the need for counter anion co-extraction and the gradual loss of chloride from the aqueous chloride extracting medium. If chloride is transferred to the stripping solution chlorine will be produced on electrolysis. Without chloride transfer, oxygen will be produced at the cathode which can be controlled more effectively.

1.2.4 Survey of hydrometallurgical zinc extractants

Over the past twenty years there has been active research into ligands that will extract zinc[24], mainly from aqueous chloride, sulphate or perchlorate solutions. Early work centred on the use of di(2-ethylhexyl)phosphoric acid (D2EHPA Fig. 1.13 (**13**)) as the extractant and several processes for hydrometallurgical zinc recovery were developed[25].

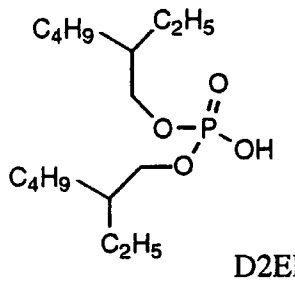

D2EHPA (**13**)

Fig. 1.13 Structure of di(2-ethylhexyl)phosphoric acid (**13**) extractant.

More recently, work using this ligand has been concerned with defining the nature of the extracted zinc species. There is now a general agreement that the major species extracted with D2EHPA (**13**) concentrations of greater than 0.1M is $[ZnL_2(HL)_2]$ from either perchlorate or sulphate-perchlorate aqueous solutions into toluene or alkane (decane, dodecane or heptane) solvents. Below ligand concentrations of 0.1M $[ZnL_2(HL)]$ is the predominant extractant[26].

Commercial extractants based on phosphorus oxoacids are available from a few companies (such as Cyanex 272 {bis(2,4,4-trimethylpentyl)phosphoric acid} American Cyanamid Company, SME 418 Shell Chemical Co., PC 88A Daihanchi Chemical Industry Company) and this has increased the interest in the use of phosphoric and phosphinic acids as metal extractants[27]. A comparison of phosphorus oxoacids (di(2-

ethylhexyl)phosphoric acid (**13**), 2-ethylhexylphosphonic acid mono 2-ethylhexyl ester (**14**) HEH[EHP] (SME 418) and di(n-octyl)phosphinic acid (**15**) HDOP) indicated[26(i)] that they extract zinc by similar mechanisms to D2EHPA (**13**).

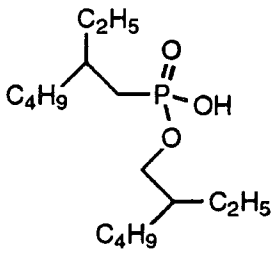

(**14**) HEH[EHP]

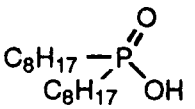

(**15**) HDOP

Fig. 1.14 Structures of HEH[EHP] (**14**) and HDOP (**15**) extractants.

The order of zinc extraction was D2EHPA (**13**) > HEH[EHP] (**14**) > HDOP (**15**), the reverse of the ligand's acidity. A similar order was found when these ligand types where used for the extraction of cobalt and nickel[28]. The branching of the alkyl chain is an important factor in the amount of zinc extracted. The ligand structure will affect its dimerization constant (Eqn. 1.3), which follows the general order[29] phosphoric > phosphonic > phosphinic. The higher the dimerization constant the greater is the contribution of $[ZnL_2(HL)_2]$ i.e. the extractant species.

Eqn. (1.3) $2[HL] \rightleftharpoons [(HL)_2]$

Using monothiophosphinic acids or dithiophosphinic acids as extractants has a direct effect on the pH range in which zinc is extracted and the nature of the extracted zinc species. A commercially available monothiophosphinic acid ((Fig. 1.15) Cyanex 302 bis(2,4,4-trimethylpentyl)monothiophosphinic acid (**16**)) has been studied for zinc extraction from aqueous sulphate[30] and chloride[31] solutions.

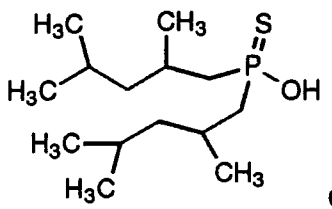

Cyanex 302 (**16**)

Fig. 1.15 Structure of Cyanex 302 (**16**).

It was found that zinc is extracted at more acidic pH values than with either D2EHPA (**13**) or Cyanex 272. This is clearly seen by comparing the $pH_{1/2}$ values (Fig. 1.16) ($pH_{1/2}$ is the acidity at which 50% of the maximum amount of zinc is extracted).

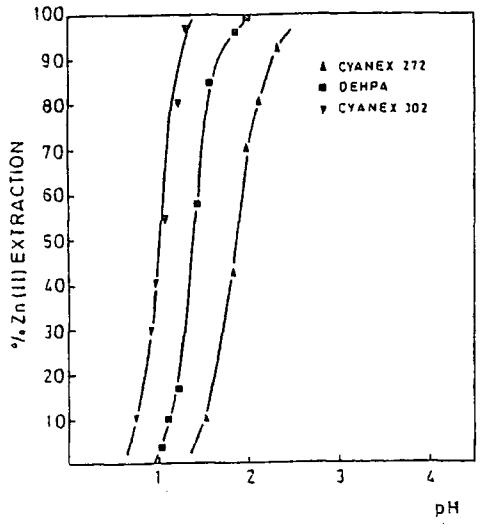

Organic phase: 20 v/v extractant in kerosene. Aqueous phase: 1.0g l zinc (II)

Fig. 1.16 Zinc extraction as a function of pH using various extractants.

Zinc is extracted in the form of $[(ZnL_2)_2 1.5(LH)_2]$ from a zinc chloride medium into kerosene. Using bis(dibutyldithiophosphinic) acid as the extractant in either heptane or tetrachloromethane the ligand was able to extract zinc from an aqueous acidic perchlorate solution as a $[ZnL_2]$ species[31].

One major disadvantage of using simple phosphorus acids is that they show poor selectivity for extraction of zinc over iron (III) and other metals (particularly copper and cadmium). Using D2EHPA (**13**) for zinc extraction necessitates the treatment of the aqueous solution to precipitate out the iron prior to zinc extraction. As at acidic pH values iron (III) is extracted in preference to zinc, the exact pH has to be carefully controlled to avoid coextraction of calcium. This increases technical difficulties and neutralization costs. Cyanex 302 (**16**) is more effective. It shows a total rejection of calcium extraction in the pH range in which zinc is extracted. There is some preferential zinc extraction over iron in the pH range 0.95 - 1.5. However copper is quantitatively extracted at pH values at which zinc is also extracted (Fig. 1.17).

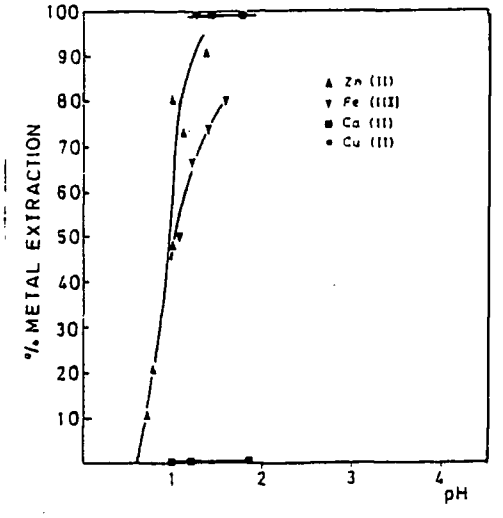

Fig. 1.17 Metal extraction by Cyanex 302 (**16**) as a function of pH.

For a commercially viable zinc extractant, high selectivity over iron (III) is required. Recent work on dithiophosphoroamides[33] (**17**) (Fig. 1.18) has resulted in a commercially usable hydrometallurgic zinc extractant for the recovery of zinc from an aqueous sulphate solution.

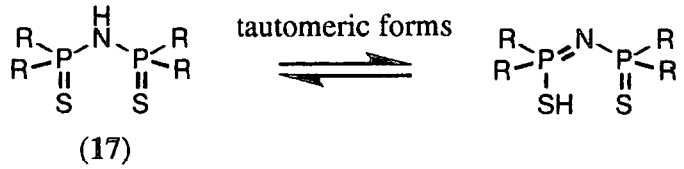

(**17**)

R is bulky and lipophilic

Fig. 1.18 Structure of the dithiophosphoroamide (**17**) zinc extractant.

The ligand (**17**) binds with zinc to form an $[ML_2]$ structure which is extracted into the organic phase (kerosene based). X-Ray crystallographic analysis of a less lipophilic derivative (R = isopropyl) indicated that zinc is bound with a good tetrahedral geometry to the sulphur atoms (i.e. S_4 donor set). Comparing this ligand (**17**) to Cyanex 302 (**16**) and D2EHPA (**13**) (Table 1.3) shows a very high zinc selectivity over iron.

Extractant	Zinc extracted	Iron extracted
dithiophosphoramide (**17**)	190	1
Cyanex 302 (**16**)	28.9	27.6
D2EHPA (**13**)	1.2	161.6

a.q. feed 2.9g/l Zn 4.3g/l iron (III) pH 2
organic 0.2M ligand in ESCAID 100 (kerosene based)
organic to aqueous contact ratio was 1/2

Table 1.3 Relative proportions of zinc and iron extraction by various extractants.

As well as zinc, other 'soft' metals (Bi, Cd, Cu, Hg, Ag, Pb) are also extracted while 'hard' metals are not taken up. In the industrial process (Section 1.2.1) copper is removed by hydrometallurgy prior to zinc extraction, while cadmium is removed from the organic layer after zinc has been stripped from the ligand. Unlike other extraction processes no neutralization at any stage is required.

The extraction from an aqueous chloride solution is more difficult than from sulphate. There have been reports of failed commercial attempts because of the inability of the process to produce a sufficiently pure solution for the ultimate recovery of the metal. One problem is that the chloride anion can act as a donor and help transfer metal impurities by an ion pairing mechanism into the organic layer (Eqn 1.4). A similar process does not readily occur in a sulphate medium.

Eqn. (1.4) $$L_{org} + H^+_{aq} + FeCl_4^-{}_{aq} \rightleftharpoons [LH]^+[FeCl_4]^-{}_{org}$$

The extractant may also be protonated and transfer hydrochloric acid into the organic phase and this effect can build up an excess chloride concentration on the stripping side. This problem has been found to be acute for zinc extraction[33]. These problems have been overcome for copper extraction using a pyridine ester reagent[34] (ACORGA CLX 50, Zeneca) which is able to extract copper selectively over iron (III).

Work on zinc extraction has been centred on substituted bisimidazole (**18**) and bisbenzimidazole compounds (**19**) (Fig. 1.19).

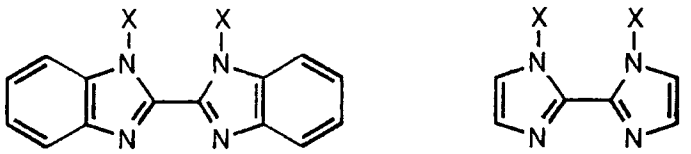

(**19**) (**18**)

X = R or C(O)OR

Fig. 1.19 Bisimidazole (**18**) and bisbenzimidazole (**19**) based ligands for zinc extraction.

The bisbenzimidazole ligand (**19**) has been thoroughly tested. It extracts zinc as a neutral chloro-complex which has been determined to be a dimeric $[M_2L_2Cl_4]$ structure[32]. Extraction shows a chloride concentration dependence (Fig. 1.20).

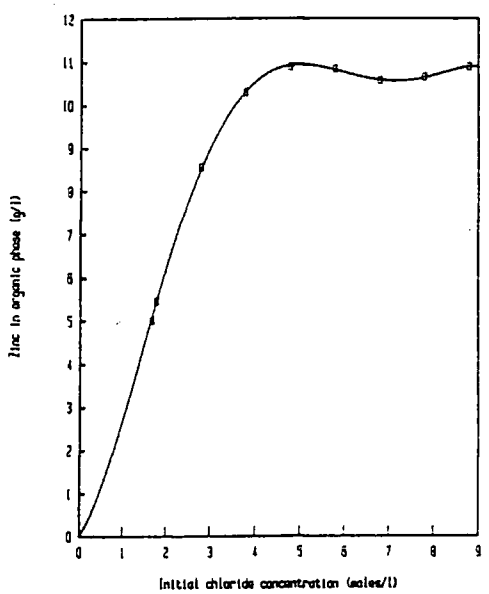

Fig. 1.20 Bisbenzimidazole ligand (**19**) chloride dependence.

The ligand exhibits fast kinetics of complexation and stripping with equilibrium being reached within two minutes for extraction and five minutes for stripping. Selectivity of zinc extraction over iron (II and III) was shown, but not over copper which was extracted preferentially over zinc (Table 1.4).

	zinc	iron	copper
Initial conc.	50 g/l	100 g/l	25 ppm
In organic after one contact	15 g/l	6 ppm	15 ppm

Table 1.4 Metal extraction data for bisbenzimidazole ligand (**19**).

1.3 Zinc coordination chemistry

Zinc compounds exist almost exclusively in the +2 oxidation state. The only exception occurs when zinc is added to molten zinc chloride at 500-700°C and a yellow diamagnetic glass is formed on cooling, in which unstable Zn_2^{2+} species can be identified. Although zinc may prefer a tetrahedral coordination arrangement in metal-ligand complexes other geometries are found. A recent survey of 490 zinc containing crystal structures has found that zinc is four coordinate in 58% of the structures and five and six coordinate in 13% and 27% respectively[19].

1.3.1 Ligand donor atoms for zinc

From examples illustrated in the literature[36] it appears that zinc binds to a variety of nitrogen, oxygen and sulphur donors. Its lack of preference for either hard or soft donors would suggest zinc (II) is a borderline cation in the Pearson classification[37] of donor and acceptor groups. The majority of complexes involve coordination to nitrogen donors. Binding to mono and polyfunctional amines is common, for example zinc binding to α(1-tert-butyl)-2-aziridinyl)benzylamine (**20**) (Fig. 1.21) which forms a tetrahedral N_2Br_2 geometry to a primary and tertiary nitrogen[38]. This example illustrates that halide ions (as well as water) are often coordinated to zinc, so increasing the coordination number.

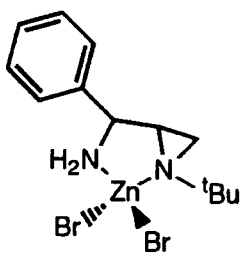

(**20**)

Fig. 1.21 Binding of zinc to α–(1-tert-butyl)-2-aziridinyl)benzylamine (**20**).

Binding to Schiff bases, hydrazones and N-heterocycles (such as pyridines, purines, imidazoles and o-phenanthrolines) is also common. Ligands that contain more

than one functionality allow a comparison of zinc's donor atom preference. Zinc readily binds to the amide functionality often via the oxygen atom. For example with a diamide substituted ethylenediamine[39] (21) zinc (II) forms an N_2O_2 donor set and the simple lactam[40] (22) is believed to coordinate only through the amide oxygen (Fig. 1.22).

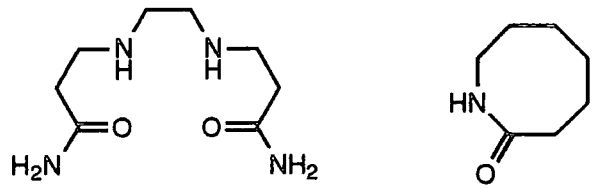

(21) (22)

Fig. 1.22 Oxygen donating amide ligands (21) and (22).

This preference can be altered by ligand design. Zinc binding enhances amide deprotonation, the nitrogen atoms can then bind especially if the amide oxygens are hindered by the resulting decrease in ligand chelating ability (Fig. 1.23). Likewise increasing the acidity favours nitrogen over oxygen donation, this can be seen with saccharin[41] (25) which acts as a unidentate nitrogen donor.

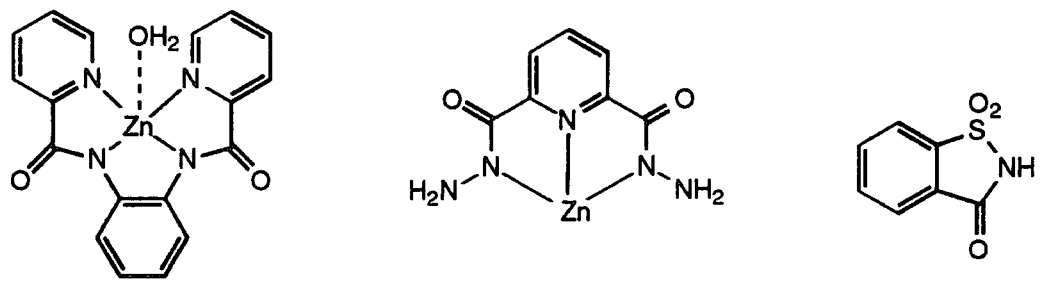

(23) (24) (25)

Fig. 1.23 Nitrogen donating amide ligands (23)[42] and (24)[43] and saccharin (25).

Preferential binding of nitrogen over sulphur can also be seen with certain ligands. Thiocyanate is generally bonded through nitrogen to zinc and cadmium (and through sulphur to mercury) for example in Zn(en)(NCS)Cl and $ZnL_2(NCS)_2$ where L = benzoquinoline. With the heterocyclic ligand[44] (26) (Fig. 1.24) tetrahedral $ZnCl_2L$ complexes are formed in which the ligand only acts as a bidentate nitrogen donor.

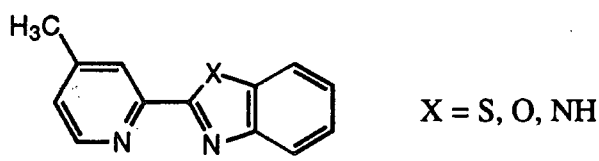

X = S, O, NH

(26)

Fig. 1.24 Heterocyclic bidentate nitrogen donor.

Functional groups containing oxygen as a donor are also common, excluding complexes with bound water, there are fewer examples of oxygen donors than of nitrogen donating ligands. Carboxylic acids are able to bind zinc in a unidentate or bidentate fashion depending on the structure of the acid. For example phenoxyacetic acid[45] (**27**) acts as a bidentate donor while the structurally similar 2,4-dichlorophenoxyacetic acid[46] (**28**) acts as a unidentate donor (Fig. 1.25). Complexes involving zinc coordination to diketones, alcohols and ethers are also known.

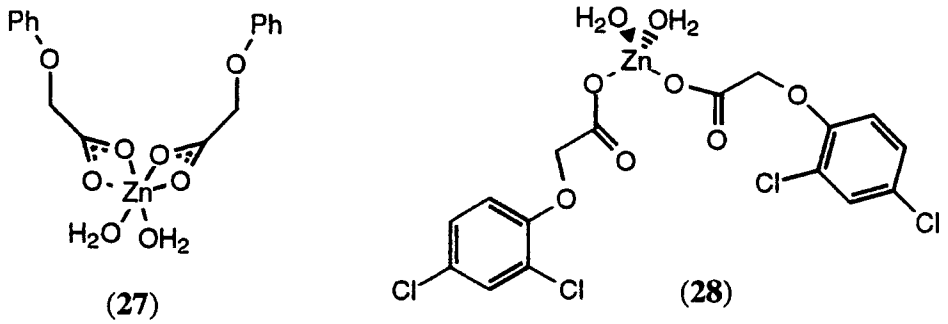

(**27**) (**28**)

Fig. 1.25 Carboxylic acid binding ligands (**27**) and (**28**).

The phosphorus (III) donor coordination chemistry of zinc is not extensive. Complexes such as $[Zn_2\{P(cych)_3\}X_4]$ where X = Cl, Br, I can be readily prepared and form halogen bonded dimers[47]. Tetrahedral species of $[ZnX_2L_2]$ (X = Cl, Br, I and L = Et_3P, Et_2PhP) have also been made and characterized[48]. Cadmium forms a greater number of phosphorus donor complexes[36].

Binding to sulphur donors is known for a range of sulphur containing ligands. Thiols and thioethers are able to readily form complexes with zinc, usually giving interesting structures. Aryl thio donors tend to have a greater tendency to form bonds with zinc than do aliphatic sulphur donors. There are also complexes with thioacids, thioamides and phosphine sulphides. Proton NMR analysis of zinc dithiocarbazo complexes $[ZnL_2]$ (HL = $R^1R^2NNHCSSH$) have indicated that a pseudo tetrahedral geometry with sulphur chelation is achieved[49]. Methylation of the thiol results in the complex configuration being dependent on the nature of the R group[50].

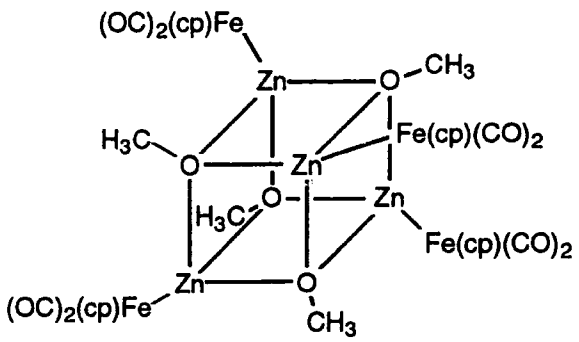

(**29**)

Fig. 1.26 Cubic structure of $[ZnFe(cp)(CO)_2OMe]_4$ (**29**) complex.

Recently a complex has been structurally characterized which shows zinc is bound to a iron carbonyl complex to form a cubic zinc(transition-metal carbonyl) alkoxide $[ZnFe(cp)(CO)_2OMe]_4$ complex[51] (**29**) (Fig. 1.26).

1.3.2 Complex stereochemistry

Zinc (II) has an electronically complete d^{10} shell and so is not subject to crystal field stabilization effects. Even though four coordination is preferred, zinc shows steric flexibility and is willing to submit readily to the structural demands of the ligand thereby resulting in many geometries. Four coordination with different groups is found in many complexes, with the majority being tetrahedral or distorted tetrahedral. Examples include the approximate tetrahedral binding of bisimidazolyl ketone[52] (**30**) with two bromides (Fig. 1.27). Greater tetrahedral distortion can be seen with an N_2Cl_2 environment from a substituted ethylenediamine[53] (**31**). It is interesting to note that the pendent arm phosphine is not coordinated to the metal

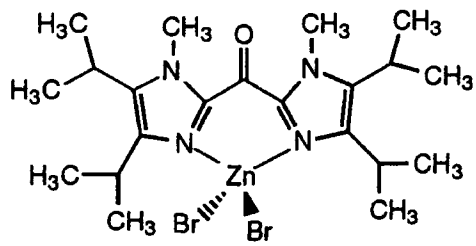

(**30**)

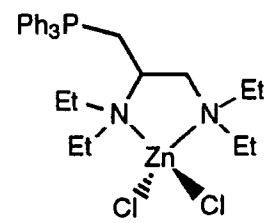

(**31**)

Fig. 1.27 Tetrahedral coordinating nitrogen donor ligands (**30**) and (**31**).

Tetrahedral donation by an oxygen donor can be seen with the diketone, 1,8-dihydoxyanthraquione[54] (**32**) which forms an $[ZnL_2]$ structure (Fig. 1.28).

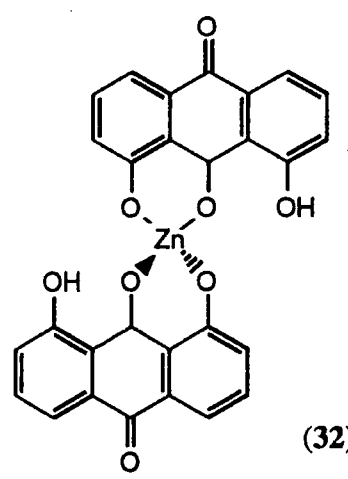

(**32**)

Fig. 1.28 Tetrahedral $[ZnL_2]$ structure with 1,8-dihydoxyanthraquione (**32**).

Dimeric and oligomeric zinc complexes are known in which the zinc adopts tetrahedral coordination. Although this is seen with nitrogen (**33**) as well as oxygen donors, many examples are observed when sulphur acts as the donor (**34**) (Fig. 1.29). With the substituted ethylenediamine[55] (**33**) ligand each zinc is bound to three nitrogens and a terminal hydride to give an interesting tetrahedral N_3H environment. The zinc complex of thiophenol[56] is a $[Zn_4(SPh)_8]$ aggregate.

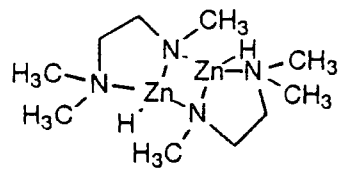

(**33**)

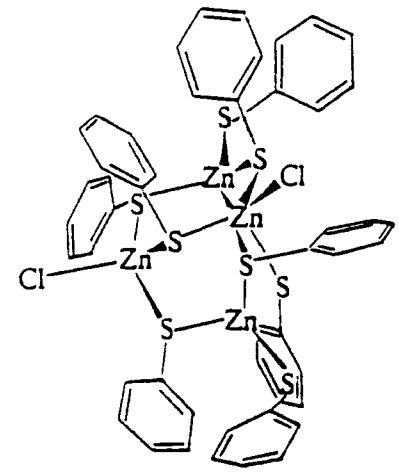

(**34**)

Fig. 1.29 Zinc dimer (**33**) and tetramer (**34**) species.

A four coordinate square planar arrangement is rare with the only example quoted being bis(glycinyl)zinc[57]. If a ligand has a square planar array of donors, zinc coordination will occur and there is often an increase in the coordination number. A square pyramidal arrangement can be seen when zinc interacts with the N_4 -azamacrocycle[58] (**35**) (Fig. 1.30) in the presence of a tertiary amine (triethyl or tri-n-propyl amine). The tertiary amine is bound in the apical position.

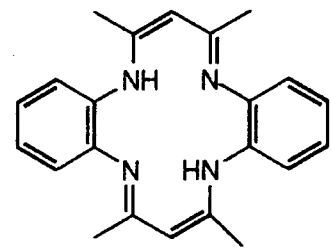

(**35**)

Fig. 1.30 14-Dibenzo-N_4-azamacrocycle (**35**).

The more common five coordination arrangement is trigonal bipyramidal and can result from a distorted tetrahedral geometry. This situation has been observed with Kimura's ligand[6] (**6**). The phenol pendent arm is too restricted to bind directly over the zinc and a cleft is produced which allows water to bind (Fig. 1.31).

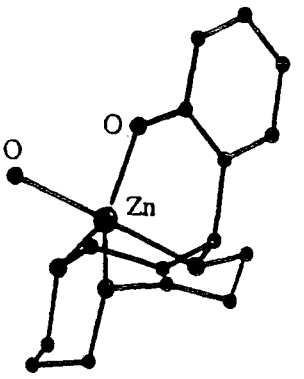

Fig. 1.31 Kimura's α–C-substituted $12N_3$ (**6**) showing trigonal bipyramidal coordination to zinc.

Ligands which may have been expected to bind in an $[ML_2]$ tetrahedral arrangement such as 8-aminoquinoline (**36**) have been shown to bind zinc in a trigonal bipyramidal environment[59] with water as the fifth donor. It is interesting that a related sulphur analogue[60] (**37**) has been crystallographically shown to bind zinc in a distorted N_2S_2 tetrahedral environment. (Fig. 1.32).

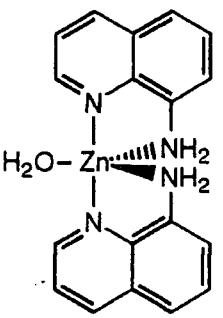

(**36**)

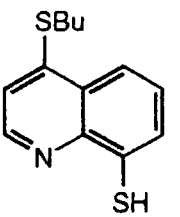

(**37**)

Fig. 1.32 Trigonal bipyramidal binding 8-aminoquinoline (**36**) and the tetrahedrally coordinating sulphur analogue (**37**).

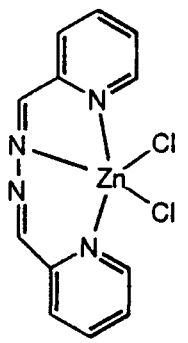

(**38**)

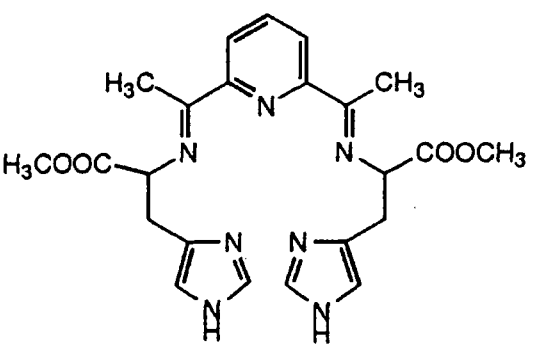

(**39**)

Fig. 1.33 Ligands that bind in geometries midway between trigonal bipyramidal and square planar.

Binding midway between trigonal bipyramidal and square planar is unusual but can be observed with ligands such as with 2-pyridinaldazine[61] (**38**) or the N_5-macrocycle[62] (**39**) which binds through sp^2 hydridized nitrogens (Fig. 1.33).

Higher coordination numbers are found but due to zinc's small ionic radius and d^{10} configuration there are fewer examples than with other cations (e.g. cadmium, iron and cobalt). With six coordination, the most common binding geometry is the octahedron. Again this is seen with both nitrogen and oxygen donors. A higher percentage of the oxygen donors (and carboxylic acids) appear to bind in an octahedral geometry rather than tetrahedral. This may be a reflection of oxygen being a 'harder' donor, but it is interesting to note there are fewer sulphur bound octahedral complexes. Zinc in a trigonal prismatic arrangement appears to be found in only one complex, namely a zinc fluoroborotris(2-aldoximino-6-pyridy)phosphine cationic complex[63].

The pentagonal bipyramidal geometry is the only arrangement found for seven coordinate complexes. This is often a result of a pentadentate ligand[64] (**40**) coordinating zinc in a near planar geometry then two other sites are occupied by water or counter anions (Fig. 1.34).

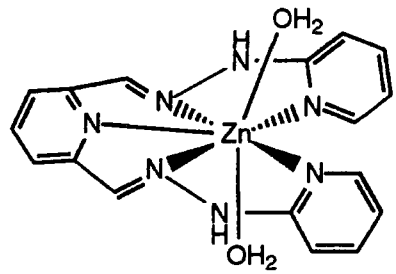

(**40**)

Fig. 1.34 N_5-Macrocycle (**40**) and water showing seven coordinate zinc binding.

A rare example of eight coordination is found in $(Ph_4As)_2Zn(NO_3)_4$ where zinc has a dodecahedral arrangement. The nitrate ions are coordinated asymmetrically to such an extent that the stereochemistry may alternatively be regarded as approaching tetrahedral[65].

1.3.3 Brief comparison with nickel and copper

The coordination chemistry of zinc is much less extensive than that of nickel and copper. There are however important differences. Nickel (II) species are the most common and form many complexes with coordination numbers of three to six. Principal geometries are octahedral and square planar, there are fewer examples of trigonal bipyramidal, square pyramidal and tetrahedral. A characteristic of nickel

complexes is the presence of complicated equilibria which give different structural types depending commonly on temperature and concentration.

The observed stereochemistry can be explained, at least in part, by considering crystal field splitting energies of the d^8 configuration. The octahedral geometry results in a lower energy configuration for the electrons than that of tetrahedral geometry. Square planar geometry, unlike octahedral or tetrahedral symmetry, is able to accommodate all 8d electrons in four low energy orbitals (d_{xz}, d_{yz}, d_{z^2} d_{xy}) and leave a vacant uppermost orbital ($d_{x^2-y^2}$). If the crystal field is thus of sufficiently low symmetry (e.g. $[NiL_2X_2]$ type) or is sufficiently strong (e.g. $[Ni(CN)_4]^{2-}$) to pair up two electrons then square planar geometry is energetically preferable.

The following stoichiometric types; $[NiX_4]^{2-}$, $[NiX_3L]^-$, $[NiX_2L_2]$, $[Ni(L\text{-}L)]_2$ give tetrahedral complexes. Apart from the first, good tetrahedral geometries do not occur. There are marked distortions reducing the tetrahedral symmetry to near planarity. With $[Ni(L\text{-}L)_2]$ complexes the bidentate ligand needs to have bulky substituents to prevent planarity.

With copper the +2 oxidation state is again the most important (however cyanide and iodide form covalent Cu (I) compounds which are stable). The most common coordination numbers are 4, 5 and 6, but regular geometries are rare. Distinction between certain geometries is difficult to make because the d^9 configuration of copper (II) is subject to Jahn-Teller distortion if placed in an environment of cubic symmetry (i.e. octahedral or tetrahedral). With six coordination, the octahedron can be greatly distorted, usually by elongation of two bonds along a C_4 axis so that it is often difficult to distinguish from square planar. Four coordinate distorted tetrahedral species are often intermediate between tetrahedral and square.

1.4 Ligand design features

Other than the geometric and coordination number preferences of the metal that have already been discussed earlier, there are other design features that have to be considered when making a ligand which is selective and has a high stability constant. There is now a vast knowledge of ligand-donor preferences that allows ligands to be designed with the required selectivity and stability[66].

1.4.1 Donor atom selection

There is a good understanding of the selection of donor atoms to bind the metal of interest (in this case zinc) with the ideas based on the hard and soft and base principle of Pearson[37] (HSAB) or the A and B type acids of Schwarzenbach[67] or Ahrland[68]. Generally, class (a) or hard acids tend to form their most stable complexes

with ligands containing nitrogen, oxygen or fluorine donor atoms, while class (b) or soft acids tend to form their most stable complexes to the heavier members of the V, VI, VII groups (Table 1.5). This is impart due to the polarizability of the donor and acceptor groups. The hard acids being electropositive form the most stable complexes with ligands favouring electrostatic bonding. Soft acids have relatively full d orbitals and form most stable complexes with ligands possessing lone pairs of electrons and empty d orbitals to accept charge from the d orbitals of the acid on binding. Certain acceptors (e.g. zinc) show borderline character and previous examples indicate zinc's ability to bind both hard and soft donors. The HSAB idea only gives a preliminary guide for donor atom selection. More detailed consideration needs to be given to the donor and the ligand architecture.

Acids	
Hard	Soft
H^+, Li^+, Na^+, K^+	Cu^+, Ag^+, Au^+, Tl^+, Hg^+
Be^{2+}, Mg^{2+}, Ca^{2+}, Sr^{2+}, Ba^{2+}	Pd^{2+}, Cd^{2+}, Pt^{2+}, Hg^{2+}
Al^{3+}, Sc^{3+}, Ga^{3+}, In^{3+}, La^{3+}	CH_3^+, Hg, $Co(CN)_6^{2-}$, Pt^{4+}
Gd^{3+}, Lu^{3+}, Cr^{3+}, Co^{3+}, Fe^{3+}	Te^{4+}, Br^+, I^+
Si^{4+}, Ti^{4+}, Zr^{4+}, Hf^{4+}, Th^{4+}	
Pu^{4+}, Ce^{4+}, WO^{4+}, Sn^{4+}	
UO^{2+}, VO^{2+}, MoO^{3+}	
Borderline	
Fe^{2+}, Co^{2+}, Ni^{2+}, Cu^{2+}, Zn^{2+}, Pb^{2+}	
Sn^{2+}, Sb^{2+}, Bi^{3+}, Rh^{3+}, Ir^{3+}, $B(CH_3)_3$	
Bases	
Hard	Soft
H_2O, OH^-, F^-, CH_3CO^{2-}, PO_4^{3-}	R_2S, RSH, RS^-, I^-, SCN
SO_4^{2-}, Cl^-, CO_3^{2-}, ClO_4^-, NO_3^-	$S_2O_3^{2-}$, R_3P, R_3As, $(RO)_3P$
ROH, RO^-, R_2O, NH_3, RNH_2,	CN^-, RNC, CO, C_2H_4, H^-, R^-
NH_2NH_2	
Borderline	
$C_6H_5NH_2$, C_5H_5N, N^{3-}, Br^-, NO^{2-}, N_2, SO_3^{2-}	

Table 1.5 Classification of acids and bases according to Pearson's HSAB principle.

From the literature[36] it would appear zinc favours binding to nitrogen donors. Indeed the effect of adding neutral oxygen donor atoms to an existing ligand leads in many cases to a decrease in zinc-ligand complex stability constant. This trend can be seen with both nitrogen and carboxylic acid donor ligands (Table 1.6). As a rule increasing the number of oxygen donors increases the selectivity of the ligand for large metal ions over small metal ions[66].

	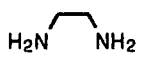	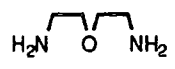	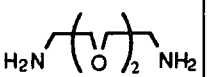	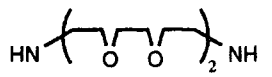	
Log K_{ZnL}	5.7	5.7	5.1	3.1	
	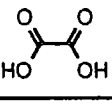	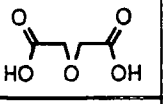	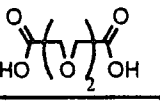	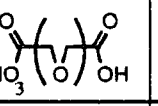	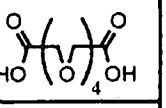
Log K_{ZnL}	3.88	3.58	2.65	2.6	2.18
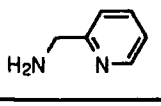		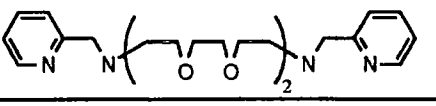			
Log $\beta_2 = 9.60$		log $K_{ZnL} = 7.0$			

Table 1.6 Log K_{ZnL} values (298K, H_2O, I = 0.1)[69] of zinc-ligand complexes when neutral oxygen donors are incorporated into the ligand.

Negatively charged oxygen donors (carboxylic acids, phenolates, hydroxamic acid groups) all tend to form their most stable complexes with metals of high charge density (e.g. their affinity for the hydroxide anion) such as Al^{3+}, In^{3+}, Fe^{3+}. Zinc only forms moderately stable complexes with these donors.

The neutral saturated nitrogen donor is widespread in coordinating ligands. Apart from its synthetic usefulness it shows stronger coordinating properties to many metal cations than the more electronegative, weaker neutral oxygen donor. The effect on complex stability by replacing a neutral oxygen by nitrogen is related to the metal affinity for the archetypal saturated nitrogen donor (i.e. the ammonia molecule). There is a large increase in stability for metals such as cobalt, zinc, nickel and copper and very little change for cations such as calcium, barium and magnesium (Table 1.7).

Ligand	Ca (II) Log K_{CaL}	Zn (II) Log K_{ZnL}
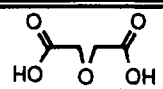	3.38	3.61
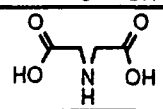	2.59	7.15
	-	4.79
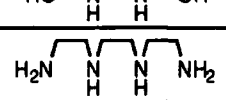	-	12.03

Table 1.7 Log K_{ML} constants (298K, H_2O, I = 0.1)[69] for calcium and zinc when nitrogen replaces oxygen.

Only in special cases, such as macrocycles, is this preference overcome and hard metals such as calcium bind strongly to nitrogen donors. Alkylating nitrogen will increase its donor potential due to the inductive effect of the substituent. However the expected increase in stability constant rarely materializes because there is an associated increase in steric strain which reduces stability. This trend can be seen with ethylenediamine-zinc complexes (Table 1.8): with nitrogen methylation there is a drop in log K_{ZnL} of up to two log units for tetramethylated ethylenediamine-zinc complex.

	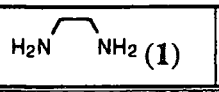 (1)		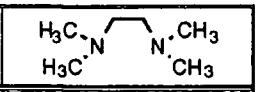
log K_{ZnL}	5.7	5.51	3.62
log β_{ML_2}	10.62	9.73	5.5

Table 1.8 Log K_{ZnL} values (298K, H_2O, I = 0.1)[69] of ethylenediamine (**1**) and alkylated derivatives.

Unsaturated nitrogen donors are also common, due to their structural and electronic properties. Often these donors (e.g. imidazole, o-phenanthroline (**2**)) are rigid units and can impart structural rigidity to the ligand. More effective preorganization is present which can result in higher stability constants. The low proton basicity may also be of use, in that under many circumstances metal-ligand complexation can occur without the relative difficulty of proton removal. The nitrogen in these donors is sp^2 or sp hybridized which leads to greater s-character in the donor orbitals used for bonding to metal cations and hence more covalent bonding. This will tend to favour borderline and slightly softer metals.

Phosphorus and sulphur donor atoms in water are poorly solvated and tend to bind softer metals (gold and mercury). Addition of sulphur only really benefits soft metal ions. Replacement of the corresponding neutral nitrogen by sulphur offers no advantage for zinc complex stability but complexes of harder cations are destabilized more markedly. This effect can be seen with the tetraamine (**41**) ligand (Table 1.9), replacing the two NH groups for sulphur results in an increase of the ligand-silver stability constant (0.69 log units), but decreases the zinc-ligand stability constant by 7 log units .

	 (41)	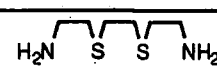
log K_{ZnL}	12.03	4.96
log K_{AgL}	7.65	8.34

Table 1.9 Log K_{ML} values (298K, H_2O, I = 0.1)[69] of zinc and silver complexes.

The thiol group is of more importance as it is weakly acidic (pKa about 9-10) and binds to many metals with high complexing strength. This effect can be seen with aromatic thiols and thio-carboxylic acids (Table 1.10).

	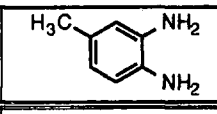	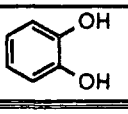	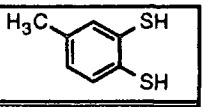
log β_2 Zn	n.d.	17.4	25.7
log β_2 Cu	8.5	24.9	
		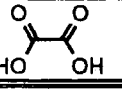	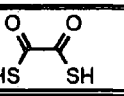
log β_2 Zn	n.d.	6.08	10.6

Table 1.10 Stability constants (298K, H_2O, I = 0.1)[69] of $[ML_2]$ complexes.

1.4.2 Chelate and macrocyclic effects

There appears to be an enhancement of complex stability when the complex contains chelate rings as compared to similar related acyclic systems (similar donor atoms with no or fewer rings). This can be readily seen with amine-zinc donors, as well as many other metal-ligand systems (Table 1.11).

	NH_3	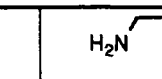	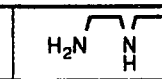	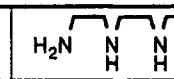
log β ZnL_{CN4}	9.65	10.62		12.03
log β ZnL_{CN6}	9.08	17.71	18.6	

Table 1.11 Stability constants of four and six coordinate zinc complexes (298K, H_2O, I = 0.1)[69].

This thermodynamic effect has been explained by considering entropy differences. There are only very slight differences in enthalpy between the above complexes. The enthalpy terms correspond to ligand and zinc desolvation, ligand reorganization and ligand-metal complexation. The main cause is the large entropy change resulting from the increase in the number of unbound molecules when polydentate ligands bind as illustrated in Eqn 1.5.

Eqn. (1.5) $[Ni(H_2O)_6]_{aq}^{2+} + 3(en)_{aq} \rightleftharpoons [Ni(en)_3]_{aq}^{2+} + 6H_2O_{aq}$

4 unbound molecules — 6 unbound molecules

The macrocyclic effect[70] is an extension of the chelate effect and refers to the increase in stability constant of a cyclic polydentate ligand as compared to the analogue

non cyclic ligand. There is generally an increase in stability, as can be seen with the following polyamine binding to zinc (Table 1.13). Similar trends are seen with other metal and ligand systems.

	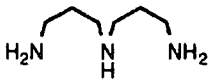	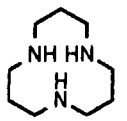		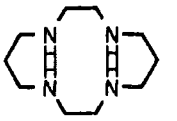
Log K_{ZnL}	7.92	8.75	11.25	15.34
Δlog K_{ZnL}	+0.83		+4.09	

Table 1.13 Log K_{ZnL} values (298K, H_2O, I = 0.1)[69] of acyclic and cyclic polyamine ligands.

This effect has its origin in both enthalpy and entropy contributions. The importance of these two contributions varies between ligand and metal[71]. However the enthalpy contribution is often the more dominant.

1.4.3 Macrocyclic pendent arms and ligand preorganization

Attaching pendent arms to macrocycles will only have a beneficial effect if they are of the correct donor type for the metal to be complexed. As mentioned (page 24) attaching oxygen donor groups to macrocycles disfavours smaller cation binding (i.e. zinc). This effect can be seen with $14N_4$ (**42**) ligands: methylation of the nitrogens causes a decrease in the complex stability constant, but adding hydroxyethyl pendent groups results in a large decrease in stability constant (Table 1.14). The low log K_{ZnL} value may indicate that the ligand is no longer behaving as an N_4-donor but as an N_2O_2 donor.

	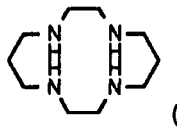 (**42**)	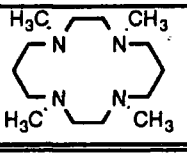	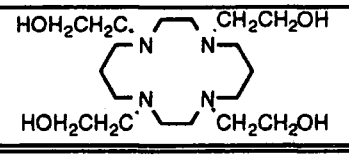
Log K_{ZnL}	15.5	10.4	6.43

Table 1.14 Log K_{ZnL} values (298K, H_2O, I = 0.M)[69] of zinc-$14N_4$ macrocycle ligands.

The length of the pendent arm affects the stability constant: long pendent arms that form large chelate rings are unlikely to enhance the stability constant of the macrocycle. However there are no reported zinc-ligand complex examples to illustrate this point. An increase in the zinc-ligand stability constant with pendent arm attachment can be seen when $12N_3$ (**43**) and a phenol α–C-substituted $12N_3$ ligand (Kimura's ligand(**6**)) are compared (Table 1.15).

	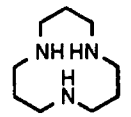 (43)	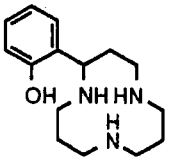 (6)
Log K_{ZnL}	8.75	12.6

Table 1.15 Zinc stability constants (298K, H_2O, I = 0.1)[69] of $12N_3$ (**43**) and Kimura's ligand (**6**).

With highly preorganized ligands such as cryptands and in particular spherands, the idea of size selectivity is of importance. With highly preorganized ligands such as Cram's spherands[72] extremely high selectivity and complex stability is exhibited and they are able to remove trace amounts of lithium and sodium from reagent grade potassium hydroxide. Apart from the size selectivity the spherands do not allow water to bind in the cavity and this effect enhances the overall complex stability as desolvation does not have to occur prior to complexation. Creating large cavity sizes is more difficult as the ligand normally has a tendency to collapse in on itself. Ligand reorganization before metal complexation requires energy and results in a lower than expected stability constant.

A more relevant example of preorganization can be seen with simpler ligands, 2,2'-bipridyl (**44**) and 1,10-phenanthroline (**2**). With the phenanthroline the two nitrogen donors are rigidly held in position so resulting in higher complex stability constants to many metals are seen (Table 1.16). The lower stability of the bipyridyl (**44**) complexes may be related in the strain introduced in the complex by the unfavourable interaction between the 3 and 3' protons.

	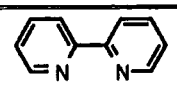 (44)	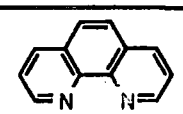 (2)
Log K_{ZnL}	5.13	6.4
Log $K_{Cu(I)L_2}$	12.95	15.82
log K_{CdL}	4.18	5.8

Table 1.16 Stability constants (298K, H_2O, I = 0.1)[69] of metal bipridyl (**44**) and phenanthroline (**2**) complexes.

1.4.4 Chelate ring size and size of metal ion

The size of the chelate ring on binding will have a large effect on the stability constant and selectivity. This applies to both linear and cyclic ligands. As a general rule an increase in the size of a chelate ring usually leads to a drop in complex stability. This drop is almost entirely due to less favourable enthalpy terms associated with increased

steric strain and the greater difficulty of bringing together dipoles and charges on donor atoms, rather than entropy effects associated with longer connecting links.

Comparing ligands where the change of chelate ring size occurs in the middle of the ligand rather than at the extremities allows certain general effects to be seen (Table 1.17). As a general observation the zinc stability constants show a gradual decrease in value with increasing number of six membered chelates rather than five membered chelate rings. Going from 2,2,2-TET (41) to 2,3,2-TET (45) there is a slight but important rise in stability constant. For lead, the decrease in stability constant with increasing number of six, rather than five, chelate rings is greater than with zinc. The protonation constant pK_1 also shows a general rise in value going from five to six chelate rings.

	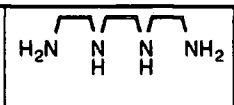 2,2,2-TET (41)	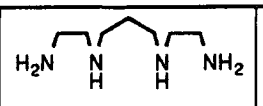 2,3,2-TET (45)	 3,2,3-TET	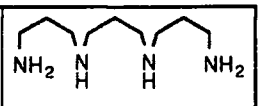 3,3,3-TET
Log K_{ZnL}	12.03	12.8	11.25	9.32
Log K_{PbL}	10.4	7.8		
pK_1	9.74	10.25	10.53	10.46

	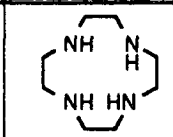	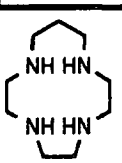	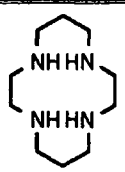	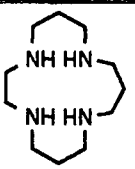	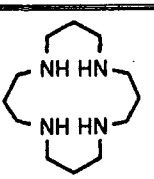
Log K_{ZnL}	16.2	15.6	15.34	15.0	13.05
Log K_{PbL}	15.9	13.48	11.3	n.d.	n.d.
pK_1	10.0	11.0	11.5	11.1	10.64

	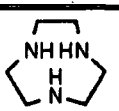	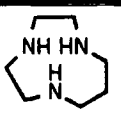	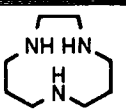	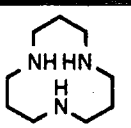 (43)
Log K_{ZnL}	11.6	11.3	10.4	8.8
Log K_{PbL}	11.0	9.8	n.d.	n.d.
pK_1	10.44	12.0	12.0	12.6

Table 1.17 Stability and first protonation (pK_1) constants (298K, H_2O, I = 0.1)[69] of polyamines with increasing chelate ring size.

Together with other formation constant data[69] the conclusion that an increase of chelate ring size leads to a drop in complex stability for the complexes of large metal ions or even small rises for smaller ions (e.g. proton) can be drawn. In other words "increase in chelate ring size leads to a greater degree of complex destabilization for larger metal ions than for smaller metal ions"[66]. Nickel and copper complex stability

data show increases for the previous ligands when going from five to six membered chelate rings.

A rationale[66] has been put forward based on simple molecular mechanics considerations. The chair conformation of a six membered ring possesses the lowest energy and minimal steric strain. Any binding arrangement which comes close to this has a low strain energy i.e. the acceptor metal must be of similar dimensions to carbon and form short metal-donor bonds. Small cations fit these criteria. For five membered chelates with the minimum strain energy, long metal-donor bonds are needed with a small donor-metal-donor angle, hence larger cations are more appropriate (Fig. 1.35).

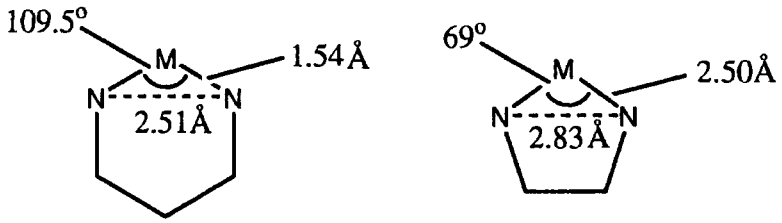

Fig. 1.35 Angles and dimensions required for minimal strain energy in chelate rings.

1.5 Scope of the present work

Using the design ideas outlined in the above sections and with reference to previous tetrahedrally binding ligands, three types of binding geometry, '3-1', '2+2', '2-2' were investigated (Fig. 1.36). These should all bind zinc in a tetrahedral manner and impart some selectivity over copper and nickel cations.

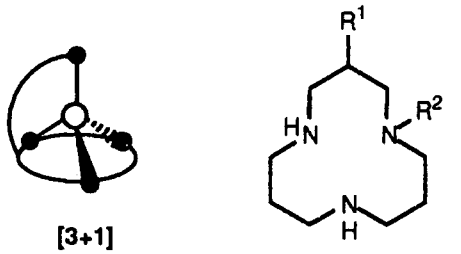

R^1 = H, R^2 = o-$CH_2C_6H_4OH$
R^1 = o-CH_2-p-BrC_6H_3OH, R^2 = H

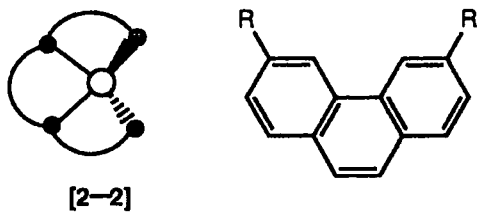

R = $CH_2PPh(O)OH$
= $CH_2PBz(O)OH$
= o-$C_6H_4CH_2COOH$

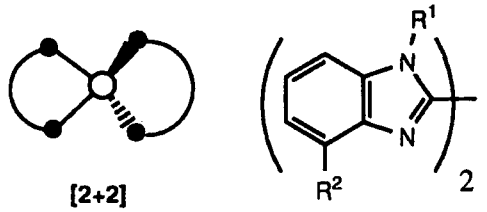

R^1 = p-$CH_2C_6H_4{}^tBu$, R^2 = COOH
= PPh(O)OEt
= PPh(S)OEt
= $P(S)(OEt)_2$

Fig. 1.36 Binding geometries and ligands synthesised in the work.

For the '3-1' binding geometry, the ligands were based on Kimura's ligand (**6**) in that the basal plane was a $12N_3$ ring and a phenol pendent arm was used. The attachment position of the pendent arm to the $12N_3$ ring was investigated. The length of the pendent arm was larger than in Kimura's ligand (**6**) to test if it enabled the fourth donor to bind in a better tetrahedral manner. For the '2-2' binding geometry phenanthroline based ligands were synthesised. The first type was similar to that of E. Cole[6] (**8**), varying only in the phosphorus substituents. A further advancement involved increasing the length of the pendent donor arm, but maintaining rigidity. This was achieved by using 1,10-phenanthroline substituted in the two and nine positions with phenyl groups appropriately functionalized with acetic acid donors. For the '2+2' binding geometry bisbenzimidazole ligands were synthesised with donor substituents (carboxylic acid or substituted phosphorus groups) in the four position. The lipophilicity of the ligand was altered by varing the N-alkyl group.

1.6 References

1) (i) G.B. Kauffman, 'Alfred Werner Founder of Coordination Theory', Springer, Berlin, 1966; (ii) R.F. Gould, ' Werner Centennial', Am. Chem. Soc., Adv. in Chemistry Series No62, Washington, 1967.

2) (i) G.N. Lewis; J. Am. Chem. Soc., 1916, **38**, 762; (ii) N.V. Sidgwick; 'The Electronic Theory of Valency', Oxford University Press, 1927.

3) E. Kimura, M. Yamaoka, M. Morioka, T. Koike; *Inorg. Chem.*, 1986, **25**, 3883.

4) N.W. Alcock, A.C. Benniston, P. Moore, G.A. Pike, S.C. Rawle; *J. Chem. Soc., Chem. Commun.*, 1991, 706.

5) (i) R. Alsfasser, A.K. Powell, H. Vahrenkamp; *Angew. Chem., Int. Ed. Engl.*, 1990, **29**, 898; (ii) A. Looney, G. Parkin, R. Alsfasser, M. Ruf, H. Vahrenkamp; *Angew. Chem., Int. Ed. Engl.*, 1992, **31**, 92; (iii) R. Alsfasser, A.K. Powell, S. Trofimenkpo, H. Vahrenkamp; *Chem. Ber.*, 1993, **126**, 685.

6) E. Cole; PhD. Thesis, University of Durham, 1993.

7) D.W. Gruenwedel; *Inorg. Chem.*, 1968, **7**, 495.

8) (i) J.A. Cras, J. Willemse;'Comprehensive Coordination Chemistry Volume 2, Ligands', Ed. G. Wilkinson, R.D. Gillard, J.A. McCleverty, Pergamon Press, Oxford, First edition, 1987, p643; (ii) A. Davison, E.S. Switkes; *Inorg. Chem.*, 1971, **10**, 837; (iii) M. R. Churchill, J. Cooke, J.P. Fennessey, J. Wormald; *Inorg. Chem.*, 1971, **10**, 1031.

9) (i) H. Groeger, A. Schmidtpeter; *Chem. Ber.*, 1967, **100**, 3216; (ii) I. Ojima, T. Iwamoto, T. Onishi, N. Inamoto, K. Tamaru; *J. Chem. Soc., Chem. Commun.*, 1969, 1501; (iii) A. Ziegler, V.P. Botha, I. Haiduc; *Inorg. Chim. Acta*, 1975, **15**, 123.

10) (i) G.F. Smith, W.H. McCurdy; *Anal. Chem.*, 1952, **24**, 371; (ii) B.G. Stephens, H.L. Felkel, W.M. Spinell; *Anal. Chem.*, 1974, **46**, 692.

11) (i) C.-H.B. Chen, D.S. Seligman; *Acc. Chem. Res.*, 1986, **19**, 180; (ii) R. Tamilarasan, D.R. McMillin; *Inorg. Chem.*, 1990, **29**, 2798.

12) (i) C.O. Dietrich-Buchecker, J.P. Sauvage, J.P. Kintzinger; *Tetrahedron Lett.*, 1983, **24**, 5095; (ii) J.P. Sauvage; *Nouv. J. Chimie*, 1985, **9**, 299; (iii) C.O. Dietrich-Buchecker, J.P. Sauvage; *Chem. Rev.*, 1987, **5**, 127.

13) J.K. Judice, S.J. Keipert, D.J. Cram; *J. Chem. Soc., Chem. Commun.*, 1993, 1323.

14) F.P. Schmidtchen; *Angew. Chem., Int. Ed. Engl.*, 1977, **16**, 720.

15) (i) E. Graf, J-M. Lehn; *J. Am. Chem. Soc.*, 1975, **97**, 5022; (ii) E. Graf, J-M. Lehn; *J. Am. Chem. Soc.*, 1976, **98**, 6403; (iii) E Graf, J-M. Lehn., *Helv. Chim. Acta*, 1981, **64**, 1040.

16) H. Irving, R.J.P. Williams; *J. Chem. Soc.*, 1953, 3192.

17) C.E. Moore, 'Ionization potential and ionization limits derived from the analysis of optical spectra', NSRDS-NBS 34, National Bureau of Standards, Washington D.C, 1970.

18) J. Bjerrum, C.K. Jørgensen; *Rev. Trav. Chim.*, 1956, **75**, 658.

19) H. Sigel, R.B. Martin; *Chem. Soc. Rev.*, 1994, 83.

20) I.D. Brown; *Acta Cryst.*, 1988, **B44**, 545.

21) (i) J.B. Hiskey, G.W. Warren, ' Hydrometallurgy Fundamentals, Technology and innovations', Soc. Min. Metall. Expl., Littleton, Colorado, 1993; (ii) F.M. Doyle;*J. Met.*, 1988, **40**, 32.

22) F. Habashi; *Chem. Eng. News*, 1982, **60**, 46.

23) P. Tasker, Private communication.

24) (i) C.S. Brooks; *Sep. Sci. Tech.*, 1995, **30**, 2055; (ii) M.A. Rabah, A.S. Elsayed; *Hydrometallurgy*, 1995, **37**, 23.

25) (i) H. Reinhardt, H. Ottertun, T. Troeng; *Inst. Chem. Eng. Symp. Ser. 41*, 1975, W1; (ii) E.D. Nogueira, J.M. Regife, P.M. Blythe; *Chem. Ind.*, 1980, 63.

26) (i) N. Miralles, A.M. Sastre, M. Aguilar, M. Cox; *Solvent Extr. Ion Exch.*, 1992, **10**, 51; (ii) M. Kunzmann, Z. Kolarik; *Solvent Extr. Ion Extr.*, 1992, **10**, 35; (iii) M. Kunzmann, Z. Kolarik; *Process Metall.*, 1992, **7A**, 207.

27) J.S. Preston, A.C. DuPreez, ' The solvent extraction of Co, Zn, Cu, Cd, Mg and rare-earth metals by organophosphorus acids', Ranburg, Council of Mineral Technology, 1988, Report (II), 37.

28) P.R. Danesi, L. Reichley-Yinger, G. Mason, L. Kaplan, E.P. Hormitz, M. Diamond; *Solvent Extr. Ion Exch.*, 1985, **3**, 435.

29) (i) M. Aguilar, N. Miralles, A.M. Sastre; *Rew. Inorg. Chem.*, 1989, **10**, 93; (ii) C. Sella, D. Bauer; *Solvent Extr. Ion Exch.*, 1988, **6**, 819.

30) C. Caravaca, F.J. Alguacil; *Hydrometallurgy*, 1991, **27**, 327.

31) F.J. Alguacil, A. Cobo, C. Caravaca; *Hydrometallurgy*, 1992, **31**, 163.

32) S. Wingefors, J. Rydberg; *Acta Chem. Scand. A*, 1980, **34**, 313.

33) P. Tasker; 'Novel Extractants', SCI conference, London, 15th March 1995.

34) D.P. Devonald, A.J. Nelson, P.M. Quan, D. Stewart, 'Process for the extraction of metal values and novel metal extractants', Europe Pat. 0196153 B1 (1986).

35) (i) R.F. Dalton, R. Price, P.M. Quan, B. Townson In M.J. Jones, R. Oblalt (editors), ' Reagents in the minerals industry', Proc. IMI Conf. Rone. Inst. Min. Metall., London, 1984, 181; (ii) R.F. Dalton, E. Hermann, B. Hoffmann, R. Price In G.A. Davis (editor), ' Reagents in the minerals industry', Ellis Horwood, London, 1987, 466; (iii) R.F. Dalton, G. Diaz, R. Price, A.D. Zunkel; *J. Met.*, 1991, **43**, 51.

36) (i) R.H. Prince, ' Comprehensive Coordination Chemistry, Volume 5, Late Transition Elements' Ed. G. Wilkinson, R.D. Gillard, J.A. McCleverty, Pergamon Press, Oxford, First edition, 1987, p925; (ii) D. Dakternieks; *Coord. Chem. Rev*, 1985, **62**, 1; (iii) D. Dakternieks; *Coord. Chem. Rev.*, 1987, **78**, 125.

37) R.G. Pearson; *J. Am. Chem. Soc.*, 1963, **85**, 3533.

38) R. Bartnik, S. Lesniak, A. Laurent, R. Faure, H. Loiseleur; *Acta Crtystallogr. Sect. C,* 1983, **39**, 1034.

39) M.C. Lim; *Aust. J. Chem.,* 1983, **36**, 19.

40) B. Dusek, F. Kutek; *Zh. Neorg. Khim.,* 1980, **25**, 2926.

41) (i) A.S. Goncalves, A.P. Chagas, C. Airoldi; *J. Chem. Soc., Dalton Trans.,* 1979, 159; (ii) C. Airoldi, A.P. Chagas; *Thermochim. Acta,* 1979, **33**, 371; (iii) B. Kamenar, G. Jovanovski; *Cryst. Struct. Commun.,* 1982, **11**, 257.

42) R.L. Chapman; R.S. Vagg; *Inorg. Chim. Acta,* 1979, **33**, 227.

43) S.K. Sahni; *Transition Met. Chem. (Weinheim, Ger.),* 1979, **4**, 73.

44) M. Massacesi, M. Biddau, G. Devato, E. Barni, P. Savarino; *Inorg. Chim. Acta,* 1984, **82**, 27.

45) G. Smith, E.J. O'Reilly, C.H. L. Kennard, K. Stadnicka, B. Oleksyn; *Inorg. Chim. Acta,* 1981, **57**, 111.

46) O.H.L. Kennard, G. Smith, E.J. O'Reilly, K. Stadnicka, B. Oleksyn; *Inorg. Chim. Acta,* 1982, **59**, 241.

47) R.G. Goel, W.P. Henry, N.K. Jha; *Inorg. Chem.,* 1982, **21**, 2551.

48) J.E. Fergusson, P.F. Heveldt; *Inorg. Chim. Acta,* 1978, **31**, 145.

49) D. Gattegnio, A.M. Guillani; *J. Inorg. Nucl. Chem.,* 1974, **36**, 1553.

50) M.F. Iskander, M. Mishrikey, L. El-Sayed; *J. Inorg. Nucl. Chem.,* 1979, **41**, 231.

51) J.M. Burlitch, S.E. Hayes, C.E. Whitwell II; *Organometallics,* 1982, **1**, 1074.

52) R.J. Read, M.N.G. James; *Acta Crystallogr., Sect. B,* 1980, **36**, 3100.

53) P.K.S.Gupta, L.W. Houk, D. Van der Helm, M.B. Hossain; *Acta Crystallogr., Sect. B,* 1982, **38**, 1818.

54) A.C. Tripis, E.G. Bakalbassis, V.P. Papageoriou, M.N. Balkola-Chistianopoutu; *Can. J. Chem.,* 1982, **60**, 2477.

55) N.A. Bell, P.T. Moseley; *Acta Crystallogr., Sect. B,* 1980, **36**, 2950.

56) I.G. Dance; *Inorg. Chem.,* 1981, **20**, 2155.

57) N.N. Greenwood, A. Earnshaw, ' Chemistry of the Elements', Pergamon Press, Oxford, First edition, 1984, 1402.

58) D.R. Neves, J. C. Dabrowiak; *Inorg. Chem.,* 1976, **15**, 129.

59) M.C. Kerr, H.S. Preston, H.L. Ammon, J.E. Huheey, J.M. Stewart; *J. Coord. Chem.,* 1981, **11**, 111.

60) O.G. Matyukhina, J. Ozols, B.T. Ibragimov, J. Lejejs, L.E. Terent'eva, N.A. Belov; *Zh, Strukt. Khim.,* 1981, **22**, 144.

61) H.W. Smith; *Acta Crystallogr., Sect. B,* 1975, **31**, 2701.

62) L. Casella, M.E. Silver, J.A. Lbers; *Inorg. Chem.*, 1984, **23**, 1409.

63) M.R. Churchill, A.H. Reis; *Inorg. Chem.*, 1973, **12**, 2280.

64) D. Wester, G.J. Palenik; *J. Chem. Soc., Chem. Commun.*, 1975, 74.

65) C. Bellito, L. Gastaldi, A.A.G. Tomlinson; *J. Chem. Soc., Dalton Trans.*, 1976, 989.

66) R.D. Hancock, A.E. Martell; *Chem. Rev.*, 1989, **89**, 1875.

67) G. Schwarzenbach; *Adv. Inorg. Radiochem.*, 1961, **3**, 257.

68) S. Ahrland, J. Chatt, N.R. Davies; *Q. Rev. Chem. Soc.*, 1958, 12.

69) R.M. Smith, A.E. Martell, 'Critical Stability Constants Vol 1 to 6', Plenum Press, London.

70) D.K. Cabbiness, W.D. Margerum; *J. Am. Chem. Soc.*, 1969, **91**, 6540.

71) M. Micheloni, P. Paoletti; *Inorg. Chim. Acta*, 1980, **43**, 109.

72) D.J. Cram, T. Kaneda, R.C. Helgeson, S.B. Brown, C.B. Knobler, C.B. Maverick, K.N. Trueblood; *J. Am. Chem. Soc.*, 1971, **93**, 6014.

Chapter Two

Bisbenzimidazole Based Ligands

2.1 Introduction

2.1.1 Bisbenzimidazoles

The first bisbenzimidazole was made by M.A. Phillips[1] in 1928, 56 years after the first benzimidazole had been synthesised[2]. Bisbenzimidazoles are generated when two benzimidazoles groups are linked together, often via the 2,2' benzimidazole positions (Fig. 2.1), but 2,4(7) and 2,5(6) bisbenzimidazoles are known .

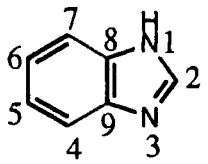

(**46**)
Benzimidazole

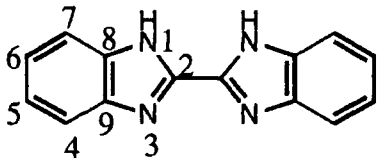

(**47**)
Bisbenzimidazole

Fig 2.1 Structures of benzimidazole (**46**) and bisbenzimidazole (**47**).

The benzimidazole units may be directly linked together or involve a spacer such as methylene groups or phenyl rings. Many examples exist where the nitrogens are substituted and the benzene ring is often substituted in the 5(6) position. Fewer examples exist with substituents in the 4(7) sites[3]. To date there are still many more known benzimidazole[3,4] derivatives than bisbenzimidazoles. A number of benzimidazoles have found commercial[5] uses as pharmaceutical, veterinary, anthelmintic agents and fungicides. However there are currently no bisbenzimidazoles made commercially on a medium or large scale.

2.1.2 Bisbenzimidazole coordination aspects

Compared to other bidentate nitrogen coordinating ligands there are comparatively few literature examples of bisbenzimidazole coordination complexes Most reported complexes utilise unsubstituted 2,2'-bis-1H-benzimidazole (**47**) and involve second or third row transition metals such as; gold[6], palladium[7], ruthenium[8], silver[9], rhodium,[10] or mixed metal complexes involving the above. There are fewer complexes involving first row transition metals. Complexes of titanium[11], iron[12], manganese[13], copper[14] and zinc[15] have been reported and apart from the iron example all the metal complexes involve other ligands.

The bisbenzimidazole ligand (**47**) is able to bind in a number of ways (Fig 2.2). The two pyridine-like nitrogens may coordinate cooperatively to a single cation without

ionising the NH groups. Mono-deprotonated bisbenzimidazole species bind via one pyridine-like nitrogen and one anionic nitrogen. Dianionic bisbenzimidazoles are able to bind two metals via all four nitrogens, or coordinate to three metals.

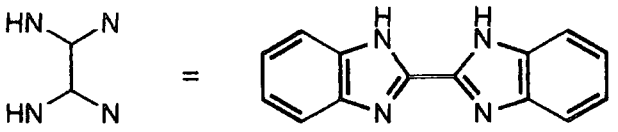

(a) via pyridine-like nitrogens:

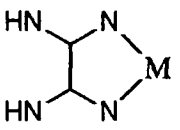

e.g. M=Fe [$Fe(BiBzImH_2)_3$]
M=Pd [$Pd(\eta^3\text{-}2\text{-}CH_3(C_3H_5)(BiBzImH_2)$]

(b) via mono anion:

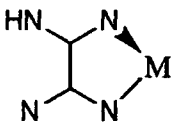

e.g. M=Pd [$Pd(\eta^3\text{-}2\text{-}CH_3(C_3H_5)_4(BiBzImH)$]

(c) via dianion:

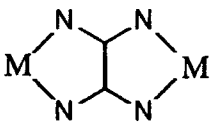

e.g. M=Mn {$[Mn(CO)_3(PPh_3)_2]_2(BiBzIm)$}

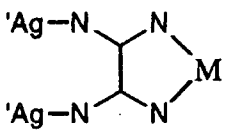

e.g. M=Rd {$[Rd(cod)(AgPPh_3)_2](BiBzIm)$}

Fig 2.2 Bisbenzimidazole (**47**) binding modes.

2.1.3 Bisbenzimidazole zinc coordination

There are two reported N-substituted bisbenzimidazoles[16,17] that bind zinc chloride in a tetrahedral fashion (Fig. 2.3). From the crystal structure (Fig. 2.4) it was observed that a dimeric neutral complex is produced involving two ligands binding via the pyridine-like nitrogens to two zinc (II) chloride molecules. In the complex, the bisbenzimidazole units are twisted around the 2,2' linkage to form two mutually perpendicular coordination planes. When the dihedral angle between the benzimidazole moieties is close to 90° two tetrahedral binding sites are produced.

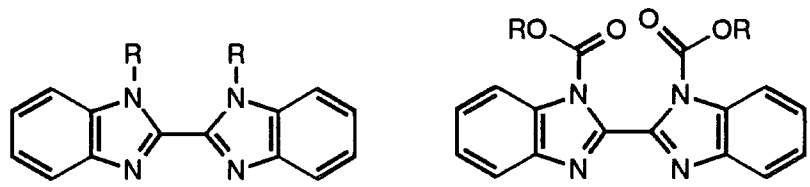

(48) (49)

Fig 2.3 Zinc coordinating bisbenzimidazoles (**48**) and (**49**).

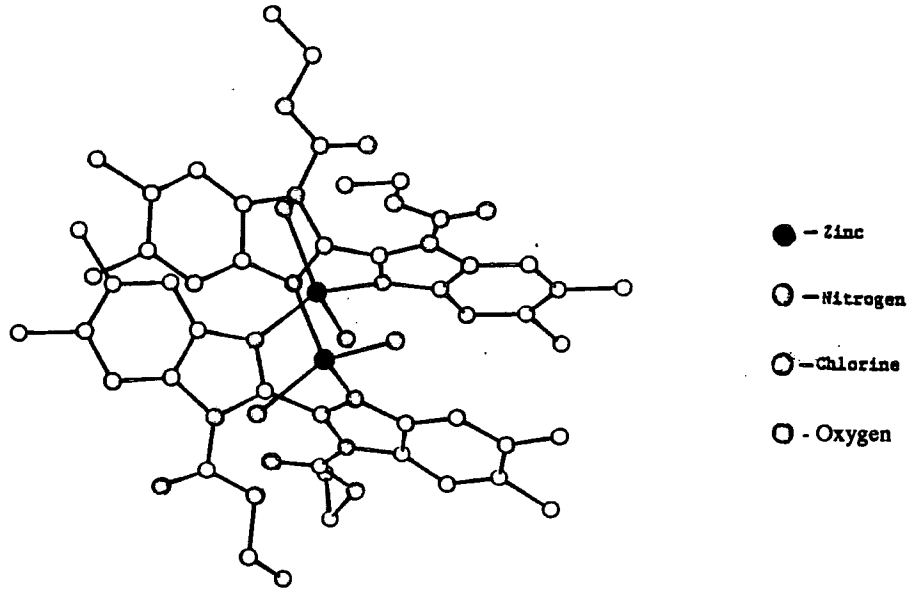

Fig 2.4 Crystal structure of zinc chloride complex of (**49**), (R = Et).

Lipophilic derivatives of (**48**) and (**49**) have been synthesised and have been tested for solvent extraction of zinc from an acidic chloride leach solution[17]. The kinetics of binding (extraction) and decomplexation (stripping) are rapid, with equilibrium being established in less than one minute. The ligand showed high selectivity for zinc over iron (II), (III) and other metals (e.g. Pb, Cd (Table 2.1)). Copper is also extracted, so in practice it would be desirable to remove copper prior to zinc extraction.

Metal	Zn (g/l)	Fe	Cu (ppm)	Pb	Cd (ppm)	Sb (ppm)
Initial aqueous	50	100 g/l	25	1.5 g/l	25	25
Organic after one contact	15	6 ppm	15	<5 ppm	<5	<5

Metal sulphides in chloride medium (5.5M Cl ion)

Table 2.1 Metal extraction data using the lipophilic deivative of ligand (**48**).

The bisbenzimidazole ligands are weak bases and are not readily protonated under the low pH (<2) conditions found in chloride leach solutions. They therefore do not readily transfer either unwanted impurity metals (by ion pairing mechanisms) or hydrochloric acid into the organic phase (equations 2.1 and 2.2) where they can cause problems in zinc decomplexation and electrochemical recovery.

Eqn. (2.1) $L_{org} + H^+_{aq} + FeCl_4^-{}_{aq} \rightleftharpoons ([LH]^+[FeCl_4]^-)_{org}$

Eqn. (2.2) $L_{org} + H^+_{aq} + Cl^-_{aq} \rightleftharpoons (LHCl)_{org}$

2.1.4 Improved ligand design

There are many advantages of a bisbenzimidazole based ligand for tetrahedral coordination and hence subsequently as a zinc selective ligand for solvent extraction. The previous complexes show zinc is bound tetrahedrally. The bisbenzimidazole unit also shows the required selectivity, rapid kinetics of complexation and stripping and is stable to air and thermal decomposition; allowing ligand recycling. Its solubility can in principle be readily altered via the N-substituent without affecting its binding properties.

Improvements can be made on ligands (**48**) and (**49**) to enhance the bisbenzimidazole unit for use in binding and zinc solvent extraction. Increasing ligand preorganisation to the required binding geometry prior to cation complexation results in a larger metal-ligand stability constant. Using substituted benzyl groups to increase the steric bulk of the N-substituent should therefore increase the likelihood that the benzimidazole moieties are not coplanar prior to complexation. Binding via the two nitrogens in a bidentate fashion in the same plane becomes impossible, so square-planar and octahedral complexation potential was removed.

The equilibrium position of zinc extraction from the aqueous phase using the ligands (**48**) and (**49**) was found to be dependent on chloride ion concentration (equation 2.3).

Eqn. (2.3) $2Zn^{2+}_{aq} + 2L_{org} + 4Cl^-_{aq} \rightleftharpoons (LZnCl_2)_{2org}$

Decomplexation was achieved by the use of a strip solution of lower chloride concentration. Ideally the ligand should avoid this dependency on counter ions, but still be charge neutral. It has been shown that aliphatic carboxylic acids[18] can be used for the extraction of zinc from weakly acidic solutions. By varying the ligand and extraction conditions, zinc selectivity over cadmium was achieved.

The ligand (**50**) was designed with these constraints in mind (Fig. 2.5).

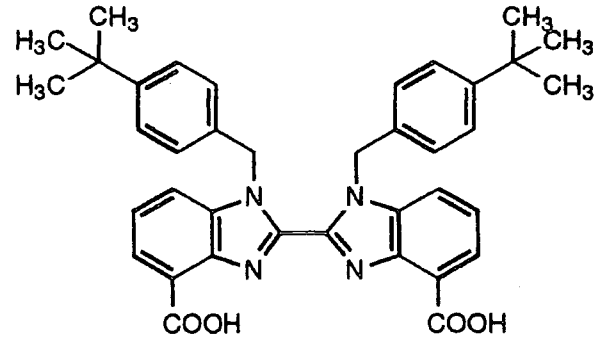

(50)

Fig. 2.5 The desired bisbenzimidazole ligand (**50**).

The aryl carboxylic acid is expected to have a lower pK_a than that of aliphatic acids so zinc extraction by this ligand (**50**) may occur at a lower pH. Binding to the acid groups should be preferred over chloride binding, resulting in a charge neutral $[L_2Zn_2]$ complex. Lipophilicity may be controlled by variation of the nitrogen substituent. Selectivity for small and tetrahedral coordinating ions should be favoured by a combination of the 6-ring chelate (favouring small ions)[19] and the ligands preferred binding conformation imposed by minimising steric interactions between the N(1) substituents.

2.2 Ligand synthesis

2.2.1 Bisbenzimidazole via 1,2-diaminobenzene (51)

2,2'-Bis-1H-benzimidazole (**47**) is a convenient starting material for the synthesis of the target ligand (**50**) as it can be readily made from inexpensive materials by a literature method[20]. Ortho diaminobenzene (**51**) was heated at 200°C with oxamide (**52**) in a minimal volume of ethylene glycol. Precipitation from hot water gave the crude bisbenzimidazole (**47**). A modified purification procedure was employed which involved recrystallization from acetic acid rather than ethylene glycol. After heating the crystals with ammonia solution and vacuum drying the residual acetic acid was removed as ammonium acetate.

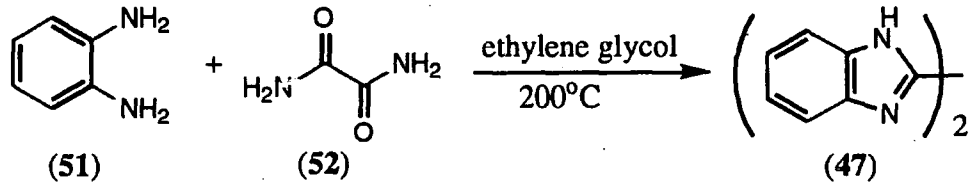

(51) (52) (47)

Fig. 2.6 Bisbenzimidazole (**47**) formation from 1,2-diaminobenzene (**51**) and oxamide (**52**).

Neutral benzimidazoles may be alkylated by an S_E2' mechanism in which electrophilic attack is directed at the pyridine-like nitrogen. The benzimidazolium intermediate reacts with uncharged benzimidazole and so yields are restricted to around 50%. Greater yields may be obtained by the use of an excess of alkylating reagent and 1.5 equivalents of base. Alkylation was achieved using 4-tert-butylbenzyl bromide (**53**) with either caesium carbonate, or sodium hydride in DMF. Tetrahydrofuran could not be used as a solvent because the bisbenzimidazole salt was too insoluble. The ^1H NMR of the crude reaction mixture from both procedures indicated that conversion to the product had occurred in high yield. However, purification by column chromatography gave only 22-27% of the desired product (**54**) as a pale yellow solid. It was noted that the product was unstable in solution, especially in chloroform with respect to air and light; this could account for the poor yield from chromatography.

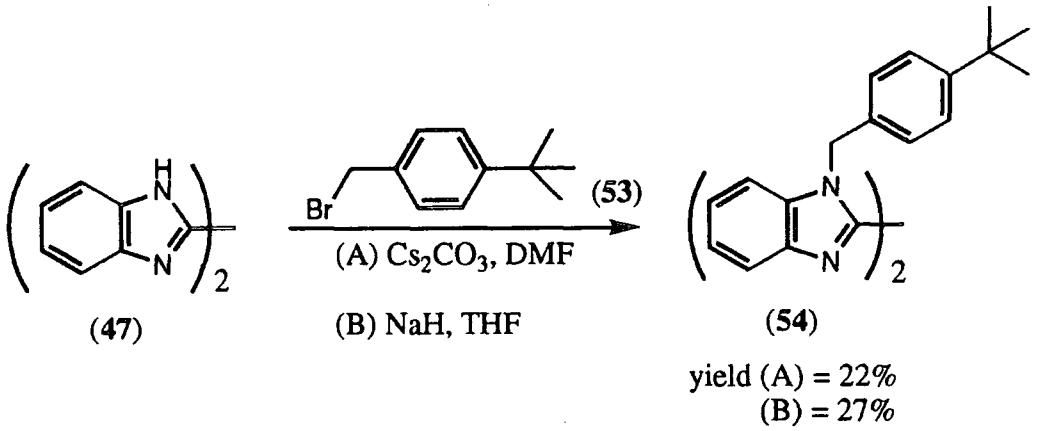

Fig. 2.7 N-alkylation of 2,2-bis-1H-benzimidazole (**47**).

The position of proton abstraction with n-butyl lithium depends on both steric and electronic considerations and whether the reaction is under thermodynamic or kinetic control. The nitrogen atoms of the bisbenzimidazole direct proton abstraction to the ortho and para positions on the benzene ring. The reaction was performed at low temperatures in an attempt to obtain the kinetic product. The benzyl group provides steric hindrance for proton abstraction ortho to the substituted nitrogen. Abstraction of the proton ortho to the pyridine-like nitrogen should be more favourable. However reaction of the bisbenzimidazole (**47**) with nBuLi at -78°C and subsequent carbon dioxide addition resulted in no carboxylated products being isolated.

2.2.2 Bisbenzimidazole via 2,3-diaminobenzoic acid (59)

Using an aromatic 1,2-diamine with a carboxylic acid group already present in the three position eliminates the need for the carboxylation reaction after coupling. 2,3-Diaminobenzoic acid (**59**) was prepared from 2-methyl-6-nitroaniline (**55**) following literature methods[21,22] . After cleavage of the amide (**57**), the product (**58**) was observed to exist in two polymorphic forms; either as yellow fibrous crystals which

were sparingly soluble in water, or yellow plate-like crystals which were insoluble in water. The relative amounts of the two forms seemed to depend on the reaction time . The longer the reaction time, the more plate-like crystals formed on cooling. Both polymorphs gave identical ^1H NMR and I.R. spectra. Reduction of the nitro group was performed by heating compound (**58**) in concentrated hydrochloric acid with tin (II) dichloride dihydrate. Use of anhydrous tin (II) dichloride resulted in a much lower yield. After two hours, the acid was neutralised to pH 7 using sodium hydroxide. The precipitated tin compounds were removed by filtration. Acidification of the filtrate resulted in formation of the diamino product (**59**) which crystallized as the dihydrochloride. The diaminobenzoic acid was unstable and decomposed with time. However, as the dihydrochloric salt it was stable to storage in air at room temperature. Vacuum sublimation allowed the free diaminobenzoic acid to be generated.

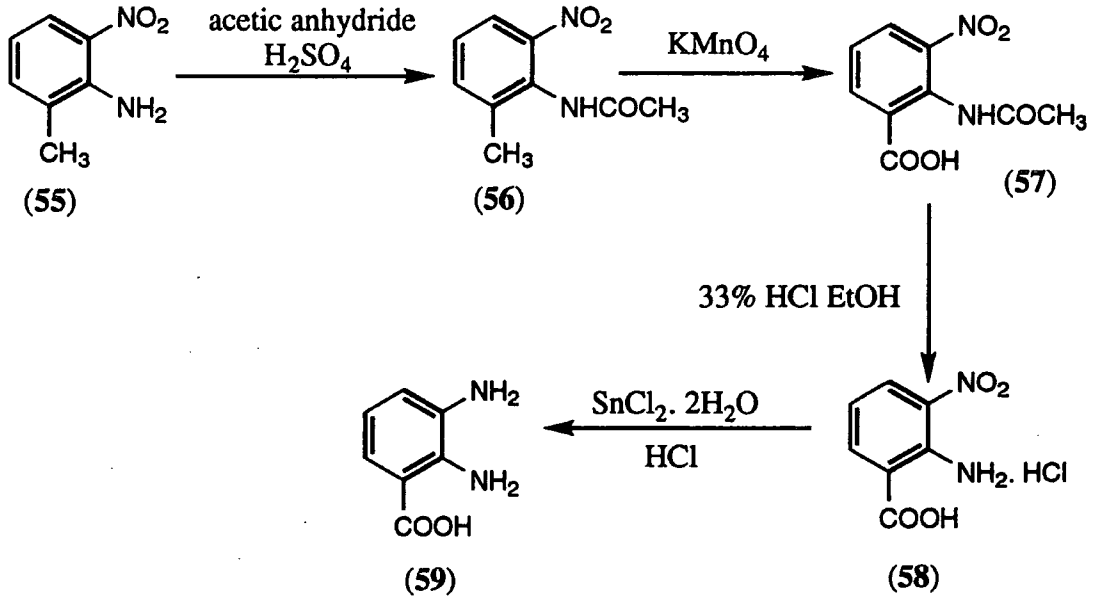

Fig. 2.8 2,3-Diaminobenzoic acid (**59**) synthesis.

Other reduction methods were also tried. Reduction using hydrogen with a 5% palladium on carbon catalyst in a variety of solvents:- ethanol, 20% v/v water/ethanol, 16:4:1 ethanol/water/acetic acid also resulted in nitro group reduction (as observed by the disappearance of the brightly yellow coloured nitro compound). However, on removal of the hydrogen atmosphere and isolation of the product, decomposition occurred. No diaminobenzoic acid (**59**) was recovered. Using ammonium formate as a catalytic hydrogen transfer agent[23] with 5% palladium on carbon in either ethanol or water also resulted in reduction but gave similar problems with product isolation.

2.2.2.1 2,3-Diaminobenzoic acid (59) coupling

The coupling of freshly sublimed 2,3-diaminobenzoic acid (**59**) with oxamide (**52**) using the same conditions as before resulted in bisbenzimidazole formation. A side

reaction resulted in decarboxylation of the bisbenzimidazole dicarboxylic acid product (**60**). The product could not be easily separated from 2,2'-bis-1H-benzimidazole (**47**) by recrystallization using either acetic acid or ethylene glycol. Chromatographic purification was not viable because of the low solubility of both materials. Derivatization of the crude acid was attempted to increase the solubility of the material and allow subsequent chromatography (Fig. 2.9).

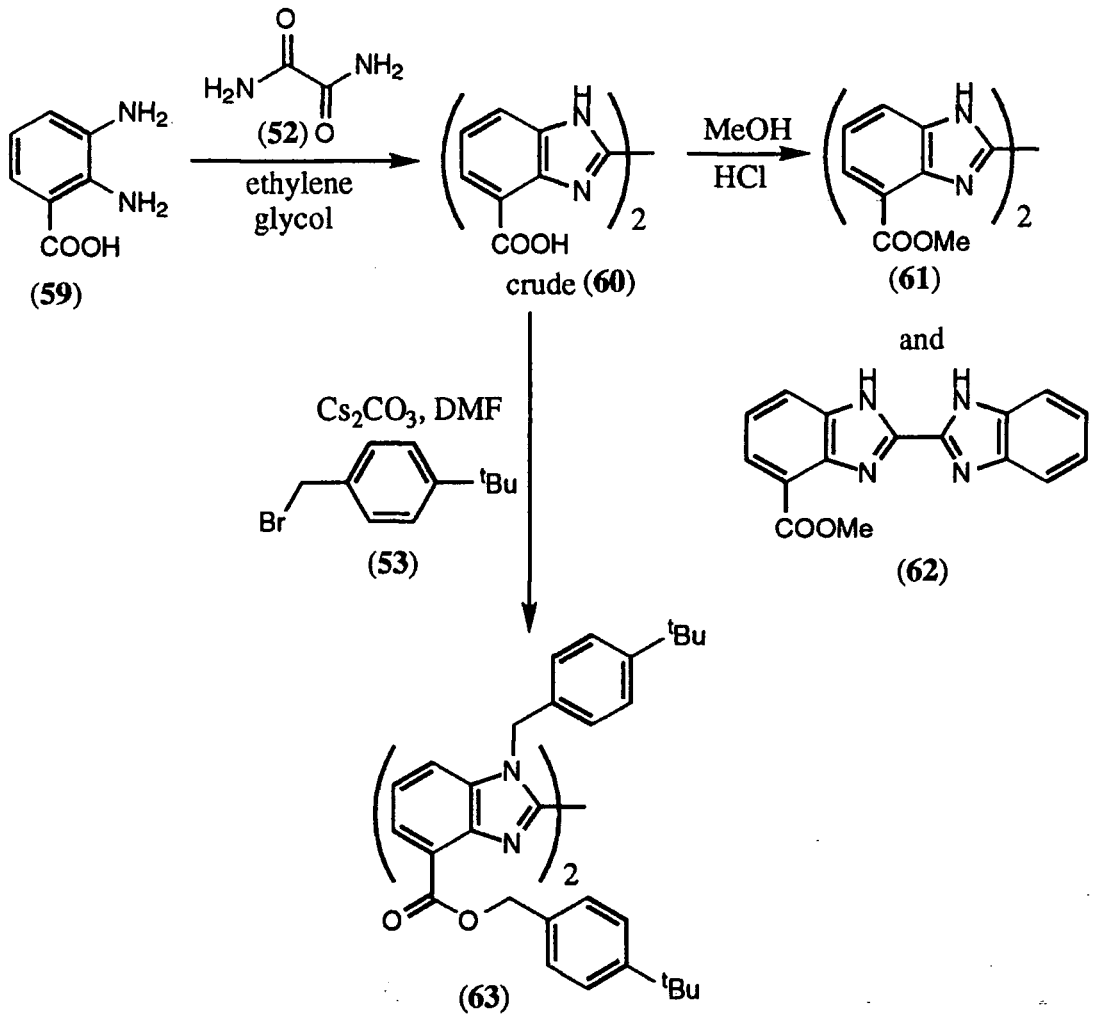

Fig. 2.9 Functionalizing crude bisbenzimidazole dicarboxylic acid (**60**).

Reaction of the crude bisbenzimidazole dicarboxylic acid (**60**) with dry methanolic hydrogen chloride gave the methyl ester. Column chromatography separated two products; the bisbenzimidazole dimethyl carboxylate ester (**61**) and the bisbenzimidazole mono-methyl carboxylate ester (**62**), both in very low yields. Reaction of the crude bisbenzimidazole dicarboxylic acid (**60**) with 4-tertbutylbenzyl bromide (**53**) in DMF using caesium carbonate as the base resulted in both N-alkylation and esterification. Chromatographic purification gave a low yield of the di-N-alkylated bisbenzimidazole dicarboxylate ester (**63**). Both of these methods are therefore unsatisfactory for purifying the desired ligand.

The observed decarboxylation was considered likely to result from the use of high temperatures in the coupling step. Variations on the coupling reaction were accordingly investigated. Using a lower temperature gave no product and using microwave energisation (thereby reducing the reaction time down to three minutes) gave the product but decarboxylated material was found to be still present. To make the use of 2,3-diaminobenzoic acid (**59**) viable, a lower temperature coupling reaction was needed. Reacting the benzoic acid (**59**) with either trichloroacetonitrile[24] in ethanol at 79°C, or 1,1'-bis(methylthio)-2-nitroethane[25] in DMF at 100°C gave a number of compounds which could not be isolated. None of the desired product was formed in either case. Coupling methods using the diamine (**59**) and CF_2=$CFCl$[26] or metallation induced coupling of the benzimidazole[27] (**66**) were not attempted because of the expected low yields and metallation complications with the carboxylic acid.

The diamine (**59**) was reacted in methanol at room temperature under an inert atmosphere using methyl trichloroacetimidate[28] as the coupling reagent. Only a monobenzimidazole (**65**) was purified from the crude reaction mixture by recrystallization from 0.1M hydrochloric acid. The literature[28] report indicates that the trichloromethyl group present on the benzimidazole (**65**) is sufficiently reactive to couple with a second diamine. However the low solubility of the product in this case probably prevented any further reaction. The reaction was initially acid catalysed and the use of protonated diamino compounds gives faster reaction times and higher yields. However, the protonated form of 2,3-diaminobenzoic acid (**59**) was too insoluble to allow reaction.

The proton of benzimidazoles may reside on either nitrogen, so in theory alkylation can occur at either site. Ortho substitution on the benzene ring provides enough steric bulk to result in selective alkylation of the less hindered site[29] (e.g. Fig. 2.10).

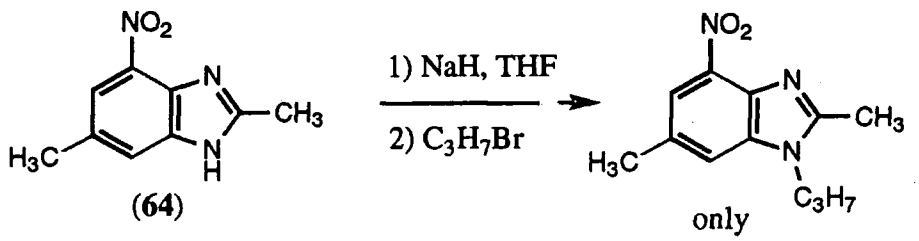

Fig. 2.10 Selective N-alkylation of benzimidazole (**64**).

N-Alkylation with 4-tert-butylbenzyl bromide (**53**) in DMF using caesium carbonate as the base selectively alkylated the benzimidazole (**65**). Esterification may have occurred, but as an aqueous acidic workup was used ester hydrolysis would have resulted. During the course of the alkylation reaction the trichloromethyl group was cleaved. The resulting compound (**66**) can act as a bidentate chelating agent and was used subsequently as a control for studies with the bisbenzimidazole dicarboxylic acid (**50**).

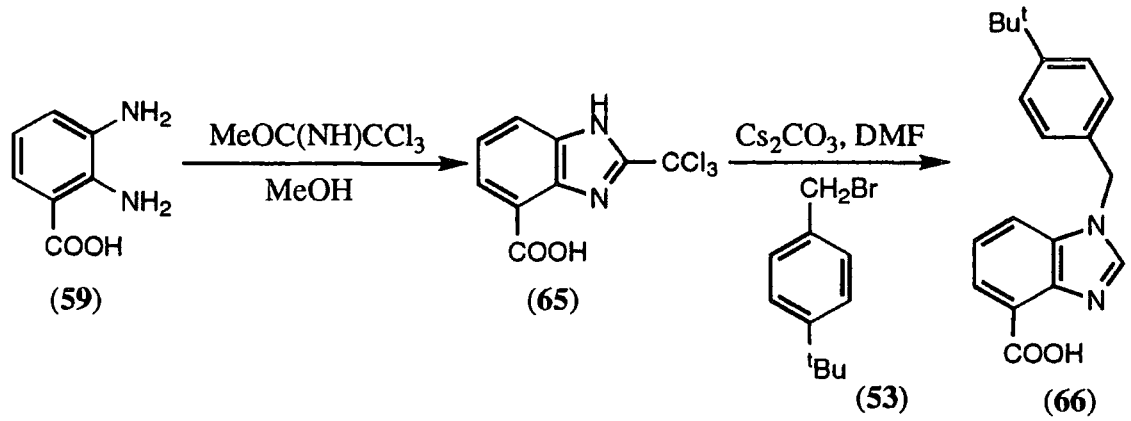

Fig. 2.11 1-(4-tert-Butylbenzyl)-benzimidazole-4-carboxylic acid (**66**) formation.

2.2.3 Bisbenzimidazole via 2,3-diaminobromobenzene (72)

It was evident that the presence of the carboxylic acid group on the diaminobenzene caused the problems in coupling. A functionality suitable for facile conversion to a carboxylic acid was sought to overcome this problem. The carboxylation of a lithiate derived from the appropriate aryl halide was therefore considered.

Direct nitration of 2-bromoaniline (**67**) was possible using 4-nitro-4-methyl-2,3,5,6-tetrabromo-2,5-cyclohexadiene-1-one[30] (**68**), which was readily made by bromination of para-methyl phenol and then activated by nitration using fuming nitric acid and acetic acid following a literature method[31]. The ortho nitrated aniline (**69**) had to be purified by chromatography and only a small yield was obtained (14%). The deactivated nitrating agent was also recovered and could be recycled. This procedure was regarded as being not viable as a preparative route to produce multi-gram quantities of bromonitroaniline (**69**).

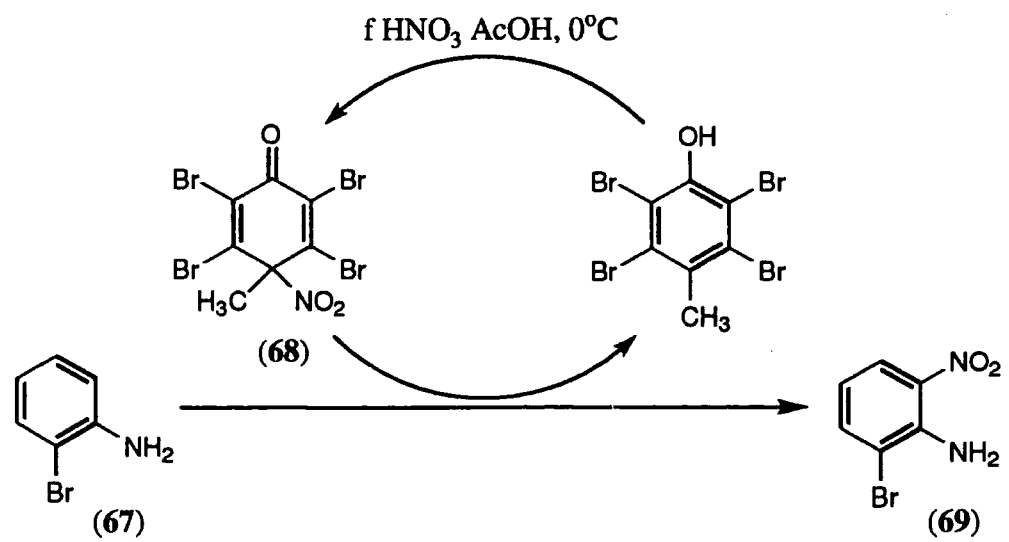

Fig. 2.12 Direct nitration of 2-bromoaniline (**67**).

The successful nitration method involved first the formation of the acetamide (**70**) of 2-bromoaniline (**67**) using acetic anhydride and a catalytic amount of sulphuric acid. Nitration[32] using a 5/4 v/v mixture of acetic acid and fuming nitric acid at room temperature occurred over two days. Precipitation by pouring the nitration mixture onto ice and water gave two products; ortho (**71**) and para nitro compounds in a 55/45 ratio. Purification by recrystallization for chloroform gave the desired product as a white solid. This purification procedure was used in preference to the literature method[33] which involved crystallization of 2-bromo-4-nitroaniline after base hydrolysis, reacetylation of the aqueous filtrate and 2-bromo-6-nitroacetanilide (**71**) precipitation. Scaling up the nitration reaction required a large increase in the reaction time (7 days) and led to a drop in the overall yield of nitrated products. Using trifloroacetic acid and fuming nitric acid at room temperature increased the reaction rate, but the ortho/para ratio was found to be 45/55. If large scale nitrations are required further investigation of nitration conditions and experiments with the reaction temperature may be worthwhile.

After hydrolysis of the amide (**71**) in 33% v/v hydrochloric acid-ethanol, the nitro group was reduced in near quantitative yield using tin (II) chloride dihydrate in concentrated hydrochloric acid. The product (**72**) was more stable in air than 2,3-diaminobenzoic acid (**59**) and could be extracted with diethyl ether from a basic solution.

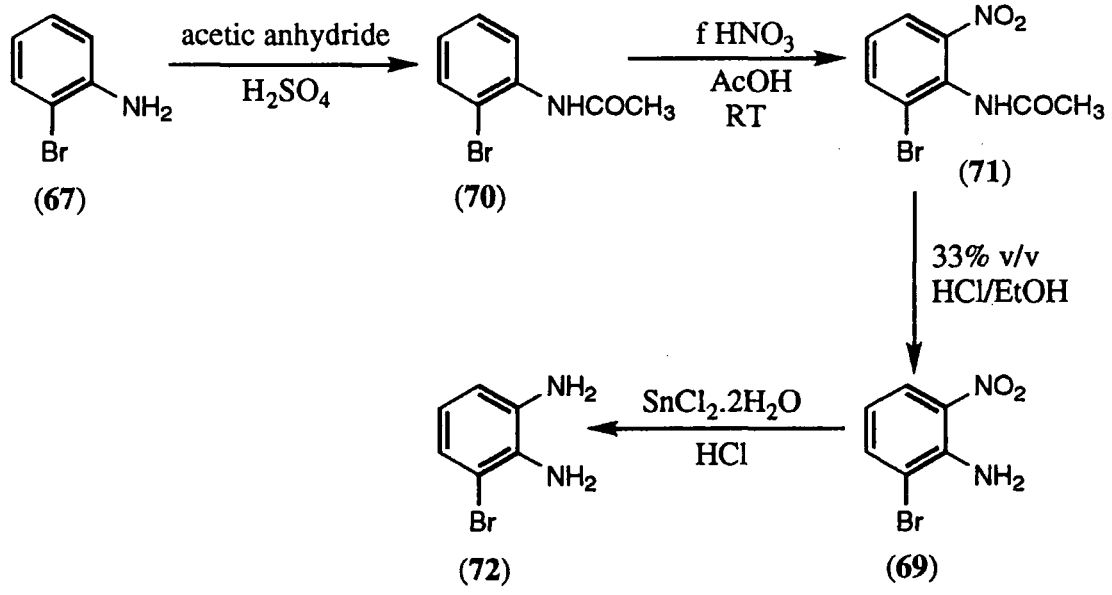

Fig. 2.13 2,3-Diaminobromobenzene (**72**) synthesis.

To initiate the coupling of diaminobromobenzene (**72**) with methyl trichloroacetimidate a few drops of concentrated hydrochloric acid were added to the methanolic solution. As the reaction proceeded, hydrochloric acid was generated and this eventually inhibited further reaction. To obtain higher yields, potassium carbonate

was added to the reaction after three hours. Yields of up to 75% resulted, compared to 45% without base addition. The dibromobisbenzimidazole (**73**) was insoluble in methanol. Purification by boiling the crude reaction mixture in methanol, allowing to cool and filtering, washing with water removed all the impurities to give the product (**73**) as a yellow solid.

The bromine substituent provided enough steric bulk to direct N-alkylation to the distant nitrogen using 4-tert-butylbenzyl bromide (**53**) in DMF with caesium carbonate as the base. A ^{1}H NMR NOE experiment on the benzylic protons showed the enhancement of two sets of aromatic proton resonances (ortho protons on the benzyl group and proton H-7 of the bisbenzimidazole (**74**)); indicating that selective alkylation had occurred. The substituted product (**74**) had low solubility in DMF and was recovered by precipitation with methanol. Recrystallization from chloroform gave a white solid. To increase the solubility in chloroform for NMR analysis 0.5% trifluoroacetic acid was added to the sample.

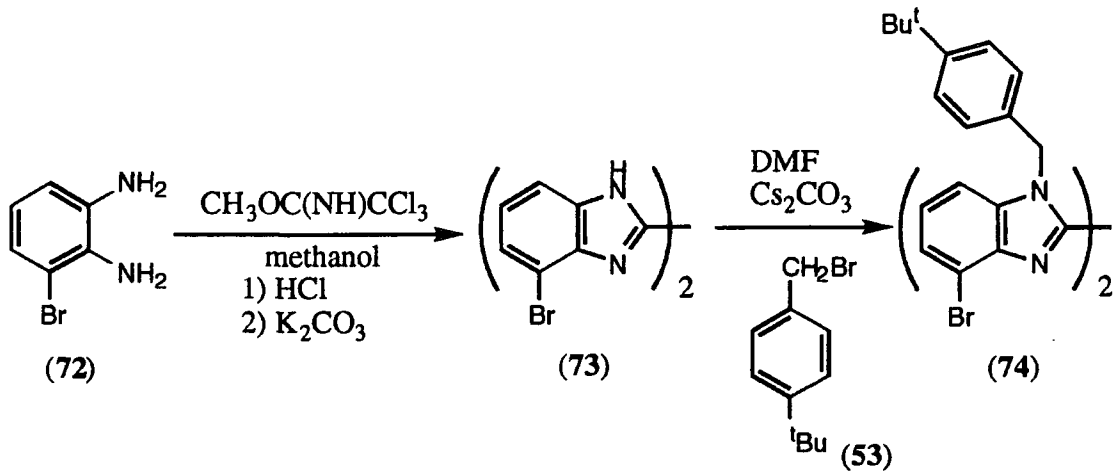

Fig. 2.14 Selective N-alkylation of 4,4'-dibromobis-1H-benzimidazole (**73**).

Carboxylation of the alkylated dibromobisbenzimidazole (**74**), which had been dried at 50°C under vacuum for 24 hours, with n-butyl lithium in THF at -78°C proceeded slowly because of its limited solubility in THF. Carbon dioxide gas was generated from solid carbon dioxide and dried with concentrated sulphuric acid and bubbled through the lithiate for ten minutes. After an aqueous acid work-up, ^{1}H NMR analysis of the crude reaction mixture indicated the presence of two bisbenzimidazole species; the product (**50**) and the starting material (**74**) in 65:35 ratio. The absence of any monocarboxylated material indicates that the second lithiation step is faster than the first. This is presumably an effect of solubility, with the rate limiting step being the solubilization of the dibromobisbenzimidazole (**74**) prior to halogen-lithium exchange.

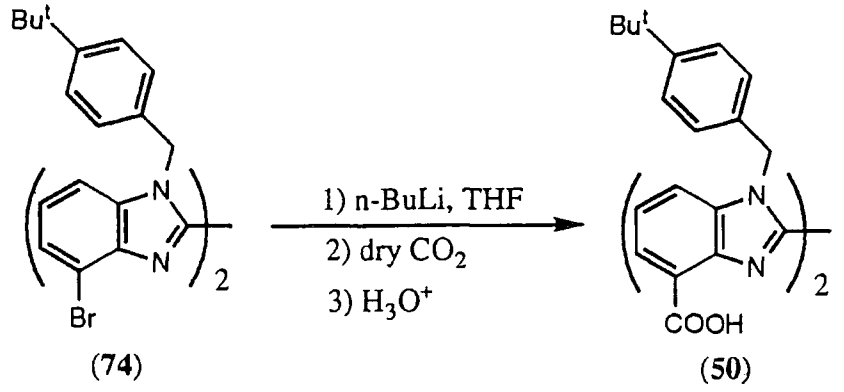

Fig. 2.15 Carboxylation of N-substituted dibromobisbenzimidazole (**74**).

The N-substituted dibromobisbenzimidazole (**74**) is less soluble than the dicarboxylic acid (**50**) so recrystallization from chloroform resulted in recovery of the starting material (**74**). Pentanoic acid, which was generated from carbon dioxide adding to excess n-butyl lithium, was removed by washing the crude with methanol. The crude product was absorbed onto silica and the dibromobisbenzimidazole (**74**) removed by washing with 2% methanol in dichloromethane. The dicarboxylic acid (**50**) was recovered using 40% methanol in dichloromethane. After solvent removal, the diacid (**50**) was no longer chloroform-soluble and C,N,H analysis indicated that the product had formed a 1:1 complex with a silicate species. To free the dicarboxylic acid (**50**), the complex was stirred with 0.1M hydrochloric acid at 40°C for 24 hours. Filtration and drying gave pure N-substituted bisbenzimidazole dicarboxylic acid (**50**) as a white solid. A ^{1}H NMR NOE experiment observing the benzylic methylene resonance at 6.06 ppm confirmed that direct halogen-lithium exchange and carboxylation had occurred with no lithium migration on the benzene ring.

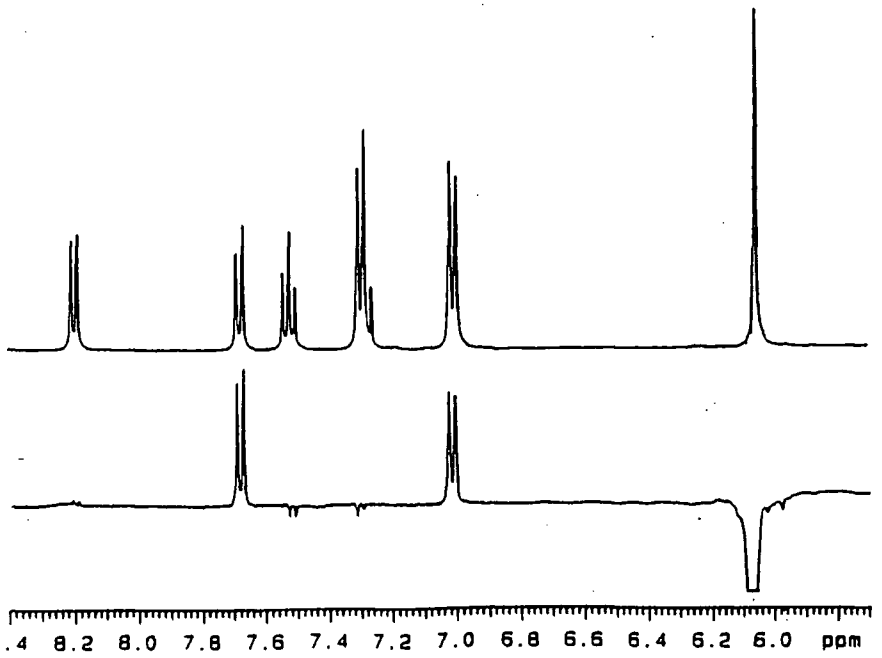

Fig. 2.16 NOE spectrum of bisbenzimidazole dicarboxylic acid (**50**).

2.2.4 N-Alkyl derivatives

By varying the lipophilicity of the reagent used in the N-alkylation of the dibromobisbenzimidazole (**73**), the solubility properties of the final dicarboxylic acid ligand can be modified.

For attempted solid state crystallographic analysis, a simple benzyl group was considered more appropiate. Benzyl bromide was reacted with the dibromo-bisbenzimidazole (**73**) and the product (**75**) recovered as before. The alkylated product (**75**) had a lower solubility in THF than its analogue (**74**). This was reflected in the longer reaction time for lithiation and the lower yield of dicarboxylic acid (**76**), which was purified as before.

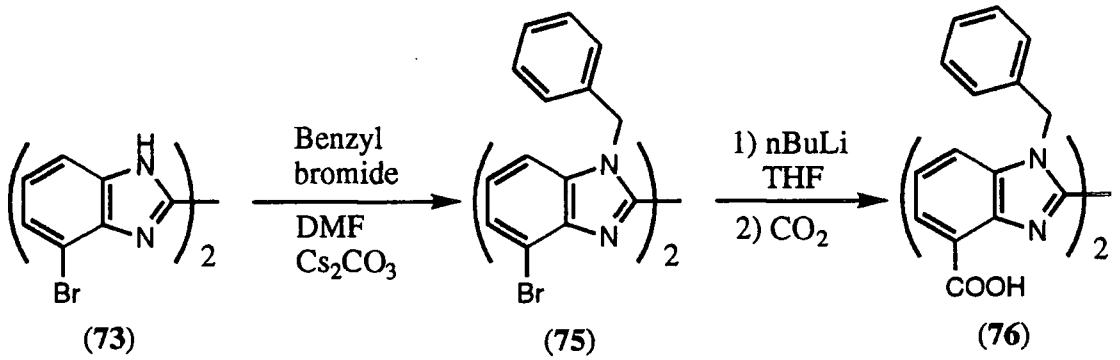

Fig. 2.17 Unsubstituted benzyl substituted bisbenzimidazole dicarboxylic acid (**76**) synthesis.

For solvent extraction tests the dicarboxylic acid needed to be soluble in the kerosene-like hydrocarbons used commercially. A lipophilic benzyl bromide derivative was made from branched dodecyl benzene (**78**) using paraformaldehyde (**77**) and phosphorus tribromide according to a known procedure[34]. Careful Kugelrohr distillation of the reaction mixture gave the dodecyl benzyl bromide (**79**) as a clear oil. The dodecyl benzene (**78**) was supplied as a mixture of highly branched structural isomers. This aids hydrocarbon solubility, but as the product (**79**) exists as a mixture of constitutional isomers a detailed analysis of the characterization of this product and subsequent compounds was not possible. N-Alkylation was performed as before and as the material (**80**) was more lipophilic it had greater solubility in DMF and could not be precipitated with methanol. The solvent was removed by vacuum distillation and the crude product recrystallized from 40-60 petroleum ether at 5°C to give the N-substituted dibromobisbenzimidazole (**80**) as an off-white solid. The alkylated product (**80**) was soluble in THF and the dianion was fully generated within 15 minutes at -78°C. Quenching by residual water was now found to be a problem and great care was taken to dry the starting material. After carbon dioxide addition as before and aqueous

work-up, the dicarboxylic acid (**81**) was purified by recrystallization from 40-60 petroleum ether at 5°C. Proton NMR analysis of the benzylic methylene resonance at 6.04 ppm revealed that the isolated product (**81**) was more than 95% homogeneous.

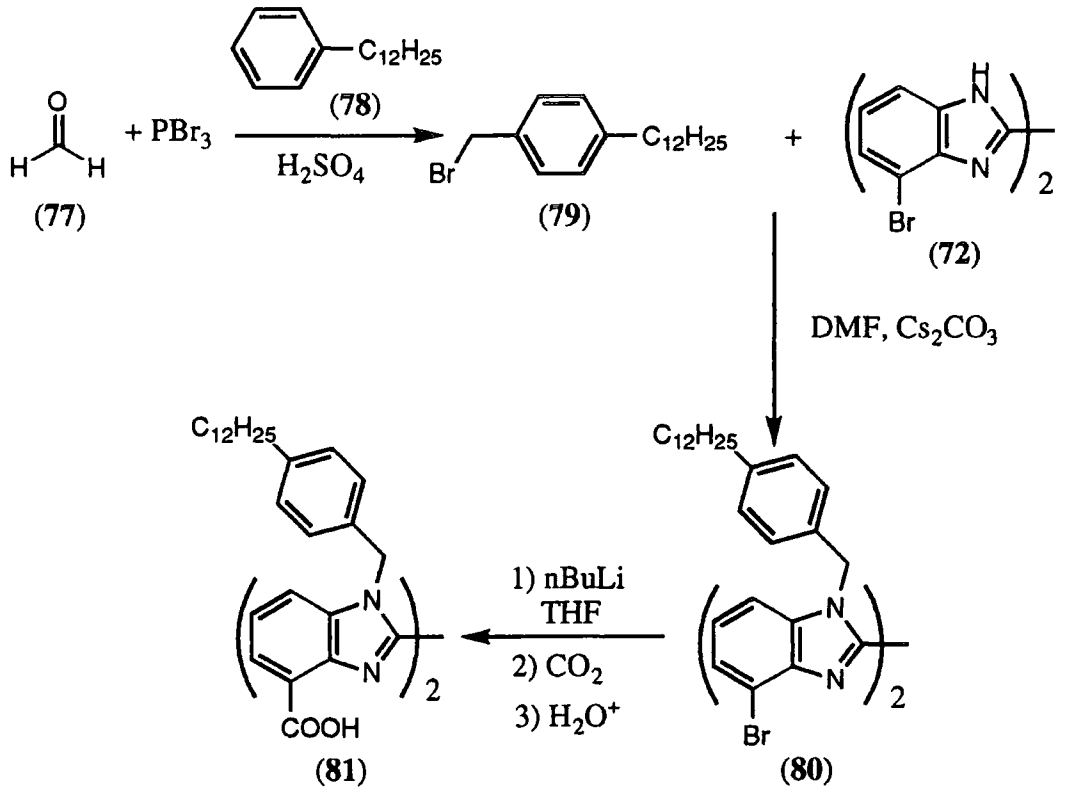

Fig. 2.18 Lipophilic bisbenzimidazole dicarboxylic acid (**82**) synthesis.

2.3 Solution complexation behaviour

In order to allow valid correlations to be made; ^{1}H NMR, IR, UV and electrospray mass spectrometric studies were carried out in methanolic solution (for NMR 25% CD_3OD, 75% $CDCl_3$; IR and UV non-deuterated solvent conditions as previous; electrospray MS 70% CH_3OH, 30% $CHCl_3$). In principle various equilibria can be set up in solution involving differently protonated mononuclear or dinuclear complex species (equations 2.4 to 2.8).

With each metal all the equilibria need not occur. The metal may react with the ligand and form a monomeric metal-ligand complex, [ML] (equation 2.4). This equilibrium has been assigned the constant K_1. The complex [ML] may be protonated by acid in the solvent to give a protonated monomeric metal-ligand complex (equation 2.5). The [ML] complex may also be produced by a different set of equilibria. Two ligands may coordinate to a metal (equation 2.6) and then to a further metal cation so producing two [ML] species (equation 2.7). Equilibrium constant K_2 has been defined as the coupling of two monomeric species to form a dimeric $[M_2L_2]$ complex (equation

2.8). Of course $[M_2L_2]$ may not be produced from two discrete [ML] units. This is especially true if K_1 is small and the metal prefers a $[M_2L_2]$ structure.

Eqn. (2.4) $M + L \overset{K_1}{\rightleftharpoons} [ML]$

Eqn. (2.5) $[ML] + H \rightleftharpoons [MLH]$

Eqn. (2.6) $M + 2L \rightleftharpoons [ML_2]$

Eqn. (2.7) $[ML_2] + M \rightleftharpoons [2ML]$

Eqn. (2.8) $[2ML] \overset{K_2}{\rightleftharpoons} [M_2L_2]$

2.3.1 Proton NMR spectroscopic analysis

Complexation of metal triflates (M = Ni, Cu, Zn, Pb, Cd) with 1,1'-bis(4-tert-butyl benzyl)-2,2'-bisbenzimidazole-4,4'-dicarboxylic acid (**50**) was examined by ^1H NMR spectroscopy (293K, 25% CD_3OD, 75% $CDCl_3$). Complexation of zinc triflate with the control ligands 1-(4-tert-butyl benzyl)-benzimidazole-4-carboxylic acid (**66**) and 1,1'-bis(4-tert-butyl benzyl)-2,2'-bisbenzimidazole (**54**) (Fig. 2.19) was also examined under identical conditions.

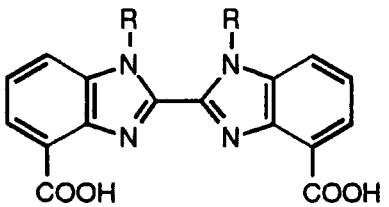

(**50**)

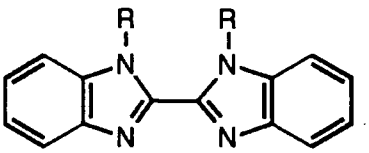

(**54**)

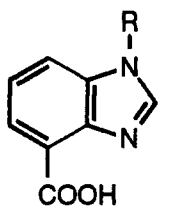

(**66**)

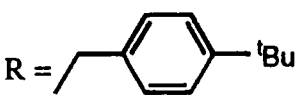

Fig. 2.19 Benzimidazoles (**50**), (**54**) and (**66**) used for proton NMR studies.

For ligands (**50**) and (**54**) stock solutions were prepared (4.06×10^{-2} M) in the desired solvent mixture. A stock solution of the metal triflate was also prepared (0.203 M). NMR samples were prepared using 0.4 ml of the ligand solution and the appropriate amount of metal solution to obtain a metal to ligand ratio in the range 0 to 5. Each sample was made up to 0.8 ml with the addition of the required amount of the NMR solvent mixture to make a final ligand concentration of about 0.2M. Insufficient

quantities of ligand (**66**) were available to make a stock solution. Instead a single NMR sample was prepared and incremental amounts of zinc triflate were added to obtain metal/ligand ratios of 0, 0.25, 0.5, 1, 1.5, 2. Each sample was examined by ^1H NMR before the next zinc triflate addition.

2.3.1.1 Lead

With increasing metal to ligand ratio there was a shift in the methylene NCH_2Ar proton resonance to lower frequency. Free and bound species were in fast exchange on the NMR time-scale (200MHz, 293K), so that a single resonance only was observed. There was no observable line-width broadening. Plotting the shift in the CH_2 proton resonance against the M/L (metal to ligand) ratio gave a titration curve. Non-linear least squares analysis for a 1:1 stoichiometric complex[35] gave an equilibrium value of 3.4 $x10^3$ and the theoretical curve shown (Fig. 2.20). The good agreement between the theoretical and experimental curves suggested other equilibria ($[ML_2]$ formation in Eqn. 2.6) were unlikely to be significantly involved (Fig. 2.20).

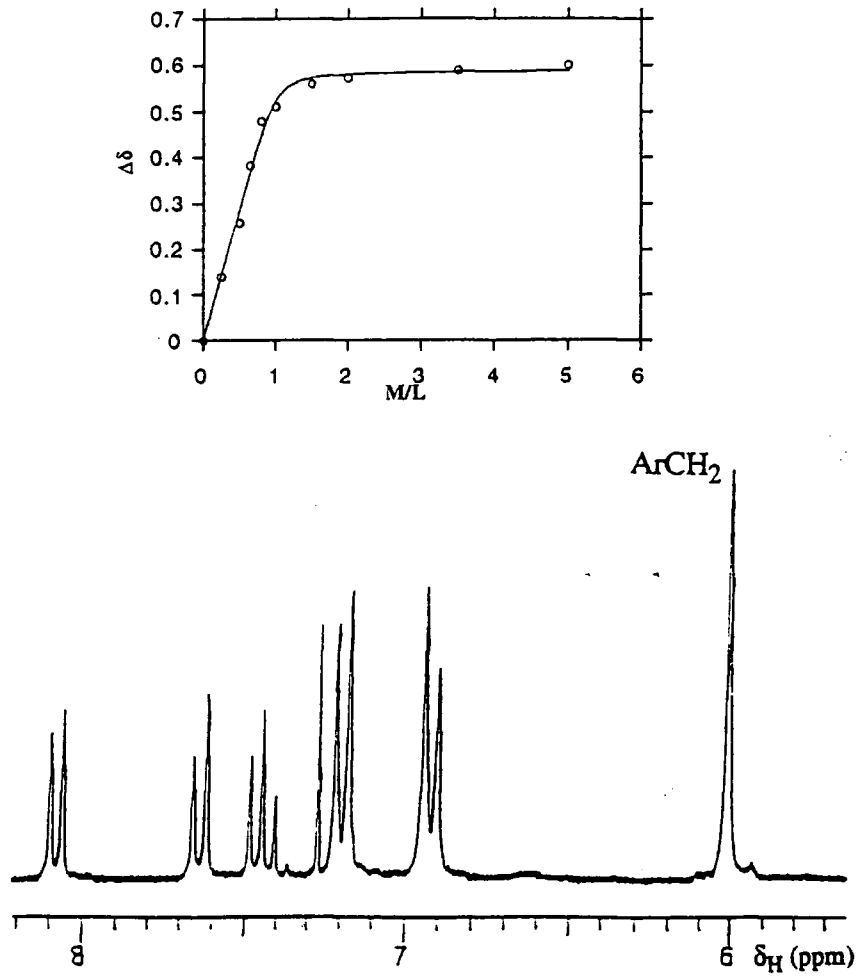

Fig. 2.20 Lead and ligand (**50**) proton NMR titration curve and spectrum of the ligand (M/L=0).

2.3.1.2 Copper and Nickel

Both copper (II) and nickel (II) are paramagnetic cations and cause NMR line broadening. For a metal to ligand ratio of up to M/L = 1.2, NMR spectra could be recorded and analysed even though there some line broadening was observed. At greater metal to ligand ratios no spectral peaks were observed. This is probably due to the presence of significant amounts of uncomplexed metal ions in solution causing extensive line broadening. As before the shift to lower frequency of the methylene proton resonance was observed and plotted against M/L ratio. Line broadening made it more difficult to determine the exact resonance position, but as the shifts were comparatively large this should not cause too much of a problem in curve plotting. Analysis for 1:1 complex formation gave estimates of $K_{NiL} = 1.1 \times 10^4$ for nickel and $K_{CuL} = 300$ for copper. With the copper titration there was a significant deviation from the best fit to a 1:1 complexation curve. This is consistent with other equilibria being present en route to [ML] complexation (Fig. 2.21). The plotted points follow a curve and are not directly proportional to the amount of metal added. The resonances also move in the same direction as with the lead experiment and are of the same magnitude, hence the shifts may be ascribed to complexation rather than any paramagnetic effect. .

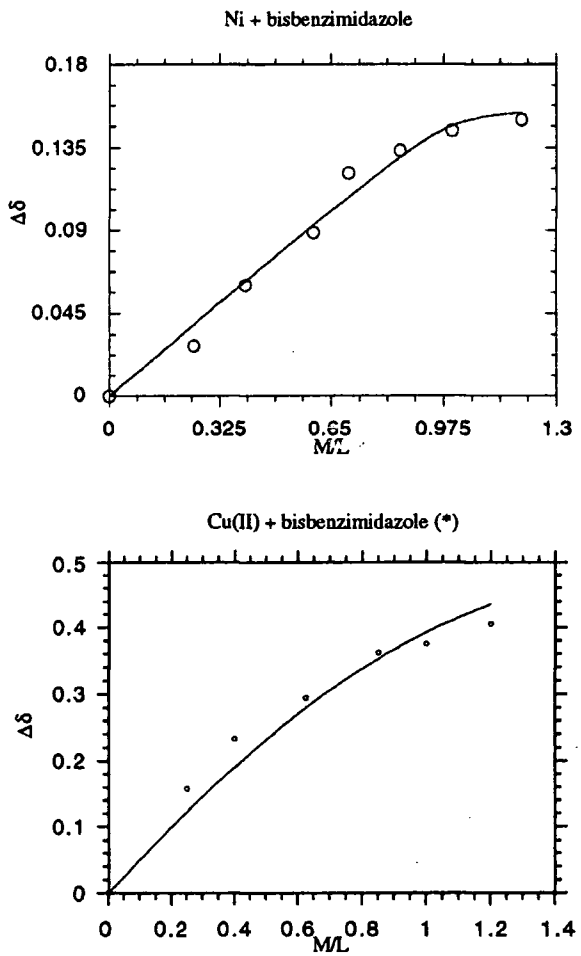

Fig. 2.21 Titration plots of ligand (**50**) with nickel and copper respectively.

2.3.1.3 Zinc

A very different set of spectra was obtained when zinc triflate was added to the ligand (Fig. 2.22). At M/L ratios of less than one, separate resonances were seen for two ligand-containing species; free ligand and a bound species, consistent with slow exchange on the NMR time-scale (i.e. $K > 10^5$). At M/L = 0.5, 50% of the signals were due to the slightly exchange-broadened ligand ($\omega_{1/2}$ = 13Hz for CH_2, 200MHz, 293K) and the remaining sharper signals for the 1:1 overall stoichiometric complex. Only the sharper set belonging to the bound complex was observed at M/L=1. No alteration was seen at higher metal to ligand ratios. Such behaviour is consistent with intermediate formation of a weak ZnL complex, followed by dimerization to give a neutral $[M_2L_2]$ complex with $K_2 > K_1$. Given that the 'nitrogen-carboxylate' 1:1 complex of zinc and ligand (**50**) is likely to be weaker than that with copper (II), it is probably that K_2 has a value of at least 10^3 (cf. 400 for Cd(II)). This ligand therefore shows 'positive cooperativity' in zinc binding, i.e. after binding one zinc it is favourable to bind a second cation to form $[M_2L_2]$. It would be possible to form a Scatchard plot[36] to show this.

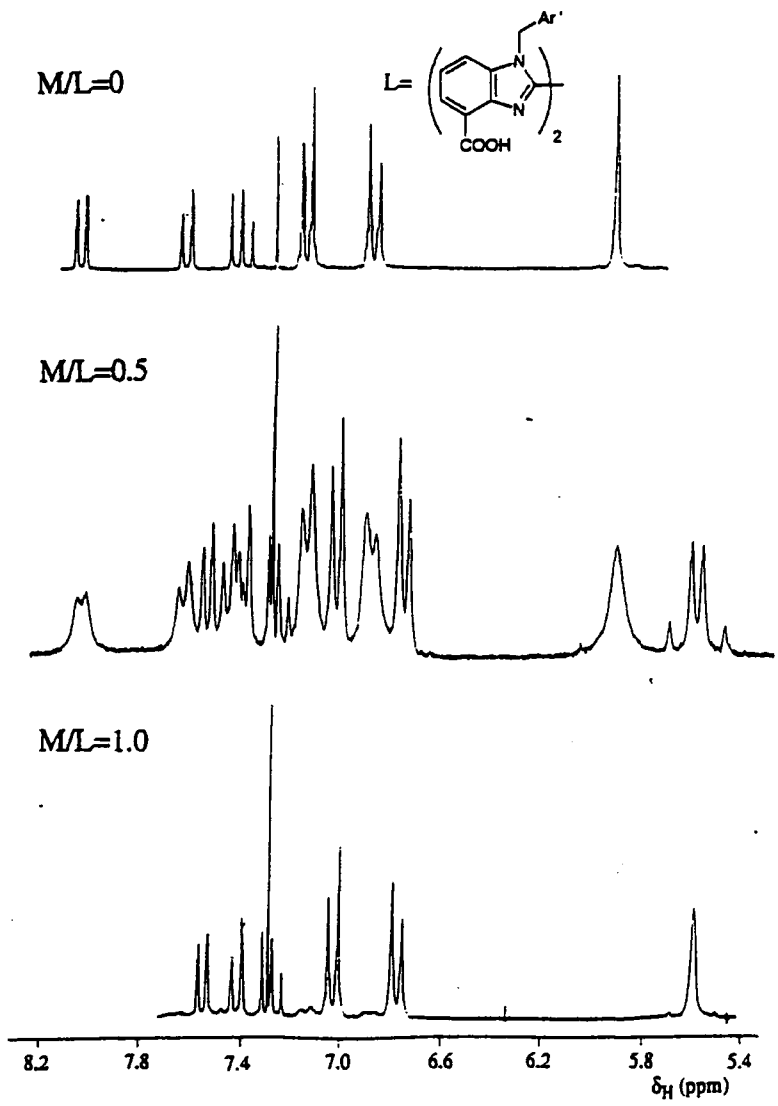

Fig. 2.22 Zinc NMR titration spectra with ligand (**50**).

2.3.1.4 Cadmium

The ^1H NMR titration using cadmium triflate showed more complicated behaviour. At low M/L ratio (≤ 0.5) there was again a shift in the methylene proton resonance to lower frequency indicative of formation of a bound complex in fast exchange with the unbound species. There were also certain very broad resonances integrating to only a small percentage of the total ligand present due to a more stable cadmium-ligand bound complex (Fig. 2.23 M/L = 0.25). At higher M/L ratios there was considerable line-broadening to all the ligand resonances. Two 'sets' of ligand peaks could be readily observed whose relative intensities varied with increasing M/L ratio. Only at M/L ratios of 2 and beyond was there a marked sharpening of the ligand resonances. At a M/L ratio of 5, signals due to a major complex species in slow exchange with at least one other different species could be defined.

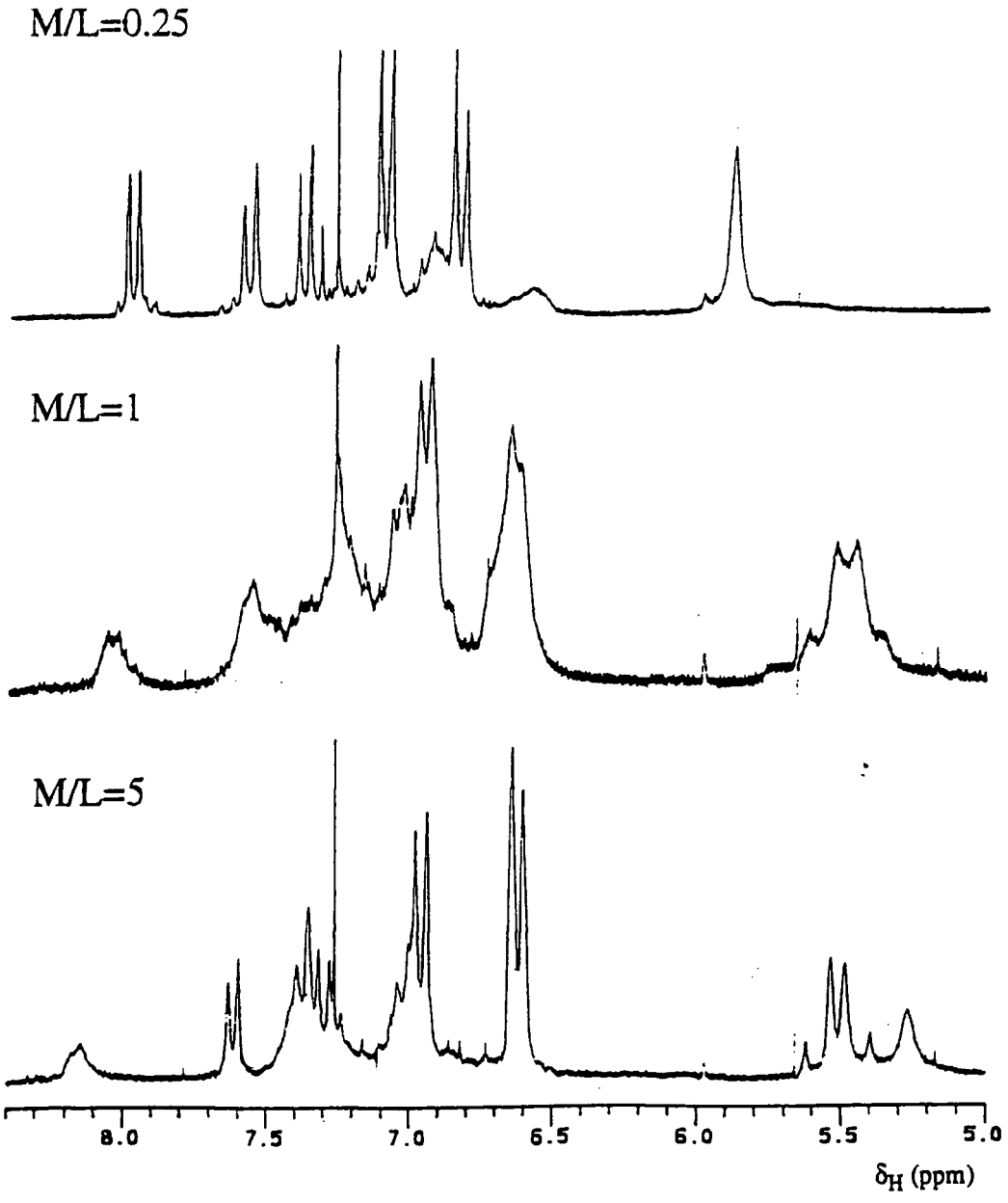

Fig. 2.23 Cadmium NMR titration spectra with ligand (**50**).

The resonances of the minor species were considerably exchange broadened. The resonances of the major species (ca. 70% of the total signal) were similar in form and chemical shift to the $[M_2L_2]$ species observed with zinc. Stepwise dilution of this sample with the deuterated NMR solvent mixture gave less and less of the major species and more of the exchanged-broadened species, consistent with the formation of a dimeric complex at higher concentrations. Assuming that the equilibria in equations 2.4 and 2.8 are operative, and knowing the relative proportions of the two species (^{1}H NMR integration) and the total concentration of the ligand used, then the association constant for formation of the $[Cd_2L_2]$ species (from [CdL]) was estimated to be 400 (± 150) dm^3mol^{-1}.

An interesting observation was noted when cadmium triflate contaminated with residual triflic acid from its manufacture was used. Generation of the second species and shifting of the ligand resonances were again observed with increasing M/L ratio, but there was much reduced line-broadening. Individual resonances were always observable. It appeared the excess acid helped to reduce the line-broadening, perhaps implying the intermediacy of protonated species (e.g. [MLH] or $[M_2L_2H]$) or even complexes involving ligation of the triflate anion. This was not studied in any further detail.

2.3.1.5 Zinc complexation with control ligands (54) and (66)

Under the same experimental conditions, the incremental addition of zinc triflate to ligand (**66**), the monomeric analogue of the bisbenzimidazole carboxylic acid (**50**) resulted in a shift to lower frequency of the methylene protons with increasing M/L ratio. The ligand would be expected to form $[ML_2]$ species and not an $[M_2L_2]$ complex. Non-linear least squares analysis of the $\Delta\delta_H$ vs. M/L titration curve (Fig. 2.24) for a 1:2 binding model (Appendix (i)) gave an estimate of $K_{ZnL} = 8 \times 10^3$.

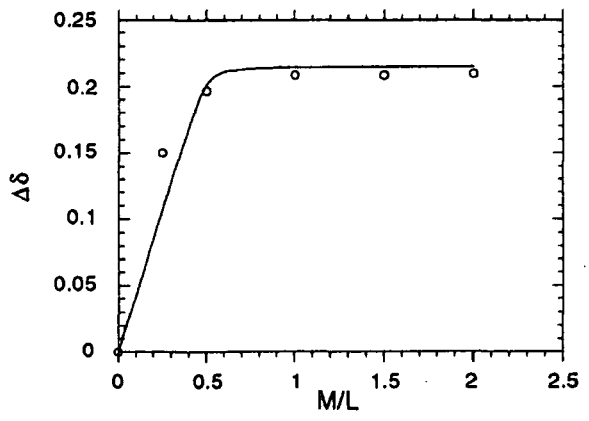

Fig. 2.24 Titration curve of ligand (**66**) and zinc.

Using the N-substituted bisbenzimidazole (**54**) with no carboxylic acid group, addition of zinc triflate gave a different titration curve. In the NMR solvent mixture the methylene resonances were no longer sharp as they were in 100% $CDCl_3$. Instead they were exchange-broadened ($\omega_{1/2}$ = 30Hz) The coordination shift was monitored by observing the major aromatic peak. With increasing M/L ratio and even at M/L ratio of 5:1, there was only a very small shift in the ligand resonances. Plots of $\Delta\delta_H$ vs. M/L gave a shallow curve. Attempts to fit the data to a 1:1 binding stoichiometric analysis gave a poor fit which was predominantly due to the negative deviation observed at low M/L ratios, consistent with the formation of more than one weak complex.

2.3.1.6 Comparison of metal stability constants

There are very few comparable ligands reported in the literature. There is one example of a carboxylic acid substituted imidazole[37] (**82**) which binds with the same chelate ring size as the bisbenzimidazole carboxylic acids (**50**) and (**66**). A direct comparison of the numbers is not meaningful because of the vastly different solvent conditions, but at least the relative order of binding constants between ligands can be compared.

Metal (II)	Bisbenzimidazole dicarboxylic acid (**50**) K_{ML} (a)	N-substituted Bisbenzimidazole (**54**) K_{ML} (a)	Benzimidazole carboxylic acid (**66**) K_{ML_2} (a)	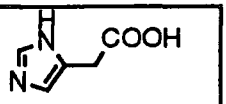 (**82**) K_{ML} (b)	K_{ML_2} (b)
Zn (c)	$>10^5$	0.16	8×10^3	7.9×10^3	1.3×10^6
Cd (d)	$10^4<K>10^5$				
Ni	1.1×10^4		(e)	5.0×10^4	2.0×10^8
Pb	3.4×10^3				
Cu	3×10^2		(e)	1.0×10^7	5×10^{12}

(a) Value determined in 25% CD_3OD/75% $CDCl_3$ at 293K by ^1H NMR.

(b) Value determined in water (0.25M ionic strenght) at 298K.

(c) Not K_{ML} but a sum of K_1 and K_2 (equations 2.4 and 2.8).

(d) Complex equilibria involving at least [ML], [M_2L_2] and triflate ligation (ESMS evidence).

(e) See 2.3.2.7 for qualitative speciation.

Table 2.2 1:1 M/L binding constants

The imidazole (**82**) binds the transition metals with stability constants that follow the Irving-Williams sequence (Cu > Ni > Zn). This is in marked contrast to the behaviour of the bisbenzimidazole dicarboxylic acid (Zn > Ni > Cu). Identical solvent conditions were employed for the benzimidazole ligands and a comparison of the

ligand-zinc binding constants is possible. The stability order was, ligand (**50**) > (**66**) > (**54**). There is a marked difference when no carboxylic acid functionality is present with the K_{ZnL} being very small under these conditions.

2.3.2 Electrospray mass spectrometry studies

Electrospray mass spectrometry is a recent technique which has advantages over other mass spectrometric techniques. The sample is injected at atmospheric pressure and the ionization method of solvent removal under vacuum is intrinsically soft. These factors have made it possible for this technique to be used in accurately assessing the solution speciation of ions[38] and their ligand complexes[39] The stock ligand solution (1.5×10^{-4}M) was prepared in a mixed solvent of 70% methanol, 30% dichloromethane to achieve solubility. To 1 ml of the ligand solution the appropriate amount of wet methanolic metal triflate solution (about 0.2 ml) was added to make a 1:1 metal, ligand ratio. Mass spectra were recorded at a final sample concentration of between 10^{-4} and 10^{-5} mol dm^{-3}, using a 30V cone voltage and 60°C source temperature.

2.3.2.1 Lead

Using a fresh sample of lead triflate with the ligand (**50**) the major observed species was uncomplexed ligand. Species corresponding to [PbL], [PbLTf], [PbLTfH] were observed but were significantly weaker. With an aged wet sample peaks corresponding to [PbL(OH)] and [Pb_2L_2(OH)] were seen.

2.3.2.2 Copper and nickel

Both spectra had peaks at 615, 616 indicating uncomplexed ligand at the concentration tested, however these were not the largest peaks. Species corresponding to [ML], [MLH], [M_2L_2] and [M_2L_2Tf] were observed with many unidentifiable signals. The entire spectrum was weaker (signal to baseline noise) when compared to other spectra at the same concentration. This may be a consequence of the large number of complex species present.

2.3.2.3 Zinc

The peak for uncomplexed ligand was relatively small when compared to the rest of the spectrum. As with other spectra the major peak corresponds to [ML] and [MLH], The second major peak is the dimeric [M_2L_2]. An excellent agreement was observed between the experimental and theoretical isotope patterns for [M_2L_2] (Fig. 2.25). At a higher cone voltage 64V and at a source temperature of 80°C, fragmentation

of this species (benzylic cleavage) gave an intense daughter cluster of peaks centred at *m/z* 1210 (Zn_2L_2- CH_2-p^{t}BuPh) (Fig. 2.26). A further set of peaks at masses 695, 696, 697 were assigned to [$ZnL(OH_2)$]. Five fold dilution of the sample had little effect on the relative intensities of the [ZnL] and [Zn_2L_2] species.

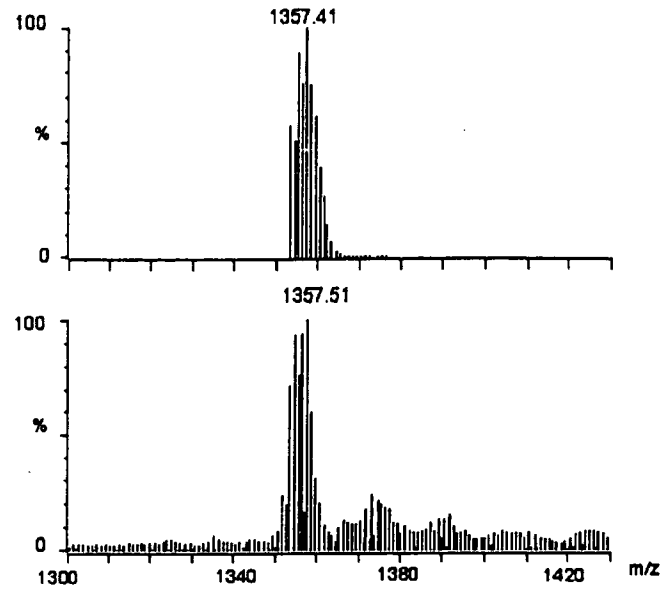

Fig. 2.25 ES MS Spectrum of [Zn_2L_2] with theoretical spectrum above (L=(**50**)).

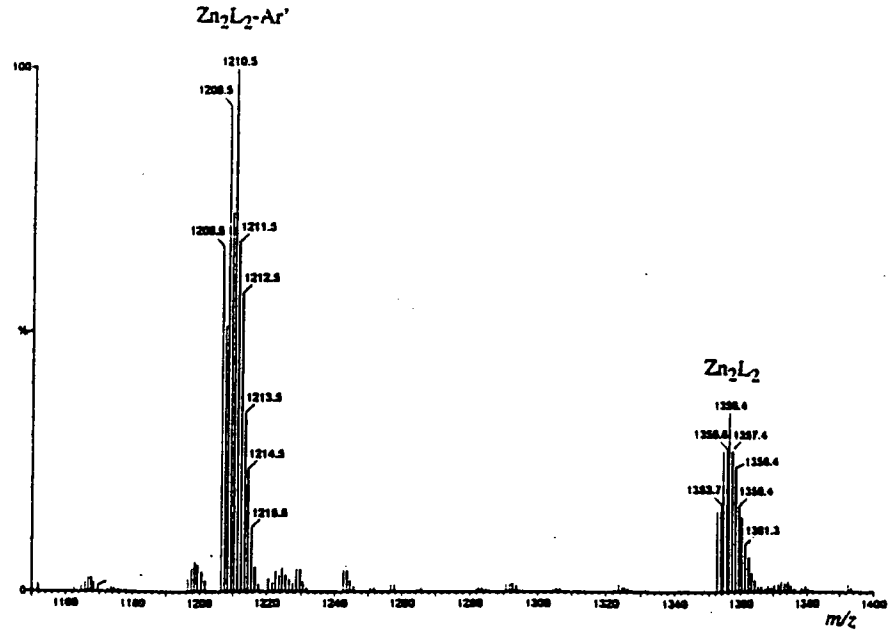

Fig. 2.26 ES MS Spectrum of [Zn_2L_2] (L= (**50**)) showing daughter fragment.

2.3.2.4 Cadmium

As in the ^{1}H NMR analysis, cadmium showed more complex behaviour. Uncomplexed ligand was observed at a higher percentage than with zinc. Species

corresponding to [CdL], [CdLH], [CdLTf] were identified. Dimeric $[Cd_2L_2]$ was seen but with significant amounts of $[Cd_2L_2Tf]$, $[Cd_2L_2Tf_2]$. With a higher Cd/L ratio of 1.5 the spectrum showed higher intensities of the oligomeric species at the expense of the mononuclear complex species and also the generation of a trinuclear $[Cd_3L_3Tf]$ complex (Fig. 2.27).

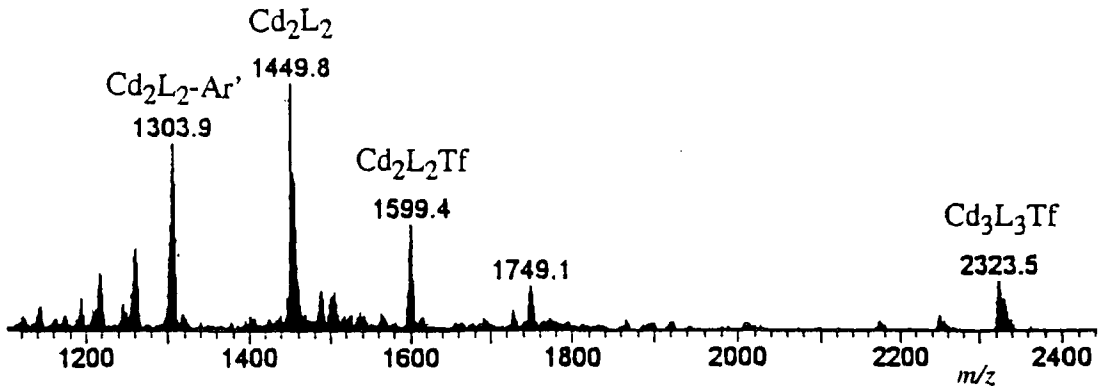

Fig. 2.27 ES MS spectrum of $[Cd_2L_2]$, M/L=1.5 (L = (**50**))

A systematic study of the effect of cone voltage (30-100V) with constant source temperature (60°C) revealed that the mononuclear species was readily broken down to the uncomplexed ligand, while the dimeric species existed throughout the whole voltage range. At voltages above 50V the dimeric species fragmented and daughter ions as a result of benzylic cleavage were observed.

2.3.2.5 Iron

With ferric chloride a single peak corresponding to [FeL] was observed. There was no uncomplexed ligand or species containing more than one ligand.

2.3.2.6 Summary of ES MS peaks observed

The following table (Table 2.3) summarizes the nature of the metal complex species observed. With cadmium and copper there were many peaks corresponding to metal-containing species (as deduced from the isotope pattern) that could not be assigned, these have not been included in the table. This technique illustrates the utility of such studies in pinpointing the solution speciation. In the table the calculated masses have been displayed adjacent to the observed mass to show the close agreement between theory and experiment (error of typically ± 0.4D). For a given pattern the strongest peak was underlined.

complex + ligand (**50**)	observed species	observed mass	calculated mass
Pb	[PbL]	819.3, 820.5, 821.8	818.3, 819.3, 820.3, 821.3
	[PbLTf]	969.5, 970.9, 972.0	969.2, 970.2, 971.2
	(weak)		
	$[Pb_2L_2]$	1638.1, 1639.2, 1640.2,	1638.5, 1639.5, 1640.5,
	(v. weak)	1641.3	1641.5
Ni	{[NiL]	670.6, 671.8, 672.7, 673.6	670.2, 671.2, 672.2, 673.2
	[NiLH]}		671.2, 672.2, 673.2, 674.2
	$[Ni_2L_2]$	1341.5, 1342.5, 1343.4,	1340.4, 1341.4, 1342.4,
		1344.2	1343.4
Cu	[CuLH]	676.2, 677.3, 678.3	676.2, 677.2, 678.2
	$[Cu_2L_2]$	1351.1, 1352.4, 1353.3,	1350.4, 1351.4, 1352.4,
		1354.5	1353.4
Zn	$[Zn_2L_2]$	1354, 1355, 1356, 1357	1354, 1355, 1356, 1357
	{[ZnL]	677.1, 678.1, 679.2, 680.2	676.2, 677.2, 678.2, 680.2
	[ZnLH]}		
Cd	{[CdL]	724.6, 725.9, 727.1, 728.1	724.2, 725.2, 726.2, 727.2
	[CdLH]}		
	$[Cd_2L_2]$	1448.6, 1450.3, 1451.4,	1449.4, 1450.4, 1451.4,
		1452.5	1452.4
	$[Cd_2L_2Tf]$	1599.5, 1600.6, 1601.5	1598.3, 1599.3, 1600.3,
			1601.3
	$[Cd_2L_2Tf_2]$	1748.6, 1749.7, 1750.7,	1747.3, 1748.2, 1749.3,
	(weak)	1751.7	1750.3
	[CdLTf]	874.7, 875.8	873.1, 874.1, 875.1
	(weak)		
Fe	[FeL]	667.7, 668.8	668.2, 669.2

Analysis was performed at, 30V cone voltage, 5V skimmer voltage, 60°C source temperature, sample concentration = 1.5 x10^{-4} M in 30% $CHCl_3$/70% MeOH.

Table 2.3 Major species of ligand (**50**) metal complex observed by ESMS , most intense peak is underlined.

2.3.2.7 Electrospray mass spectrometry studies of the control ligands (54) and (66)

With the bisbenzimidazole without carboxylic acid groups (**54**), only uncomplexed ligand was observed with zinc triflate. The N-substituted benzimidazole

carboxylic acid (**66**) showed different behaviour to the bisbenzimidazole dicarboxylic acid (**50**) (see Table 2.4).

complex + ligand (**66**)	observed species	observed mass	calculated mass
Pb	Ligand		
Ni [(a)]	$[LNi(OH_2)_2]$	400.8, 401.5, 402.6	401.1, 402.1, 403.1
	[LNiTf]	514.7, 515.4, 516.5, 517.4	515.0, 516.0, 517.0, 518.0
	$[L_2Ni\text{-}Ar'H^+]$	527.2, 528.6, 529.5	527.1, 528.1, 529.1
	$\{[L_2NiH_2O]$	690.5, 691.5 692.7, 693.6	(H^+) 691.2, 692.3, 693.2
	$[L_2NiH_3O^+]\}$		
	$[L_2NiTfH]$	822.7, 823.8, 825.0	822.2, 823.2, 824.2, 825.2
Cu [(a)]	$[L_2Cu\text{-}Ar'H^+]$	532.1, 533.6, 534.7	532.1, 533.1, 534.1
	$[L_2CuH^+]$	678.0, 679.8, 680.8	678.2, 679.2, 680.2, 681.2
	$[L_2Cu(H_2O)_2H^+]$	714.0, 715.0, 715.8, 716.7	714.3, 715.3, 716.3, 717.3
	$[L_2CuTfH]$	827.9, 828.9, 830.4	827.2, 828.2, 829.2
Zn [(a)]	$[L_2Zn\text{-}Ar']$	532.6, 533.4, 534.6	532.1, 533.1, 534.1
	$[L_2Zn(H_2O)_2]$	714.8, 715.8, 716.9, 717.7	714.2, 715.3, 716.2, 717.3
	$[L_2ZnTfH^+]$	828.4, 829.4, 830.6	828.2, 829.2, 830.2
Cd	Unidentified	'767.7'	
		'1071'	
Fe	$\{[LFe(OH)_3]$	414.2, 415.4, 416.5	414.1, 415.1, 416.1
	$[LFe(OH)_2H_2O]\}$		
	$[LFeCl_2(OH)]$	449.8, 450.5, 451.6, 452.2	450.0, 451.0, 452.0

(a) Water is being observed as a ligand in contrast to previous ligand (**50**).

Table 2.4 Major metal-ligand (**66**) species observed by ESMS , most intense peak is underlined.

With lead no metal containing species could be identified, only free ligand. Complexation of copper gave rise to strong signals for metal-bound species which were significant in intensity compared to the free ligand signal. Complexes of 2:1 L/M stoichiometry were the most common; $[L_2Cu\text{-}Ar'H^+]$, $[L_2CuH^+]$, $[L_2Cu(H_2O)2H^+]$ and $[L_2CuTfH]$. With nickel the metal-ligand peaks were of much lower intensity, and a large number of species both of 1:1 and 1:2 stoichiometry; $[L_2Ni\text{-}Ar'H^+]$, $\{[L_2NiH_2O]$, $[L_2NiH_3O]\}$, $[L_2NiTfH]$, $[LNi(H_2O)_2]$ and [LNiTf] were identified. With zinc the major species was the uncomplexed ligand, however species corresponding to $[L_2Zn$-

$Ar'H^+$], $[L_2Zn(H_2O)_2]$ and $[L_2ZnTf]$ were identified. No species could be identified corresponding to cadmium complexes even though two sets of peaks centred at 768 and 1071 were observed which by their isotope patterns contained cadmium cations. These were very weak in intensity compared to uncomplexed ligand. With iron (III) chloride and ligand (**66**) the major peaks corresponded to {$[LFe(OH)_3]$ $[LFe(OH)_2H_2O]$} and $[LFeCl_2(OH)]$ with no free ligand present.

The ligand (**66**) follows the Irving-Williams sequence for metal-ligand binding stability, i.e. Ni < Cu > Zn with a preference for the smaller cations over the larger lead and cadmium cations. The more highly charged iron (III) cation bound strongly as expected, but no $[ML_3]$ complex was observed. Preferential binding to chloride or hydroxide occurred. The amount of fragmentation was higher than with the bisbenzimidazole (**50**) at the same cone voltage and source temperature.

2.3.3 Solution FTIR studies with ligand (50)

Solution FTIR spectra were performed in 25% MeOH, 75% $CHCl_3$ using a calcium fluoride solution cell. The carbonyl stretching frequency of the free ligand and its 1:1 metal complexes was observed at the same concentration (8.1×10^{-3}M) to allow direct comparisons. The ligand (**50**) had a stretching frequency of 1734 cm^{-1} consistent with a protonated carboxylic acid. The carbonyl frequency altered depending on the nature of the metal. With zinc the frequency shifted to 1636 cm^{-1}, consistent with metal-bound carboxylate in the major solution $[Zn_2L_2]$ complex. Lead showed a carbonyl stretch at 1657 cm^{-1}, while cadmium gave two carbonyl stretches at 1650 and 1637 cm^{-1}. The lead result is consistent with a free-carboxylate stretch, while cadmium exhibits a mixture of free and metal bound carboxylates. With nickel only a single stretch at 1634 cm^{-1} was measured again showing carboxylate-metal coordination. Copper had a broad less well defined band between 1620-1640 cm^{-1} suggestive of a series of related complexes with varying degrees of carboxylate binding.

Species	ν_{CO} (cm^{-1})
ligand	1734
'ZnL'	1636 (bound carboxylate)
'PbL'	1657 (free carboxylate)
'CdL'	1650 and 1637
'NiL'	1634
'CuL'	1620 - 1640 (broad)

Table 2.5 Infra-red carbonyl stretching frequencies of ligand (**50**) metal complexes.

2.3.4 U.V-visible solution studies with ligand (50)

A ligand (**50**) stock solution (0.001 M) was made up in 25% MeOH, 75% $CHCl_3$. To 3ml of the ligand solution in a quartz cuvette the appropriate amount (typically 0.1 ml) of methanolic metal triflate solution was added (M = Zn, Cd, Pb, Cu, Ni, 0.01M) or methanolic ferric (III) chloride (0.01M), to make a final concentration of 9.1 $x10^{-4}$M. Only the extinction coefficient for the copper complex was accurately determined

$$\lambda_{MAX} = 732.0 \text{ nm} \qquad \varepsilon = 56 \text{ M}^{-1}\text{cm}^{-1}$$

Dilution of the samples (x12.5) with the same solvent enabled the lower wavelength absorption spectra to be recorded. Benzimidazoles possess characteristic absorption spectra in the U.V. region which can be used for their identification, but there are fewer reported examples for bisbenzimidazoles. The relative shapes and shifts could be compared to the free ligand (**50**). The free ligand (**50**) had four major absorption peaks. With lead, cadmium and iron all four absorptions were observable and although their relative intensities had changed, only small shifts had occurred. As there was only a small variation with metal addition it can be assumed that metal ligand coordination was weak at these concentrations.

Ligand		Lead		Cadmium		Iron	
λ (cm^{-1})	ε (M^{-1} cm^{-1})	λ (cm^{-1})	ε (M^{-1} cm^{-1})	λ (cm^{-1})	ε (M^{-1} cm^{-1})	λ (cm^{-1})	ε (M^{-1} cm^{-1})
228	17000	228	24800	228	18400	226	19700
246	13300	shoulder		245	11000	244	14200
302	11200	294	12300	296	14100	302	14800
346	20200	348	18500	346	9950	338	12600

Table 2.6 U.V absorption bands of ligand (**50**) and in the presence of [$PbTf_2$], [$CdTf_2$], [$FeCl_3$].

Ligand		Nickel		Copper		Zinc	
λ (cm^{-1})	ε (M^{-1} cm^{-1})	λ (cm^{-1})	ε (M^{-1} cm^{-1})	λ (cm^{-1})	ε (M^{-1} cm^{-1})	λ (cm^{-1})	ε (M^{-1} cm^{-1})
228	17000	226	16200	226	16800	228	16300
246	13300					shoulder	
302	11200	298	11800	288	16800	304	13700
346	20200	shoulder				shoulder	

Table 2.7 U.V absorption bands of ligand (**50**) and Ni, Cu, Zn metal complexes.

With nickel, copper and zinc there was a substantial change in the absorption spectra. Only two U.V. bands predominate (Table 2.7), the others had greatly reduced extinction coefficients. A greater degree of metal ligand complexation existed.

2.3.5 Aqueous metal extraction studies

^{1}H NMR and ESMS studies had indicated that the bisbenzimidazole dicarboxylic acid ligand (**50**) was able to bind zinc with selectivity over copper, nickel, cadmium and lead. Ideally this ligand would be used for the extraction of zinc into a kerosene based organic medium from an aqueous acidic (below pH 2) metal chloride solution. The more lipophilic dodecylbenzyl-bisbenzimidazole dicarboxylic acid (**81**) ligand was used. Studies were performed to determine at what pH zinc was tranferred from the aqueous to the organic layer and also to test the ligands (**81**) selectivity over iron (III) and copper (II) under these experimental conditions.

2.3.5.1 Zinc extraction isotherm

To achieve reasonable solubility the dodecylbenzyl-bisbenzimidazole dicarboxylic acid (**81**) was dissolved in dichloromethane instead of the preferred kerosene based organic solvent to give an 0.1M solution (15 ml). An equal volume of zinc (II) chloride solution (0.5M) in sulphuric acid (pH 2) was prepared. The two phases were vigorously shaken together for 15 minutes and then allowed to separate. The pH of the upper aqueous layer was measured and equal aliquots of both layers were removed. The acidity of the aqueous layer was varied by adding sodium hydroxide solution and the extraction process repeated. Aliquots were taken over the pH range 0.7 to 5.1. The ligand's solubility was not optimal, as at higher pH phase separation was extremely slow and a third layer between the aqueous and organic layers was observed. The metal content of the organic samples was determined by atomic absorption after decomplexation with a known volume of 1M hydrochloric acid.

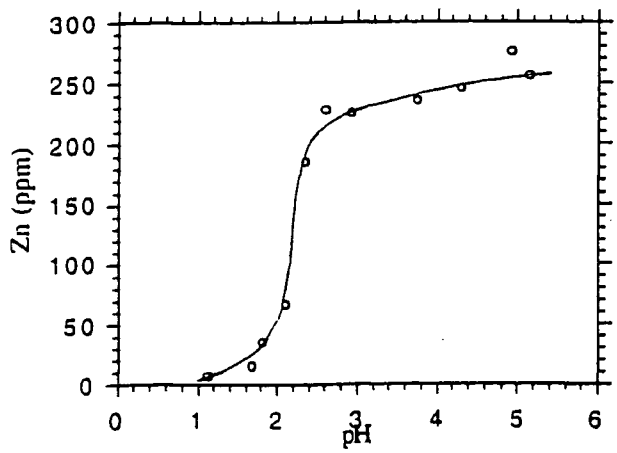

Fig. 2.28 Zinc pH dependent extraction curve with ligand (**81**).

From the extraction curve (Fig. 2.28) the aqueous acidity at which 50% of the maximum amount of zinc was extracted was found to be pH 2.3. This value is defined as the ligand's $pH_{1/2}$ and enables comparisons between extractants to be made.

2.3.5.2 Competitive zinc extraction

In commercial applications other competing cations will be present in the aqueous feed solution. To test the ligand's suitability in extracting zinc selectively, the ligand was exposed to a binary mixture of metal ions (zinc, iron (III) and zinc, copper). An identical procedure as before was followed, except the ligand was in excess over the metals (each metal concentration was 0.025 M).

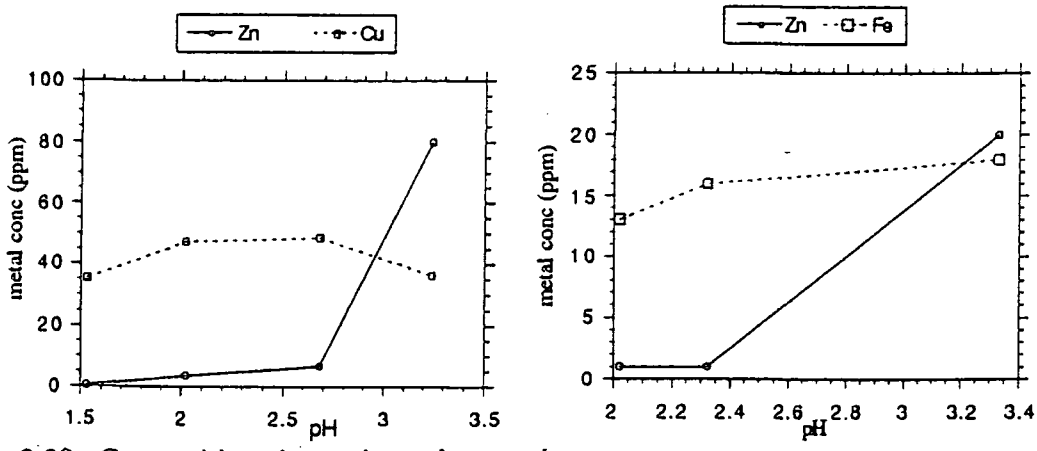

Fig. 2.29 Competitive zinc and metal extraction curves.

The extraction curves indicated there was a virtually constant background of the interferent metal, while zinc uptake was pH dependent. This was either a result of a lower $pH_{1/2}$ for the competing ion so as a result over the pH range measured the interferent metal was always extracted, or the metals were being transported into the organic solvent by a different route (i.e. not via a simple $[M_2L_2]$ complex). Performing the extraction test without the presence of the ligand resulted in no metal transference into the organic layer, hence metal extraction is ligand dependent.

2.4 Summary and conclusion

From comparison between the desired ligand (**50**) and the control ligands (**54**) and (**66**) it can be seen that to achieve the required selectivity the bisbenzimidazole structure was required and not the simple benzimidazole moiety (ESMS and NMR evidence). Indeed the benzimidazole carboxylic acid (**66**) followed the same trend in metal binding (ESMS) as the imidazole carboxylic acid (**82**) i.e. the Irving-Williams sequence Ni (II) < Cu (II) > Zn (II). The higher binding constant was a result of the presence of the carboxylic acids and not just the benzimidazole structure (evidence from Zn ^{1}H NMR titrations).

Considering all the solution studies a number of conclusions can be drawn about the selectivity and stability of metal-bisbenzimidazole dicarboxylate (**50**) complexes. Both proton NMR and ESMS studies indicate that zinc forms a stable 2:2 charge neutral complex, with an overall stability $>10^5$ (^{1}H NMR). The zinc must be tetrahedrally bound involving N(3) and a carboxylate (IR evidence) of two cooperating bisbenzimidazoles (**50**). Copper forms a weaker complex with many species present (ESMS, IR, ^{1}H NMR). An ill-defined 1:1 complex is generated, probably via other metal-ligand bound species such as $[Cu_2L]$ or even [LCuTf] (evidence from poor 1:1 NMR titration analysis). The bisbenzimidazole dicarboxylic acid (**50**) was unable to present a well-defined square planar array of donor atoms to bind copper either as an $[ML_2]$ complex or more importantly [ML] or $[M_2L_2]$ complexes. Nickel (II) is known to bind in a tetrahedral manner in certain complexes. This tendency was manifested in the higher stability constant for a 1:1 stoichiometric complex, as determined by ^{1}H NMR. A number of complexes are in equilibrium (ESMS) which involved carboxylate binding (IR).

Lead represents a simple case, a weak 1:1 complex is formed (NMR) with no carboxylate binding (IR). The complex must have involved only nitrogen coordination with the carboxylates uncoordinated because of the relatively large size of the lead (II) cation. The more favourable interaction between a six-ring chelate and small metal ions (e.g. Zn (II) and Ni(II)) compared to the larger ions such as Pb (II), is now well-defined in coordination chemistry[19]. Cadmium shows a more complicated picture, for which NMR and ESMS indicated that a mixture of mono and dinuclear species e.g. [CdLX], $[Cd_2L_2]$ and $[Cd_2L_2X]$ was present in solution. This is consistent with the observation of the infra-red spectra of bound and free carboxylates. Cadmium (II) can be bound tetrahedrally and this was observed in the formation of $[M_2L_2]$ complexes (ESMS, ^{1}H NMR). The relatively large cationic size (Cd^{2+} 0.78Å, Zn^{2+} 0.60Å, Pb^{2+} 0.98Å for 4 coordinate complexes)[40] resulted in unfavourable strain energy and a reduction in the degree of tetrahedral binding (NMR) and the lower stability constant. Binding to the weakly nucleophilic triflate anion apparantly becomes competitive.

The ligand (**50**) preferred to bind the tetrahedral zinc (II) ion and the observed order of overall complex stability (Zn > Cd > Ni > Pb > Cu) reflects a combination of steric requirements imposed by the ligand and the intrinsic metal ion selectivity resulting from the N,O chelating donors favouring small cations.

Solvent extraction results under the experimental conditions used do not mirror the above trend and there was not a high degree of selectivity for zinc over iron (III) or copper. A direct comparison cannot be made as the solvent conditions were vastly different. The effects of high hydration of both the ligand (**81**) and metal ions, and the presence in solution of more strongly coordinating anions (Cl^-, OH^-, SO_4^{2-}) than triflate are important factors. If the ligand was unable to complex readily via an $[M_2L_2]$ species as a result of low metal-ligand concentration or competitive anion or water coordination

much of the desired zinc selectivity would be lost. The equilibrium defined as K_2 (i.e. 2[ML] going to $[M_2L_2]$ equation 2.8) will be concentration and solvent dependent. ESMS studies had indicated that [LFe] was a predominant complex and this could have been transported into the organic layer as an ion pair (see section 2.1.3).

2.5 Phosphinate or thiophosphinate donor groups

The extraction tests showed that a carboxylic acid is perhaps not the best donor group for selective zinc extraction from an aqueous solution. There are examples of phosphinates[41], thiophosphinates[42] and dithiophosphinates[43] used as hydrometallurgic extractants[44]. The high selectivity shown by the N-substituted bisbenzimidazole (**50**) for zinc was not present for the simple phosphinates. The coupling of the phosphinate group to the bisbenzimidazole should have many advantages over both the individual extractants and the previous carboxylic acid ligand (**50**).

Using an N-functionalized bisbenzimidazole as before but replacing the carboxylic acid with a phosphinate or thiophosphinate donor will still allow a tetrahedral $[M_2L_2]$ structure to form on zinc binding. Phosphinate and thiophosphinate acids have lower pK_a's than carboxylic acids (Table 2.8).

	EtCOOH	$(Et)_2P(O)OH$	$(Et)_2P(O)SH$	$(Et)_2P(S)SH$
pKa	4.67 (a)	3.29 (b)	2.54 (b)	1.71 (b)

(a) reference 37 vol 3 (b) reference 48

Table 2.8 pK_a values of related acids.

This will have an effect of lowering the $pH_{1/2}$ valve to below pH 2.0 (Table 2.9).

	Di(2-ethylhexyl) phosphoric acid	2-ethylhexyl phosphonic acid mono-2-ethylhexyl ester	Di(n-octyl) phosphinic acid	Di(4-dimethyl-2-methylpentyl) thiophosphonic acid
$pH_{1/2}$	1.65 (a)	2.05 (a)	1.95 (a)	1.05 (b)

(a) Ref. 41 (b) Ref. 43

Table 2.9 $pH_{1/2}$ values of selected phosphonate and thiophosphonate extractants.

Using thiophosphinates metal-ligand binding will occur through the 'softer' sulphur and hence intrinsically favour zinc binding over iron (III). Even though the previous ligand had utilized lipophilic N-substitutents, the molecule itself was still strongly dipolar with the charged groups on one end and the 'greasy' chain on the other. The organic solubility was not as good as it should have been, i.e. not kerosene soluble. The poor phase separation at near neutral pH's may also have been a result of this dipolar nature. Phosphinates allow substitution close to the binding centre and with appropriate design, minimal disturbance to the binding geometry. Greater overall lipophilicity can be generated with resultant kerosene solubility and increased phase separation.

2.5.1 Synthesis

Substituted phosphinate esters (**84**) are generally made by an Arbuzov reaction between an electrophilic reagent and a substituted phosphorus (III) diester (**83**) (Fig. 2.30).

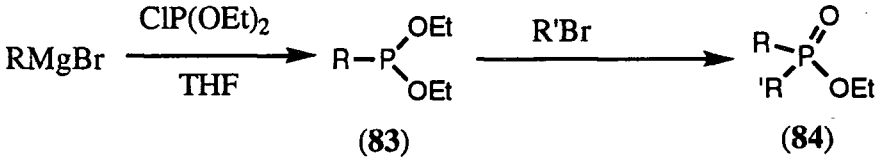

(**83**) (**84**)

Fig. 2.30 Phosphinate ester (**84**) preparation.

Identical methology can be applied to the bisbenzimidazole system. The bromobisbenzimidazole (**74**) was reacted with nBuLi at -78°C in dry THF to produce the lithiate. The lithiate was reacted with diethylchlorophosphonite and then allowed to warm to room temperature. The bisbenzimidazole diethylphosphinite was detected by ^{31}P NMR (product 154ppm). To increase the reaction rate with benzyl bromide the solvent was changed to acetonitrile. Care was taken to exclude oxygen and water during THF removal and acetonitrile addition. Heating the reaction mixture at 60°C resulted in complete reaction after 18 hours as indicated by the disappearance of the P(III) NMR resonance (Fig. 2.31). Chromatographic purification on alumina gave the product as the only bisbenzimidazole-phosphinate species (**85**) with some contamination (<8% by ^{31}P NMR) with other phosphinate species. ^{1}H NMR analysis showed the product was reasonably pure therefore the two close singlets observed in the ^{31}P NMR being consistent with the non-selective formation of RR/SS and RS diastereoisomers. Clean hydrolysis of the phosphinate ester (**85**) proved very difficult. The lipophilic nature of the ester (**85**) meant that for aqueous alkali (NaOH or LiOH) hydrolysis, addition of methanol was required to achieve solubility. There was no ester cleavage at room temperature even after a few weeks. Boiling with 3M hydrochloric acid in 1/2 v/v

water/methanol for 3 days also resulted in no observable hydrolysis (as deduced by ^{31}P and ^{1}H NMR analysis).

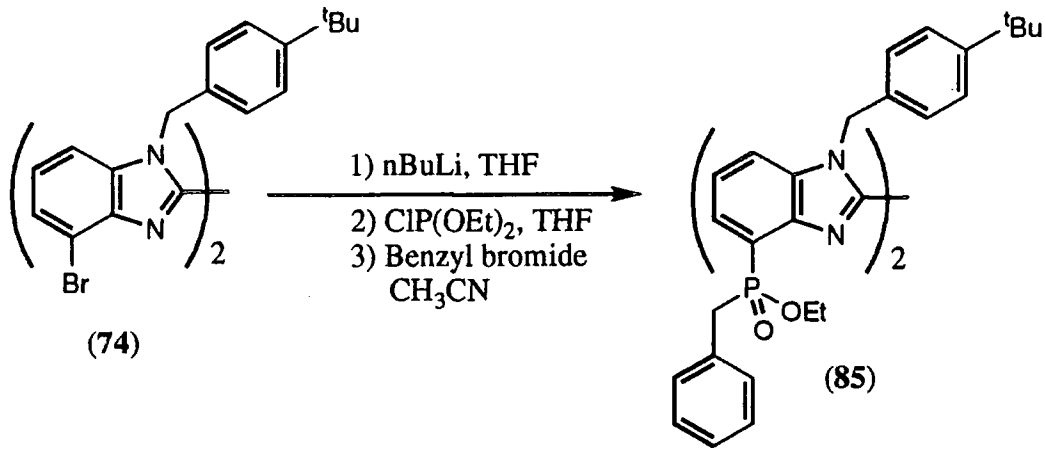

Fig. 2.31 Synthesis of benzyl phosphinate (**85**).

The previous synthesis had shown that a phosphinate group can be added to the bisbenzimidazole. The ideal target should possess a thiophosphinic acid donor. Elemental sulphur will directly add to certain phosphorus (III) species to give a P=S bond. A mixed phosphinite (**87**) was required to add to the bisbenzimidazole lithiate. One equivalent of sodium ethoxide was reacted with dichlorophenyl phosphinite (**86**) in dry THF to produce the mixed phosphinite species (**87**) as the major product (75%) (Fig. 2.32). Purification was not easy: THF was removed under reduced pressure without allowing moisture to enter to give an oily mixture of product and sodium salts. Attempted distillation from the sodium salts resulted in the isolation of dichlorophenyl phosphonite (**86**). The presence of the chloride ions had reversed the reaction on heating. Instead of direct distillation the product was dissolved in dry toluene and filtered through a fine sinter under an inert atmosphere to remove the sodium salts. Concentration and distillation gave the product (**87**) in 80% purity.

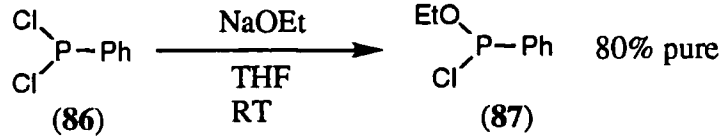

Fig. 2.32 Chloroethylphenyl phosphonite (**87**) via sodium ethoxide nucleophilic attack.

An alternative and synthetically simpler method was found. The equimolar addition of neat dichlorophenyl phosphinite (**86**) and neat diethylphenyl phosphinite (**88**) at 0°C resulted in the clean production of the mixed phosphinite (**87**). The reaction can be envisaged as the exchange of choride and ethoxy groups between phosphorus species in a four membered tranisition state.(Fig. 2.33).

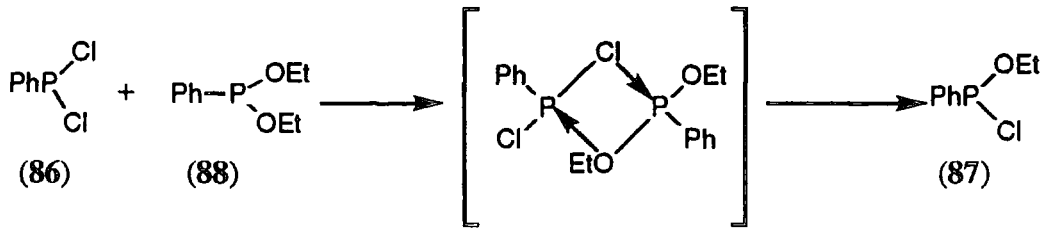

(86) (88) (87)

Fig. 2.33 Chloroethylphenyl phosphonite (**87**) via interchange reaction.

Reaction of the mixed phosphinite (**87**) with the bisbenzimidazole lithiate was performed as before. Without isolating the intermediate, elemental sulphur was added, the reaction was allowed to warm to room temperature and stirred under an argon atmosphere for 15 hours. From ^{1}H NMR analysis there were 2 major bisbenzimidazole species, corresponding to the desired product (**89**) and starting material (**74**).

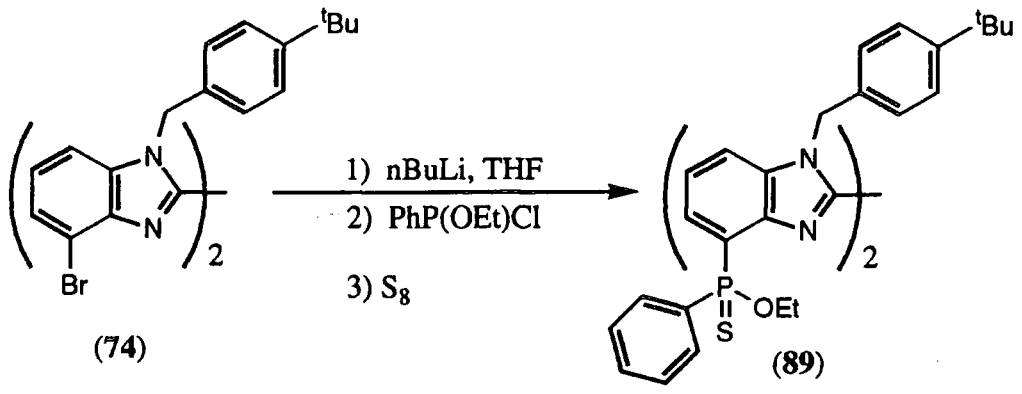

(74) (89)

Fig. 2.34 Preparation of phenylthiophosphinate ester (**89**).

Separation of the product (**89**) from the starting material either by column chromatography or preparative HPLC using normal phase (hexane, propan-2-ol) or reverse phase (water, acetonitrile) conditions was not possible. Formation of the thiophosphonic acid and subsequent separation should have been easier to perform as the two materials would have different polarities. The ester (**89**) could not be hydrolysed using either methanolic aqueous alkali or acid, phase transfer catalysis with dichloromethane and aqueous alkali, or TFA in water. The use of 48% v/v HBr/acetic acid caused degradation of the molecule with the only product identifiable by mass spectroscopy being debenzylated dibromobisbenzimidazole.

Hydrolysis may have been prevented by the steric bulk around the phosphinate ester. Accordingly a less sterically demanding thiophosphonate ester (**91**) was produced (Fig. 2.35). Reaction of the bisbenzimidazole diethylphosphonate (**90**) which was prepared as before with sulphur gave a diethylthiophosphonate ester (**91**). After

extensive chromatographic separation the diethylthiophosphonate ester (**91**) was separated from the starting bromobisbenzimidazole (**74**).

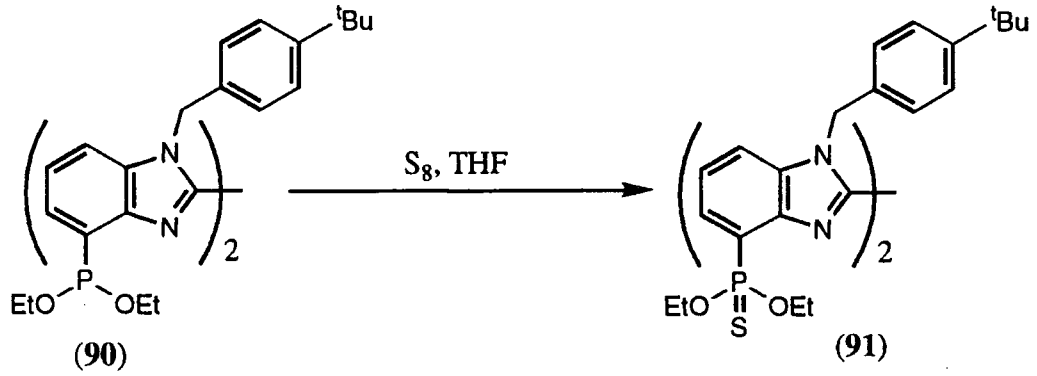

(**90**) (**91**)

Fig. 2.34 Preparation of diethylthiophosphonate ester (**91**).

Hydrolysis of one ethyl group will be easier than the second, so a mono thiophosphonic acid should be generated. However, as before, hydrolysis was not possible. In addition to the described hydrolytic methods, nucleophilic cleavage using sodium thiolate in acetonitrile or toluene also failed. From a detailed search of the literature many of the reported thiophosphinate esters appear to be surprisingly hydrolytically stable. Only activated esters (**92**) (Fig. 2.36) have been hydrolysed using micellar[45] or enzyme[46] catalysed conditions.

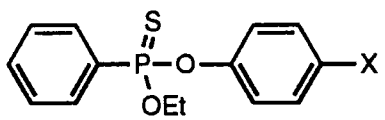

X = CN or NO_2

(**92**)

Fig. 2.36 Activated thiophosphonate ester (**92**).

More recently a diethyl arylphosphonate[47] has been hydrolysed under mild conditions. First the ethyl groups were exchanged with bromotrimethylsiliane to give O-trimethylsilyl groups that were subsquently hydrolysed using an aqueous acetone base mixture at room temperature. This technique was not investigated for the bisbenzimidazole thiophosphonate (**91**).

2.5.2 Binding studies

The unhydrolysed ligand (**91**) should be able to bind zinc cations, either to produce a cationic $[M_2L_2]$ structure or a neutral [ML] complex involving anions. A ^1H NMR titration was performed as before using ligand (**91**) and zinc (II) chloride in the mixed NMR solvent with M/L ratios of 0, 0.5, 1.0, 1.5, 2.0, 3.5, 5. Analysis for a 1:1

complex gave a K_{ZnL} value of 0.42. There was a deviation from the expected 1:1 binding curve (Fig.2.37) suggesting the presence of other complex species.

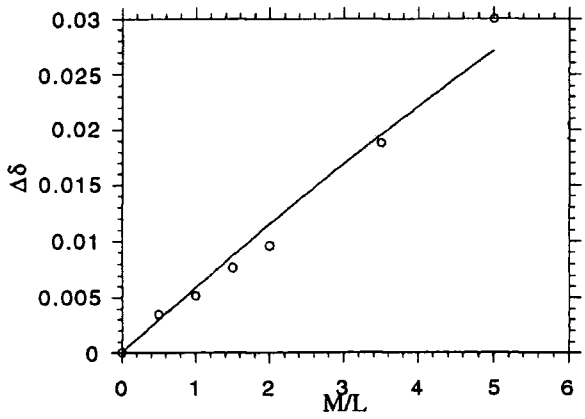

Fig. 2.37 Titration curve of ligand (**91**) and $ZnCl_2$ for 1:1 binding.

The value was slightly higher than for the N-substituted bisbenzimidazole (**54**) (K_{ZnL} = 0.16). However as both values are small and both ligands exhibit significant deviations from 1:1 binding a fair comparison cannot be made. It was apparent that an anionic donor group on the ligand was required to obtain a higher binding constant.

2.5.3 Future synthesis

The major problem in the synthesis of bisbenzimidazole phosphinic or thiophosphonic acids lies with the hydrolysis of the ester. Ideally the acid group should be generated directly and not produced subsequently by the hydrolysis of the ester. The two synthetic routes shown in (Fig. 2.38) may allow the synthesis of the desired thiophosphonic (**94**) and thiophosphinic (**97**) acids.

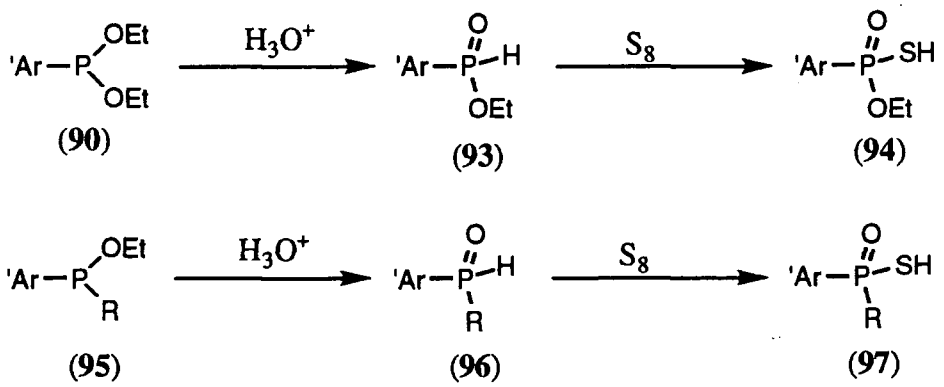

Ar' = bisbenzimidazole

Fig. 2.38 Proposed synthetic routes.

Both of the bisbenzimidazole P (III) compounds (**90**) and (**95**) have been made, and it is known that controlled aqueous hydrolysis of these species will give a P-H containing acid[48]. Direct addition of elemental sulphur should be possible. The P (V) phosphorus species (**93**) and (**96**) will exist in equilibrium with their tautomeric P (III) form e.g. (**98**). This P (III) form would be the species where sulphur insertion could occur (Fig. 2.39).

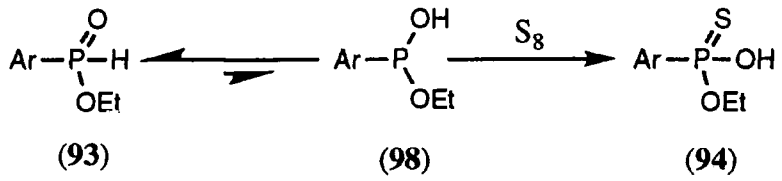

(**93**) (**98**) (**94**)

Fig. 2.39 Phosphorus tautomerism and sulphur addition.

2.6 References

1) M.A. Phillips; *J. Chem. Soc.*, 1928, 2393.

2) F. Hobrecker; *Ber,*. 1872, **5**, 920.

3) P.N. Preston; 'Heterocyclic Compounds, Benzimidazoles and Congeneric Tricyclic Compounds Part 1', John Wiley and Sons, Chichester, 1981 p8 and p211.

4) (i) P.N. Peston, *Chem. Rev.*, 1974, **74**, 279; (ii) M.R. Grimmett; *Int. Rev. Sci. Org. Chem.*, Serl., 1973.

5) P.N. Preston; 'Heterocyclic Compounds, Benzimidazoles and Congeneric Tricyclic Compounds Part 2', John Wiley and Sons, Chichester, 1981 chapter 10.

6) R. Usón, J. Gimeno, J. Formies, F. Martinez, C. Fernandez; *Inorg. Chim. Acta,* 1982, **63**, 91.

7) R. Usón, J. Gimeno, L.A. Oro, J.M. M. de Ilarduya, J.A. Cabezo, A. Tiripicchio, M.T. Camellini; *J. Chem. Soc., Dalton Trans.*, 1983, 1729.

8) M-A. Haga; *Inorg. Chim. Acta,* 1983, **75**, 29.

9) R. Usón, A. Laguna, J.A. Bbad; *J. Organomet. Chem.*, 1983, **246**, 341.

10) R. Usón, L.A. Oro, M.A. Ciriano, M.M. Naval, M.C. Apreda, C. Foces-Foces, F.H. Cuno, S. Garcia-Blanco; *J. Organomet. Chem.*, 1983, **256**, 331.

11) B.F. Fieselmann, D.N. Hendrickson, G.D. Stucky; *Inorg. Chem.*, 1978, **17**, 2078.

12) D. Boinnard, P. Cassoux, V. Petrouleas, J-M. Savariault, J-P. Tuchagues; *Inorg. Chem.*, 1990, **29**, 4114.

13) R. Usón, J. Grimeno; *J. Organomet. Chem.*, 1981, **200**, 173.

14) M.S. Haddad, D.N. Hendrickson; *Inorg. Chem.*, 1978, **17**, 2622.

15) P.A. Tasker; private communication.

16) D.P. Devonald, A.J. Nelson, P.M. Quan, D. Stewart; 'Process for the extraction of metal values and novel metal extractants', Europe Pat. 0196153 B1 (1986).

17) R.F. Dalton, A. Burgess, P.M. Quan; *Hydrometallurgy,* 1992, **30**, 385.

18) (i) J.S. Preston; *Solv. Extr. and Ion Exchange*; 1994, 12, 1; (ii) F. Bergakademie, J. Berger, L. Hinz, W. Charewicz, J. Strzelbricki; Patent DD 258 179 A1 (1987)

19) R.D. Hancock; *Chem. Rev.*, 1989, **89**, 1893.

20) E.S. Lane; *J. Chem. Soc.*, 1953, 2238.

21) C.W. James, J. Kenner, W.V. Stubbings; *J. Chem. Soc.*, 1920, **117**, 775.

22) J.B. Jones, K.E. Taylor; *Can. J. Chem.*, 1977, **55**, 1653.

23) S. Ram, R.E. Ehrenkaufer; *Tetrahedron Lett.*, 1984, **25**, 3415.

24) E.L. Holljes, E.C. Wagner; *J. Org. Chem.*, 1944, **9**, 31.

25) H. Schaefer, K. Gewald; *Z. Chem.*, 1976, **16**, 272. Chem. Abstr. 86:55339y.

26) W. Reid, H. Lohewasser; *Angew. Chem., Int. Ed. Eng*, 1966, **5**, 835.

27) (i) B.A. Tertov, A.V. Koblik, Y.V. Kolodyazhuy; *Tetrahedon Lett.*, 1968, **42**, 4445. (ii) P.W. Alley, D.A. Shirley; *J. Org. Chem.*, 1958, **23**, 1791.

28) G. Holan, E.L. Sammual, B.C. Ennis, R.W. Hinde; *J. Chem. Soc., (C)*, 1967, 20.

29) R.E. Lyle, J.L. LaMattina; *J. Org. Chem.*, 1975, **40**, 438.

30) M. Lemaire, A. Guy, P. Boutin, J.P. Guette; *Synthesis*, 1989, 761.

31) M. Lemaire, A. Guy, J. Roussel, J.P. Guette; *Tetrahedron*, 1987, **43**, 835.

32) H. Franzen, F. Engel; *J. Prakt. Chem.*, 1921, **102**, 187. Chem. Abstr. 1921, 15:3633.

33) C.J. Gibson, J.D.A. Johnson; *J. Chem. Soc.*, 1928, 3092.

34) D.Thorpe, (ZENECA), private communication.

35) L. Collie, J.E. Denness, D. Parker, F. O'Carroll, C. Tachon; *J. Chem. Soc., Perkin Trans. 2*, 1993, 1747.

36) B. Perlmutter-Hayman; *Acc. Chem. Res.*, 1986, 19, 90.

37) A.E. Martell, R.M. Smith; 'Critical Stability Constants Vol 1', Plenun Press, London, 1974, p78.

38) (i) G.T. Agres, G. Horlich; *Appl. Spectrosc.*, 1994, 48, 655; (ii) J.M. Curtis, P.J. Derrick, A. Schell, E. Constantin, R.T. Gallagher, J.R. Chapman; *Org. Mass Spectrom.*, 1992, **27**, 1176.

39) (i) F. Bitsch, C.O. Dietrich-Buchecker, A.K. Khemiss, J-P. Sauvage, A.Van Dorsselaer; *J. Am. Chem. Soc.*, 1991, **113**, 4023; (ii) E. Leise, A. Van Dorsselaer, R. Kramer, J-M. Lehn; *J. Chem. Soc., Chem. Commun*, 1993, 990.

40) R.D. Shannon; *Acta. Cryst. A*, 1976, **32**, 751.

41) N. Miralles, A.M. Sastre, M. Aguilar, M. Cox; *Solv. Extr. and Ion Exch.*, 1992, **10**, 51.

42) F.J. Alguacil, A. Cobo, C. Caravaca; *Hydrometallurgy*, 1992, **31**, 163.

43) S. Wingefors, J. Rydberg; *Acta. Chem. Scand. A*, 1980, **34**, 313.

44) G. Cole, D. Bauer; *Rev. Inorg. Chem.*, 1989, **10**, 121.

45) P.K. Danikhel, Purnanand; *Indian J. Chem., Sect. A*, 1990, **29**, 256.

46) (i) R. Honeycutt, L. Ballantine, H. LeBaron, D. Paulson, V. Seim, C. Ganz, G. Mibol; *Am. Chem. Soc., Symp. Ser.*, 1984, **259**, 343. (ii) W. Steurbaut, W. Dejonckheere, R.H. Kips; *Meded. Fac. Landbowwnet Rijksuniv Gent.*, 1980, **45**, 943; Chem. Abstr. 94: 78413x.

47) T.L. Schull, J.C. Fettinger, D.A. Knight; *J. Chem. Soc., Chem. Commun.*, 1995, 1487.

48) D.E.C. Corbridge;' Studies in inorganic chemistry 10. Phosphorus, an outline of its chemistry, biochemistry and technology', Elsevier, Oxford, 1990.

Chapter Three

Phenanthroline Based Ligands

3.1 Ligand Design

The extraction experiments with bisbenzimidazole carboxylic acids (section 2.3.5, page 64) highlight the intrinsic problem of relying on $[M_2L_2]$ formation. Production of this species is concentration dependent for both metal and ligand. There is a possibility that other metal complex species such as [ML] can occur. To overcome this it would be better to have all the donors in a single molecule. The same ligand requirements as before are needed i.e. complex charge neutrality, high zinc selectivity via tetrahedral coordination and pH dependent complexation and decomplexation.

A '2-2' system (section 1.2.2, page 4) could fulfil the basic requirements (Fig. 3.1).

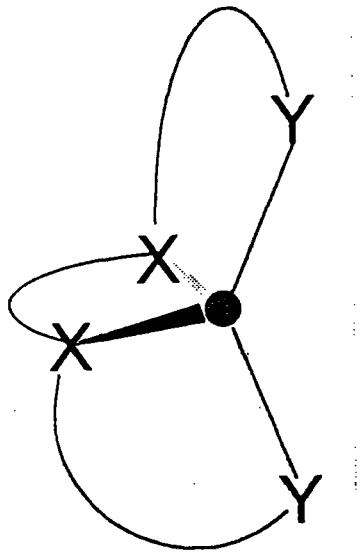

Fig. 3.1 Diagrammatic '2-2' ligand representation.

The two 'X' donors need to be rigidly held together and the pendent arms must be able to bind cooperatively to give the tetrahedral geometry. There should not be too much flexibility in the pendent arms otherwise selectivity and high binding stability may be lost. Using a 1,10-phenanthroline (**2**) as the rigid backbone, the addition of two anionic donor groups allows ligands of this type to be made.

3.1.1 1,10-Phenanthroline as a ligand

Compared to other common bidentate diamine donors such as ethylenediamine (**1**) and 2,2'-bipyridyl (**44**), 1,10-phenanthroline (**2**) has several distinct advantages. In ethylenediamine there is free rotation about the C-C and C-N sigma bonds, whereas in 1,10-phenanthroline nitrogen donors are always held in juxtaposition. Even with 2,2'-dipyridyl (**44**) free rotation about the linkage allows the two nitrogens to be trans disposed (Fig. 3.2). In acidic solutions both nitrogen atoms may be cis orientated and

cooperatively bind a proton, while in non-acidic media they may be trans disposed. As a result there is an entropic advantage associated with 1,10-phenanthroline (**2**) binding.

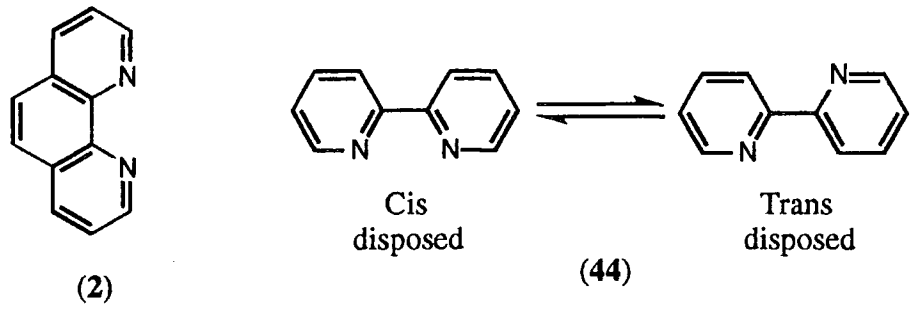

(**2**) (**44**)

Fig. 3.2 Structures of the rigid 1,10-phenanthroline (**2**) and the freely rotating 2,2'-bipyridyl (**44**)

In the last decade the phenanthroline group has been used often in studies of ionic recognition and self-assembling systems[1]. Most of the studies reporting aqueous speciation and metal-ligand stability constants have been concerned with 1,10-phenanthroline (**2**) itself. Simple, 2 and 9 substituted (methyl or chloro) phenanthrolines or more rarely the 4 and 7 substituted phenanthrolines also have been examined[2]. The ability of 1,10-phenanthroline to bind many metals has in the past been exploited in analytical chemistry[3] for example in the production of oxidation and reduction indicators, in the spectrophotometic determination of metals (ferrous and copper ions) and as organic precipitators for anions. 2,9-Substituted-1,10-phenanthrolines (substituted with mostly aliphatic chains) have been investigated as ionophores in lithium ion-selective electrodes[4]. Likewise Chandler has produced a potentiometric sensor e.g. (**99**) based on a phenanthroline[5], (Fig. 3.3).

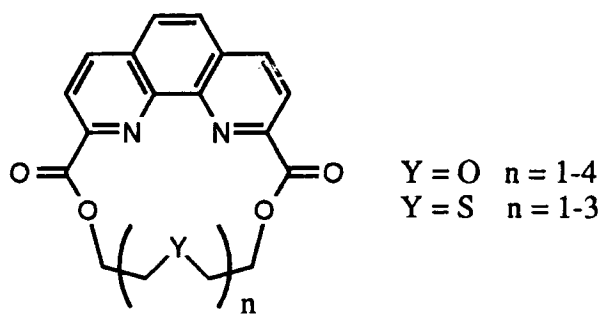

(**99**)

Fig. 3.3 Phenanthroline based potentiometric sensor (**99**).

Substituted phenanthrolines e.g. (**100**) (Fig. 3.4) have been investigated as sensitizing ligands for europium ions[6]. Such complexes may be used as luminescent probes in a variety of diagnostic applications.

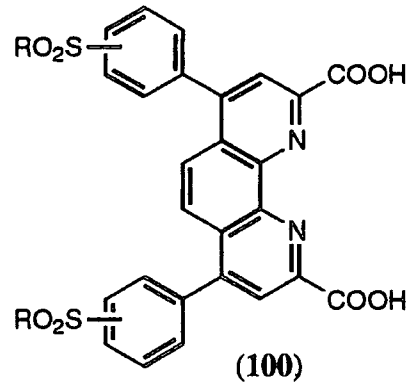

(100)

Fig. 3.4 Phenanthroline based europium ion sensitizing ligand (**100**).

There are many examples of 2,9-substituted phenanthrolines which have been used for general metal coordination chemistry[7]. 2,9-Dimethyl-1,10-phenanthroline (neocuproine) is known to bind copper (I) in a tetrahedral manner in an $[ML_2]$ complex. This effect has been exploited by Sauvage to construct many catenanes and molecular knots using copper (I) templated phenanthroline based cyclizations (section 3.4 for more details). More recently a neocuproine copper (I) complex has been used for sequence-specific scission of DNA[8] and has led to other phenanthroline derivatives being synthesised for this purpose[9]. Chiral phenanthroline zinc and cobalt complexes[10] have also been investigated for use as enzyme mimics.

3.1.2 The desired ligand

Past work[11] had indicated that a 1,10-phenanthroline substituted in the 2 and 9 positions with methylene(methylphosphinate) donors was apparently able to bind zinc selectively over copper and nickel (Fig. 3.5). This would be novel and very interesting.

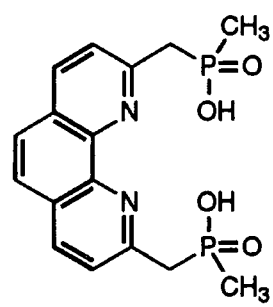

(8)

Metal	Zn	Cu	Ni
$\log K_{ML}$	8.86	4.11	5.39

Determined by aqueous pH titration (298K, H_2O, I = 0.1 Me_4NNO_3) [11]

Fig. 3.5 1,10-Phenanthroline-2,9-bis(methylene(methylphosphinate)) (**8**).

It would be desirable to make other phosphinate derivatives to investigate whether this was a general effect or whether it was specific to this ligand. Knowing the answer will allow further development of the pendent arm or donor group to increase selectivity and examine its extraction potential.

3.2 Synthesis

3.2.1 Synthesis of benzyl (107) and phenyl (108) substituted phosphinic acids

Following a literature method[12] 2,9-bis(bromomethyl)-1,10-phenanthroline (**104**) was synthesised from 2,9-dimethyl-1,10-phenanthroline (**101**) (Fig. 3.6). The first two steps proceeded as reported in high yield. It was essential to filter the dialdehyde (**102**) while it was hot as crystallisation occurred rapidly on cooling. The conversions were probably near quantitative and the lower reported yields are a reflection of material lost in workup and recrystallization.

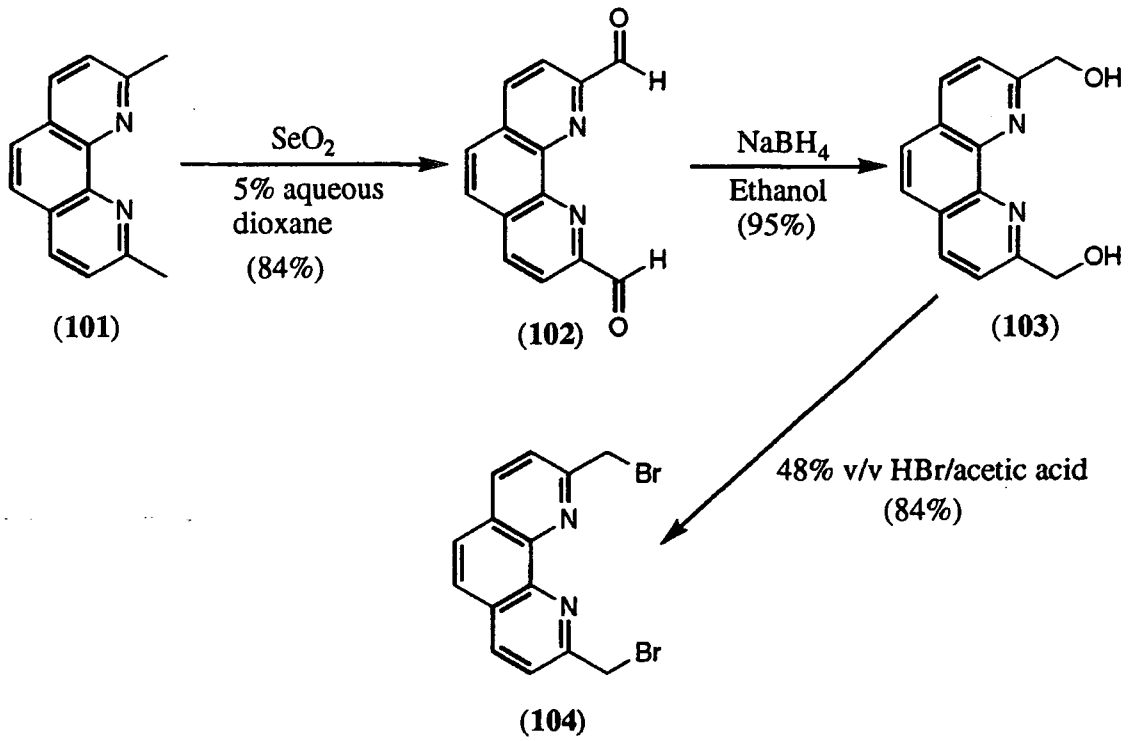

Fig. 3.6 Formation of 2,9-dibromo-1,10-Phenanthroline (**104**).

An improved procedure to form the dibromide (**104**) was performed. Instead of boiling the dialcohol (**103**) in aqueous hydrobromic acid, recovering the material and purifying by column chromatography and recrystallization, 48 % v/v HBr/acetic acid was used at 100°C. The product (**104**) was precipitated as the hydrobromide salt from diethyl ether. The salt was stable and could be stored over many months. Just prior to

use the salt was neutralized with sodium carbonate in water and extracted into chloroform to give the pure dibromo-phenanthroline (**104**)

An Arbuzov reaction between the dibromophenanthroline (**104**) and either diethyl phenylphosphonite or diethylbenzylphosphonite yielded the required phosphinate esters (**106**) and (**105**) respectively, as the major products (by ^{31}P NMR analysis). Purification by column chromatography on neutral alumina using 2% methanol/98% dichloromethane gave the desired compounds (**105**) and (**106**). The high conversion reflected in both the ^{1}H and ^{31}P NMR analysis was not reflected in the isolatable yields. Hydrolysis of the ester may have occurred to some extent on the chromatographic column.

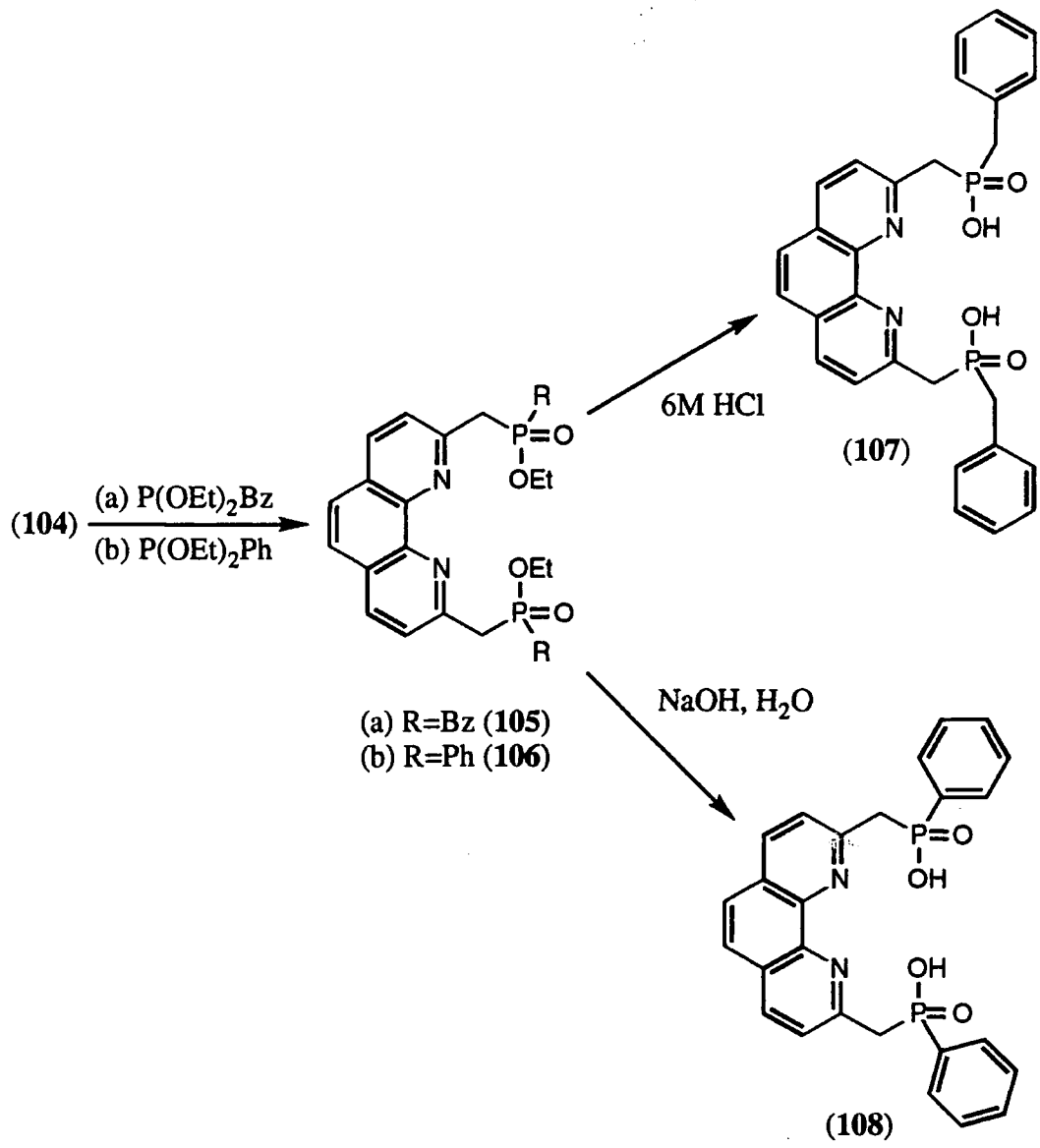

Fig. 3.6 Phosphinic acid (**107**) and (**108**) formation.

Different hydrolysis conditions were required depending on the phosphorus substituent (Fig. 3.6). With the benzyl derivative (**105**), hydrolysis using 6M hydrochloric acid occurred cleanly to give the desired acid (**107**) with one resonance for the acid observed by ^{31}P NMR. Proton NMR analysis in deuteriated methanol indicated

that the phenanthroline methylene protons underwent hydrogen-deuterium exchange. After 18 hours 88% exchange had occurred (by ^1H NMR integration compared to the PCH_2Ph resonance). Performing the ^1H NMR in $CDCl_3$ in the presence of trifluoroacetic acid (0.5%) which was added to aid solubility showed both sets of methylene resonances. Recrystallization of (**107**) from methanol gave the acid as a fine white powder.

Hydrolysis of the phenyl derivative (**106**) under identical conditions resulted in a material whose ^1H NMR suggested a loss of symmetry. This could have been a result of either addition across the phenanthroline 5,6 position or a change in one of the pendent arms, but this was not investigated. Instead, hydrolysis with aqueous sodium hydroxide (at pH 13) was undertaken and this occurred cleanly after 48 hours. The desired acid (**108**) was recovered from the sodium salts by ethanol extraction of the dried, neutralized reaction mixture. Again hydrogen-deuterium exchange of the phenanthroline methylene protons occurred in CD_3OD. This exchange must occur through an enolate intermediate (Fig. 3.7)

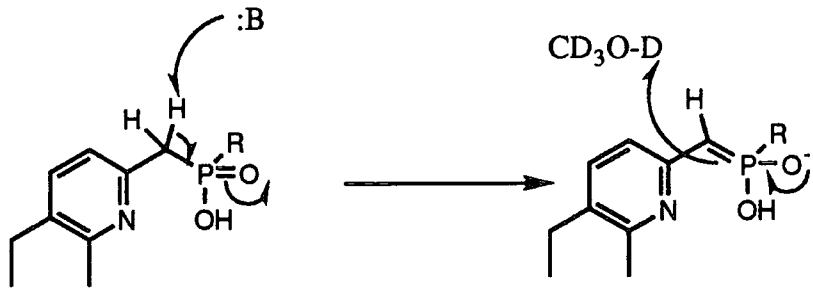

Fig. 3.7 Enolate intermediate and H-D exchange mechanism.

This process was not thoroughly investigated, but from general ^1H NMR observations it appeared the rate of hydrogen-deuterium exchange varied with the P-R substituent on the phosphinate (benzyl faster than phenyl which was quicker than methyl).

3.2.1 Synthesis of methyl substituted phosphinic acid(8)

The same procedure to that reported by E. Cole[11] was followed but the reaction did not give the same results as reported. The required diphosphinate ester was produced in a low yield (2.5% compared to 47%). Two other compounds were recovered; 2,9-dimethyl-1,10-phenathroline (**101**) (yield = 22%) and 2-methyl-1,10-phenanthroline-9-(methylene(methylphosphinic acid)) (**109**) (yield = 9%). These two compounds could have resulted from the breakdown of the dibromophenanthroline (**104**) prior to reaction.

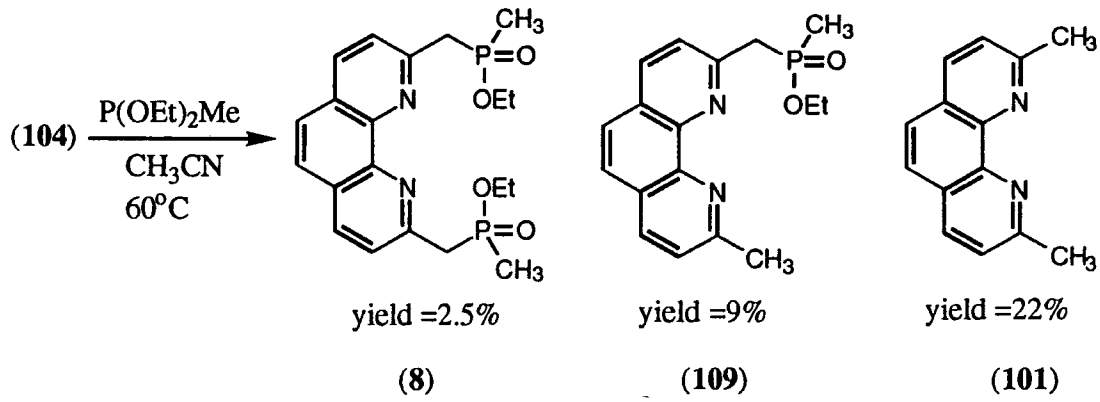

Fig. 3.8 Reaction of the methylphosphonite with the dibromophenanthroline (**104**).

The Arbuvoz reaction takes place by the nucleophilic attack of the diethyl phosphonite at the benzylic bromine, displacing the bromine and forming a P-C bond. The rearrangement then follows (Fig. 3.10). If instead the diethylphosphonite reacts with the benzylic bromine and causes C-Br cleavage a salt can be produced. Any traces of water would react rapidly to form the methyl substituent.

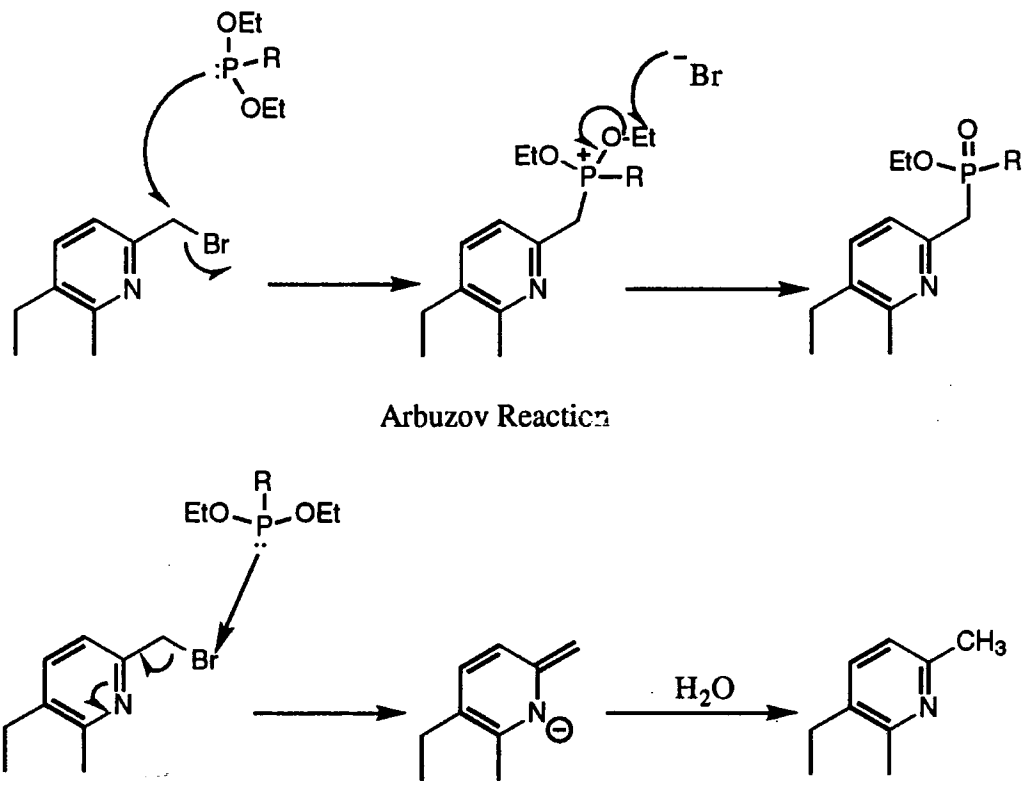

Fig. 3.10 Diethylphosphonite reactions.

There are analogous reactions known for chloro (**111**) and bromo ketones. Triphenylphosphine (**110**) reacts with the halogen to give an enolate which picks up a proton to form the ketone[13] (**112**) (Fig. 3.11).

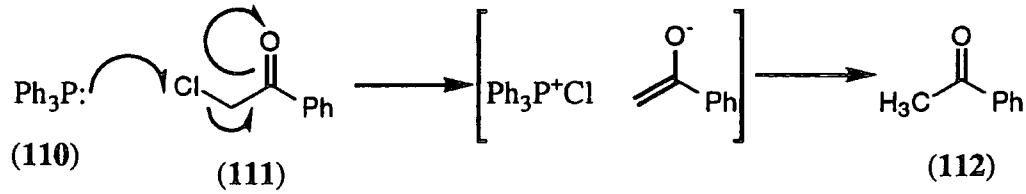

(**110**) (**111**) (**112**)

Fig. 3.11 Known reaction of chloride extraction by a phosphine (**110**).

However Ohta[14] found when attempting to prepare the phosphonium salt of 2-bromoacetophenone, that the addition of a catalytic amount of triethylamine gave a 92% yield of the desired phosphonium salt, whereas in the absence of triethylamine only 3% was formed, with the major product being acetophenone (Fig. 3.12). It was conceivable that the triethylamine was reacting with the 2-bromoacetophenone to provide a better leaving group. A similar situation may be expected with the bromobenzylic phenanthroline, however, this was not tested.

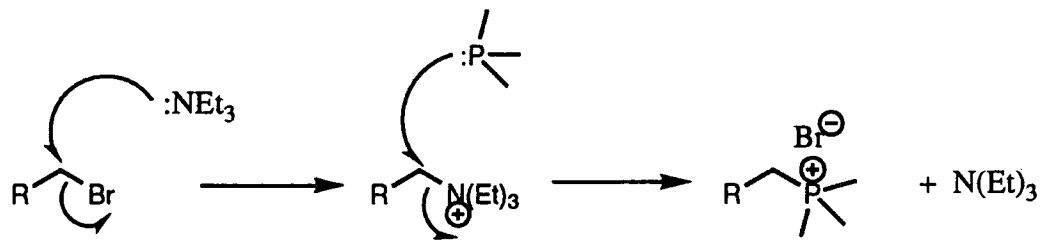

Fig. 3.12 Catalytic use of triethylamine in phosphonium salt production.

3.2.1 Synthesis of lipophilic substituted phosphinates (113) and (114)

For aqueous-organic extraction tests (section 2.3.5, page 64), lipophilic derivatives were required. It was decided to synthesis two lipophilic phosphinic acid derivatives based on phenyl and alkyl groups. (Fig. 3.13).

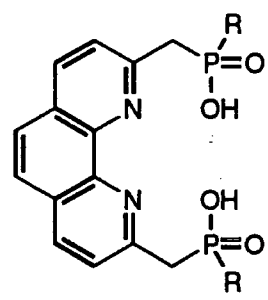

$R = C_{12}H_{25}$ (**113**)
or
$R = -C_6H_4OC_{12}H_{25}$ (**114**)

Fig. 3.13 Lipophilic derivatives (**113**) and (**114**) for extraction tests.

Dodecylmagnesium bromide (**115**) is commercially available, using diethyl ether as the solvent at 0°C the reaction with diethyl chlorophosphonite proceeded in high conversion. The magnesium salts were removed by filtration under an inert atmosphere. Washing the residue with dry benzene and concentration (to remove any volatile species) gave the dodecyldiethylphosphonite (**116**). The thick oil was dissolved in a known volume of dry benzene and the exact concentration of product determined using ^{31}P NMR with diethyl phenylphosphonite as the reference. Both ^{1}H and ^{31}P NMR analysis indicated that the product was about 95% pure.

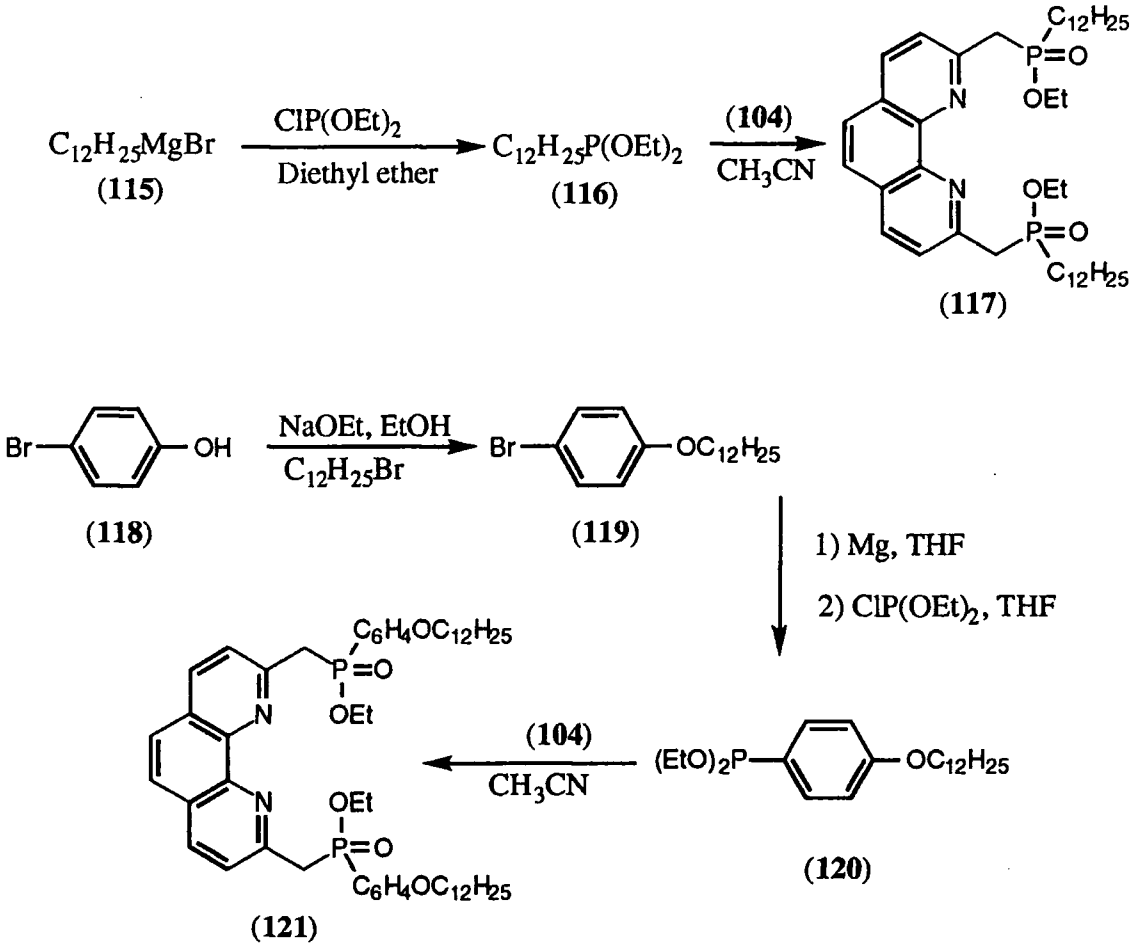

Fig. 3.14 Lipophilic phosphinate esters (**117**) and (**121**) synthesis.

Producing the substituted phenylphosphonite (**120**) was more involved. p-Bromophenol (**118**) was deprotonated in ethanol with sodium ethoxide as the base and then alkylated with dodecylbromide. A high conversion took place and the product (**119**) was recrystallized from 40-60 petroleum ether at -18°C to give colourless crystals. The use of sodium hydride in THF formed the phenolate but alkylation was very slow with less than 5% conversion after two days. Grignard formation needed a high temperature (60°C) to cause initiation after which the exothermic reaction maintained the temperature. Excess magnesium was removed by filtration under an argon atmosphere. Diethylchlorophosphonite reacted rapidly with the Grignard at 5°C.

After the reaction had stopped the solvent was carefully removed under vacuum and dry benzene added. An identical workup procedure as before was followed. ^{31}P NMR analysis indicated only one phosphorus containing species was present, however ^{1}H NMR showed that the material was only 85% pure. The remaining 15% was not unreacted starting material.

Reaction with the dibromophenanthroline (**104**) was performed as outlined previously (section 3.2.1). ^{31}P and ^{1}H NMR analysis of the crude reaction mixture indicated that a reasonable conversion to the desired compounds (**117**) and (**121**) had occurred. However after alumina or silica chromatography only a small fraction of the total material taken to be purified was recovered. Again there was material isolated with a methyl substituent in the 2 position. There was insufficient time for further synthetic investigation especially as it seemed that chromatographic separation was not ideal.

3.3 Metal-ligand complexation analysis

3.3.1 pH Potentiometric titrations

pH Potentiometric titrations enable aqueous protonation and metal-ligand complex constants to be determined, together with the aqueous speciation of the ligand and metal at any given pH (in the pH range 2.5-10.5).

All potentiometric titrations were performed in a water thermostatically temperature controlled cell (approximately $5cm^3$ capacity) and the contents mixed with a magnetic stirrer. A PC program, 'Molspin' was used to collect and store the measured pH readings during the titration and operate the 1ml capacity autotitrator (syringe) containing the base solution. The base used was tetramethylammonium hydroxide (Me_4NOH about 0.05M) in a background of constant ionic strength (I = 0.1 Me_4NNO_3). Both the cation (Me_4N^+) and anion (NO_3^-) will have negligible effect on metal-ligand complexes or ligand protonation constants because they are non-interferent ions (i.e. they tend not to bind). The titrant (base) was delivered to the titration cell through a fine rigid plastic tube which was held in place so it touched the side of the titration cell above the test solution. The tube was not placed in the solution so to avoid the potential problem of titrant diffusion into the test solution. The volume added per increment and the time between additions (which was governed by the pH stability over the pre-sent 'time delay') were controlled by the software and set before the titration. The pH electrode was calibrated using pH buffers of 4.008 and 6.865. The exact base concentration was determined by titrating against a standard hydrochloric acid solution (3ml, 0.01M) at 25°C.

3.3.1 pK_a Determination of the phenyl substituted phosphinic acid (108) derivative

A stock solution of the ligand (**108**) (0.001M, I = 0.1 Me_4NNO_3) was prepared in 'Purite' water which had previously been boiled under a nitrogen atmosphere for thirty minutes to remove any dissolved carbon dioxide. During the preparation of the ligand solution it was necessary to add three equivalents of inorganic acid (hydrochloric acid) to produce a solution of initial acidity between pH 2.5-3.0. Using 3ml of the ligand solution, at 25°C the base was added in increments of 0.0025ml with a preset time-delay of twelve seconds. The titration curve was analysed using two non-linear least squares programs; firstly Superquad and then with the resultant output SCOGS2. Three titrations were performed and analysed to obtain consistent results.

Two pK_a values were determined for 1,10-phenanthroline-2,9-bis(methylene-(phenylphosphinic acid)) (**108**) of 5.93 and 2.7, whereas for the previously reported methyl derivative (**8**)[11] only one was reported. However there was a close agreement between the first protonation constant (Table 3.1). It should be noted that the value of 2.7 does contain a greater error and was at the limit of accurate determination using this method. It is likely that this protonation constant is lower than reported.

	$logK_1$	$logK_2$
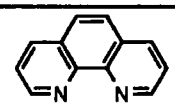 (2)	4.93	1.9
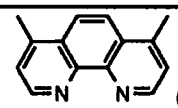 (122)	5.85	-
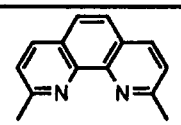 (101)	5.95	-
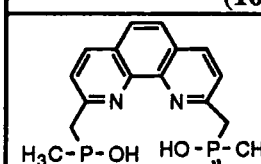 (8)	5.96	-
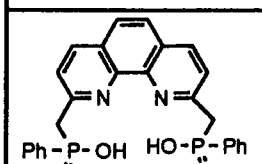 (108)	5.93 (±0.02)	[2.7] (±0.1)

Table 3.1 Protonation constants of phenanthroline based ligands (298K, H_2O, I = 0.1).

The protonation constants of the phosphinic acid substituted phenanthrolines (**8**) and (**108**) can be compared to other phenanthroline based ligands. An electron donating group (e.g. methyl) para (**122**) or meta (**101**) to the phenanthroline nitrogens has an

inductive effect and makes the nitrogen atoms better donors, as a result there is an increase in the protonation constant. A similar increase is observed with the methylene phosphinic acid substituents. There is likely to be an added steric effect, in that the pendent arms make it more difficult for [LH] deprotonation as compared to 1,10-phenanthroline (**2**). The parent 1,10-phenanthroline (**2**) has been quoted to have two protonation constants. This is consistent with the phenyl phosphinic acid substituted phenanthroline (**108**). As there was an increase in $\log K_1$ there was also likely to be a change in $\log K_2$. However there were no such protonation constants quoted for the other phenanthroline ligands suggesting that $\log K_2$ was not observed or not quoted because it was subject to large error.

3.3.1.2 Determination of metal-ligand (Ni and Cu) stability constants

Metal nitrate stock solutions (copper and nickel, 25ml, 0.001M, I = 0.1 Me_4NNO_3) were prepared in Purite water as before. The exact metal concentration was determined by atomic absorption spectroscopy prior to use. The titrations were performed as for the protonation constant determinations, using 3ml of the ligand solution and the appropriate volume of metal solution (about 0.3 ml) were mixed together and titrated with base. The time-delay was increased to 25 seconds to allow equilibrium to be obtained. If it was necessary to use a longer time-delay the top of the titration cell was covered with a layer of lab film that only allowed the electrode and base delivery tube through. This was to prevent excessive solvent evaporation and carbon dioxide absorption. Using the determined protonation constants, metal-ligand complex stability constants were determined using Superquad and then SCOGS2.

During analysis of the copper and nickel titration curves it was found necessary to omit the second protonation constant and points below pH 3.2 to obtain metal-ligand stability constants. This would indicate that there was an error in pK_2. Both metals analysed for the formation of an [ML] and an [ML_2] species, even though care was taken to try to obtain a 1:1 metal-ligand stoichiometry.

3.3.1.3 Zinc-ligand complex stability determination

For the zinc titration in 100% aqueous solution, there was a rapid precipitation of a zinc-ligand complex on zinc addition to the ligand. To obtain a stability constant the complex needs to be in solution. It was found that in 30% methanol/70% water the complex remained soluble, at the concentrations involved in this experiment. This relatively small percentage of methanol should only have a minimal effect on the stability constant as compared to the 100% aqueous values.

The electrode was calibrated in aqueous buffer solution as before. The base solution (about 0.05M, I = 0.1 Me_4NNO_3) was prepared in the new solvent conditions

(30% methanol/70% water) and calibrated by titrating against standard hydrochloric acid in the same solvent. Ligand and zinc nitrate solutions were prepared as before but in the new solvent conditions. Ligand and ligand-zinc titrations were performed. Before the titration curves could be analysed a correction factor[15] (subtraction of 0.0314) was applied to all the measured pH titration points. This was to compensate for the different solvent conditions between electrode calibration and pH measurement during titration. In the analysis the pK_w constant[16] for water was set at 14.055 and ligand protonation and zinc-ligand stability constants were determined as before. To enable a better analysis of the lower part of the titration curve the value of pK_2 was lowered to that of 1,10-phenanthroline (**2**). This should not strictly be performed in a metal-ligand titration. In this case it was believed to be justified, its absence resulted in the lower pH values not being used in the analysis and its present value ($logK_2 = 2.8$) appeared too large during zinc-ligand analysis.

3.3.1.4 Comparison of protonation and metal-ligand stability constants

The measured protonation constants in the two solvent mixtures were very similar in value (Table 3.2). As expected the methanol is having little influence. In both solvent compositions the second protonation constant was subject to the greatest error.

Solvent	$logK_1$	$logK_2$
100% H_2O	5.93 ±0.02	2.7 ±0.1
70% MeOH 30% H_2O	5.92 ±0.02	2.8 ±0.1

Table 3.2 Protonation constants of ligand (**108**) (298K, I = 0.1 Me_4NNO_3)

As with copper and nickel, the zinc titration curve also analysed for an [ML] and [ML_2] species. The values indicate that this ligand forms both [ML] and [ML_2] complexes which follow the Irving-Williams sequence of stability (Table 3.3)

	$logK_{ML}$	$logK_{ML_2}$
nickel	6.24 ±0.01	3.9 ±0.09
copper	6.95 ±0.05	4.22 ±0.02
zinc	6.64 ±0.02	3.97 ±0.03

Table 3.3 Metal-ligand (**108**) complex stability constants (298K, I = 0.1 Me_4NNO_3)

The presence of an [ML_2] species for all three metals indicates that the phosphinic acid group was behaving as a poor donor and there was competitive binding to a second phenanthroline group to produce an N_4 donor set. All the metal-ligand

stability constants are of similar magnitude and this can be observed if the titration curves are compared (Fig. 3.15)

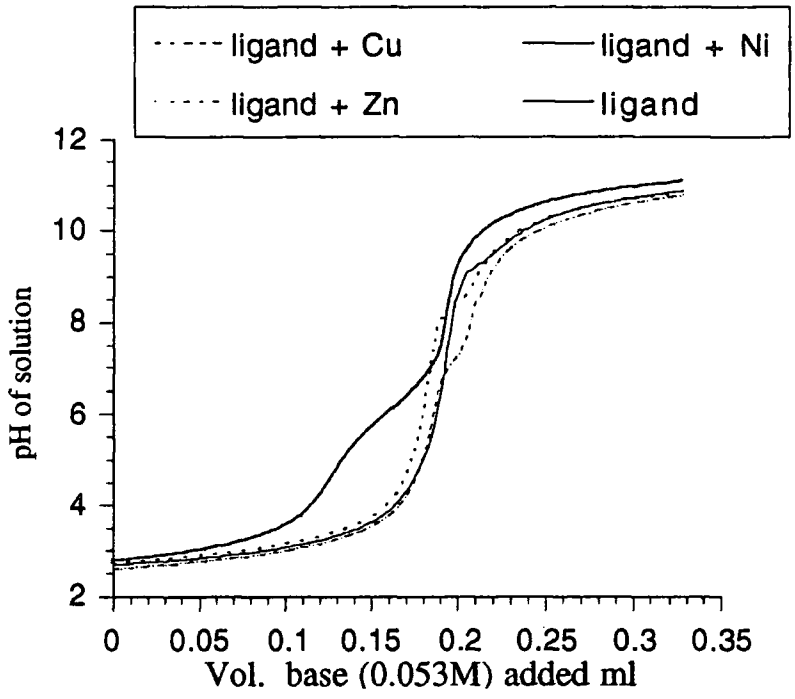

Fig. 3.15 Titration curves of phenanthroline ligand (**108**) and metals (Ni, Cu, Zn).

Allowing for the error in the initial acidity between the solutions and the slight variation in amount of metal added all three titration curves appear very similar. The [ML] complex was formed at low pH values (i.e. the plateau region of pH 2.7 to 3.4). the 'step' that can be observed after the initial vertical portion probably corresponds to deprotonation of bound water molecules (i.e. Eqn. 3.1). It was not possible to analyse this behaviour accurately.

$$\text{Eqn. (3.1)} \quad LM(H_2O)_x + OH^- \underset{}{\overset{K_a}{\rightleftharpoons}} LM(OH)(H_2O)_{x-1} + H_2O$$

The low protonation constant and comparatively large metal-ligand complex stabilities make analysis of the entire titration curve difficult. At the starting acidity (pH 2.7) there was already significant amount of metal-ligand complex (about 50%). Ideally a lower initial pH should be used so [ML] formation can be analysed rather than its conversion to other species. However there would then be errors in the pH measured as a result of pH electrode acid errors.

It is known that 2,9-dimethyl substituted phenanthroline will produce [ML_2] species with comparatively high values (Table 3.4). The phosphinic acid groups can readily rotate out of the binding plane to allow two phenanthroline units to bind.

	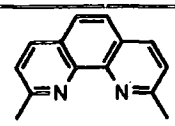 (101)	
	$\log K_{ML}$	$\log K_{ML_2}$
Nickel	5.0	3.5
Copper	5.2	5.8
Zinc	4.1	3.6

Table 3.4 Metal-ligand (**101**) complex stability constants (298K, H_2O, I = 0.1)[2]

3.3.1.5 Comparison of phenanthroline phosphinic acid ligands (8) and (108)

A comparison of the stability constants of the two phenanthroline phosphinic acid derivatives (**8**) and (**108**) shows that there is an inconsistency between the values (Table 3.5)

		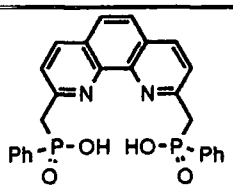 (108)	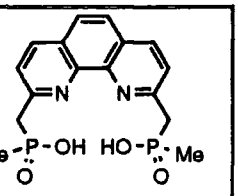 (8)
nickel (II)	$\log K_{ML}$	6.24	5.39 [a]
	$\log K_{ML_2}$	3.9	n.d
copper (II)	$\log K_{ML}$	6.95	4.11 [a]
	$\log K_{ML_2}$	4.22	n.d.
zinc (II)	$\log K_{ML}$	6.6 [b]	8.86 [a]
	$\log K_{ML_2}$	4.0 [b]	4.67 [a]

(a) Reference 11
(b) Solvent conditions 30% v/v methanol/water

Table 3.5 Metal-ligand stability constants of phenanthroline phosphinic acid ligands (**8**) and (**108**) (298K, I = 0.1 Me_4NNO_3).

The methyl derivative (**8**) appeared to show a high selectivity over copper, but this feature was not reproduced with the phenyl derivative (**108**). The methyl derivative (**8**) zinc titration was repeated, and reproducible data were obtained. However, data analysis proved to be exceedingly difficult and no values could be determined. On re-examination of the original titration data of the methyl derivative (**8**) with copper it was found that the titration curve was similar in shape to those obtained with nickel and zinc and the data had only been analysed in the higher pH region (> 5.5). This was likely to be outside the main region for [ML] formation and hence there is the possibility of larger errors on the quoted value.

The substituent on the phosphorus will have a direct effect on the donor character of the oxygen donor. It is possible there is a slight difference between the stability constants of the ligand-metal complexes, but probably not as large as those originally suggested. Comparison with other phosphinic acid substituted amine ligands is important to see if there are any definite trends.

3.3.1.6 Disubstituted phosphinic {-PR(O)OH} and phosphonic {-PH(O)OH} acid ethylenediamine ligands

Ethylenediamine ligands with methylene-phenyl (**126**) and methyl (**124, 125**) substituted phosphinic acids and methylenephosphonic (**122, 123**) groups have been produced and studied with nickel, copper and zinc (Table 3.6).

	Ni (II) log K_{ML}	Cu (II) log K_{ML}	Zn (II) log K_{ML}
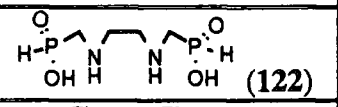 (122)	7.52 (a)	10.72 (a)	6.16 (a)
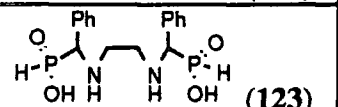 (123)	6.17 (a)	10.10 (a)	5.52 (a)
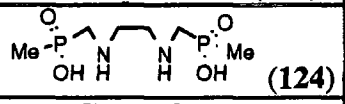 (124)	8.34 (b)	8.03 (b)	n.d
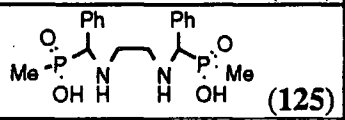 (125)	6.91(a)	10.32 (a)	n.d
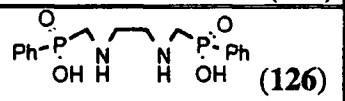 (126)	8.13 (b)	6.56 (b)	7.03 (c) $\log K_{ML_2}$ 5.1(c)

(a) Reference 2
(b) Reference 11
(c) This work solvent conditions 30% v/v methanol/water

Table 3.6 Metal-ligand stability constants of ethylenediamine phosphinates (298K, I = 0.1).

Firm trends concerning the variation of the phosphorus substituent cannot be drawn from the tabulated values. Replacing the PH group (**122, 123**) with either PMe (**124, 125**) or PPh (**126**) tends to increase the nickel and zinc complex stability constants but each has little or no effect on copper complex stability. Phenyl substitution of the methylene group (**123, 125**) slightly destabilizes the complexes and lowers the stability constants. Of greater importance is the fact that all the stability constants are of similar magnitude and therefore no particularly enhanced values over those of the parent ethylenediamine (**1**) or the N,N'-diethyl substituted ethylenediamine (**127**) (Table 3.7).

	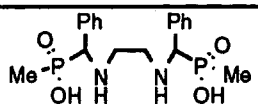 (125)	 (127)	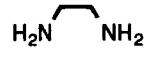 (1)
Copper $\log K_{CuL}$	10.10 (a)	8.85 (a)	10.50 (a)
$\log K_{CuL_2}$	n.d.	5.75 (a)	9.1 (a)
	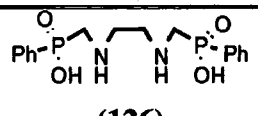 (126)		
Zinc $\log K_{ZnL}$	7.03 (c)	5.47 (b)	5.7 (a)
$\log K_{ZnL_2}$	5.1 (c)	3.53 (b)	5.1 (a)

(a) 298K, H_2O, I = 0.1 Reference 2
(b) 298K, H_2O, I = 0.48 Reference 2
(c) 298K, H_2O, I = 0.1 This work

Table 3.7 Stability constants of copper and zinc [ML] and $]ML_2]$ complexes with ethylenedimaine based ligands **(125)**, **(127)**, **(126)** and **(1)**.

Having two non-coordinating ethyl substituents on the parent ethylenediamine (**1**) decreases the metal complex stability constant with respect to the parent ethylenediamine (**1**), probably as a result of an increase in unfavourable steric interactions. with the phosphinate donor group there is not a substantial decrease hence they must be coordinating to a certain extent. Binding to copper and zinc is different, Comparing to the parent ethylenediamine there is a small decrease in $\log K_{CuL}$ with copper and a slight increase in $\log K_{ZnL}$ with zinc. The value obtained for $\log K_{ZnL_2}$ with L = **(126)** is consistent with what can be expected when compared to the same complex stabilities with 1,2-diethylethylenediamine (**127**) and the parent ethylenediamine (**1**) ($\log K_{ZnL_2}$ = 3.53 and 5.1 respectively).

Other ethylenediamine substituted ligands with carboxylic or phenol groups give much larger metal-ligand binding constants (Table 3.8).

	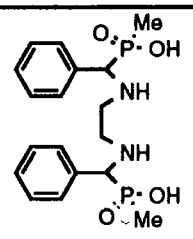 (125)	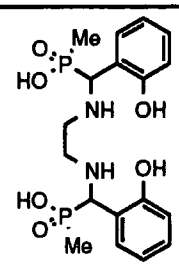 (128)	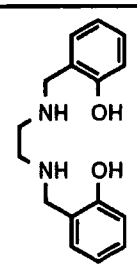 (9)	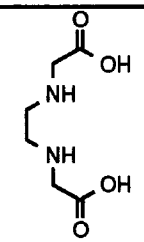 (129)
Cu (II)	10.10	20.14	20.5	16.2
Zn (II)	n.d.	n.d.	11.97	11.22

Table 3.8 Stability constants for [ML] complexes (298K, H_2O, I = 0.1)[2]

From the observed copper complex stability constant of the ligand with both a phenolate and a phosphinate donor (**128**) it would appear that binding was occurring through the phenolate. This suggests that the phosphinate group is a particularly poor donor for copper (II) but is slightly better for zinc.

3.3.2 Phosphorus-31 NMR analysis

The sequential addition of zinc (II) triflate to an aqueous (D_2O, pD = 8.5) sample of 1,10-phenanthroline-2,9-bis(methylene(methylphosphinic acid)) (**8**) saw the appearance of a second singlet resonance in the ^{31}P NMR (uncomplexed ligand δ_P = 40.72 ppm, metal-ligand complex δ_P = 42.51ppm at M/L=0.25). This corresponds to a zinc-ligand complex in slow exchange with uncomplexed ligand and zinc on the NMR time-scale (i.e. $\log K_{ZnL} > 5$). The proportion of this complex increased proportionately with the amount of zinc triflate added. There was an associated slight shift to higher ppm without significant line-broadening. At M/L ratios of greater than unity only one signal was observed. A similar experiment using the phenyl derivative (**108**) could not be performed. At the NMR sample concentration (0.02M in 30% CD_3OD, D_2O) there was a rapid precipitation of the 1:1 zinc complex when zinc triflate was added to the ligand solution.

The experiment with the methyl derivative (**8**) was repeated with copper (II) triflate. On incremental addition there was no observable generation of a second signal. The observable signal showed line-broadening with increasing metal/ligand ratio (298K, 101MHz, M/L = 0.25 $\omega_{1/2}$ = 28Hz, M/L = 0.75 $\omega_{1/2}$ = 74Hz). A decrease in the signal to noise ratio also occurred, so at M/L = 1 there was no observable resonance. The absence of a second resonance does not necessarily indicate that the complex stability was lower than 10^5 (i.e. $\log K_{CuL} < 5$). It is possible that the observed signal was uncomplexed ligand being exchange broadened by small amounts of copper, while the resonance due to the copper-ligand complex was paramagnetically broadened and was not observed. On standing, a micro-crystalline material formed. Attempted recrystallization did not result in large enough crystals for X-ray crystallography.

The ^{31}P NMR results confirm that the pH potentiometrically determined $\log K_{ZnL}$ was greater than five. As the resonance was not sharp ($\omega_{1/2}$ = 30Hz, 298K, 101MHz) an exchange with other species may also be occurring (such as $[ML_2]$).

3.3.3 Solid metal-ligand complex formation and analysis

Molecular modelling of the diphosphinic acid substituted phenanthrolines indicated that the metal would bind in a geometry between that of square planar and tetrahedral (Fig. 3.16). To test if this was correct single crystals would be required for solid state structure determination by X-ray crystallography.

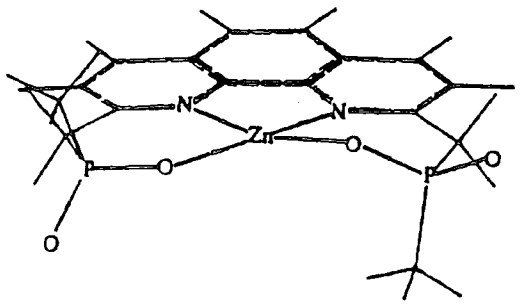

Fig. 3.16 Molecular model of methyl derivative (**8**) and zinc.

The addition of zinc perchlorate solution to either an aqueous or methanolic solution of 1,10-phenanthroline-2,9-bis(methylene(benzylphosphinic acid)) (**107**) (7.8 x 10^{-3} moldm^{-3}) resulted in a rapid precipitation of a white solid. The complex was recovered by centrifugation, washed with methanol and vacuum dried. Combustion analysis indicated that the solid was not a simple [ML] complex. There was possible the presence of a counter anion (i.e. $LZnHClO_4$). Recrystallization was not possible because no solvent could be found to dissolve the complex. To examine whether a counter ion was involved complexes were formed from a range of zinc salts ($ZnCl_2$, $Zn(OAc)_2$, $Zn(CF_3SO_3)_2$). Again there was a rapid precipitation from methanol. Combustion analysis and atomic absorption spectroscopy gave similar carbon, nitrogen, hydrogen and zinc ratios regardless of the anion used. This would suggest a counter ion is not involved. Combustion analysis was not consistent even if non-stoichiometric amounts of water were present. The zinc analysis gave a value that was more than expected for an [ML] complex. Solid state FTIR analysis gave near identical spectra for all the samples. On close examination there did appear to be small amounts of the anion present (e.g. complex from zinc acetate Fig. 3.17). The broad band at 3420cm^{-1} indicated water was involved in the complex. A fully spectral interpretation was not performed. It is likely that a definite solid complex formula cannot be determined because water is present together with trapped non-stoichiometric amounts of the zinc salt used as a result of the rapid complex precipitation. Repeating the experiment with copper perchlorate resulted in rapid precipitation of a green complex. Again an exact elemental formula could not be determined. Leaving the mother liquor resulted in a more crystalline solid forming, but of insufficient quality for X-ray crystallographic analysis. The addition of nickel perchlorate did not result in any significant precipitation. Further investigation with this ligand (**107**) or its solid complexes was not carried out because of the solubility problems.

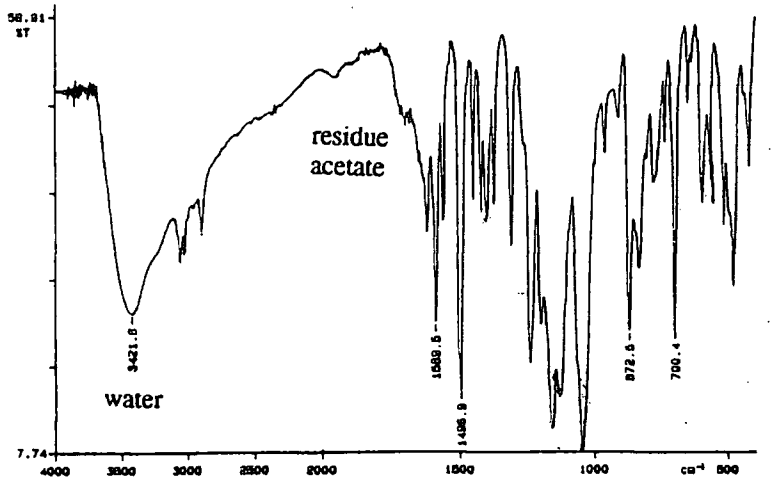

Fig. 3.17 FTIR spectrum of solid complex of (**107**) and zinc acetate.

Using 1,10-phenanthroline-2,9-bis(methylene(phenylphosphinic acid)) (**108**) in either water or methanol gave solid complexes on the addition of copper, zinc and cadmium salts (perchlorate and chloride). Precipitation was slower than with the previous ligand (**107**). Combustion analysis and metal percentage determination indicated that hydrated metal-ligand complexes were formed for zinc and cadmium (Table 3.9), while for copper this was less clear. FTIR Studies supported the elemental analysis results.

	$LZn(H_2O)_{1/2}$		$LCd(H_2O)_{1/2}$	
	Experimental percentages	Calculated percentages	Experimental percentages	Calculated percentages
C	55.49	55.33	51.14	51.38
H	3.76	3.96	3.50	3.48
N	4.98	4.87	4.61	4.61
Metal	11.82	11.62	18.43	18.49

Table 3.9 Elemental analysis of solid state complexes of phenyl derivative (**108**) with zinc and cadmium.

For the methyl derivative (**8**) no solid was produced when zinc perchlorate was added. On slow evaporation no crystalline material was produced.

The immediate precipitation from water when the metal cations are added would suggest that a neutral species were produced. The insolubility was a function of the phosphorus substituent, the more lipophilic the substituent (e.g. benzyl) the more insoluble the complex. With the complexes involving the benzyl derivative (**107**) the lack of solubility in any solvent may suggest an oligomeric type structure.

3.3.4 Electrospray mass spectrometry analysis

ES Mass spectrometry studies using the three phenanthroline diphosphinic acid derivatives (**8**), (**107**) and (**108**) were performed, as outlined in section 2.3.2 (page 57). As a general observation, all three ligands behaved very similarly. The results for the phenyl (**108**) derivative will be discussed and any differences to the benzyl (**107**) or methyl (**8**) derivatives will be noted.

The spectrum of the ligand (**108**) appeared more complicated than expected, with many closely related peaks being observed. The major species were sodium and potassium mono-cationic species such as $[LNa_3^+]$ and $[LNa_2K^+]$ (L is the dianion of (**108**)). Hydrated species were also seen. These alkali metal cations are likely to have been present as the ligand (**108**) was isolated as the sodium salt. However the same feature was seen for the methyl (**8**) and benzyl (**107**) derivatives which were isolated in their protonated forms. The cations must be coming from the surrounding solvent probably from the glassware[17]. The addition of trifluoroacetic acid to the ligand solution resulted in $[LH_3^+]$ species being seen.

3.3.4.1 Copper, nickel and zinc

The results for copper, nickel and zinc addition to the phenyl derivative (**108**) were all very similar. The major species observed were [MLNa] complexes. Copper gave the strongest peak, while for nickel and zinc it was sightly weaker. A dimeric $[L_2M_2Na]$ complex was also detected. This was not a discrete species (i.e. $[M_2L_2]$) as on sample dilution (by a factor of four) these peaks were no longer observed. Species pairing (i.e. 2[ML]) is known to occur with certain types of molecules or if the sample concentration is too high. For the benzyl (**107**) derivative the major species observed were due to [MLH] rather than [MLNa] complexes.

3.3.4.2 Cadmium and lead

With these metals there was a difference in the spectrum depending on the ligand used. With the phenyl (**108**) derivative cadmium gave a large number of cadmium containing species but only a few could be assigned. Lead gave one major [PbLNa] complex peak and a large number of minor lead-containing species. For the benzyl (**107**) derivative cadmium and lead gave a clear [CdLH] and [PbLH] respectively together with other metal containing species. For the methyl (**8**) derivative cadmium showed an [CdLNa] complex, while for lead the major species was uncomplexed ligand and a less intense [PbLNa] peak together with other lead containing unassigned peaks.

3.3.4.3 Summary of major complexes

With all the ligand and metal combinations no [ML_2] species were detected. This is not surprising considering the low concentrations used together with the fact that [ML_2] formation has a much lower stability constant than for [ML]. For the benzyl (**107**) derivative the [MLH] species were more common, this was probably a result of the variation in the protonation state of the ligand used. With the phenyl (**108**) derivative the disodium salt was used, while for the benzyl (**107**) the protonated form (LH_3^+) was utilized, hence there are more protons in solution on complexation.

	observed peaks	calculated peaks
ligand	[LNa_3] 554.9, 555.9	555.0, 556.0
	unknown 560.8, 561.8	
	[LNa_2K] 571.2, 572.2	571.0, 572.0
	[LNa_3H_2O] 573.6, 574.6	573.1, 574.1
L + Cu	[CuLNa] 571.5, 572.4, 573.5, 574.5	572.0, 573.0, 574.0
L + Ni	[NiLNa] 567.0, 569.0, 570.7	567.0, 569.0, 570.0
L + Zn	[ZnLNa] 572.5, 573.4, 574.5, 575.5	573.0, 575.0, 577.0
L + Cd	[CdLNa] 620.4, 621.5, 622.5	621.0, 622.0, 623.0
L + Pb	[PbLNa] 715.9, 717.1	715.1, 716.1, 717.1

Table 3.10 Major species of ESMS analysis of phenyl (**108**) derivative with various metals. (Most intense peak of the cluster is underlined).

	observed peaks	calculated peaks
ligand	[LH_3] 516.6, 517.6, 518.7	517.1, 518.2, 519.2
	[LH_2Na] 538.7, 539.6	539.1, 540.1, 541.1
	[LH_2K] 554.5, 555.5, 556.6	555.1, 556.1, 557.1
L + Cu	[CuLH] 578.0, 579.5, 580.5	578.1, 579.1, 580.1
	[CuLNa] 560.0, 561.6, 602.6	600.0, 601.0, 602.0
L + Ni	[NiLH] 573.1, 574.4, 575.4, 576.5	573.1, 574.1, 575.1, 576.1
L + Zn	[ZnLH] 578.8, 580.4, 581.5, 582.5	579.1, 580.1, 581.1, 583.1
L + Cd	[CdLH] 626.1, 627.5, 628.6, 629.6	627.1, 628.1, 629.1
L + Pb	[PbLH] 721.8, 722.8, 723.8	721.1, 722.1, 723.1

Table 3.11 Major species of ESMS analysis of benzyl (**107**) derivative with various metals. (Most intense peak of the cluster is underlined).

	observed peaks	calculated peaks
ligand	[$LHNa_2$] 408.7, 409.6	409.1, 410.1
	[LHKNa] 425.6, 526.6	425.0, 426.0
	[LNa_3] 430.7, 431.6	431.0, 432.0
	[LNa_2K] 447.4, 448.3, 449.5	447.0, 448.0
L + Cu	[CuLNa] 447.7, 448.5, 449.6	448.0, 449.0, 450.0
L + Ni	[NiLNa] 442.7, 443.5, 444.5	443.0, 444.0, 445.0
L + Zn	[ZnLNa] 448.5, 450.5, 452.6	449.0, 451.0, 453.0
L + Cd	[CdLNa] 496.3, 497.3, 498.5	496.0, 497.0, 498.0, 499.0
L + Pb	[PbLNa] 590.3, 591.3, 592.3	591.0, 592.0, 593.0

Table 3.12 Major species of ESMS analysis of methyl (**8**) derivative with various metals. (Most intense peak of the cluster is underlined).

3.4 Creation of a tetrahedral binding site

Molecular modelling of the binding of the previous phenanthroline ligands (**8**) and (**108**) to zinc indicates a 'poor' tetrahedral geometry in the energetically most favourable state. Zinc is tetra-coordinated in a geometry that lies between tetrahedral and square planar (Fig. 3.18a).

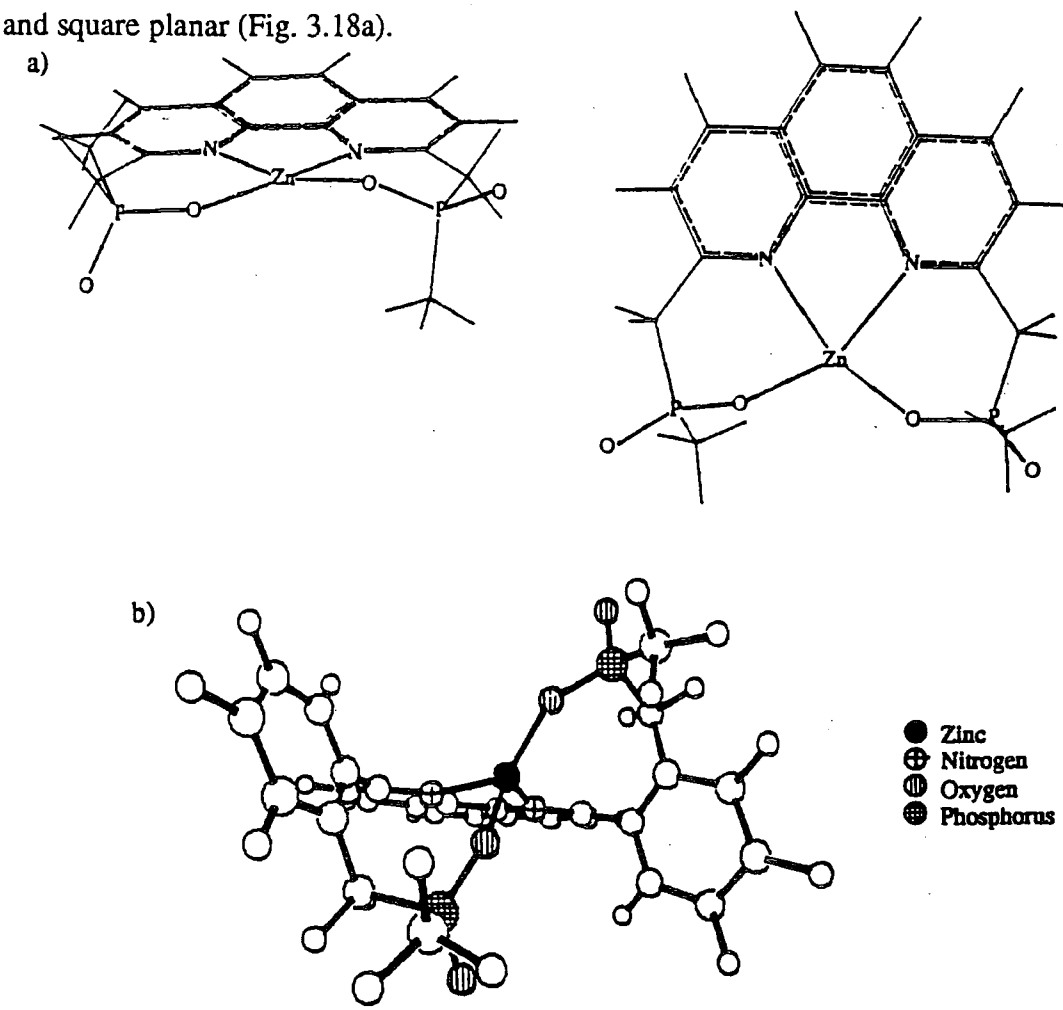

Fig. 3.18 Binding geometries of phenanthroline based ligands.

By increasing the length of the pendent arms while still maintaining rigidity, a binding geometry closer to tetrahedral should be generated. Molecular modelling indicates the attachment of a phenyl group will achieve this objective (Fig. 3.18b). Greater stability and selectivity for zinc, which favours tetrahedral binding over copper, should result. The increased length of the pendent arms means a square planar geometry is virtually impossible to obtain due to unfavourable steric interactions between the arms.

3.4.1 2,9-Phenyl substituted phenanthrolines

There are many examples of 1,10-phenanthrolines with phenyl groups in the two and nine positions. The phenyl rings often lie perpendicular to the phenanthroline plane especially in metal complexes[18] (Fig. 3.19), and also in uncomplexed ligands[19].

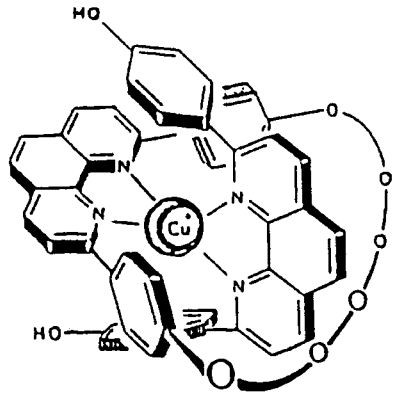

Fig. 3.19 Binding of 2,9-diphenyl substituted phenanthrolines with orthogonal phenyl/phenanthroline groups.

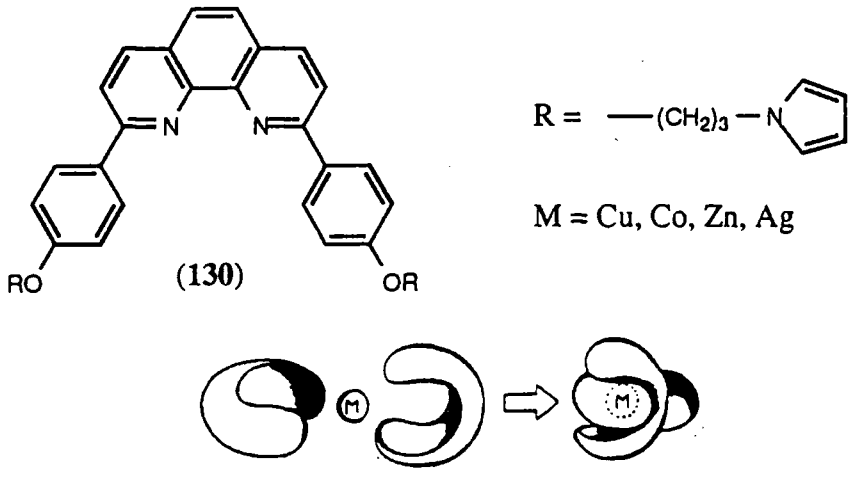

Fig. 3.20 2,9-Phenyl substituted phenanthroline (**130**) that forms a '2+2' tetrahedral donor array with various metals (Cu, Co, Zn and Ag).

The 2,9-diphenyl-1,10-phenanthrolines have been shown to bind Cu(I) in a tetrahedral manner[18], this has been exploited by Sauvage for use in metal cation

templating in catenane synthesis[20] and by others in molecular knot synthesis[21]. Other metals (Zn, Co, Ag) have been shown to bind with two 2,9 phenyl substituted phenanthrolines (**130**) in a tetrahedral manner[22] (Fig. 3.20). The 2,9-diphenyl-1,10-phenanthroline unit has been used as a rigid spacer. A substituted pyrrole group has been attached to the four position on the phenyl groups[23]. Such molecules have been investigated for possible intramolecular electron or energy transport.

3.4. 2 Past routes to the desired geometry

A donor such as a carboxymethyl or phosphinoxymethyl group on the phenyl ortho position was required to bind to the metal. There has been much work on the addition of para substituted phenyl groups[20,21,22,24,25] to the 2 and 9 positions of 1,10-phenanthroline and their subsequent reaction. However there is comparatively little work reported on ortho substituted compounds. Known examples only involve small substituents such as methyl, methoxy and ethoxy[26]. Examples exist where all the ortho phenyl positions are substituted[27], again with simple substituents. With these systems orthomethoxy ethers have been cleaved and subsequent functionalization has linked the phenyl groups together[28]. Almost all the phenyl substituted phenanthrolines have been synthesised by the reaction of the phenanthroline with lithiated species. However reaction of 1,10-phenanthroline with ortho substituted lithiated species[11] (Fig. 3.21) resulted in monosubstitution only, with the second addition not being observed even when the purified mono-substituted phenanthroline (**133, 134**) was reacted with more lithiated species.

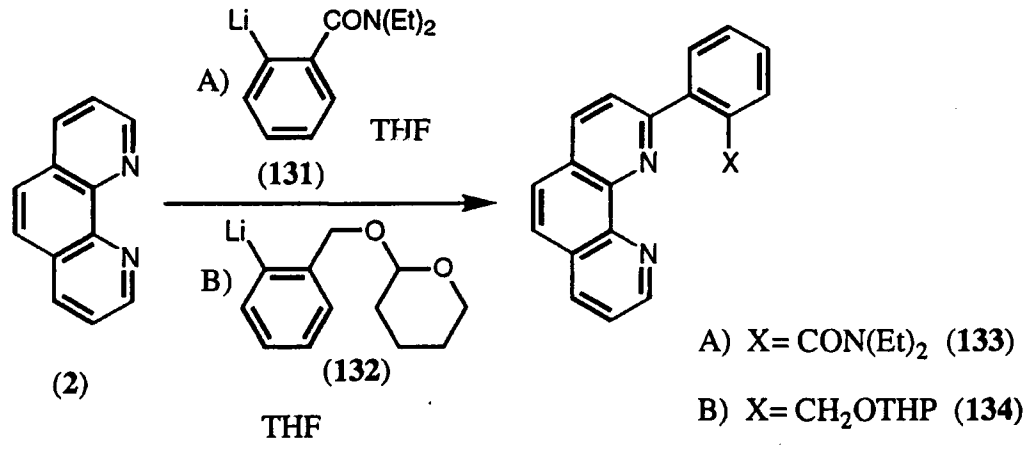

Fig. 3.21 Reaction of 1,10-phenanthroline (**2**) with ortho lithiated species (**131**) and (**132**).

From the literature 2,9-di(2-methylphenyl)-1,10-phenanthroline[29] can be prepared from the 2-methylphenyl lithiate and phenanthroline. Attempted

functionalization of the methyl groups either by oxidation (using SeO_2 or potassium permanganate) or radical bromination using N-bromosuccinimide resulted in no isolable products.

3.5 Ligand synthesis

3.5.1 Synthesis via 2,9-bis(2-bromomethylphenyl)-1,10-phenanthroline (141)

A 2,9 substituted bromobenzylic compound (**141**) is potentially a useful precursor to the desired ligand. Phosphinic acid donors with varied substituents could be made via an Arbuzov reaction followed by hydrolysis. In addition a carboxylic acid derivative could be synthesised by nucleophilic displacement of the bromine with cyanide and subsequent acid hydrolysis.

There are many examples of radical bromination of toluene groups to produce benzyl bromides, by peroxide[30], AIBN and light initiation[31]. Bromination of the structural isomer 2,9-bis(4-methylphenyl)-1,10-phenanthroline[23] using NBS and light initiation has been reported. Trying to improve on previous work freshly crystallized 2,9-bis(2-methylphenyl)-1,10-phenanthroline, NBS with AIBN or light initiation failed to give any products. The use of bromotrichloromethane[32] which has been shown to impart selectivity for benzylic bromination was also tested, but failed in this case to give any observable products.

The cleavage of benzylic ethers and subsequent bromination by the use of HBr in acetic acid is known. Following the patent literature[4(ii)], the required benzylic ether (**139**) can be synthesised (Fig. 3.22). 2,9-Dichloro-1,10-phenanthroline (**136**) was prepared in a six step synthesis from 1,10-phenanthroline[33] (**2**). Halogen-lithium exchange on 2-methoxymethylphenyl bromide[34] (**137**) and reaction with trimethylborate followed by an aqueous workup gave the boronic acid (**138**). The acid was only formed in moderate yield (about 50 %) and could not be purified above 80% despite repeated alternate acid and base extractions. As the acidic product was an oil, crystallization to higher purity was not possible. Cross coupling using a Suzuki reaction[35] gave the desired biaryl (**139**) in higher yield (82%) than that previously reported (47%). Treatment of the ether with HBr/acetic acid at 100°C gave a dark material, ^1H NMR analysis showed that C_2 symmetry had been lost. An intramolecular cyclization reaction had occurred producing a stable monocationic species (**140**). Only when HBr/acetic acid was used at room temperature and the material isolated by diethyl ether precipitation was the dibromobenzyl HBr species (**141**) recovered, as the mono-hydrobromide salt.

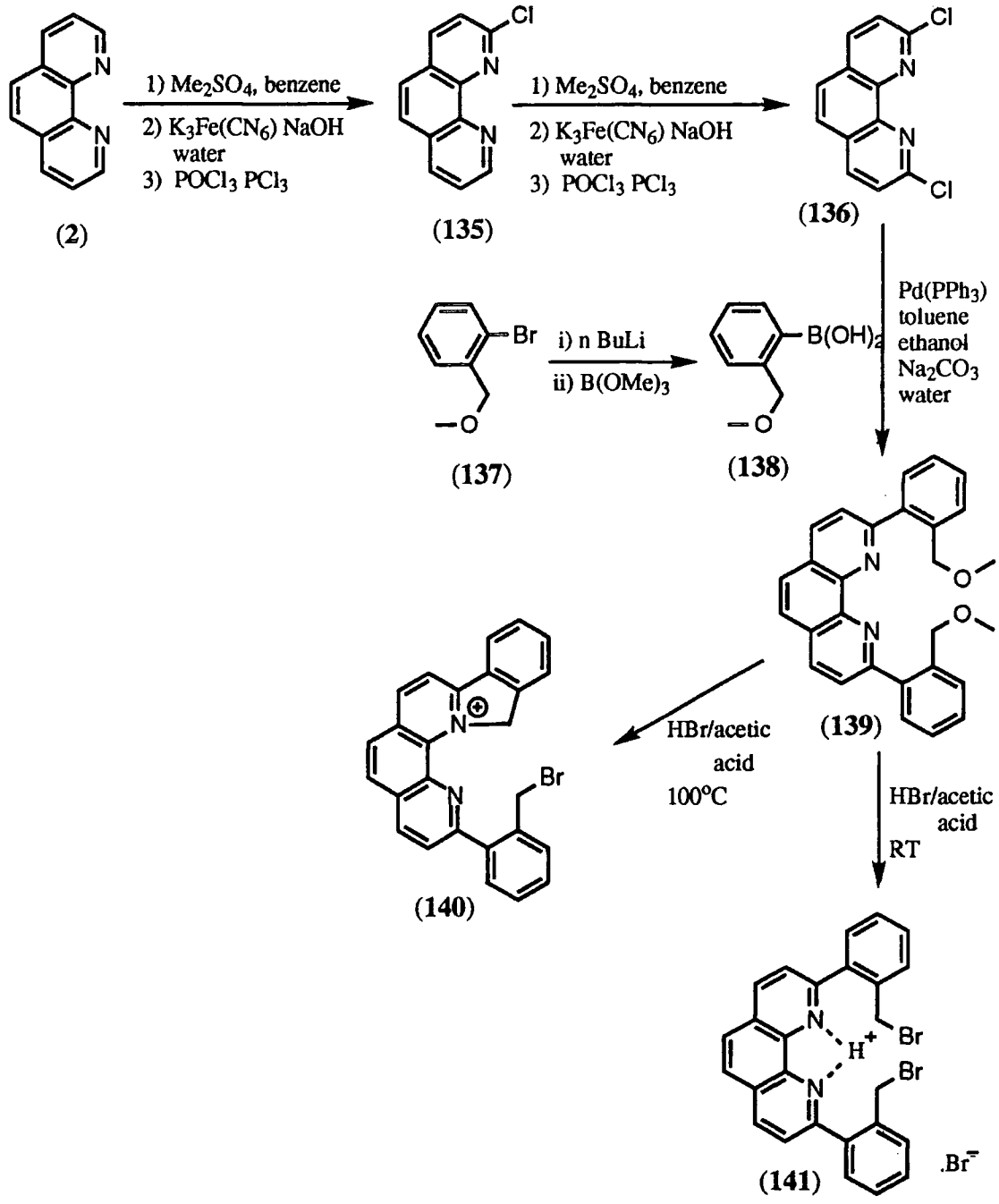

Fig. 3.22 Synthesis of 2,9-bis(2-bromobenzyl)-1,10-phenanthroline (**141**).

3.5.1.1 Reaction of the bromobenzyl derivatives (140) and (141) with nucleophiles

Using the cationic phenanthroline (**140**) an Arbuzov reaction was carried out with diethylphenyl phosphonite in dry acetonitrile to give a deep red coloured material. Proton NMR and mass spectroscopy analysis showed only one phosphorus group had added (Fig. 3.23). The benzylic bromine had reacted, but the phosphine had not proved to be sufficiently reactive to open the five membered ring. The positive charge is likely to be delocalized over the aromatic rings so stabilizing the five membered ring .

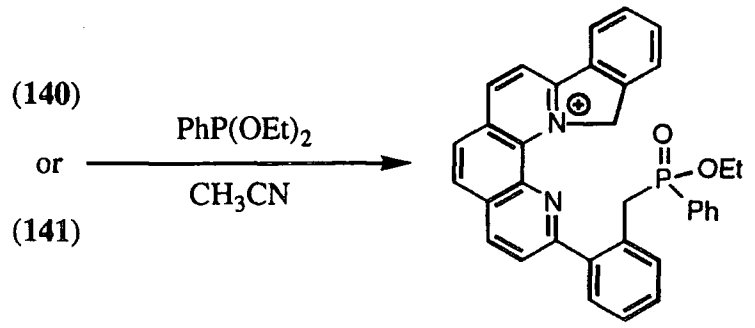

(142)

Fig. 3.23 Reaction of the bromobenzyl derivatives (**140**) and (**141**) with diethylphenyl phosphonite.

Using the proton stabilised di(bromobenzylic) species (**141**) the same red coloured product as before (**142**) was obtained. The other major species from the reaction was identified as an aryl phosphinous ester (**143**). This species was readily identified from the large proton phosphorus coupling constant in the ^{1}H NMR (J_{PH} = 563Hz) and the doublet in the non-decoupled ^{31}P NMR. Phosphinous esters are known to be produced rapidly from phosphonite esters in acidic media[36]

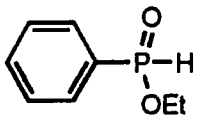

(143)

Fig. 3.24 O-Ethylphenylphosphinous ester (**143**).

Varying the order and rate of reagent addition, having zinc present or using very nucleophilic conditions (DMF, 18-crown-6, NaCN, caesium carbonate) only resulted in the addition of one nucleophilic moiety with consistent intramolecular cyclization. An exception to this occurred when diethylphenyl phosphonite was used in DMF with caesium carbonate. As well as the phosphinous ester which was produced, a black coloured material was formed, which was insoluble in chloroform unlike previous reactions. In methanol the ^{1}H NMR showed one very broad resonance in the aromatic region. It was postulated that a radical cationic species was present, perhaps formed by two intramolecular cyclizations. This was not investigated further.

3.5.1.2 Other boronic acid coupling intermediates

Using boronic acids in the Suzuki coupling reaction allows ortho substituted phenyl rings to be added to the phenanthroline sub-unit. Other 2-bromophenyl substituted compounds with useful functionalities were also prepared (Fig. 3.25)

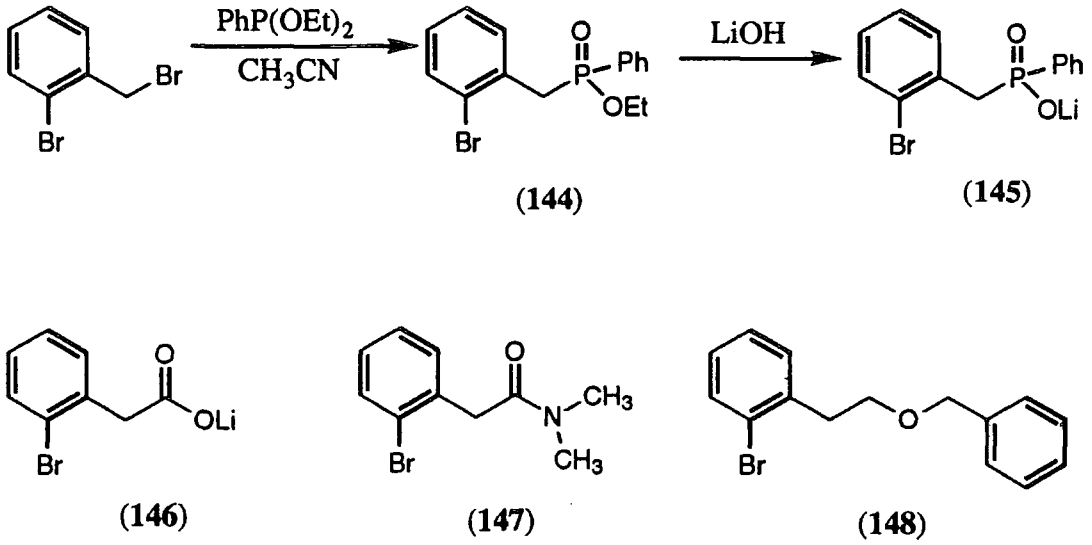

Fig. 3.25 2-Bromophenyl substituted intermediates (**144** to **148**).

Using nBuLi or the more reactive tBuLi (with 144 - 148) for halogen lithium exchange and subsequent reaction with trimethyl borate did not result in any of the required boronic acid, only starting material or from the acid base extractions small amounts of unidentifiable material. On anion generation the typical red colour of the aryl lithium species was not observed, instead a light yellow colouration was seen. Benzylic proton abstraction rather than halogen lithium exchange was occurring. Use of the salts (**145** and **146**) should help disfavour benzylic proton abstraction but the reaction still resulted in the desired product. Using the phosphonate ester (**144**) the anion that was generated was trapped with methyl iodide (Fig. 3.26) confirming that competitive deprotonation was occurring.

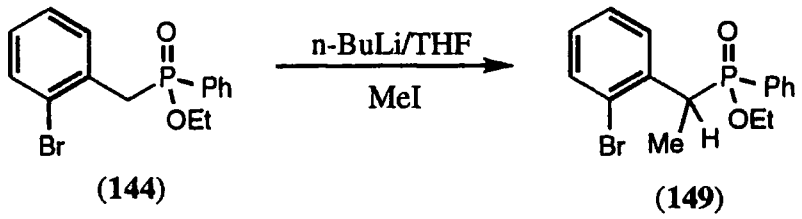

Fig. 3.26 Benzylic methylation.

There is a possibility of 4 diastereoisomers because of the 2 chiral centres present in (**149**). From previous work, the streochemistry of the phosphonate esters can not be determined by either proton or phosphorus NMR. The purified product (**149**) appeared to exist as a mixture of two diastereoisomers in a near 50/50 ratio as determined by ^{1}H and ^{31}P NMR. In the reaction excess nBuLi and methyl iodide were used, but as dimethylation at carbon was not seen, the second benzylic proton may now not be as acidic. This material could have been used for halogen lithium exchange, but later compounds and NMR's would have been over-complicated by the diastereoisomeric mixture. Referring to the molecular model (Fig. 3.18) the extra

methyl groups would probably not have interfered with binding. Despite this, the synthetic route was abandoned in favour of alternative tin-based coupling strategies.

3.5.2 Synthesis via stannane mediated aryl coupling

In the past 15 years there have been many examples of aromatic stannane formation[37] often involving palladium catalysed coupling of either hexamethyl or hexabutylditin to an aromatic halide. The stannanes can then be coupled to other aromatic halides using palladium catalysts[38]. As ortho stannanes are required, hexamethylditin was used as this would be sterically less bulky than tributylstannanes, so promoting better yields. Aromatic iodides appear to give better yields than the corresponding bromides[37a] but this is not always the case.

2-Iodophenylacetonitrile(**150**) was reacted with two equivalents of hexamethylditin using freshly prepared tetrakis(triphenylphosphine) palladium (0)[39] in dry, degassed toluene at 100°C under argon. The stannane (**151**) was hydrolytically and air stable and could be purified by column chromatography to give a colourless oil in high yield (86%). Cross coupling with 2,9-dichloro-1,10-phenanthroline, (**136**), which had been recrystallized from chloroform was performed under the same conditions as for the stannane formation. The phenanthroline dichloride (**136**) was not as reactive as the aromatic iodide and this necessitated a longer reaction time and resulted in a poorer yield in coupling. From the crude reaction mixture a number of products (**152** - **154**) were isolated (Fig. 3.27).

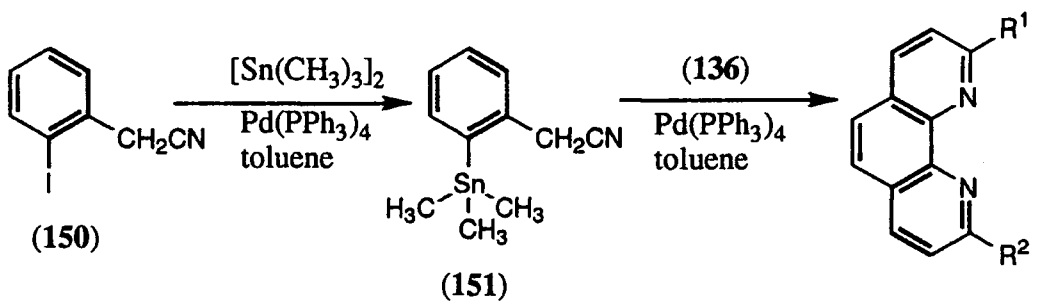

(**150**) (**151**)

(A) $R^1 = Cl$; $R^2 = C_6H_4CH_2CN$ (**152**)

(B) $R^1 = R^2 = C_6H_4CH_2CN$ (**153**)

(C) $R^1 = CH_3$; $R^2 = C_6H_4CH_2CN$ (**154**)

Fig. 3.27 Stannane (**151**) reaction with dichlorophenanthroline (**136**).

The major compound (**152**) that was isolated possessed only one additional aromatic group. As well as aromatic transfer from the stannane intermediate a product was isolated where a methyl group had been coupled (**154**). Both these observations

suggest that the second phenyl coupling is slower than the first. The complete removal of triphenylphosphine, which is generated in the reaction, from the desired product (**153**) also proved surprisingly difficult. Even after two chromatographic separations it still remained. It is possible that triphenylphosphine is forming a weak 1:1 complex with the product (**153**) through favourable π-π interactions of the phenyl pendent arms. Evidence of some interaction can be seen in the ^{13}C NMR spectra, the resonances corresponding to the triphenylphosphine have shifted in the presence of the ligand (**153**).

3.5.2.1 Carboxylic acid formation by cyano hydrolysis

Hydrolysis of the mono-nitrile (**152**) using 6M hydrochloric acid occurred readily and the resultant compound (**155**) was recrystallized from methanol to give colourless fibrous needles. From analysis of this material it appeared nucleophilic chloride displacement had occurred thereby forming a hydroxyl group (Fig. 3.28).

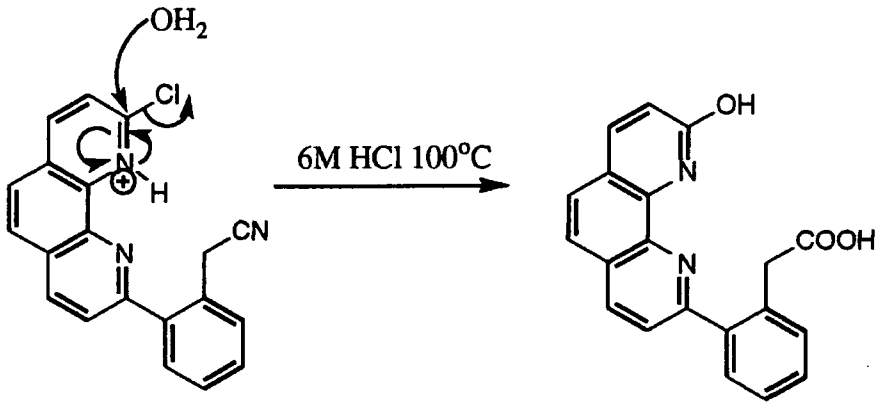

(**152**) (**155**)

Fig. 3.28 Cyano hydrolysis and chloride substitution (**152**).

Attempted hydrolysis of the dicyano compound (**153**) under the same conditions resulted in no detectable hydrolysed material. Formation of the more reactive imidate ester was then considered which would allow subsequent cyano hydrolysis to occur more readily. Reaction of the dicyanophenanthroline (**153**) with ethanol and dry hydrochloric acid in benzene resulted in a stable intermediate (**156**) that could be detected by ES MS. No further reaction occurred when aqueous hydrochloric acid was added. Mass spectrometry showed the same intermediate (**156**) (*m/z* = 504) and neither starting material (**153**) nor product (**157**) peaks were observed. The intermediate (**156**) could have been generated by an intramolecular cyclization between the phenanthroline nitrogen and the imidate ester. The resultant type of functionality would normally be expected to be readily hydrolysed. However the low solubility in the hydrolysing solvent and the close proximity of adjacent NH_2 and OEt groups, which would lead to

intramolecular hydrogen bonding may be sufficient to stabilise the structure in the solid state. Only after using more forcing conditions of 50/50 v/v, 6M hydrochloric acid/ acetic acid was the phenanthroline dicarboxylic acid (**157**) finally produced in a 34% yield from the dinitrile (**153**).

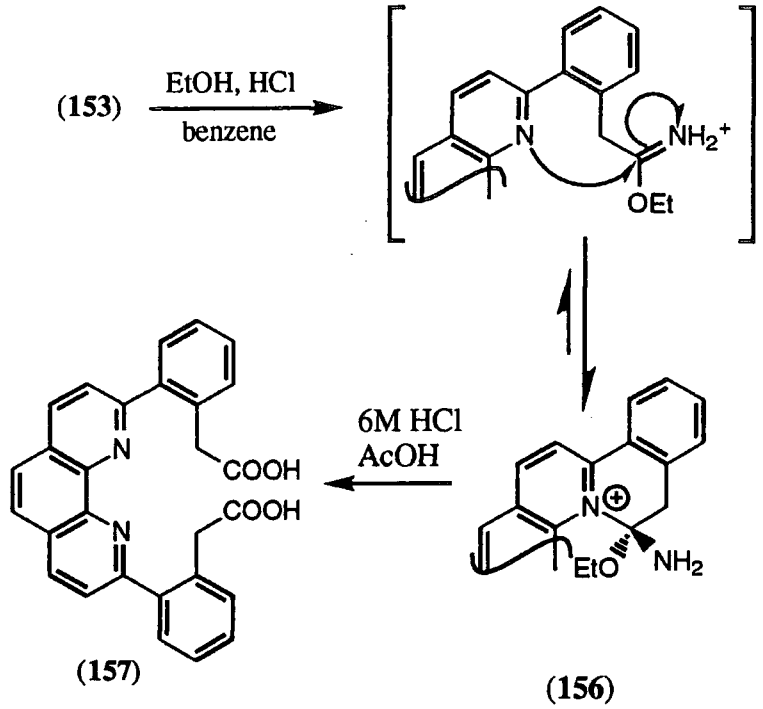

Fig. 3.29 Hydrolysis of phenanthroline dinitrile (**153**).

3.5.3 Future possibilities

Reaction of hexamethylditin with o-ethyl-(2-bromophenyl)methylene-(phenylphosphinate) (**144**) under the same conditions as before resulted in a number of compounds being formed over a period of 72 hours. Analysis of the product by GC-MS showed the presence of the desired product (**158**), but no attempts were made to isolate it, because of the small amount of material available.

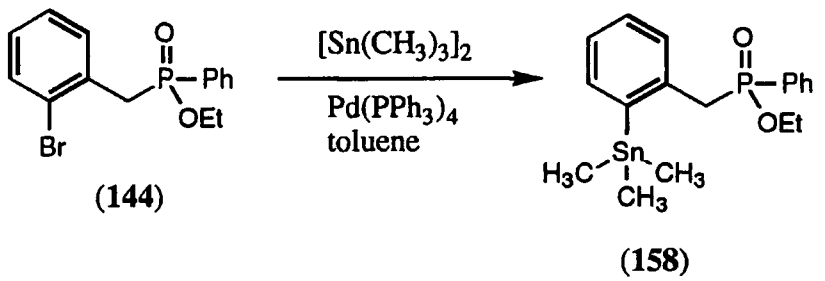

Fig. 3.30 Stannane addition to (**144**).

As mentioned previously if an aromatic iodide had been used a higher yield of the stannane may have resulted. Coupling to the dichlorophenanthroline (**136**) may be more difficult than before because of the greater steric bulk of the substituent ortho to the trimethyl stannane group. However this method of coupling may open the way to

generate other derivatives with varying phosphinate and thiophosphinate ester functionalities.

3.6 Metal-ligand complexation analysis

3.6.1 Zinc-ligand (157) ^{1}H NMR titration

The appropriate amount of zinc triflate was added incrementally to the ligand (**157**) NMR sample (0.0222M, CD_3OD) so that M/L ratios of 0.25, 0.5, 0.75, 1.0, 1.5 and 2.0 were obtained. After each addition the sample was thoroughly mixed and left for fifteen minutes to equilibrate before the NMR spectrum was acquired. Plotting $\Delta\delta_H$ (for the phenanthroline H-6) against M/L ratio gave a curve that analysed for 1:2 M:L binding (Fig. 3.31). A complex stability constant of $K_{ML_2} = 300$ ($\log K_{ML_2} = 2.5$) was estimated.

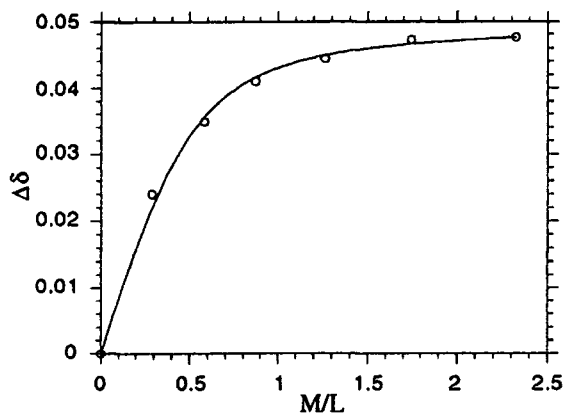

Fig. 3.31 Titration curve of (**157**) on zinc addition analysed for $[ML_2]$ formation (298K, CD_3OD).

The ligand was behaving as an N_2 donor with the carboxylic acid groups not involved in binding. The complex stability constant was of similar magnitude to $[ML_2]$ formation with 2,9-dimethyl-1,10-phenanthroline (**101**) ($\log K_{ML_2} = 3.6$, 298K, H_2O). The difference was probably the result of the different solvent conditions and the extra steric interactions caused by the phenyl groups. The lack of [ML] formation may have been a result of the carboxylic acids being protonated prior to zinc addition. However, if the stability constant was sufficiently high deprotonation should have readily occurred on metal addition.

3.6.2 Electrospray mass spectrometric analysis

A similar procedure was performed as outlined previously (section 2.3.2, page 57). The ligand was dissolved in methanol and left for twenty four hours. ESMS

Analysis indicated that the methyl ester had formed. As aqueous metal salts (nickel, copper, zinc triflate and ferric chloride) were added to the ligand it could be expected that ester hydrolysis would occur.

With nickel the spectrum was identical to that of the ligand with not even a phenanthroline methyl ester nickel complex being observed. For zinc there appeared to be a small peak corresponding to [ML] (L = phenanthroline dicarboxylic acid (**157**)). However this was very small with a poor match to the calculated isotope pattern. The addition of ferric (III) chloride again did not give a clear spectrum. A peak corresponding to $[L_2Fe]$ was seen indicating that some hydrolysis had occurred. Over three days there was no significant change in any of the three spectra.

With copper addition, more interesting spectra observed. Just after copper addition, peaks were observed for [ML] type species with one and two methyl groups hydrolysed. Another group of related species was seen for $[ML_2]$ complexes, again with no, one or two methyl groups hydrolysed. After three days the spectrum had altered. There was no longer any uncomplexed ligand or [ML] species. A series of complexes was identified for $[ML_2H_3]$, $[ML_2H_2Me]$, $[ML_2HMe_2]$, $[ML_2Me_3]$ and $[ML_2Me_4]$ with the major species corresponding to $[ML_2HMe_2]$ (Me represences the carboxylate methyl ester). There was also a second series of peaks of lower intensity that could not be assigned. Leaving this sample over a significantly longer time (55 days) only had a small effect on the ESMS spectrum. Only $[ML_2]$ type species were present $[ML_2H_3]$ was now of higher intensity than $[ML_2HMe_2]$ with significantly lower amounts of $[ML_2Me_3]$ (Fig. 3.32). There was however a visible change in the solution colour, over time the sample had become more yellow in colour. From related work (see Chapter 4) this may suggest that copper is bound in a tetrahedral environment (i.e. in this case an N_4 donor array). The continued presence of methyl esters would suggest that this ester was particularly stable with respect to hydrolysis.

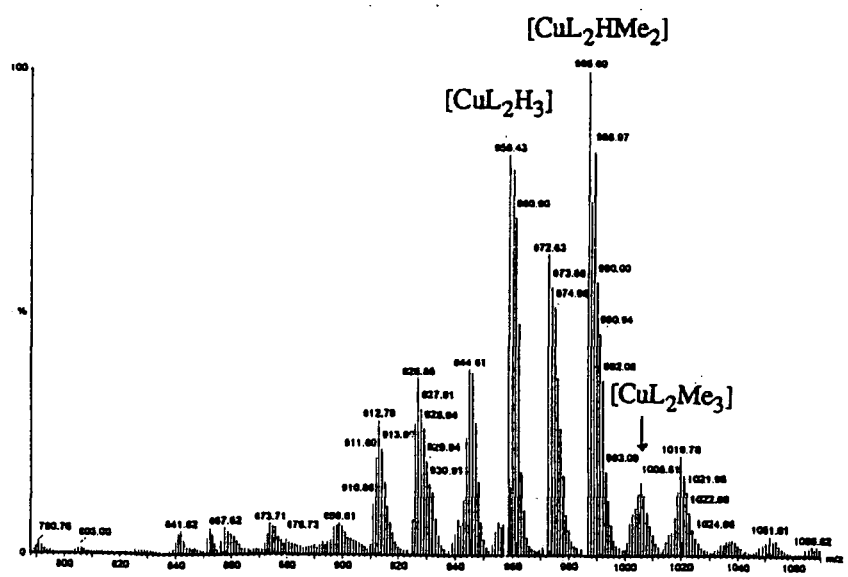

Fig. 3.32 ESMS of copper (II)-phenanthroline dicarboxylate (**157**) after 58 days.

In a further attempt to observe [ML] formation, a ligand solution was prepared in 50/50 v/v water/isopropanol mixed solvent in the presence of potassium carbonate (to neutralize the carboxylic acid) The solution acidity was measured (pH paper) to be pH 8.5. Samples were prepared as before and tested within two hours of metal addition. For the ligand a number of species were seen, corresponding to varying degrees of potassium and proton addition (i.e. $[LNa_3]$, $[LH_2K]$, $[LHK_2]$ and $[LK_3]$). With cadmium and lead triflate there was no observable [ML] species suggesting there was no binding compared to the potassium cation. For nickel and zinc, there was only a trace of [ML] complex species and the major species observed was due to the ligand. As before, only copper showed a significant presence of transition metal-ligand complex. There was a weak peak for [ML], and a more intense signal for [LCuK]. Significantly there was a substantial amount of $[L_2CuH_3]$ and a species that appeared to be $[L_2CuH_2(H_2O)]$. The solution was pale yellow in colour.

3.6.3 Future work

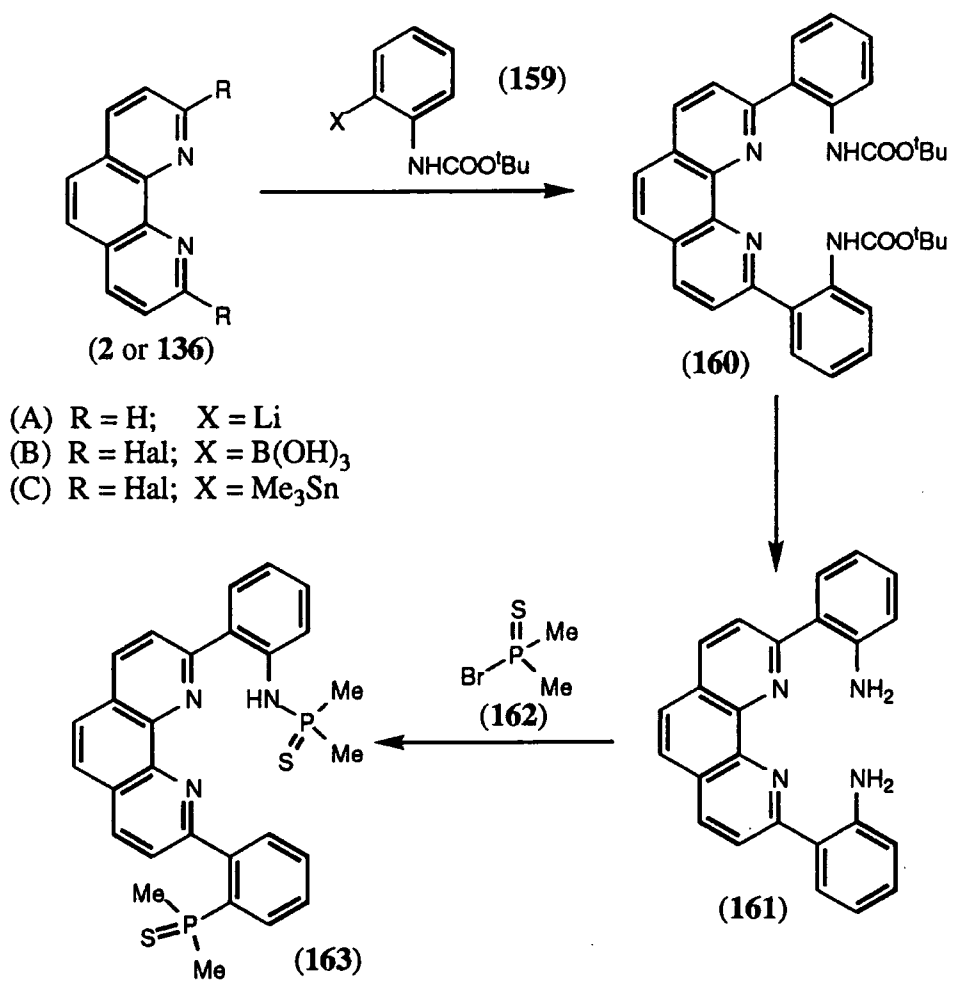

Fig. 3.33 Possible route to a thiophosphoroamide donor group.

From the proton NMR titration and ESMS studies it would appear that the carboxylic acid donor is not ideal. (There was also evidence of the carboxylic acid group's lack of selectivity over copper and iron (III) from the bisbenzimidazole work Chapter 2). An improved donor may be a thiophosphinate or thiophosphoramide donor. The sulphur groups may act as a better donor than oxygen because of its softer nature. Current investigations[40] suggest that the thiophosphinate donor may be difficult to produce in good yields and purity. The thiophosphoramide group appears more accessible and plausible synthetic routes to this group can be outlined (Fig. 3.33)

Aromatic addition to a phenanthroline unit (**2** or **136**) has been shown to be possible using at least three coupling routes (using the lithiate, boronic acid or stannane groups). The carbamate (**106**) should be readily cleaved to yield the phenanthroline diamine (**161**). The thiophosphoryl bromide (**162**) is a literature[41] compound and has been used to couple to other amines[42]. Coupling to the diamine (**161**) should be possible to yield the desired compound (**163**). On binding, the NH proton dissociates and a N=P-S^- functionality is formed.

3.7 Conclusion

A number of conclusions can be drawn regarding 2,9-disubstituted phenanthrolines as metal complexing ligands. The 1,10-phenanthroline-2,9-bis (methylene(phenylphosphinic acid) (**108**) (Fig. 3.34) was shown to readily form [ML] complexes with a wide range of metals (e.g. nickel, copper, zinc, cadmium and lead) (ESMS evidence). Solid complexes were obtained from either aqueous or methanolic ligand solutions with copper, zinc and cadmium salts. If precipitation was not instantaneous the complexes had a definable composition of [ML1/2(H_2O)]. Likewise if precipitation was too rapid (as with the benzyl derivative (**107**)) some uncomplexed metal salts were coprecipitated in the solid matrix (I.R., elemental analysis). pH Potentiometric titrations showed the phenyl derivative bound nickel, copper and zinc with stabilities that followed the Irving-Williams sequence (i.e. Cu > Ni > Zn). The presence of [ML_2] species was also detected (pH potentiometric analysis). The order of stability constants observed for the methyl derivative (**8**) (i.e. Zn >> Ni > Cu) was not reproduced with the phenyl derivative (**108**). Comparison to other phosphinic acid substituted ligands (e.g. ethylenediamine) indicated that the donor group only had a marginal effect on increasing metal-ligand complex stability above that of the parent ligand. In general the phosphinate group slightly enhances the zinc binding constant with respect to that of copper and nickel. The end result is similar stability constants for all three 1:1 complexes.

Although a better tetrahedral donor arrangement could be generated by increasing the length of the pendent arms by inserting a phenyl group (e.g. **157**) (molecular modelling), there did not appear to be an enhancement in the zinc selectivity

over copper (ESMS). The most probable reason was that the wrong donor group was used. Phenylacetate donor groups do not have a particularly affinity for zinc[2] Binding kinetics may be slow for [ML] formation and faster for [ML_2] generation (Evidence can be seen with ESMS, copper initially forms an [ML] complex with is converted to an [ML2] species). The observation of an [ML_2] species is further evidence that 2,9-disubstituted phenanthrolines (such as the phosphinic acids) are able to form such species readily.

A better donor group for zinc may involve thiophosphinate or a thiophosphoroamide group. The low protonation constants would enable metal complexation to occur at low pH, while the donor ability would be greater than that of the phosphinate or carboxylate groups.

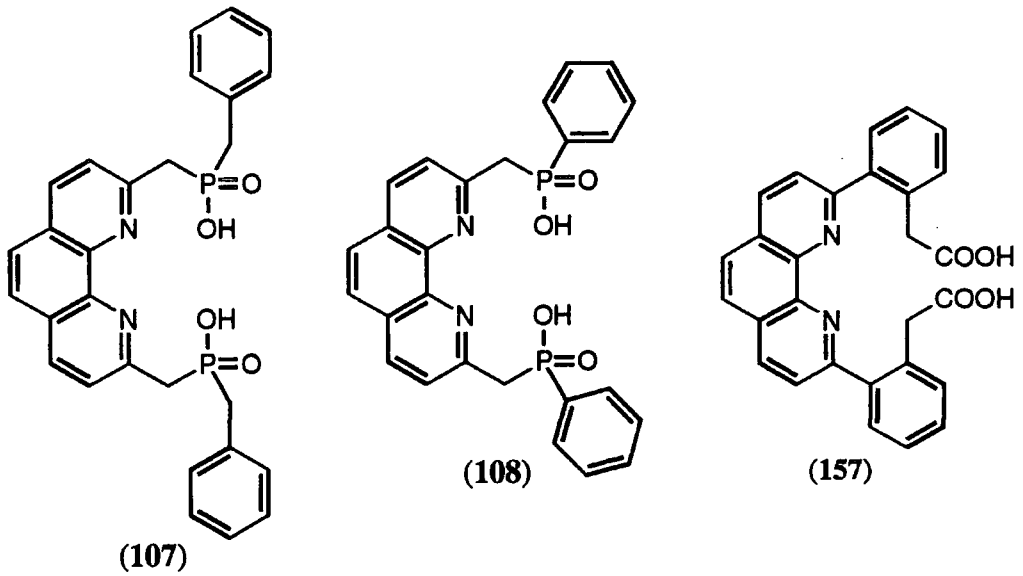

(107) (108) (157)

Fig. 3.34 Phenanthroline based ligands

3.8 References

1) J-M. Lehn; *Angew. Chem., Int. Ed. Engl.,* 1988, **27**, 89; 1990, **29**, 1304.

2) A.E. Martell, R.M. Smith,'Critical Stability Constants Vol 1-6', Plenum Press, London.

3) C.F.H. Allen; ' The Chemistry of Heterocyclic Compounds. Six Membered Heterocyclic Nitrogen Compounds with Condensed Rings', Wiley and Sons, London, 1958.

4) (i) H. Sugihara, T. Okada, K. Hiratani; *Chem. Letters,* 1987, 2391; (ii) M.H. Delton, H.C. Warren (III), patent EP339.973, Cl C07 D471/04.

5) C.J. Chandler, L.W. Deady, J.A. Reiss; *J. Heterocycl Chem.,* 1986, **23**,1327.

6) (i) E.P. Diamandis; *Clin. Biochem.*, 1988, **21**, 139; (ii) R.A. Evangelista, A. Pollock, B. Allore, E.F. Templeton, R.C. Morton, E.P. Diamandis, *Clin. Biochem.*, 1988, **21**, 173.

7) J. Lewis, T.D. O'Donoghue; *J. Chem. Soc., Dalton Trans.,* 1980, 736.

8) (i) C-H.B. Chen, D.S. Seligman; *Acc. Chem. Res.,* 1986, **19,** 180; (ii) R. Tamilarasen, D.R. McMillin; *Inorg. Chem.,* 1990, **29**, 2798.

9) C-H.B. Chen, D.S. Seligman; *Acc. Chem. Res.,* 1988, **110**, 6570.

10) J.G.J. Weijnen, A. Koudijs, J.F.T. Engbersen; *J. Org. Chem.,* 1992, **57**, 7258.

11) E. Cole; Ph.D. Thesis, University of Durham, 1993, Chapter 4.

12) C.J. Chandler, L.W. Deady, J.A. Reiss; *J. Heterocycl. Chem.,* 1981, **18**, 599.

13) (i) A.J. Kirby, S.G. Warren; 'The organic chemistry of phosphorus', Elsevier, 1967, p117; (ii) A.J. Spezlale, L.J. Tayor; *J. Org. Chem.,* 1966, **31**, 2451; (iii) R.D. Partos, A.J. Spezlale; *J. Am. Chem. Soc.,* 1965, **87**, 5068.

14) M. Ohta, K.K. Fuku, R. Sudo, M. Masuke; *J. Org. Chem.,* 1968, **33**, 3504.

15) R.G. Bates, 'Determination of pH', Wiley, New York, 1964, Chapters 7 and 8.

16) S. Rondinini, P. Longhi, P.R. Mussini, T. Mussini; *Pure Appl. Chem.,* 1987, **59**, 1693.

17) (i) S.R. Wilson, Y. Wu; *Supramolecular Chem.,* 1994, **3**, 273; (ii) G.J. Langley, D.G. Hamilton, M.C. Grossel; *J. Chem. Soc., Perkin Trans. 2*, 1995, 929.

18) (i) C.O. Dietrich-Buchecker, J-P. Sauvage, J.P. Kintzinger; *Tetrahedron Lett,* 1983, **24**, 5095; (ii) J-P. Sauvage; *Nouv. J. Chimie,* 1985, **9**, 299; (iii) C.O. Dietrich-Buchecker, J-P. Sauvage; *Chem. Rev.,* 1987, **87**, 795.

19) J.A. Wytko, J. Weiss; *J. Org. Chem.,* 1990, **55**, 5200.

20) (i) C.O. Dietrich-Buchecker, J-P. Sauvage; *Tetrahedron Lett.,* 1983, **24**, 5091; (ii) J-C. Chambron, J-P. Sauvage; *Tetrahedron Lett.,* 1986, **27**, 865; (iii) C.O. Dietrich-Buchecker, J-P. Sauvage, J. Weiss; *Tetrahedron Lett.,* 1986, **27**, 2257; (iv) J-F. Nierengarten, C.O. Dietrich-Buchecker, J-P. Sauvage; *J. Am. Chem. Soc.,* 1994 **116**, 375.

21) D.M. Walba, Q.Y. Zheng, K. Schilling; *J. Am. Chem. Soc.*, 1992, **114**, 6259.

22) G. Bidan, B.D. Blohorn, M. Lapkowski, J-M. Kern, J-P. Sauvage; *J. Am. Chem. Soc.*, 1992, **114**, 5956.

23) S. Chardon-Noblat, J-P. Sauvage; *Tetrahedron*, 1991, **47**, 5123.

24) C.O. Dietrich-Buchecker, J-P. Sauvage; *Tetrahedron Lett.*, 1983, **24**, 1275.

25) (i) C.J. Chandler, L. W. Deady, J. A. Reiss, V. Tzimos; *J. Heterocycl Chem..*, 1982, **19**, 1017.

26) (i) Md. A. Mosood, P. S. Zacharias; *J. Chem. Soc., Dalton Trans.*, 1991, 111; (ii) C.O. Dietrich-Buchecker, J-P. Sauvage, P.A. Marnot; *Tetrahedral Lett.*, 1982, **23**, 155.

27) U. Luning, M. Muller; *Chem. Ber.*, 1990, **123**, 643.

28) U. Luning, M. Muller, M. Gilbert, K. Peters, H.G von Schnering, M. Keller; *Chem. Ber.*, 1994, **127**, 2297.

29) U. Luning, M. Muller; *Chem. Ber.*, 1990, **123**, 643.

30) M. Tashiro, T. Yamoto; *J. Org. Chem.*, 1985, **50**, 3939.

31) L. Anzalone, J.A. Hirsh; *J. Org. Chem.*, 1985, **50**, 2128.

32) E.S Huyser; *J. Am. Chem. Soc.*, 1960, **82**, 391.

33) J. Lewis, T.D. O'Donoghue; *J. Chem. Soc., Dalton Trans.*, 1980, 736.

34) M.E. Bos, W.D. Wulff, R.A. Miller, S. Chamberlin, T.A. Brandvold; *Tetrahedron*, 1991, **47**, 4739.

35) N. Miyaura, T. Yanagi, A. Suzuki; *Synth. Commun.*, 1981, **11**, 513.

36) D.E.C. Corbridge; 'Studies in Inorganic Chemistry 10, Phosphorus. An outline of its Chemistry, Biochemistry and Technology', Elserier, Oxford, 1990 p335.

37) (a) H.Azizian, C.Eaborn, A. Pidcock; *J. Organomet. Chem.*, 1981, **215**, 49. (b) D. Azarian, S.S. Dua, C. Eaborn, D.R.M. Walton; *J. Organomet. Chem.*, 1967, **117**, C55.

38) (a)Y. Yamamoto, Y. Azuma, H. Mitoh; *Synthesis*, 1986, 564. (b) T.R. Bailey; *Tetrahedron Lett.*, 1986, **27**, 4407. (c) D.R. McKean, G. Parrinello, A.F. Renaldo, J.K. Stille; *J. Org. Chem.*, 1987, **52**, 422.

39) M. Schlosser; 'Organometallics in Synthesis', Wiley, Chichester, 1994 p448.

40) M.A.M. Easson; Private communication.

41) H.J. Harwood, K.A. Pollart; *J. Org. Chem*, 1963, **28**, 3430.

42) A. Schmidpeter, J. Ebeling; *Chem. Ber.*, 1968, **101**, 815.

Chapter Four

$12N_3$ Based Ligands

4.1 $12N_3$ Ligand Binding

4.1.1 Introduction

The third tetrahedral geometric arrangement to be considered was the use of three donors linked together to form a basal plane with the fourth donor on a pendent arm. The metal was envisaged to bind above the three basal donors and the pendent arm to bind from above to form a tetrahedral geometry (Fig. 4.1). 1,5,9-Triazacyclododecane ($12N_3$) was selected as the basal plane for the ligands.

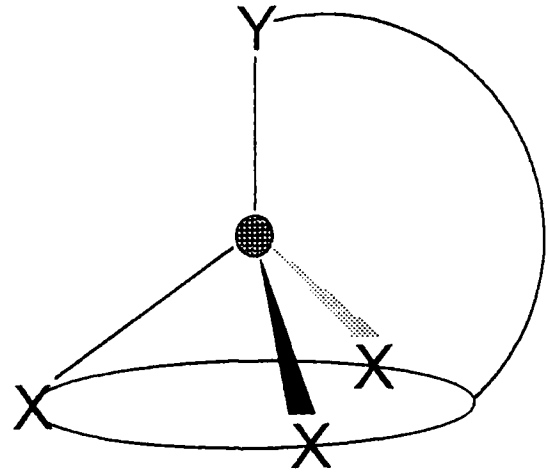

Fig. 4.1 Illustration of '3-1' binding.

4.1.2 Past Work

In solution, unsubstituted macrocyclic triamines coordinate with transition metals either facially, to form 3-coordinate 1:1 complexes with the remaining coordination site unoccupied or solvated[1], or they form six coordinate 2:1 complexes[2]. Substituted $12N_3$ ligands have been synthesised and investigated as 'proton sponges'[3] and for use in diagnostic nuclear medicine[4]. More importantly they have been studied as models to mimic the active site of zinc (II) containing enzymes e.g. carboxypeptidase A and carbonic anhydrase[5] and as ligands to impose tetrahedral coordination[6].

From published crystal structures, the design of the pendent arm is important if tetrahedral binding is required. The pendent arm has a direct effect on the N-Zn bond lengths and the N-Zn-N bond angles. If on binding a cleft remains in the structure, either water or a counter anion can readily bind to give 5-coordinate zinc. This has been shown to occur when the pendent arm only forms a five ring chelate on binding[6] (Fig. 4.2). For example when the pendent arm was pyrrolidinylethyl[6] (7), a sufficiently large cleft was generated to allow a strong interaction with a perchlorate counterion, which normally behaves as a non-coordinating anion. With the less sterically demanding 2-hydroxyethyl group[5(ii)] as the pendent arm, a cleft was also produced. This allowed formation of a dimeric $[L_2Zn_2]$ structure which was observed in the solid state. As

another example, the 3-propylamine donor[6(ii)] forms a 6-membered chelate ring on binding but the lack of steric bulk means a counter anion is able to bind. When the donor is conformationally restricted and cannot come directly over the top of the 12N$_3$ plane a cleft is again produced on zinc binding[7] e.g. Kimura's ligand (**6**) (Fig. 4.2).

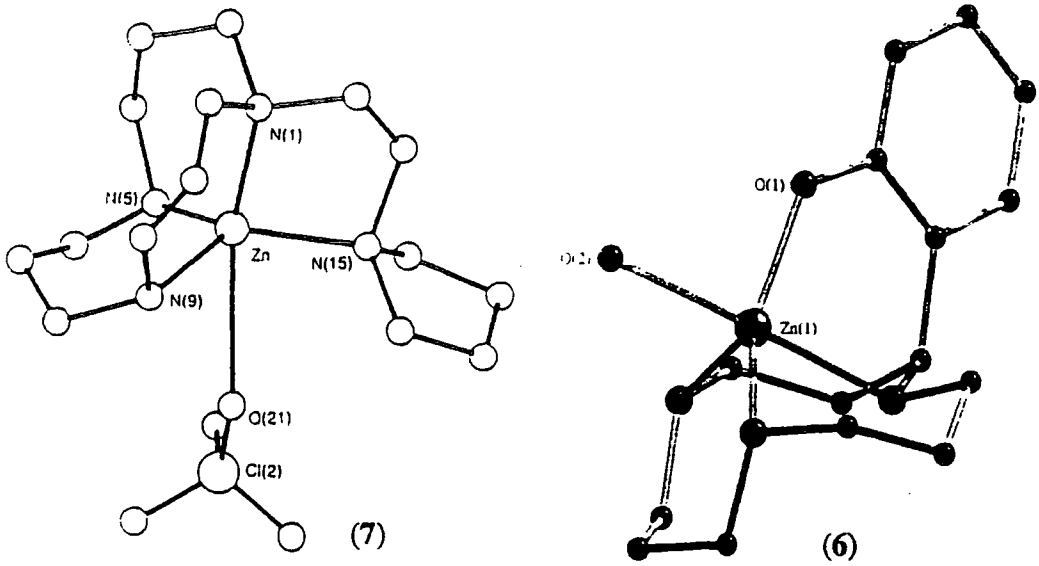

Fig. 4.2 12N$_3$ substituted ligands showing a cleft in the solid state.

Anionic nitrogen as a donor (e.g (**164**), Fig. 4.3)[8] has been used to produce a slightly distorted tetrahedral complex. All the chelating N-Zn-N angles are in the range 99.5-105.5°. Stronger coordination will exist to the anionic nitrogen donor than to the neutral nitrogen donor hence the sulphonamide N-Zn bond distance was the shortest. A slight cleft was still produced but no anion or water was bound, at least in the solid state structure.

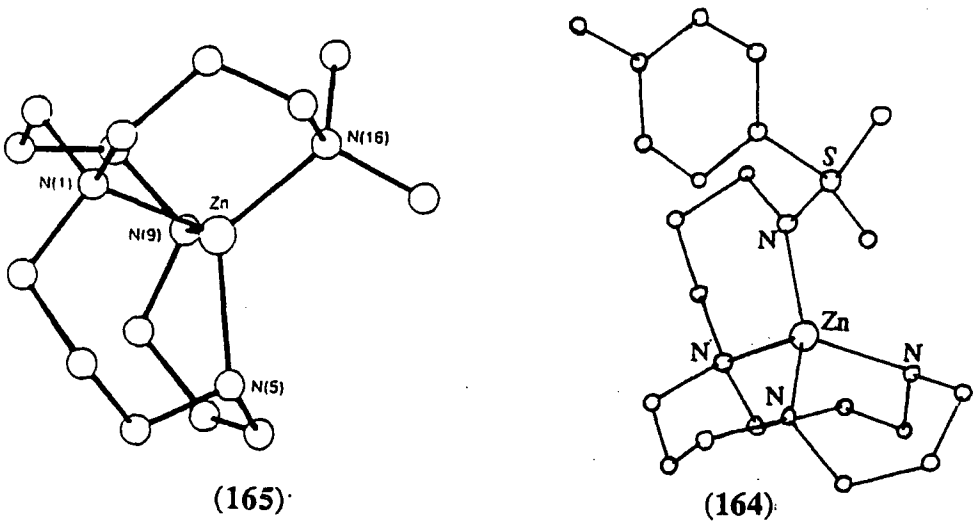

Fig. 4.3 Slightly distorted tetrahedral complexes (**164**) and (**165**).

When all the donors are neutral nitrogens, such as in [1-(3-dimethylaminopropyl)-$12N_3$][6] (**165**) (Fig. 4.3) all the N-Zn distances are virtually identical (2.00Å), with average chelate N-Zn-N angles of 104.8°. Again the non-chelating angles were relatively large (118°) and a cleft was produced. The perchlorate anion was not bound, as seen in the solid state crystal structure.

4.2 Ligand Design

A number of criteria need to be considered, mainly concerning the elimination or reduction of the cleft to hinder penta-coordination. Optimal zinc tetrahedral complexes seem to be produced when the chelate ring size is six[9] and the pendent arm is attached to a $12N_3$ nitrogen. The pendent arm needs to be as rigid as possible to reduce 5-coordination by a counter anion and to increase the metal to ligand binding constant, but should not be too conformationally restrictive. Steric bulk close to the donor atom should reduce counter anion-zinc interactions. Using an anionic donor not only gives stronger complexes with the bound metal, but also reduces the complex charge density and the subsequent likelihood of counter anion binding.

Two ligands have been synthesised (Fig. 4.4).

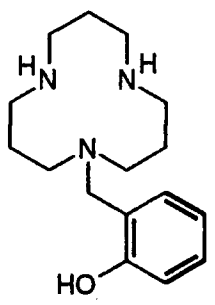

(**166**) N-linked $12N_3$

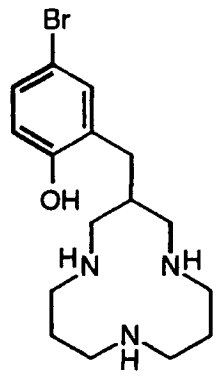

(**167**) C-linked $12N_3$

Fig. 4.4 $12N_3$ based ligands (**166**) and (**167**) synthesised in this work.

In ligands (**166**) and (**167**) the donor sets are essentially identical. The pendent arms are of equal rigidity and the phenol donor is equidistant from the $12N_3$ ring. The phenol group may be readily ionised and can act as an ionic donor to zinc. The presence of the bromine para substituted to the hydroxyl group in ligand (**167**) is advantageous as it lowers the pKa of the phenol (e.g. pK_a phenol = 10.0, 4-bromophenol = 9.35) so making it a better donor. The C-substituted $12N_3$ ligand (**167**) represents the first example where the pendent arm is attached to the central carbon atom. On binding to a metal the N-substituted ligand (**166**) produces a six membered chelate ring while (**167**) produces an eight membered chelate. CPK Space-filling molecular modelling indicated

that both ligands are able to bind zinc in a near tetrahedral manner. The ligands allow a direct comparison of the effect of ring chelate size and should help define the optimal position for pendent arm attachment.

4.2.1 Synthesis of N-substituted $12N_3$ (166)

Reported syntheses of $12N_3$ ring derivatives have often involved selective protection[10] or functionalization of a ring precursor prior to Richman-Atkins cyclization[11] or have involved the intermediacy of tricyclic orthoamides[12]. Twelve membered rings are relatively easy to form especially when a nitrogen heteroatom is incorporated.

The $12N_3$ ring was formed using a medium dilution cyclization of diethyl malonate (**170**) and 1,5,9-triazanonane (**171**) in boiling ethanol[4]. After 14 days a 16% yield was obtained following chromatographic purification. Insignificant amounts of the 24 membered ring were detected and most of the starting materials were recovered unreacted. The first condensation reaction appeared to be the rate limiting step with ring closure occurring more readily. Two types of nitrogen are present in the product: the secondary amine and the two amides. Selective mono-alkylation of the $12N_3$ ring (**172**) was performed with freshly made ortho-methoxylbenzyl chloride[13] (**173**) (made from reaction of thionyl chloride with ortho-methoxylbenzyl alcohol), in dry acetonitrile utilising fine-mesh potassium carbonate as the base. After solvent removal, the N-alkylated $12N_3$ diamide (**174**) was purified by washing off the base with water and excess alkylating agent (**173**) with diethyl ether. The only minor impurity that was detected by mass spectrometry was due to over-alkylation at one of the amide nitrogens. Recrystallization of the product (**174**) from methanol gave colourless crystals in 85% yield. The amides were quantitatively reduced by boiling with borane in THF for two days, monitoring the loss of the carbonyl group (1643 cm^{-1}) by infra-red spectroscopy. It has been shown[4] that very stable $12N_3$-boron complexes (**169**) and (**168**) can be made (Fig. 4.5).

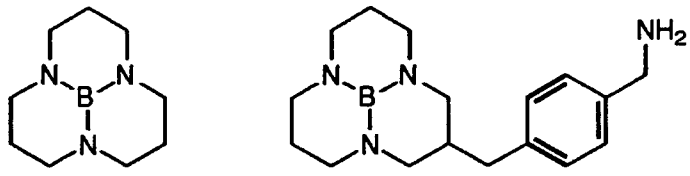

(**168**) (**169**)

Fig. 4.5 Acid stable $12N_3$-boron complexes (**168**) and (**169**).

The boron was efficiently bound in the plane of the triaza ring to form an acid stable, neutral complex. In the present example (**174**) the presence of the ring nitrogen substituent prevented a neutral, stable complex being formed. Decomplexation of the

boron by boiling with 6M hydrochloric acid generated boronic acid which was removed by azotroping with methanol. Slow recrystallization from toluene gave the N-substituted $12N_3$ (**175**) as white needle shaped crystals.

Demethylation was more difficult than expected. Nucleophilic cleavage using sodium thiolate in DMF[14], boron tribromide in dichloromethane[15] and treatment with trifluoroacetic acid in dichloromethane[16] at room temperature all failed to give any deprotected compounds. Starting material was recovered in all cases. Methods were avoided that used metals that may bind to the ligand such as aluminium, zinc and iron. Boiling the compound (**175**) in 48% v/v HBr/acetic acid[17] for 15 hours resulted in demethylation. It was necessary to add a small amount (about 2%) of p-hydroxyphenol to prevent radical bromination of the phenol ring in the para-position. The resultant N-substituted 2-hydroxylbenzyl $12N_3$ (**166**) was dark in colour and this colouration persisted despite acid/base extractions. Purification of the product to yield a light yellow solid was achieved using reverse phase HPLC.

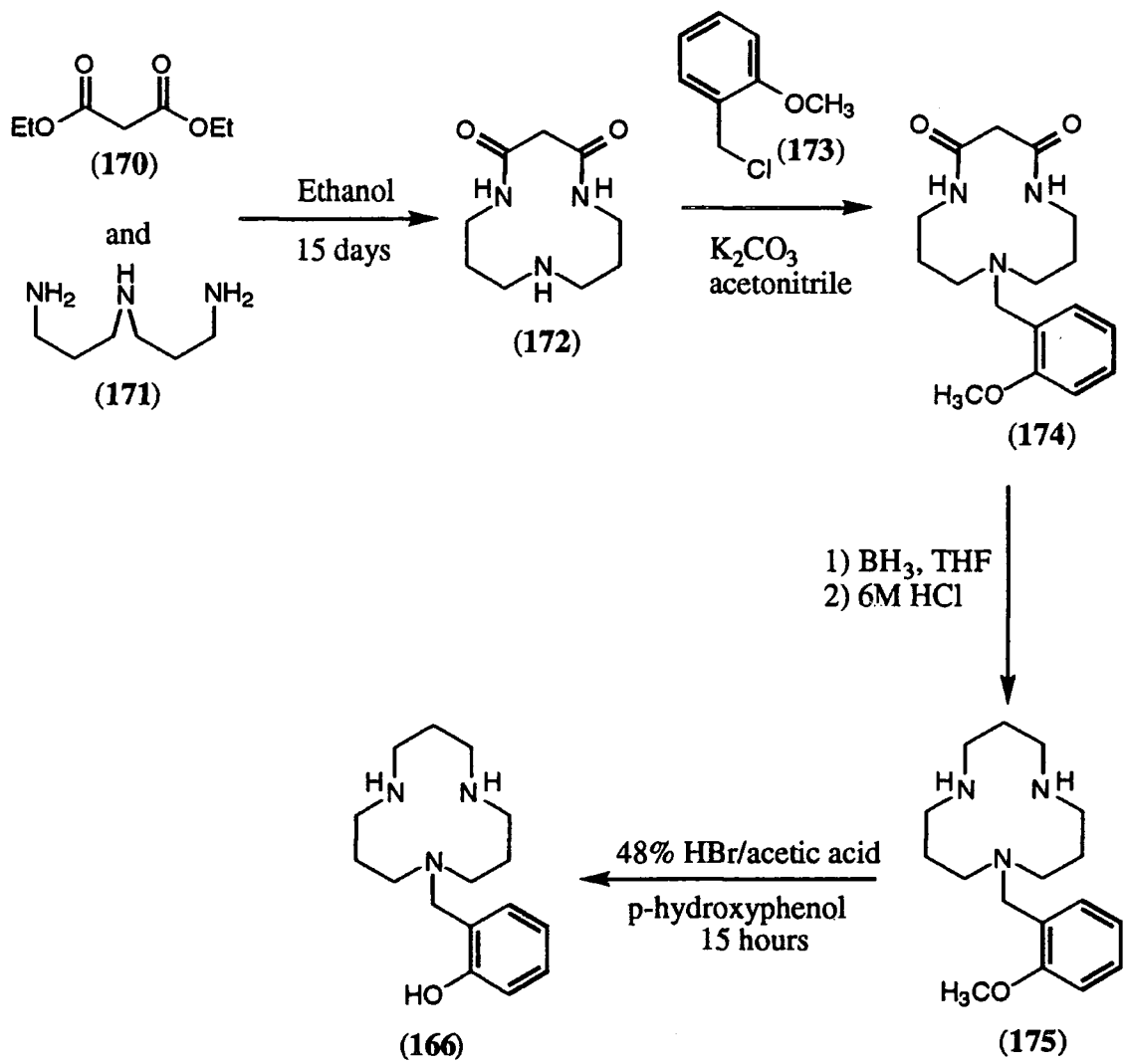

Fig. 4.6 Synthetic route to N-substituted $12N_3$ (**166**) ligand.

4.2.2 Synthesis of C-substituted $12N_3$ (167).

C-Benzyl substituted diethyl malonate esters have been used in $12N_3$ synthesis using the medium dilution cyclization methodology outlined previously[4]. The substituted diethylmalonate ester (**176**) was synthesised from diethyl malonate (**170**) and ortho-methoxybenzyl chloride (**173**) in ethanol using sodium ethoxide as the base. The substituted malonate (**176**) was a high boiling point liquid that was purified by vacuum distillation (0.05 mmHg, 125-127°C) to give a clear oil. The malonate was envisaged to be used as outlined in Fig. 4.7.

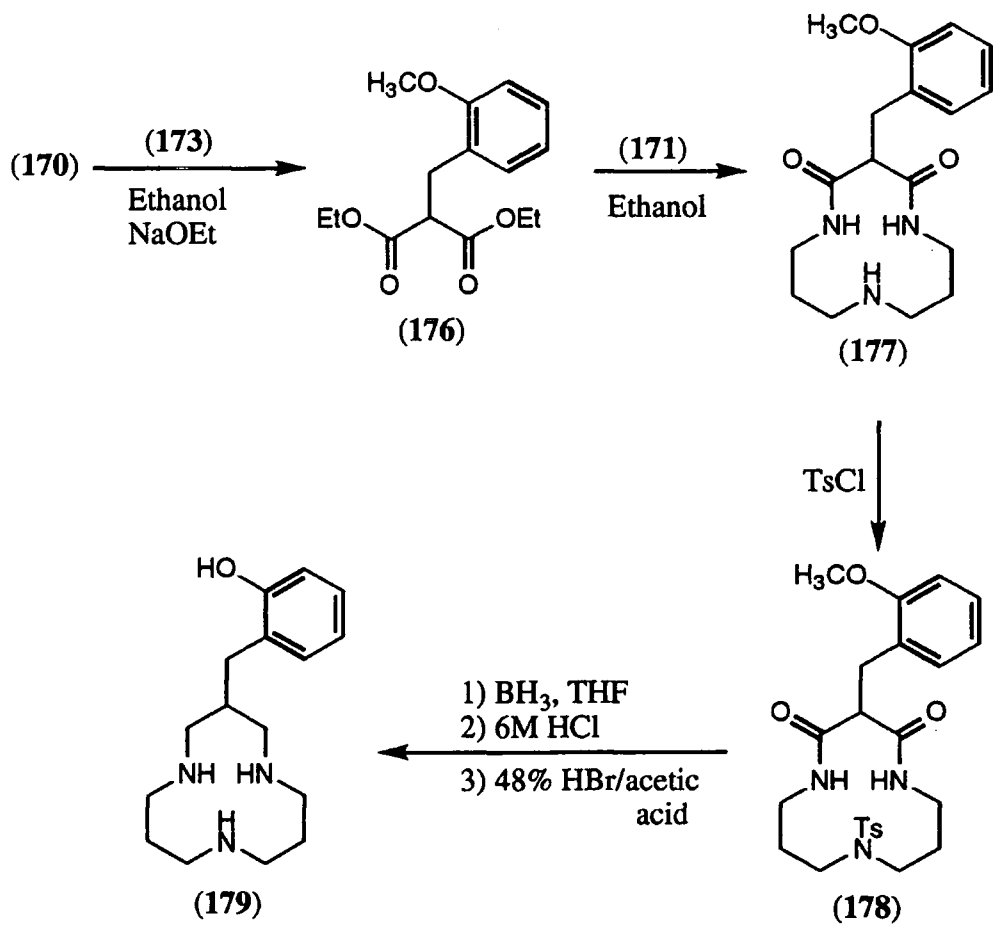

Fig. 4.7 Proposed synthesis of C-substituted $12N_3$ (**179**) via substituted malonate cyclization.

Cyclization of the substituted diethylmalonate ester (**176**) with the triamine (**171**) in a medium dilution reaction after 40 days only resulted in a low yield (2.2%) of the desired C-substituted $12N_3$ (**177**). The major compound isolated from column chromatography was the half cyclized material (**180**) (Fig. 4.8).

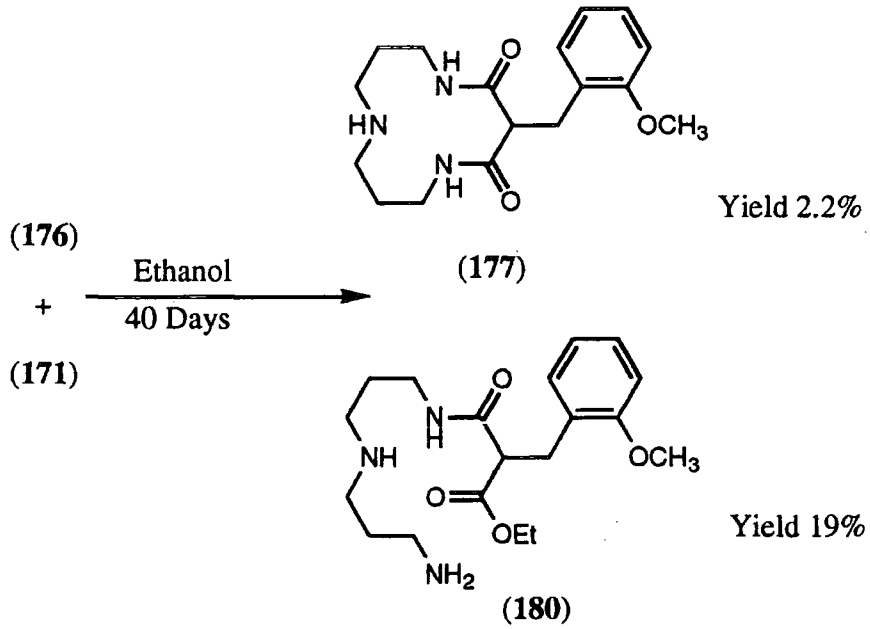

Fig. 4.8 Compounds isolated (**177**) and (**180**) from cyclization.

Metal ions are often used as templates in cyclization reactions, however there are no obvious metal cations for this example. Acetonitrile as the solvent may favour the second condensation. After boiling the half-cyclized material (**180**) in acetonitrile for a further seven days no appreciable amount of desired product (**177**) could be detected. Oligomerisation was seen to be occurring. The presence of the ortho methoxy group on the benzene ring had a steric influence, which resulted in the second cyclization being rate limiting and hard to achieve. Mono-tosylation to give (**178**) prior to reduction would have been necessary to prevent a stable 12N$_3$-borane complex being generated on borane reduction. Even though a small amount of material was isolated the synthesis as outlined (Fig. 4.7) was not taken any further because not enough of the final desired ligand would have been produced.

A higher yielding cyclization reaction was used to synthesise the desired ligand in usable amounts. 'Anionic' nitrogen is a better nucleophile than neutral nitrogen and an O-tosyl group is a good leaving group in S_N2 displacement. The synthesis was carried out as outlined in Fig. 4.9.

Ester reduction using lithium aluminium hydride in diethyl ether gave the diol (**181**) as a clear oil in 87% yield after an aqueous workup and dichloromethane extraction from the lithium and aluminium salts. Proton NMR analysis indicated the diol was of sufficient purity to be used without further purification. The diol (**181**) was dissolved in dry pyridine and at -20°C a pyridine solution of tosyl chloride was slowly added. The reaction was maintained at -18°C for three days, the reaction course was visually monitored by the production of pyridine-hydrochloride crystals. Adding the mixture to ice-water resulted in crystallization of the ditosylate (**182**), which was collected by filtration and washed with dilute hydrochloric acid to remove residual pyridine. An analytical sample was prepared by recrystallization from toluene giving

needle-shaped crystals. The tritosylamide (**183**) was prepared by tosylation of the triamine (**171**) in a mixed solvent system (THF and water) with potassium carbonate as the base. The tritosylamide (**183**) was extracted from the organic/aqueous mixture and concentrated. Recrystallization from toluene gave the product as a fine white solid. The mixed solvent method is more convenient than using large volumes of pyridine.

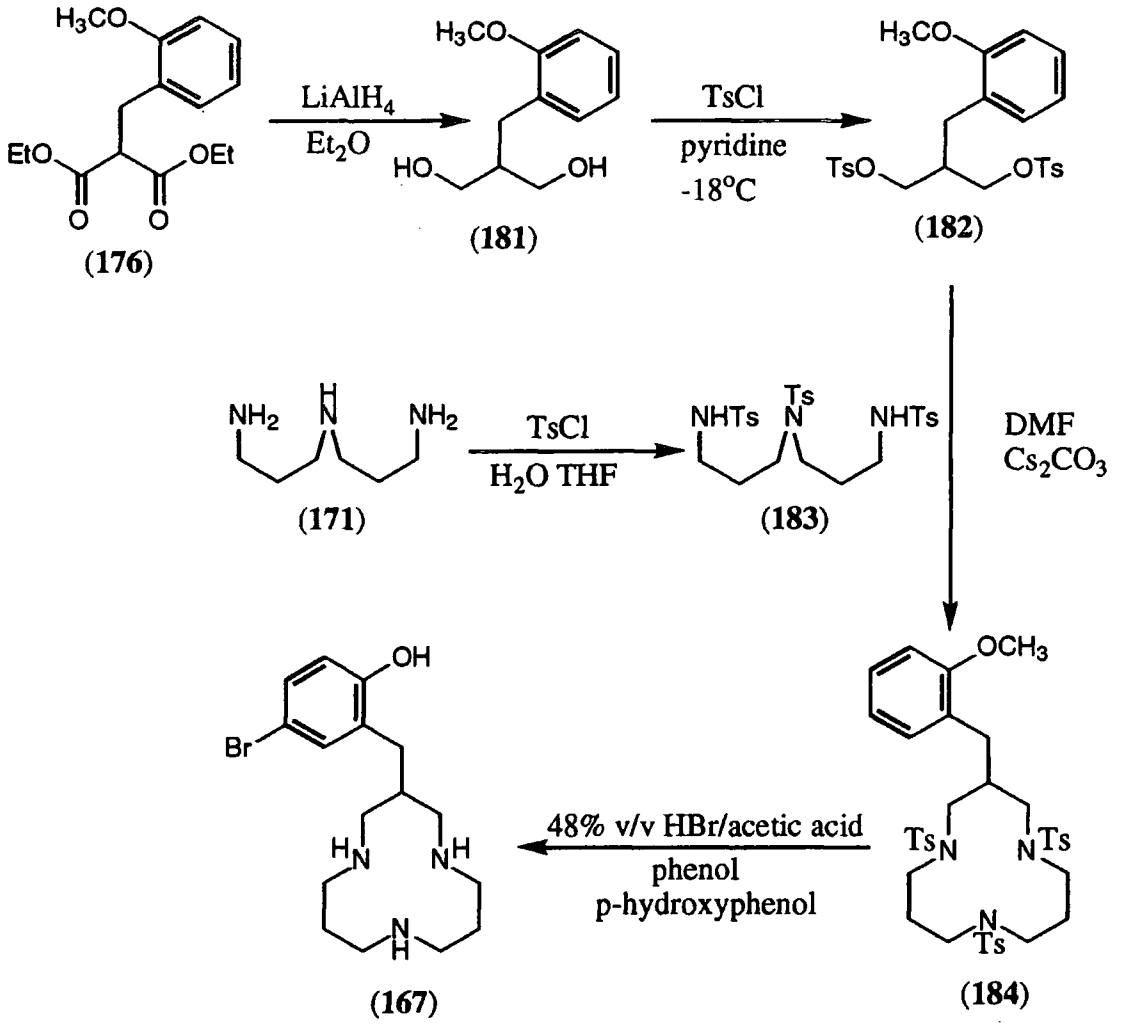

Fig. 4.9 Synthesis of C-substituted $12N_3$ (**167**) via tosylates.

The cyclization reaction was performed in dry DMF using two equivalents of caesium carbonate as the base. Once the nitrogen anion was formed cyclization proceeded via an S_N2 reaction. It was possible to monitor the formation and subsequent reaction of the half-cyclized material by tlc. The caesium cation played an active role in the cyclization. It is large and very polarizable therefore it will be poorly solvated in good coordinating solvents such as DMF. This makes the caesium ion form in close proximity to its counter anion hence promoting intra as opposed to intermolecular reactions[18]. Its large surface promotes the S_N2 displacement of OTs on its surface with the NTs and CH_2OTs centres being brought close together. After five days the solvent was removed by distillation and the $12N_3$-tritosylamide (**184**) was purified by extraction and recrystallization from toluene to give the desired product (**184**) in

moderate yield (27%). The yield was on the low side from what can be expected from tosylate cyclization reactions. This observation and the fact the first route produced very little product would suggest that this macrocyclic ring is perhaps rather difficult to form.

Detosylation using boiling 48% v/v hydrobromic acid in acetic acid worked efficiently and the methoxy group was also removed. The major isolated product (**167**) had a bromine atom para to the hydroxyl group. Performing the detosylation in the presence of a large excess of phenol with or without para-hydroxyphenol as a radical scavenger still resulted in bromine addition. The presence of bromine para to the phenol group had the effect of lowering the phenol pK_a, with the result that binding should occur more readily. Purification from ethanolic hydrochloric acid crystallization and subsequent reverse phase HPLC gave the desired ligand as a trifluoroacetate salt.

Alternative methods of detosylation are known. The use of lithium in liquid ammonia[19] was not used because of the probability of the partial reduction of the methoxybenzene ring. Detosylation with boiling 7:3 v/v perchloric acid/ acetic acid[20] resulted in only partial detosylation as indicated by ^1H NMR and MS analysis, complete detosylation only occurred in a very low yield.

4.3 Aqueous speciation by potentiometric titrations

Ligand solutions (N-linked (**166**) and C-linked (**167**) macrocycles, 50ml, 0.001M) were prepared in an ionic background of 0.1M tetramethylammonium nitrate as before (section 3.3 page 86). Potentiometric titrations were carried out using the same procedure as described in chapter three (page 86) to obtain titration curves for the ligand and the ligand-metal mixtures (M = Ni, Cu, Zn).

4.3.1 pK_a Determination

Plotting a graph of solution pH against volume of base added clearly shows that the two ligands, (**166**) and (**167**) have different pK_a values (Fig. 4.10). During preparation of the ligand solution more inorganic acid was added to the C-linked (**167**) macrocycle sample than the N-linked (**166**) macrocycle solution. The offset of the end points (first vertical portion of the titration curve) was a reflection of this different initial acidity.

Each ligand will have four pK_as as there are four sites susceptible to protonation (three nitrogens and the phenol). However they are not all measurable using this method. Acidity constants that are either too low (<2) or too high (>12) are unable to be measured because they lie outside the working pH range of this technique. Analysis indicated that the N-linked macrocycle (**166**) only had two determinable pKa values while C-linked macrocycle (**167**) had four (Table 4.1 and Fig. 4.11).

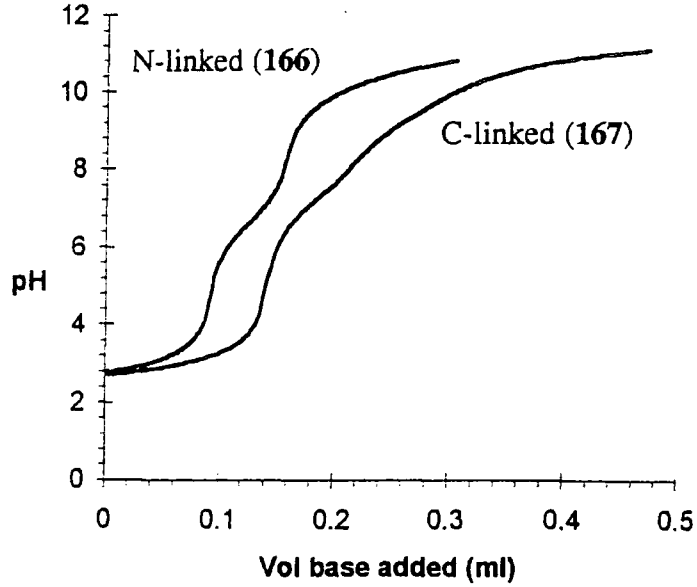

Fig. 4.10 Titration plots of the N-linked (**166**) and C-linked (**167**) macrocyclic ligands.

Ligand	pK_1	pK_2	pK_3	pK_4
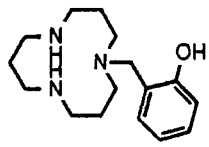 N-linked macrocycle (**166**)	>12	9.87	6.64	<2
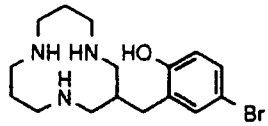 C-linked macrocycle (**167**)	10.1	8.72	6.92	2.55
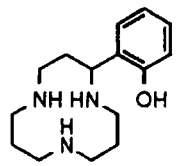 Kimura' ligand (**6**)	>12	9.67	7.09	<2

Table 4.1 Ligands (**166**), (**167**) (298K, H_2O, I = 0.1 NMe_4NO_3) and Kimura's (**6**) pK_a values.

The first, third and fourth protonation constants correspond to ring protonations while the second pK_a is that of the phenol. The variation in values can be explained by the different ligand structures. The N-linked macrocycle (**166**) behaves like Kimura's ligand[7] (**6**). The first and fourth protonation constants were not measurable. The phenol protonation constant (pK_2 = 9.87) is slightly below that of phenol (pKa = 10) indicating that there was only a minor interaction between the phenol and the monoprotonated cyclic triamine. The difference between the pK_2 (9.67) of Kimura's ligand (**6**) and that

of the N-linked macrocycle (**166**) was only 0.2 log units indicating both phenols are behaving very similarly.

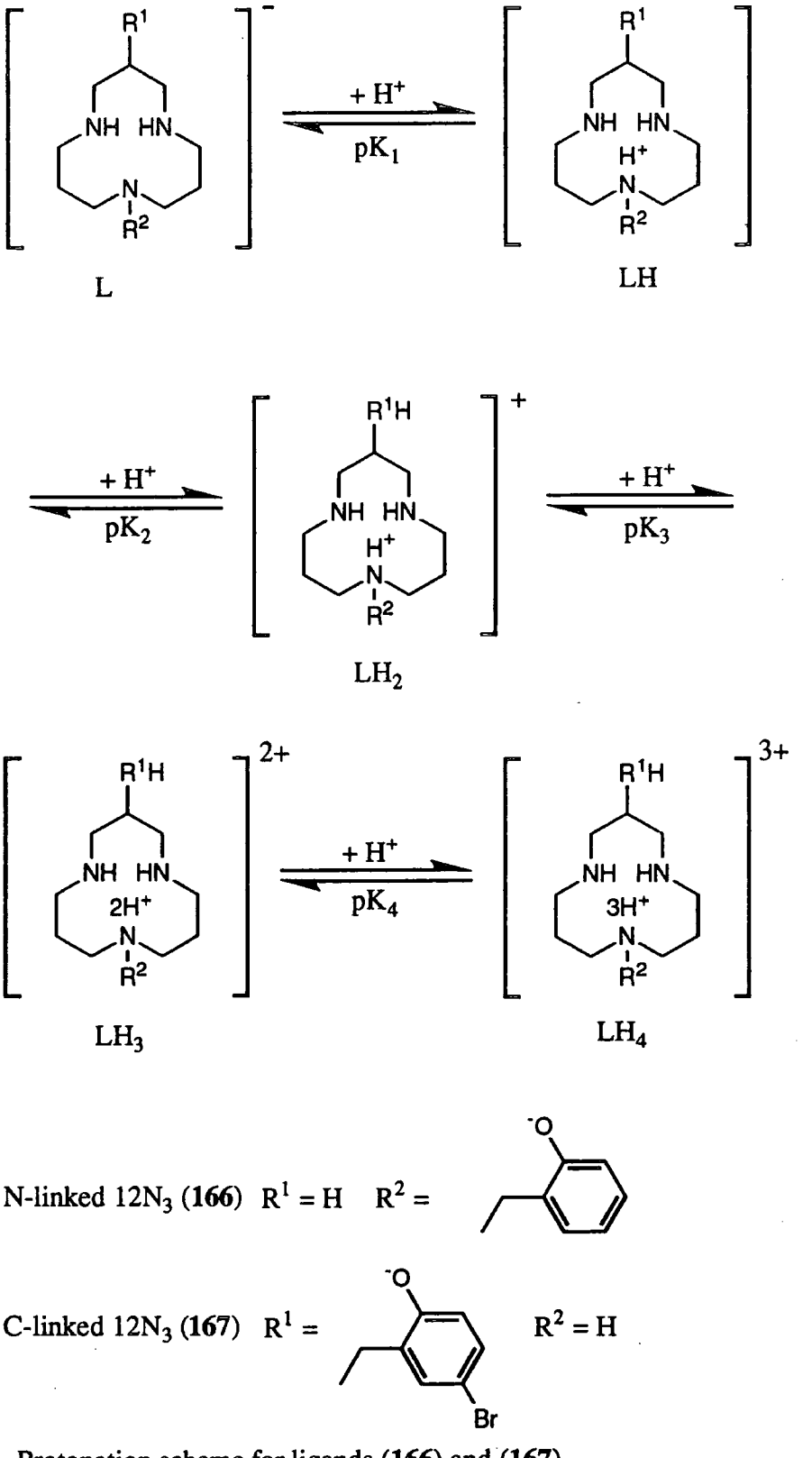

N-linked $12N_3$ (**166**) $R^1 = H$ $R^2 =$

C-linked $12N_3$ (**167**) $R^1 =$ $R^2 = H$

Fig. 4.11 Protonation scheme for ligands (**166**) and (**167**).

The C-linked macrocycle (**167**) behaved differently from Kimura's (**6**) and the N-linked macrocycle (**166**). All three nitrogen protonations were measurable; pK_1 was

lower than expected while pK_4 was higher. This would be consistent if the ring was unable to obtain its conformationally preferred geometry of chair-chair-chair. If a higher energy conformation is favoured all three nitrogens may be further from each other so enabling protonation of the last nitrogen to occur at a higher pH. Likewise if the ring was unable to adopt a conformation that allowed the first proton to reside symmetrically in the ring between all three nitrogens, then this protonation state would not be as stabilized as in $12N_3$ (**43**) and its pK_a would be lowered. Such behaviour can be seen in comparing the pK_as of the two azamacrocycles, $12N_3$ (**43**) and $13N_3$ (**186**). The latter (**186**) is unable to adopt such a favourable geometry as $12N_3$ and as a result the first protonation constant is depressed while the third is elevated (Table 4.3). Likewise with an α,α'-dimethyl-C-substituted $12N_3$ ligand (**185**) when compared to $12N_3$ (**43**) there was a slight rise in pK_3 and a lowering of pK_1, i.e. the same trend to that seen with the C-linked macrocyclic ligand (**167**). As before, the ligand's phenolate pK_a was lowered to $pK_2 = 8.72$ compared to that of bromophenol (pKa = 9.35). Some interaction of the phenol with the ring nitrogens must have occurred in order to give such a change.

Ligand	pK_1	pK_2	pK_3
$12N_3$ (**43**)	12.60 [a]	7.57 [a]	2.41 [a]
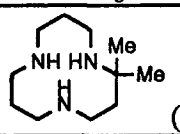 (**185**)	12.30 [b]	7.34 [b]	2.51 [b]
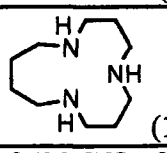 (**186**)	9.79 [b]	8.13 [b]	4.18 [b]

(a) 0.1M KNO_3, 298K; Reference1.
(b) Reference 2

Table 4.3 Protonation constants of $12N_3$ (**43**), (**185**) and $13N_3$ (**186**) (298K, H_2O, I = 0.1).

4.3.2 Metal-ligand stability constant determination

Metal-ligand complex stability constants were determined by pH potentiometric titrations as outlined in Chapter 3 (page 88). The individual ligand solutions (0.001M, I = 0.1 Me_4NNO_3) of the N-linked (**166**) and C-linked (**167**) macrocycles were tested with three metals (nickel, copper and zinc). From the titration curves and knowledge of the protonation constants, metal-ligand stability constants were determined using non-linear least squares analysis (Superquad and SCOGS). Both ligands formed complexes with all three metals and the determined stability constants are tabulated (Table 4.4). There are significant differences in the behaviour of the two ligands.

	Ni (II)		Cu (II)		Zn (II)	
	$logK_{ML}$	$logK_{MLH}$	$logK_{ML}$	$logK_{MLH}$	$logK_{ML}$	$logK_{MLH}$
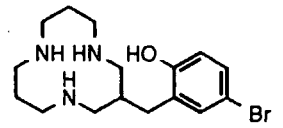 (**167**)	6.11	8.14	10.16	8.00	7.32	7.50
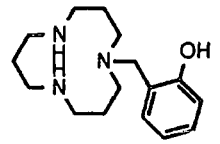 (**166**)	n.d.	n.d.	18.72	n.d.	14.1	n.d.

Table 4.4 Measured $logK_{ML}$ and $logK_{MLH}$ formation constants for N-linked (**166**) and C-linked (**167**) macrocycles (298K, H_2O, I = 0.1 Me_4NNO_3).

4.3.2.1 N-linked macrocycle (166) stability constants

For the N-linked macrocyclic ligand (**166**) a nickel [ML] stability constant could not be determined. The titration curve showed a ragged appearance at around pH 8 (Fig. 4.12), indicating that the measurements of nickel complexation were not taken at equilibrium. Increasing the 'delay-time' (time over which the pH electrode should read a steady value before the next base addition) of the syringe operator to fifty seconds (which effectively resulted in delays of fifteen to twenty-five minutes between 0.002ml additions) did not reduce the ragged appearance. More time would be required for the system to equilibrate. However, using this method it would not have been possible: there would have been unacceptably large errors associated with electrode drift and potentially solution evaporation as well as the need to control carbon dioxide absorption.

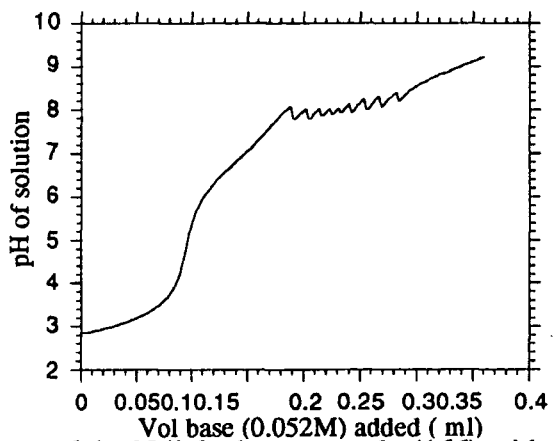

Fig. 4.12 Titration curve of the N-linked macrocycle (**166**) with nickel showing that beyond pH 8 equilibrium was not obtained.

With the copper and zinc titrations, only the value for [ML] formation could be determined with the required accuracy and reproducibility. Both titration curves were

analysed for the presence of an [MLOH] species (Eqn. 4.2), but with poor statistical reproducibility. The error associated with the [MLOH] formation constant had negligible effect on the [ML] stability constant because this equilibrium (Eqn. 4.1) occurs at a much lower pH than [MLOH] formation.

$$\text{Eqn. (4.1)} \quad M^{2+} + LH_n^{(n-1)+} \overset{K_{ML}}{\rightleftharpoons} ML^+ + nH^+$$

For the copper titration, metal hydrolysis constants for Cu(OH) and $Cu_2(OH)_2$ (LogK = -7.71 and -10.99 respectively) were included in the analysis. For zinc it proved impossible to analyse for any complexation constants when values for Zn(OH) or $Zn(OH)_2$ (logK = -5.11, -8.3 respectively) were included.

Overall the observed stability order was $\log K_{ZnL} < \log K_{CuL}$ and hence followed the Irving-Williams sequence. This order can be seen graphically by comparing the protonation titration with the metal-ligand titration curves (Fig. 4.13). The larger the [ML] stability constant the more the plateau region of the metal-ligand titration curve deviates from the protonation curve, i.e. the copper curve is below that of zinc between 0.1-0.21 ml of base added ([ML] formation region).

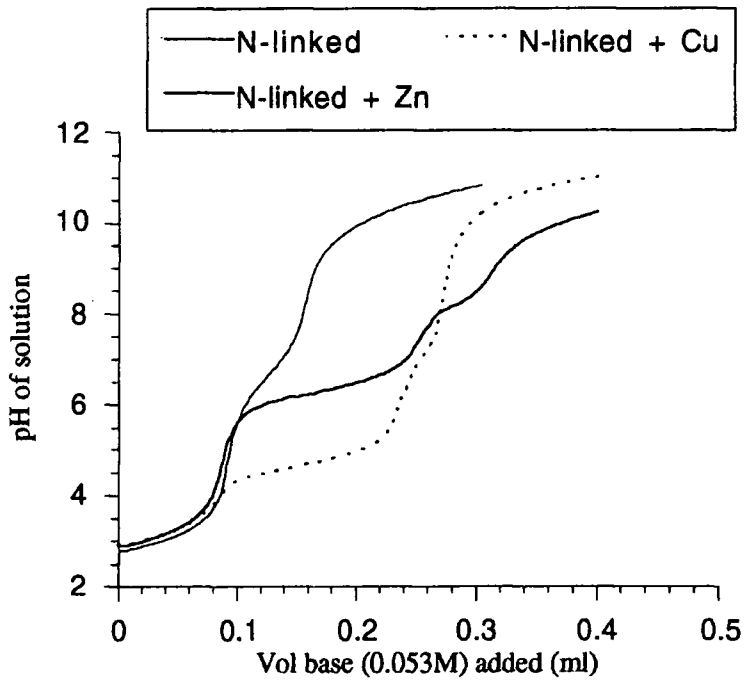

Fig. 4.13 Titration curves of N-linked macrocycle (**166**) and with Cu and Zn added.

The step at about 0.25 ml of base added probably corresponds to the generation of a hydrolysis product via proton dissociation (i.e. Eqn. 4.2). Similar curves are observed for $12N_3$ (**43**) interacting with copper and zinc[1].

$$\text{Eqn. (4.2)} \quad LM(H_2O)_x^+ \overset{K_a}{\rightleftharpoons} LM(OH)(H_2O)_{x-1} + H^+$$

4.3.2.2 C-Linked macrocycle (167) metal complex stabilities

Stability constants for [ML] and [MLH] formation could be determined for all three metals. Again nickel needed the longest delay time to allow equilibrium and pH stabilization to be attained. The $\log K_{ML}$ values follow the order Cu (II) > Zn (II) > Ni (II). The stability constant for [ZnL] is larger than for [NiL] but this can be seen with many ligands and is not so unusual[2]. All three metal titrations analysed for an [MLH] constant, corresponding to the phenol being protonated in the complex. Thus all three metals react with the protonated ligand to form an [MLH] species which subsequently loses a proton with increasing basicity (Eqn. 4.3).

Eqn. (4.3) $LH_3^{2+} + M^{2+} \underset{}{\overset{\log\beta_{(MLH)}}{\rightleftharpoons}} MLH^{2+} \underset{pK_{a(MLH)}}{\overset{\log K_{a(MLH)}}{\rightleftharpoons}} ML^{+} + H^{+}$

$\log K_{(ML)}$

With the [MLH] species the ligand is acting as an N_3 tridentate ligand with the protonated phenol not interacting. All the pK_{MLH} values are of similar magnitude and follow the order Ni (II) > Cu (II) > Zn (II) (pK_{MLH} 8.14, 8.0, 7.5 respectively). On phenol deprotonation the stability of the metal-ligand complex alters. Copper forms the most stable complex followed by zinc then nickel i.e. $\log K_{ML}$ Cu (10.16) > Zn (7.32) > Ni (6.11).

All of the values for the equilibrium constants are relatively small. The phenol only interacted with copper, producing a slightly more stable complex. With zinc and nickel there is no indication of phenol interaction and deprotonation actually reduces the stability of the metal-ligand complex. This may be a result of a conformational change in the N_3 donor set as the deprotonated phenol would take up a different geometric position.

The presence of [ML(OH)] species could be determined, but in each case the values determined were of low reproducibility. This was partially due to the expected presence of polyhydroxy and polymeric hydrolysed species (e.g. $[ML(OH)_2]$, $[M_2L_2(OH)]$). Only with copper was the analysis performed with metal hydrolysis constants included. For both zinc and nickel complex constants could not be obtained when metal hydroxide constants were included in the analysis.

Overall stability constants for metal-ligand complexes followed the Irving-Williams sequence Cu (II) > Zn (II) > Ni (II). This can be graphically observed from the titration curves (Fig. 4.14). Even though the nickel-ligand experiment appeared to be in equilibrium, it should be noted that with other cyclic triamines equilibrium was achieved over longer times (one hour for Kimura's ligand (**6**)[7], three to four months for $9N_3$-$12N_3$ systems [1]).

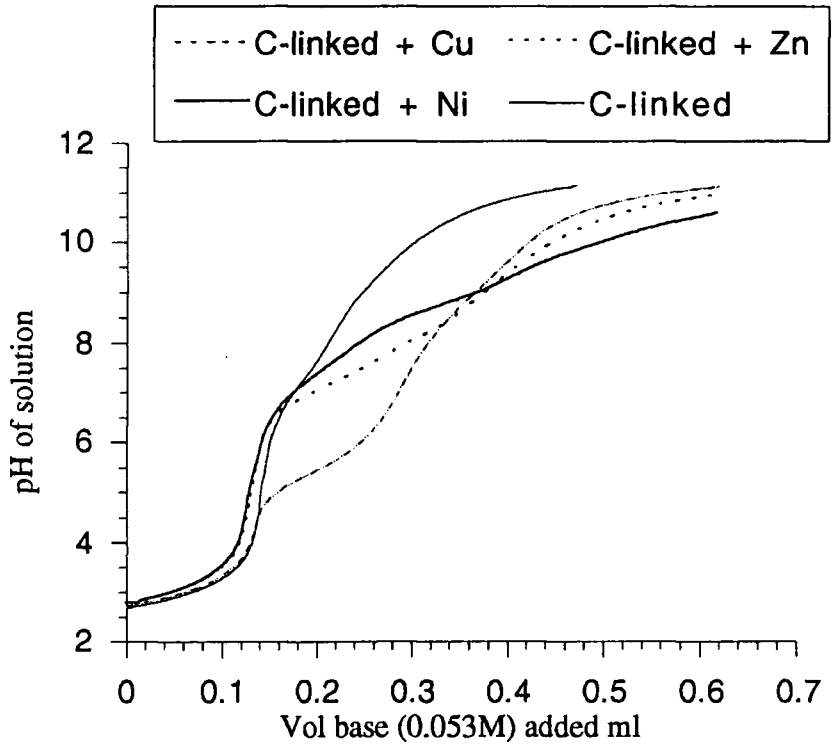

Fig. 4. 14 Titration curves of the C-linked macrocycle ligand (**167**) alone and with copper, nickel and zinc present (298K, H_2O, I = 0.1).

4.3.2.3 Comparison of $12N_3$ ligands

The N-linked (**166**) and C-linked (**167**) macrocycles behave quite differently, with the first being similar to Kimura's ligand (**6**). The N-linked macrocycle (**166**) has similar protonation constants and $logK_{CuL}$ value to Kimura's (**6**) (Table 4.5). Binding to zinc was stronger with an increase in the stability constant of 1.5 log units. This would suggest that the phenol pendent group was interacting with the metal to a greater degree than with Kimura's ligand (**6**).

	pK_2	pK_3	$logK_{NiL}$	$logK_{CuL}$	$logK_{ZnL}$
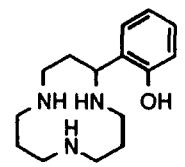 (**6**)	9.67	7.09	14.00	18.4	12.6
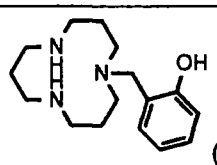 (**166**)	9.87	6.64	n.d.	18.72	14.1

Table 4.5 Protonation and $logK_{ML}$ constants of N-linked macrocycle (**166**) and Kimura's (**6**) ligand (298K, H_2O, I = 0.1), (n.d. = not determined).

The C-linked macrocycle ligand (**167**) behaved differently. For all three metals an [ML] and [MLH] formation constant could be measured. This indicated that the phenol was interacting poorly with the metal. The $logK_{ML}$ values are of similar magnitude to unsubstituted $12N_3$ (**43**) suggesting that the ligand is behaving only as an N_3 donor. Carbon substitution with a non-interacting group is known to reduce metal-ligand stability constants as can be seen with α,α'-dimethyl-$12N_3$ (**185**) which has lower [ML] stabilities than for $12N_3$ (**43**) (Table 4.6).

	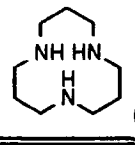 (43)	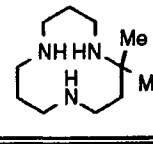 (185)	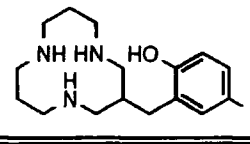 Br(167)
$logK_{NiL}$	10.9	9.8	6.1
$logK_{CuL}$	12.6	11.6	10.2
$logK_{ZnL}$	8.8	7.7	7.3

Table 4.6 Metal-ligand stability constants of $12N_3$ based ligands (298K, H_2O, I = 0.1).

There was an interesting difference between the colour of the copper complexes of the N-linked (**166**) and C-linked (**167**) macrocycles. With the N-linked macrocycle (**166**) the solution was light yellow in colour while the C-linked macrocycle (**167**) was blue. On standing in a sealed container for fourteen days there was no observable change in colour for either complex. The yellow colour of the N-linked macrocycle-copper complex may imply there is a degree of charge transfer from the phenol to the copper imparting copper (I) character (copper (I) normally forms yellow or colourless complexes depending on the nature of the donor set). The ligand's donor set could accommodate copper (I) which normally binds in a tetrahedral manner.

4.4 Speciation by ^1H NMR titrations

Given the observation of the variation in colour between copper complexation with the N-linked macrocycle (**166**) (which was yellow) and the C-linked macrocycle copper complex (blue), the possibility that the copper was being reduced to a copper (I) species with the N-linked macrocycle (**166**) ligand was further investigated. It is known that copper (I) binds in a tetrahedral geometry usually to soft donors[2]. If it bound to a triaza system with a high stability constant it would be most unusual. Copper (I) perchlorate is stabilized with four coordinated acetonitrile molecules. To prevent rapid copper (I) disproportionation to copper and copper (II) the NMR experiments were performed in deuterated acetonitrile. The different solvent conditions between the aqueous and ^1H NMR titrations of course mean that a direct numerical comparison. cannot be made. Ligand complexation to zinc (II) was also investigated by ^1H NMR. This acts as a further comparison with the copper (I) experiment.

The initial protonation state (i.e. the protonation state of the ligand before any metal is added) of the ligand may be of greater importance in the acetonitrile NMR titration than in the aqueous titration because of the increased difficulty in transferring a proton to acetonitrile than to water. The protonation state of the ligands was initially set in an aqueous solution with the pH being varied with either hydrochloric acid or sodium hydroxide respectively to final values of pH 7 and pH 10. Vacuum drying of the ligand gave the desired protonated ligand (this will be referred to as the 'initial protonation state'). The N-linked macrocycle (**166**) was tested with zinc and copper (I) at pH 7 and pH 10 'initial protonation states', while the C-linked macrocycle (**167**) was only tested with zinc at pH 7. As a control, the unsubstituted $12N_3$ (**43**) ligand was tested with zinc and copper (I) at pH 7 'initial protonation state'. The resonances that were monitored and subsequently used in plotting a titration curve ($\Delta\delta_H$ verse M/L ratio) were dependent on the ligand studied.

4.4.1 Comparison of N-linked macrocyclic ligand (166) ^{1}H NMR spectra at pH 7 and pH10 'initial protonation states'

The ligand (**166**) spectra at M/L=0 differed slightly according to the 'initial protonation state' (Fig. 4.15).

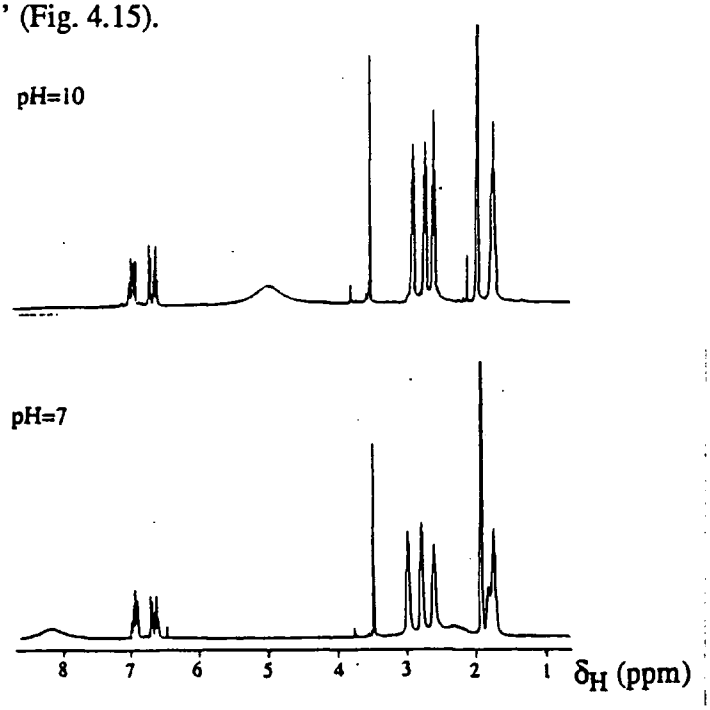

Fig. 4.15 ^{1}H NMR of N-linked macrocycle ligand (**166**) in different protonation states.

At pH 7, the three sets of triplets corresponding to the ring NCH_2 groups were less well defined than those at pH 10. There were two distinct types of $CH_2CH_2CH_2$ resonances at pH 7, while at pH10 these tended to merge into one 'set' of signals. The broad NH resonance occurred at δ = 8.5ppm at pH 7 and at δ = 5.1ppm at pH 10. These variations can be attributed to the different ring protonation states. At pH 10 the

molecule has a single proton in the ring and the phenol is ionized, while at pH 7 the ring is diprotonated. The monitored resonance was the singlet due to the $ArCH_2$ methylene signal, as this was a sharp singlet and was well-separated from the other resonances.

4.4.2 Zinc titrations

4.4.2.1 N-Linked macrocycle (166) titration at pH 7 'initial protonation state'

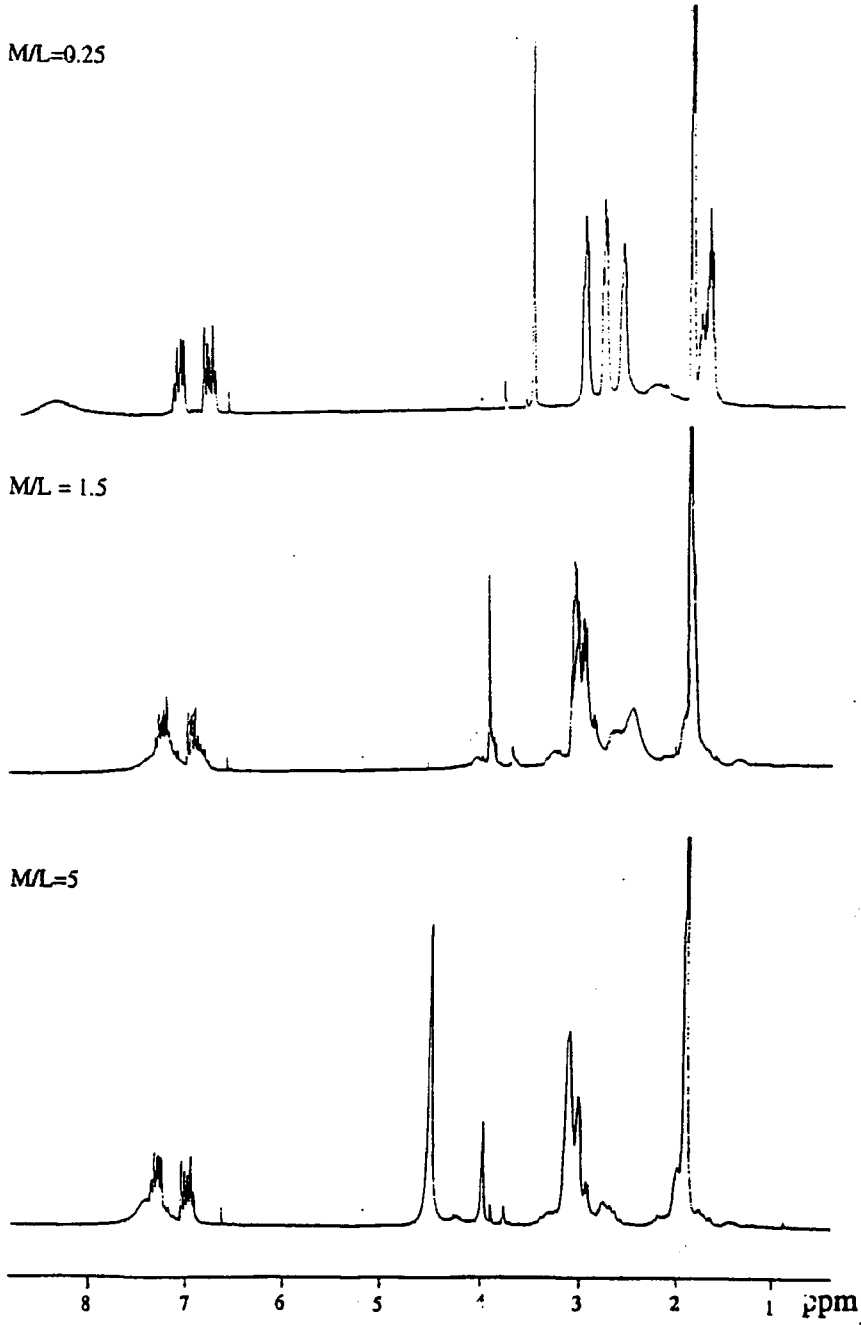

Fig. 4.16 Zinc-N-linked macrocycle (**166**) ^1H NMR titration spectra.

With increasing M/L ratio, there was a shift in the $ArCH_2$ methylene resonance to higher frequency. There was an increased line broadening and a shift to lower

frequency of the broad NH resonance. At M/L ratios of 0.75 and higher, a second set of resonances corresponding to another species could be observed which were broader in form with poorly defined splitting patterns. The relative intensity of these signals increased to a maximum at M/L=1.5, after which there was no change in intensity compared to the other signals. The three NCH_2 resonances showed a lot of variation with M/L ratio. Going from M/L=0 to M/L=1.5 there was a merging of these signals into two 'sets' of resonances, splitting could still be observed. At higher M/L ratios the splitting pattern was lost but there was no more coalescence of the signals.

With increasing M/L ratios a resonance corresponding to water was observed, which grew in intensity and shifted to higher frequency as more zinc triflate was added (Fig. 4.16). Plotting $\Delta\delta_H$ ($ArCH_2$) verus M/L ratio gave an S shaped curve (Fig. 4.19) consistent with the presence of more than one species in solution, in agreement with what is observed in the ^1H NMR spectra .

4.4.2.2 N-Linked macrocycle (166) titration at pH 10 'initial protonation state'

Again relatively complicated behaviour was observed which was similar in nature to that seen with the ligand at pH 7 initial protonation state. At M/L=0.2 there was a greater change in the spectrum than at pH 7 (M/L=0.25). A second species could be clearly seen with the aromatic signals showing a clear splitting pattern (Fig. 4.17). The broad NH resonance shifted to higher frequency to the same position as in the previous experiment (pH 7). With increasing M/L ratio this resonance behaved identically as before.

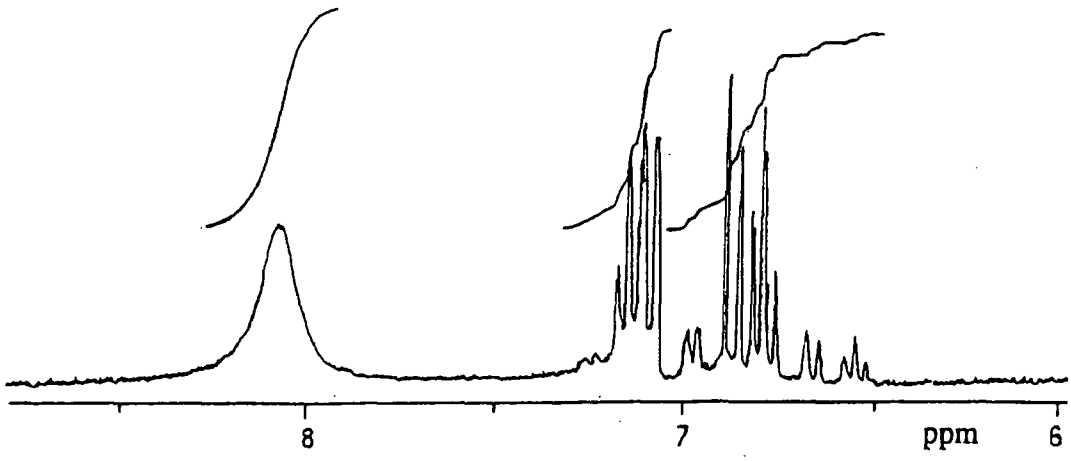

Fig. 4.17 ^1H NMR spectrum of N-linked macrocycle (**166**) and zinc M/L=0.2

The methylene $ArCH_2$ resonance was again monitored and showed a shift to higher frequency with increasing M/L ratio. The relative amount of the second zinc bound species increased to a maximum at M/L=1, but the unbound ligand was still present as the major species. The aromatic signals tended to merge and overlap

resulting in the loss of a clear indicator of the degree of metal bound complex. At higher M/L ratios the relative percentage of the bound zinc-ligand complex did not increase and as before there were large shifts in the unbound ligand. There were very small changes in the bound species with increasing M/L ratio. The final spectrum at M/L=5 was very similar to the spectrum obtained with the ligand at pH 7 'initial protonation state'. This would indicate that the same species distribution was present in both experiments. Again an S-shaped curve was produced when $\Delta\delta_H$ ($ArCH_2$) was plotted against M/L ratio (Fig. 4.19).

4.4.2.3 $12N_3$ Ligand (43) titration at pH 7 'initial protonation state'

At pH 7 the $12N_3$ (**43**) ligand was approximately mono-protonated. The initial $12N_3$ spectrum was very simple when compared to the N-linked macrocycle (**166**). Three sets of signals were present, corresponding to the NH (δ = 5.9 ppm), NCH_2 (δ = 2.81 ppm) and $CH_2CH_2CH_2$ (δ = 1.69 ppm) resonances. There was also a significant amount of water present. The shift in the NCH_2 resonance was monitored as a function of zinc addition (Fig. 4.19). With increasing M/L ratio there was a general shift to higher frequency as with the previous ligand. At M/L=0.5 a bound metal-ligand species was observed with sharp resonances. The unbound ligand resonances showed a loss in splitting pattern and slight broadening. The relative amount of this bound ligand increased at the expense of the unbound ligand up to a maximum at about M/L=1, after which there was no change. Again the ('water') resonance showed a large shift to higher frequency after M/L=1. As before an S-shaped curve was produced with increasing M/L ratio (Fig. 4.19).

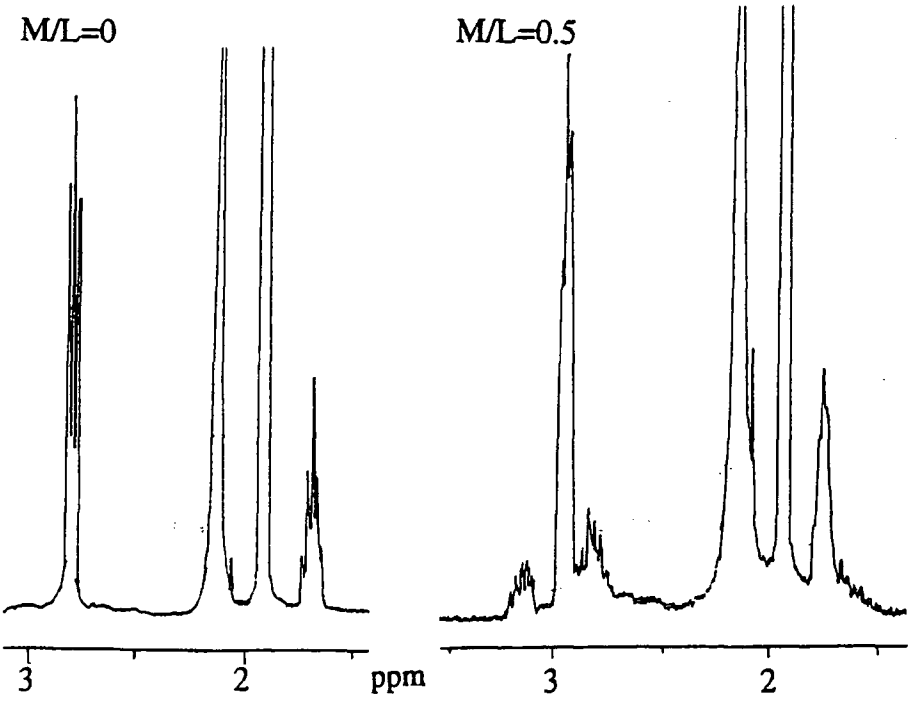

Fig. 4.18 ^1H NMR spectra of the$12N_3$ (**43**) ligand with zinc addition.

4.4.2.4 Comparison of ^{1}H NMR titration results

All three of the ^{1}H NMR titrations can be compared together (Fig. 4.19) and a number of comments made. No K_{ZnL} values could be determined for 1:1 binding because of the form of the graph and the presence of at least two species. From a visual inspection, it was not possible to tell which ligand binds zinc more strongly.

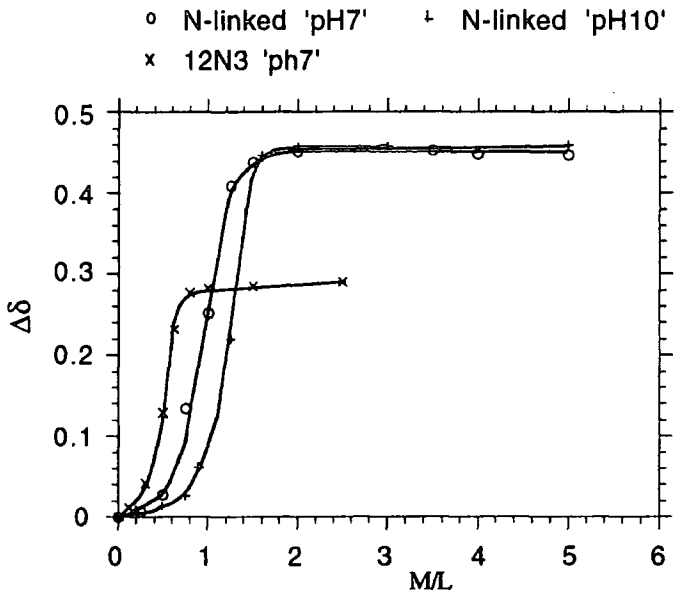

Fig. 4.19 Combined ^{1}H NMR titration graphs of zinc addition to $12N_3$ (**43**) and N-linked macrocycle (**166**).

Comparing the behaviour of the N-linked macrocycle ligand (**166**) at the two 'initial protonation states' it is evident that at pH 10, the metal complex was first produced at a lower M/L ratio (M/L=0.2 at pH 10 and between M/L 0.25-0.5 for pH 7). The monitored resonance also reached its maximum shift at a slightly lower M/L ratio for pH 10 (M/L=1.25) compared to M/L=1.5 for pH 7. The same limiting shift was observed at both 'initial protonation states' studied. The integrations were not precise enough to allow a good comparison of the amount of each complex species to be compared between the different titrations. Under conditions of fast exchange in the NMR time-scale the stability constant is an approximate function of the steepness of the curve prior to levelling off. Using this knowledge and other factors being similar (i.e. concentration and limiting shift) the vertical line section of the pH 10 curve was slightly steeper than for pH 7 indicating a higher stability constant. All these observations can be related to the difference in protonation state. As not all of the ligand was used in forming a bound complex and there was a levelling off at just over M/L=1 this may indicate that the build up of acid in the solvent caused ligand protonation and inhibited further metal binding. Beyond the ratio M/L=1, the large $ArCH_2$ resonance shift may be

due to ligand protonation rather than fast exchange between unbound ligand and complex. This would explain why at M/L=1 the ligand at pH 7 showed a larger $ArCH_2$ methylene shift than that at pH 10 as there would have been more 'free' acid in the solvent.

At pH 7 'initial protonation state'

$$LH_2^+ + Zn^{2+} \overset{K_1}{\rightleftharpoons} [LZn]^+ + 2H^+$$

$$\text{then } LH_2^+ \overset{H^+}{\rightleftharpoons} LH_3^{2+}$$

At pH 10 'initial protonation state'

$$LH + Zn^{2+} \overset{K_1}{\rightleftharpoons} [LZn]^+ + H^+$$

$$\text{then } LH \overset{H^+}{\rightleftharpoons} LH_2^+ \overset{H^+}{\rightleftharpoons} LH_3^{2+}$$

Fig. 4.20 Possible ligand (**166**) protonation and binding equilibria with zinc.

As more acid was displaced following metal binding the amount of fully protonated ligand increases eventually inhibiting further zinc binding. Overall $K_1 > 10^5$ as a stable metal bound complex, on the NMR time-scale was observed in the ^1H NMR.

The curve for zinc binding to 12N$_3$ (**43**) began to level off before M/L=1 while for the N-linked macrocycle (**166**) this was after M/L=1. This could be an indication that the 12N$_3$ ligand was forming an [ML$_2$] species rather than an [ML] species.

4.4.2.5 C-Linked macrocycle (167) titration at pH 7 'initial protonation state'

The sample used for the ^1H NMR titration was contaminated with about 5% C-linked macrocycle ligand without the bromine present. Within the accuracy of the experiment this slight contamination of a very similar material would have a negligible effect.

At M/L=0, a broad NH resonance ($\omega_{1/2}$ = 180Hz) resided at δ = 7.9 ppm. With increasing M/L ratio there was a shift to lower frequency of this signal and a sharpening after M/L=1 ($\omega_{1/2}$ = 20Hz, δ = 6.97ppm at M/L=2). At no M/L ratio was there evidence in the aromatic region of a second bound metal-ligand complex. In the aliphatic region there was the appearance of other signals with M/L > 0.2, however they were only of low intensity and their relative amount never increased significantly with more zinc added. There was however a slight sharpening of these signals with increasing zinc addition. All the shifts of the unbound ligand were small in magnitude. It was not possible to obtain titration curves that allowed analysis for a 1:1 metal-ligand binding stoichiometry using either the NCH_2 or $ArCH_2$ resonances. Using one of the aromatic resonances (proton H-6), analysis of the titration curve for a 1:1 complex gave an estimated value of $K_{ZnL} = 6.3 \times 10^3$ (at 298K, CD_3CN).

The absence of a separate set of aromatic resonances would indicate that the phenol was not involved in zinc complexation. The stability constant refers to Eqn 4.4.

$$\text{Eqn. (4.4)} \qquad LH_3^{2+} + Zn^{2+} \overset{K_1}{\rightleftharpoons} [LZn]^{+} + 3H^{+}$$

Not fully defined

4.4.2.6 Comparison with N-linked macrocycle (166) and parent $12N_3$ (43) ligands

There was a marked difference in the behaviour between the N-linked macrocycle (**166**) and $12N_3$ (**43**) ligands to that of C-linked macrocycle (**167**). Both (**166**) and (**43**) formed relatively stable metal complexes which were in slow exchange with the free ligand on the ^1H NMR time-scale, i.e. $\log K_{ZnL} > 10^5$. The titration curves of (**166**) and (**43**) indicated the presence of other equilibria in solution and hence 1:1 metal binding stability constants could not be determined. With the C-linked macrocycle (**167**) a weak zinc-ligand complex was generated with $K_{ZnL} = 6.3 \times 10^3$. This result suggests that the C-linked macrocycle (**167**) was a poorer donor to zinc than the other two ligands (**166**) and (**43**) and may not form a well defined tetrahedral complex.

4.4.3 Copper (I) titrations

The copper (I) salt, $Cu(CH_3CN)_4ClO_4$ was recrystallized from dry acetonitrile to remove any traces of copper (II) salts prior to use. Any copper (II) present would have a detrimental effect on the accuracy of the ^1H NMR titration, either by causing line-broadening or by inducing a paramagnetic shift. This could be a great problem if only small shifts were recorded. The NMR spectrum of the recrystallized copper (I) salt gave a sharp singlet (CH_3CN, $\omega_{1/2} < 2Hz$) indicating no copper (II) species.

4.4.3.1 N-Linked macrocycle (166) titration at pH 7 'initial protonation state'

NMR Samples were run within two minutes of adding the copper (I) salt and mixing. The shift to higher frequency of the methylene $ArCH_2$ resonance was monitored as a function of M/L ratio. Considering the entire spectrum, there were only small changes on copper addition. Unlike with the zinc experiment no second species could be seen and all the resonances only showed marginal shifts. There was a slight loss of splitting pattern definition mainly of the NCH_2 and $CH_2CH_2CH_2$ resonances at higher M/L ratios.

With time (30 minutes) the samples could be seen to go light green in colour. This was likely to arise from the generation of copper (II) complexes, as a result of copper (I) oxidation. Samples of M/L=0.5 and M/L=5 were left for 12 hours after which

both were green in colour with the latter being much darker in shade. A spectrum was obtained for both. At an M/L ratio of 0.5 the NCH_2 and $CH_2CH_2CH_2$ resonances had lost their splitting patterns with no appreciable line-broadening. While for M/L=5, all the lines were broadened with no definition and the entire spectrum was weaker in overall signal to noise ratio. There must therefore have been some free copper (II) present, but not in large excess over ligand otherwise the entire spectrum would have been unobservable.

From the plot of $\Delta\delta_H$ ($ArCH_2$) versus M/L, analysis for 1:1 metal-ligand binding gave a value of K_{CuL} = 37. As a curve (Fig. 4.21) was produced and not a linear response proportional to copper added, the observed resonance shifts are believed to be a result of copper-ligand binding and not a paramagnetic copper (II) shift.

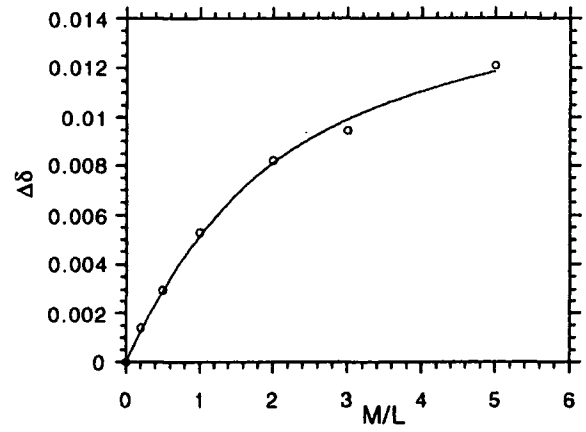

Fig. 4.21 Titration curve of N-linked macrocycle ligand (**166**) at pH 7 'initial protonation state' with Cu(I) addition.

4.4.3.2 N-Linked macrocycle (166) titration at pH 10 'initial protonation state'

The ^1H NMR experiment was performed as before and it was noted that the green colouration developed more rapidly than at pH 7, so the samples were tested quickly after they had been made up. The ligand resonances behaved similarly to before with small shifts to higher frequency on metal addition and a loss of the NCH_2 and $CH_2CH_2CH_2$ resonance splitting pattern with increased M/L ratio. The NH resonances gave an initial large high frequency shift from δ = 5.1ppm to δ = 8.1ppm on metal addition (M/L=0.5) after which there was very little change in shift. There was an increased amount of line-broadening with higher M/L ratio (>2), indicating the presence of copper (II).

A plot of $\Delta\delta_H$ ($ArCH_2$) against M/L was obtained. The plot indicated that at ratios of M/L=1.5 and beyond there was a linear rise in $\Delta\delta_H$. This was likely to be a paramagnetic shift as a result of the increased amount of copper (II) that was more

rapidly generated at this pH. Analysis for 1:1 metal-ligand binding did not give a good fit even when the later points were ignored.

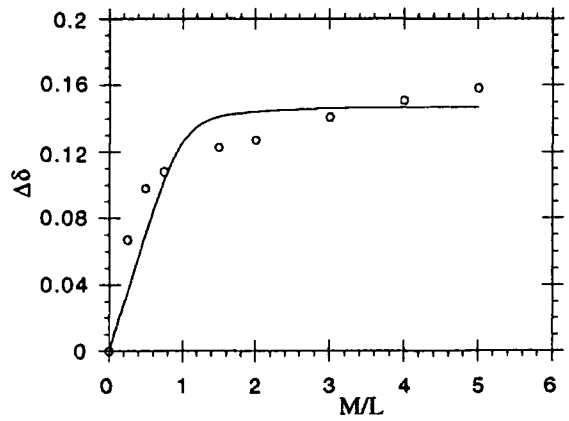

Fig. 4.22 Titration curve for N-linked macrocycle (**166**) at pH 10 'initial protonation constant' with Cu(I) addition, showing poor 1:1 analysis and the high ratio (M/L>1.5) paramagnetic shift.

Fitting the curve for a 1:2 metal-ligand complex gave a much better fit especially when only the early M/L ratio values were considered (the most accurate values). An estimate for the [ML_2] stability constant was obtained of K_{CuL_2} = 720 (Fig. 4.23).

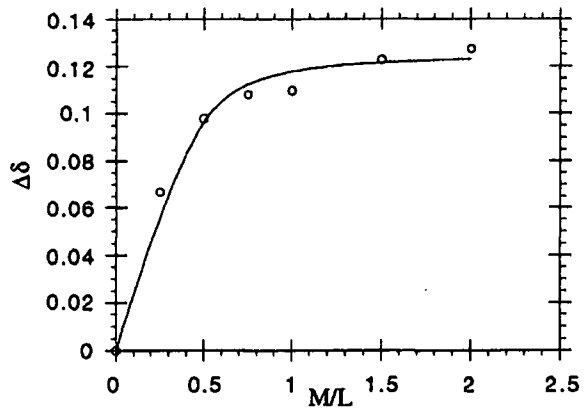

Fig. 4.23 Titration curve for N-linked macrocycle (**166**) at pH 10 'initial protonation state' with Cu(I) addition. Analysis is for 1:2, M:L complex formation.

4.4.3.3 12N$_3$ Ligand (43) titration at pH 7 'initial protonation state'

The shift in the NCH_2 resonance was monitored as a function of increasing M/L ratio. The NH resonance shifted to lower frequency with increasing metal addition (from δ = 5.9ppm to δ = 5.4ppm) and there was only a slight increase in broadening. The other resonances showed a shift to higher frequency with no broadening and only a

The other resonances showed a shift to higher frequency with no broadening and only a slight loss of definition. Plotting $\Delta\delta_H$ (NCH_2 methylene) against M/L ratio gave a curve that was analysed for 1:1 binding giving K_{CuL} = 880 (Fig. 4.24).

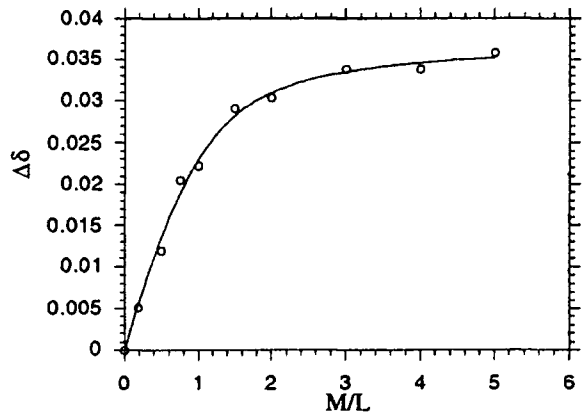

Fig. 4.24 Titration curve for $12N_3$ (**43**) with Cu(I) addition (298K, CD_3CN).

After a few hours the NMR samples turned light blue in colour, indicating copper (I) oxidation to copper (II). This process was slow compared to the speed of sample preparation and testing. There was no evidence of any paramagnetic shifting. After 24 hours the M/L=0.75 sample was retested, a large amount of broadening and a reduction in signal to noise intensity was observed, consistent with copper (II) being present.

4.4.3.4 Comparison of $12N_3$ (43) and N-linked macrocycle (166) copper (I) complex formation

All three titrations indicated that copper (I) was being weakly bound under these experimental conditions (298K, CD_3CN). At pH 7 'initial protonation state' the parent $12N_3$ (**43**) ligand bound copper (I) with a higher binding constant than the N-linked macrocycle (**166**) (K_{CuL} = 880, 37 respectively).

$$\text{At pH7} \quad [\text{N-linked}]H_2^+ \overset{K_1}{\rightleftharpoons} [LCu] \quad K_1 \text{ is small}$$

$$[12N_3]H_2^{2+} \overset{K_1}{\rightleftharpoons} [LCu] \quad K_1 \text{ is larger.}$$

$$\text{At pH10} \quad [\text{N-linked}]H^+ \overset{K_1'}{\rightleftharpoons} [L_2Cu]$$

$[CuL_x]$ not fully defined

Fig. 4.25 Summary of copper (I) binding to $12N_3$ based ligands (**43**) and (**166**).

It appeared that the initial ligand protonation state was of some importance as when there were fewer initially bound protons i.e. the N-linked macrocycle (**166**) at pH 10 'initial protonation state' binding to copper occurred in a different manner. An $[ML_2]$ complex was generated $K_{CuL_2} = 720$. The phenol may not be used in copper binding as $K_{(N\text{-linked})Cu} > K_{12N_3Cu}$ would have been expected, also the N-linked macrocycle (**166**) at pH 10 would have been the most likely to form an [ML] complex. It is quite possible that the copper-ligand species was still protonated to some degree.

4.4.3.5 Comparison between ^{1}H NMR and pH potentiometric titrations

^{1}H NMR titration analysis indicated that all the ligands bound to zinc strongly with one of the species being formed with $K_{ZnL} > 10^5$. This is in contrast to copper (I) binding where all the ligands exhibited low metal-ligand stability constants ($K_{ML} < 10^3$). In CD_3CN, K_{ML} Zn >> Cu (I) for both the $12N_3$ and the N-linked macrocycle (**166**) ligands. The C-linked macrocycle (**167**) bound zinc as a 1:1 complex with a binding constant of $K_{ZnL} = 6.3 \times 10^3$, lower than the other two ligands tested i.e. $K_{ZnL1} > K_{ZnL2}$ where L1 = $12N_3$, N-linked macrocycle (**166**) and L2 = C-linked macrocycle (**167**).

From the pH potentiometric titration data, the relative order for zinc and copper binding was K_{ML} Cu > Zn (II) for $12N_3$, N-linked (**166**) and C-linked (**167**) macrocycles. The N-linked macrocycle (**166**) bound both metals with a higher stability constant than unsubstituted $12N_3$ (**43**) and the C-linked macrocycle (**167**) (Table 4.7).

Metal	$12N_3$ (**43**) ($\log K_{ML}$)	N-linked macrocycle (**166**) ($\log K_{ML}$)	C-linked macrocycle (**167**) ($\log K_{ML}$)
Zinc	8.8 (a)	14.1 (b)	7.32 (b)
Copper	12.6	18.72 (b)	10.16 (b)

(a)Reference 2
(b) 298K, H_2O, I = 0.1 NMe_4NO_3

Table 4.7 Aqueous metal-ligand stability constants ($\log K_{ML}$) of $12N_3$ based ligands.

Comparing the relative orders between the different titration methods was valid even though the solvent conditions were different. Both methods indicate $K_{(N\text{-linked})M} > K_{(C\text{-linked})M}$ for zinc. ^{1}H NMR analysis showed that zinc was bound more strongly than copper (I) while the aqueous titration gave $\log K_{ML}$ Cu > Zn. Taken together this information strongly suggests that the copper (II) centre is not reduced to copper (I) to give the observed yellow colour in the N-linked macrocycle (**166**) aqueous pH titration.

4.5 Spectrophotometric analysis of metal-ligand formation

A similar procedure to that outlined in section 2.3.4 (page 63) was followed. The N-linked macrocycle (**166**) at pH 7 'initial protonation state' was examined in an aqueous and an acetonitrile solution while the C-linked macrocycle (**167**) at pH 10 'initial protonation state' was only tested in water. Both ligands gave similar u.v. spectra in water with two major bands observed at 224nm, 293nm at pH 10 and 226nm, 272nm at pH 7.

4.5.1 U.V. Analysis of the C-linked macrocycle (167)

On metal addition there was a slight shift to lower wavelength (to 282 nm) of the 294nm ligand band, the change in extinction coefficient was not accurately determined but from inspection of the spectra the relative order of intensity was Cu > Ni = Zn. It is possible that the pH of the solution could cause a change in band intensity. The ligand solutions were at identical pH before metal addition, but the resultant solutions were of slightly different pH (Cu = 6.5, Ni = 7.0-7.5, Zn = 7.0). This of course is an indication of the extent of binding and ligand deprotonation but the variation was too small to draw firm conclusions. Only the copper (II) spectra allowed a d-d transition extinction coefficient to be determined. The copper complex was blue in colour with λ_{max} = 690 nm (ε = 110 $dm^3mol^{-1}cm^{-1}$).

4.5.2 U.V. Analysis of the N-linked macrocycle (166) with copper

In acetonitrile, the addition of copper (I) perchlorate resulted in no observable change to the U.V. spectrum. The addition of copper (II) triflate to the aqueous ligand (**166**) solution gave a greatly altered spectrum. There was a shift in the 294nm band to 276 nm with an associated increase in extinction coefficient. The presence of two other bands were observed one at 420nm (ε = 344 $dm^3mol^{-1}cm^{-1}$) and the other at 664nm (ε = 44 $dm^3mol^{-1}cm^{-1}$).

A systematic pH-absorption study was performed with the aqueous copper (II) complex over the pH range 2 to 11.5. The pH was altered using minimal volumes of either hydrochloric acid or potassium hydroxide solution depending on the pH required. For the wavelength starting at λ = 432 nm (pH 3) there was a general trend to lower wavelength with decreasing acidity. The corresponding extinction coefficient went through a maximum in the pH 7.2 region. The tailing off may be partially a result of increased dilution, but this was minimal and the trend was real. The d-d transition remained at a fairly constant wavelength with decreasing acidity (except at high pH).

The associated extinction coefficient also went through a maximum centred at about pH 7.2.

pH	Wavelength /nm (ε / $dm^3mol^{-1}cm^{-1}$)		
2	276 (2121)	-	-
3	274 (2354)	432 (32)	-
4	274 (>3200)	426 (320)	658 (42)
5		428 (540)	654 (82)
7.2		418 (1080)	660 (158)
8.5		416 (1050)	658 (155)
9.5		410 (1000)	660 (146)
10.5		406 (950)	666 (137)
11.5		396 (870)	672 (120)

Table 4.8 Wavelengths and extinction coefficients of copper-ligand (**166**) complex as a function of pH.

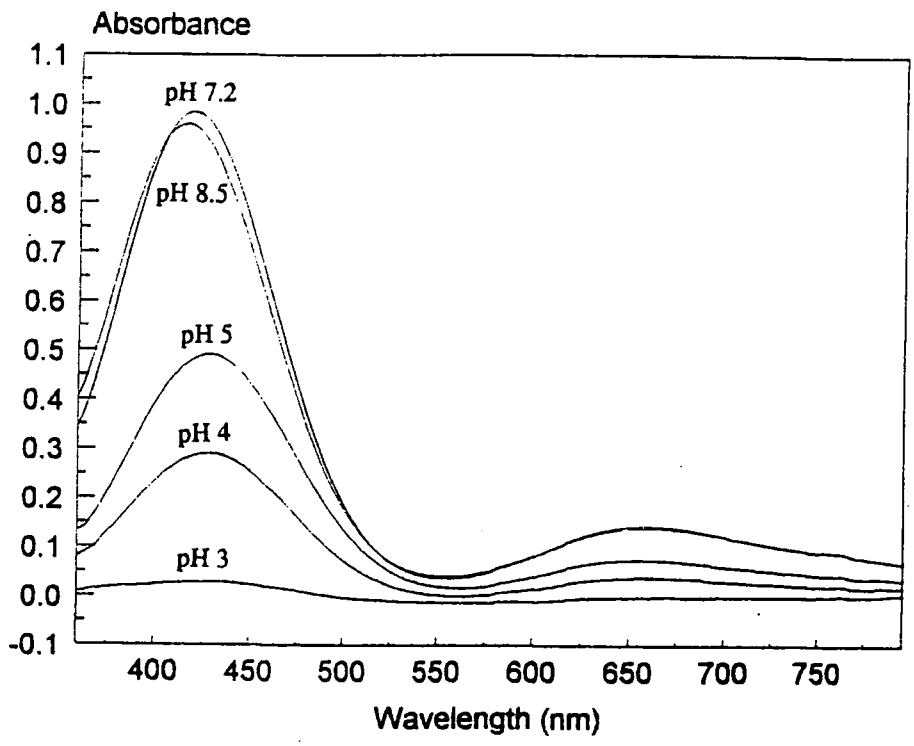

Fig 4.26 U.V. Spectra of N-linked macrocycle (**166**) with Cu (II) at varying acidities.

The observed yellow colour of the ligand (166)-copper aqueous solution, mentioned in section 4.3.2.3 was due to the presence of the 400-420nm band with its high extinction coefficient. This band may be associated with charge transfer from the phenol to copper. Aqueous titration analysis had indicated that complexation was complete by pH 7, this was consistent with the observed maximum extinction coefficient at around pH 7-8. At more alkaline pH the hydroxide ion will tend to

compete in binding resulting in a lesser degree of phenolate binding and as a result causing a slight drop in the extinction coefficient.

4.5.3 U.V. Analysis of N-linked macrocycle (166) with nickel and zinc

Adding zinc to the ligand (**166**) in either acetonitrile or water resulted in very little observable change. There was a slight (6nm) shift in the 272nm ligand band but there was insignificant change in the extinction coefficient.

Nickel also only altered the spectrum by a small amount with very small ligand band shifts (2nm) and no change in extinction coefficient. At pH 7 in water a charge transfer transition was observed λ_{max} = 389 nm (ε = 14 $dm^3mol^{-1}cm^{-1}$). Altering the pH of the solution to pH 12 only resulted in the ligand band shifting (274 to 293 nm) in the same manner as the ligand without nickel present.

4.5.4 Comparison of the N-linked (166) and C-linked (167) macrocycles to Kimura's ligand (6).

From the results it is clear that there is a marked difference in the behaviour between the N-linked macrocycle (**166**) and the C-linked macrocycle (**167**) with the former behaving rather similarly to Kimura's ligand (**6**). This was clearly seen in copper complexation. No charge transfer band was seen for the C-linked macrocycle (**167**), while for the N-linked macrocycle (**166**) this transition was much more intense than for Kimura's ligand (Table 4.9). If this is an indication of the degree of phenolate participation, the N-linked macrocycle (**166**) must be able to adopt the most favourable binding geometry for phenol binding.

	Wavelength /nm (ε / $dm^3mol^{-1}cm^{-1}$)	
Kimura's (**6**)	392 (120)	690 (110)
N-linked macrocycle (**166**) pH 7.2	418 (1080)	660 (158)

Table 4.9 U.V. Absorption bands for Kimura's (**6**) and the N-linked macrocycle (**166**) with copper (II) (298K, H_2O).

4.6 Differential pulse voltametric analysis

The redox behaviour of the phenol and the bound metal can be studied using differential pulse voltammetry. This technique monitors the current passing through the electrolyte as a function of the applied stepped voltage. Stock solutions of $12N_3$ (**43**) and N-linked macrocycle (**166**) (0.001M) at pH 10 (aqueous protonation state) were prepared in dry, degassed acetonitrile with a background electrolyte of 0.1 $moldm^{-3}$

tetramethylammonium perchlorate. Similarly copper and zinc triflate solutions (0.01M) in the same solvent and background were prepared. Using 5ml of the ligand solution and where necessary the appropriate amount of metal solution, the experiment was performed by Dr. Ritu Kataky (University of Durham) on a model 263 EG&G potentiostat. The experiments were performed using a micro glassy carbon electrode and a non-aqueous reference electrode. An E^o value[21] (E^o = 0.503V) for this electrode was used to take account of the non-aqueous solvent, rather than the standard value for a calomel electrode.

The phenol oxidation was observed as a single peak at +1.8 V. In the presence of about one equivalent of zinc triflate no such signal was observed (Fig. 4.27). This indicates clearly that there was no free phenol present in solution, i.e. the phenol was involved in zinc binding.

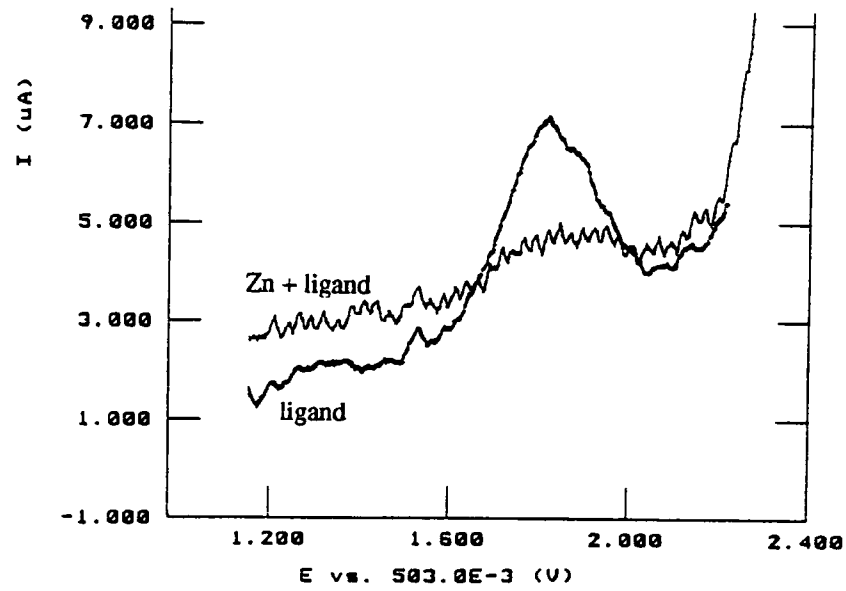

Fig. 4.27 Phenol reduction with and without zinc present.

4.6.1 Copper reduction with and without ligands

Copper can be stepwise reduced from copper (II) to copper (I) and finally to copper (0). The ease of reduction will depend on the extent to which each oxidation state is stabilized. Using a blank sample (acetonitrile and background electrolyte) showed no indication of any redox behaviour in the -0.6V to -1.0V region. Testing copper triflate without any ligands gave two peaks of roughly equal intensity. The peak at -0.72V was assigned to a copper (II) reduction while the peak at -0.99 is likely to be due to copper (I) reduction.

With the ligands $12N_3$ (**43**) and the N-linked macrocycle (**166**) present there was a change in the peak positions and their relative intensities. For $12N_3$ (**43**) there was a general shift to lower (more negative) voltages. The peak for copper (II) reduction now appeared more intense and sharper than the copper (I) reduction peak.

While for N-linked macrocycle (**166**) the peak for copper (I) reduction was more intense and both reduction peaks appeared closer together (Fig. 4.28).

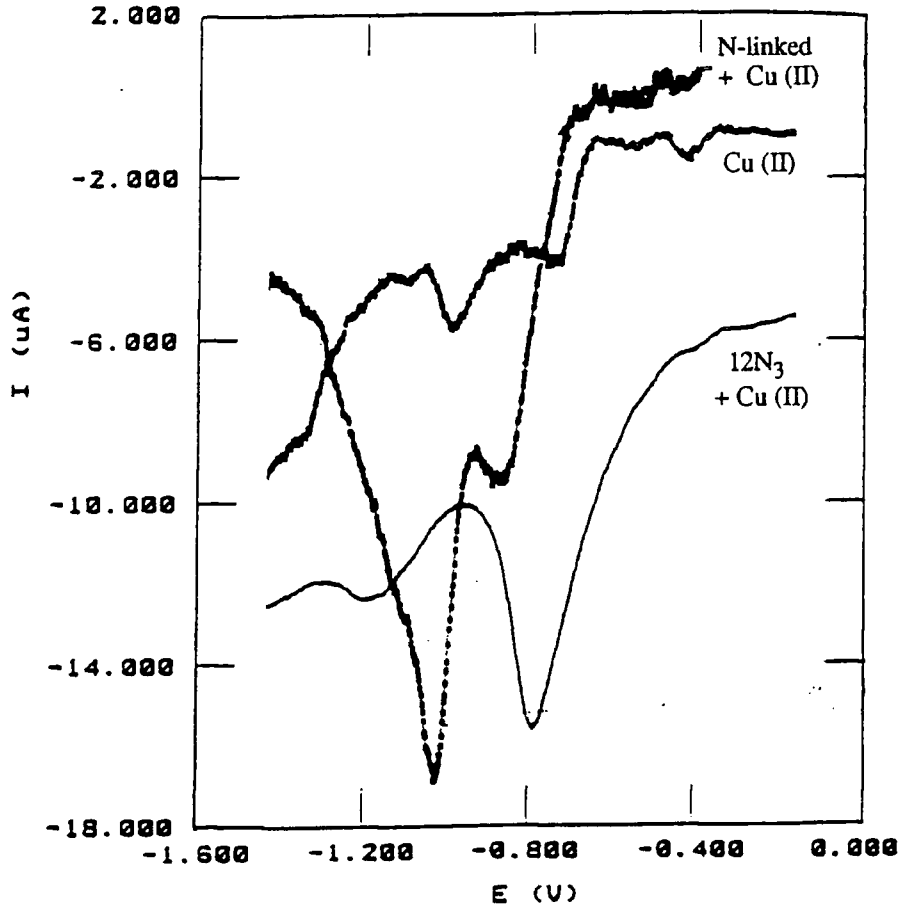

	Cu(II) to Cu(I) E(V)	Cu(I) to Cu(0) E(V)
Cu (II) only	-0.72	-0.99
Cu (II) + $12N_3$ (**43**)	-0.81	-1.11
Cu (II) + N-linked macrocycle (**166**)	-0.9	-1.02

Fig. 4.28 Copper reductions without ligand and with either $12N_3$ (**43**) or N-linked macrocycle (**166**).

It is not possible to draw firm conclusions, especially as there are very few literature reports of reduction potentials in acetonitrile. Considering the relative size of the peaks implies the two ligands are behaving differently, the large peak for copper (I) reduction for N-linked macrocycle (**166**) may mean that the ligand was stabilizing this oxidation state relatively more than copper (II). The opposite situation occurred with copper and $12N_3$ (**43**). More work in this area would be necessary to draw more positive conclusions. Cyclic voltammetry with the N-linked macrocycle (**166**) showed that reduction of the ligand-copper complex was irreversible.

4.7 Electrospray mass spectrometry analysis

The same experimental procedure as that outlined in chapter 2 (page 57) was followed. The two substituted $12N_3$ ligands (**166**) and (**167**) and $12N_3$ (**43**) as a control ligand were tested with nickel, copper and zinc. For all the samples the major species observed was the protonated uncomplexed ligand. The intensity of the metal-ligand complex depended on the nature of the metal involved. Copper (II) formed the most intense complex peaks with all the ligands, while for zinc and nickel the amount of complex species was significantly lower.

The N-linked macrocycle (**166**) ligand gave the strongest [ML] complex signal for copper, then zinc and there was no observable [NiL] species even after the sample was left for two hours. There was a good agreement between observed and theoretical peaks (Table 4.10). Using copper (I) instead of copper (II) resulted in a lower intensity [ML] peak. It was likely that this corresponds to bound copper (II) as a result of copper (I) disproportionation. The older the sample the more metal bound species were observed. Increasing the M/L ratio up to five had the effect of increasing the observed amount of [ML] complex.

	observed peaks	calculated peaks
Cu (II) [ML]	339.3, 340.7, 341.7	339.1, 340.1, 341.1
Zn (II) [ML]	340.2, 341.8, 343.8	340.1, 342.1, 344.1

Table 4.10 Assigned peaks in ESMS spectra of N-linked macrocycle (**166**) with copper and zinc (underlined mass indicates the major peak).

For the C-linked macrocycle (**167**) a more concentrated sample was used. Again copper showed the strongest [ML] peaks, then nickel and finally zinc. The zinc/nickel order was the reverse of that observed for N-linked macrocycle (**166**). For zinc the region for [ML] mass contained many peaks making it difficult for a proper assignment. As well as [ML] species being seen there appeared to be an $[M_2L]$ complex. However there was poor agreement between the theoretical and observed masses and it is likely that these could have been other unknown complexes.

	observed peaks	calculated peaks
Ni (II) [ML]	412.0, 414.2, 415.8	413.1, 415.1, 417.1
Cu (II) [ML]	417.3, 418.9, 420.6	418.0, 420.0, 422.0
	other major complexes	
Ni (II)	472.0, 474.0, 475.6	
Cu (II)	477.0, 479.0, 480.6	
Zn (II)	477.7, 479.9, 481.5	

Table 4.11 Assigned peaks in ESMS spectra of C-linked macrocycle (**167**) with nickel, copper and zinc (underlined mass indicates the major peak).

The parent $12N_3$ (**43**) showed complicated behaviour with the presence of many unassignable metal-ligand complex peaks (Table 4.12). Using copper (I) gave no [CuL] peaks, however as the sample aged, copper containing complexes were seen. This shows $12N_3$ (**43**) has higher binding constants to copper (II) than copper (I).

	observed peaks	theoretical peaks
ligand [LH]	171.99	172.2
Zn (II)	261.3, 263.3, 265.3 269.9, 271.9, 274.8	[ZnL] 235.0, 237.0, 239.0
Cu (II)	210.3, 212.0 233.5, 235.3 260.3, 262.4 269.2, 271.2	[CuL] 234.1, 236.1

Table 4.12 Observed mass peaks for $12N_3$ (**43**) with zinc and copper.

4.8 Conclusion

There are similarities between both substituted $12N_3$ ligands (Fig. 4.29) as a result of the N_3 basal donor set. Both ligands form 1:1 complexes with the metals; nickel, copper and zinc (pH potentiometric and ESMS evidence). The order of metal-ligand complex stability follows the Irving-Williams sequence i.e. Cu(II) > Zn(II) > Ni(II). Copper binding was the strongest and this is consistent with the behaviour observed with other $12N_3$ ligands such as the parent $12N_3$ (**43**), Kimura's C-linked derivative (**6**) and dimethyl-α-C-substituted $12N_3$ (**185**) ligands.

Of more interest is the *difference* in their behaviour. Both the ligand protonation constants and metal-ligand complex stabilities are different. The N-substituted ligand (**166**) was similar to Kimura's ligand (**6**) with regards to value of the measurable protonation constants. The ligand was acting as a slightly better donor with larger metal-ligand stability constants for copper and zinc (pH potentiometric analysis). Also a much larger degree of charge transfer from the phenolate to the copper (U.V. evidence) was observed. It was this charge transfer which gave the copper complex its distinctive yellow colour. The copper may be taking on more 'copper (I) character' (D.P.V evidence) as it is forced into a tetrahedral binding geometry by the ligand design. In the ^1H NMR experiment (in deuteriated acetonitrile), zinc (II) bound more strongly than copper (I). This order of binding was not consistent with the aqueous speciation study which showed copper binding more strongly than zinc. Hence copper (II), in the aqueous pH potentiometric analysis, was not being reduced to copper (I). It should be noted that in water the addition of either copper (II) or copper (I) to the N-linked macrocycle (**166**) gave rise to the same u.v. spectrum, probably as a result of rapid copper (I) oxidation.

The carbon substituted ligand was notably different. All four protonation constants were measurable by pH potentiometric titrations. Even though 1:1 metal-ligand complexes were generated (ESMS), there was little evidence of a strong phenol interaction. The ligand (**167**) was essentially behaving as an N_3 donor. Both [MLH] and [ML] species were observed with stability constants of the same magnitude as the parent $12N_3$ ligand (**43**) (pH potentiometric evidence). The copper complex was blue in colour (as is the parent $12N_3$ (**43**) copper complex), with no absorption band at 420nm (U.V. evidence) again indicative of little or no phenol participation.

The variation between the two substituted $12N_3$ ligands may be attributed to two features. Carbon substitution may have forced the $12N_3$ ring into a conformation that does not bind as efficiently. This may explain the variation in protonation constants and the lower metal-ligand complex stabilities. If the [MLH] complex forms with the phenol group in the same plane as the $12N_3$ ring, on phenol deprotonation there would have to be a large conformational change to enable phenolate binding. This requires energy and would result in a lower than expected [ML] stability constant. Secondly the size of the chelate ring on binding may be of importance. Both Kimura's (**6**) and the N-linked macrocycle (**166**) formed an N-Zn-O six membered chelate. It is known that this is favourable for small cations[22]. The C-linked macrocyclic (**167**) ligand forms an eight membered N-Zn-O chelate, which is less favourable and results in lower metal-ligand complex stabilities. Compared to acyclic ligands the N-linked macrocycle (**166**) will not have as much flexibility, as a $12N_3$ and a phenol unit are present. Hence the drop in stability going from six to eight membered chelates should not be as great as it would be with acyclic ligands.

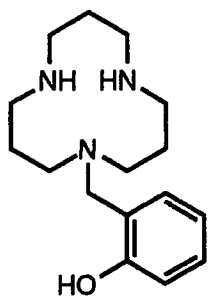

(**166**)

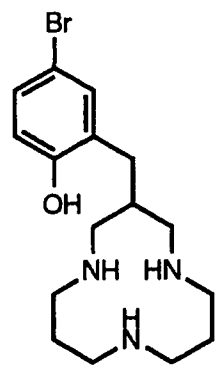

(**167**)

Fig. 4.29 $12N_3$ ligands synthesised in this work.

4.9 References

1) L.J. Zompa; *Inorg. Chem.*, 1978, **17**, 2531.

2) A.E. Martell, R.M. Smith, 'Critical Stability Constants Vol 1-6', Plenum Press, London.

3) T.W. Bell, H.J. Choi, W. Hawle; *J. Am. Chem. Soc.*, 1986, **108**, 7427.

4) I.M. Helps, D. Parker, K.J. Jankowski, J. Chapman, P.E. Nicholson; *J. Chem. Soc., Perkin Trans. 1*, 1989, 2079

5) (i) E. Kimura, T. Koike, K. Toriumi; *Inorg. Chem.*, 1988, **27**, 3687; (ii) E. Kimura, I. Nakamura, T. Koike, M. Shionoya, Y. Kodama, T. Ikeda, M. Shiro; *J. Am. Chem. Soc.*, 1994, **116**, 4764.

6) (i) N.W. Alcock, A.C. Benniston, P. Moore, G.A. Pike, S.C. Rawle; *J. Chem. Soc., Chem. Commun.*, 1992, 706; (ii) S.C. Rawle, A.J. Clarke, P. Moore, N.W. Alcock; *J. Chem. Soc., Dalton Trans.*, 1992, 2755.

7) E. Kimura, M. Yamaoka, M. Morioka, T. Koike; *Inorg. Chem.*, 1986, **25**, 3883.

8) T. Koike, E. Kimura, I. Nakamura, Y. Hashimoto, M. Shiro; *J. Am. Chem. Soc.*, 1992, **114**, 7338.

9) M.L. Turorek, P. Moore; Poster, RSC U.K. Macrocyclic Group 1995.

10) A.E. Martin, T.M. Ford, J.E. Bulkowski; *J. Org. Chem.*, 1982, **42**, 412.

11) T.J. Atkins, J.E. Richman, W.F. Oettle; *Org. Synth.*, 1978, **58**, 86.

12) G.R. Weisman, D.J. Vachan, V.B. Johnson, D.A. Gronbeck; *J. Chem. Soc., Chem. Commun.*, 1987, 888.

13) R. Grise, L.N. Owen; *J. Chem. Soc.*, 1963, 1947.

14) G.I. Feutrill, R.N. Mirrington; *Tetrahedron Lett.*, 1970, 1327.

15) F.L. Benton, T.E. Dillon; *J. Am. Chem. Soc.*, 1942, **64**, 1128.

16) E.J. Corey, R.L. Danheiser, S. Chardrasekavan, P. Siret, C.E. Keck, J-L. Gras; *J. Am. Chem. Soc.*, 1978, **100**, 8031.

17) K.M. Doxsee, M. Feigel, K.D. Stewart, J.W. Canary, C.B. Knobler, D.J. Cram; *J. Am. Chem. Soc*, 1987, **109**, 3098.

18) R.M. Kellogg, J. Buter, B.K. Vriesema; *J. Org. Chem.*, 1984, **49**, 110.

19) C.H. Heathcock, K.M. Smith, T.A. Blumenkopf; *J. Am. Chem. Soc.*, 1986, **108**, 5022.

20) D.P. Kudav, S.P. Samant, B.D. Hosangadi; *Synth. Commun.*, 1987, **17**, 1185.

21) A.K. Covington, T. Dickinson; 'Physical Chemistry of Organic Solvent Systems', Plenum Press, London; 1973 p168 and p196.

22) R.D. Hancock, A.E. Martell; *Chem. Rev.*, 1989, **89**, 1875.

Chapter Five

Experimental

5.1 Experimental Methods

All reactions were carried out in apparatus which had been oven-dried and cooled under argon. All solvents were dried from an appropiate drying agent and water was purified from the PURITE system.

Alumina refers to Mersk Alumina activity II-III that was soaked in ethyl acetate for at least 24 hours prior to use. Silica refers to Mersk silica gel F60 (230-400 mesh). Preparative tlc was carried out using either Merck 5726 Alumina plc 150 F_{254} (type T) pre-coated 1.55mm plates or Mersk Silica Plc 60 F_{254} precoated 2mm plates.

Analytical and preparative HPLC were performed on a Varian Vista 5500 or Star 5065 instrument fitted with a reverse phase column ("Dynamax").

^{1}H and ^{13}C NMR spectra were obtained with a Bruker AC 250 operating at 250.13 and 62.90 MHz respectively, Varian Gemini 200 operating at 200 and 50 MHz respectively, Varian XL 200 operating at 200 MHz and Varian VXR 400S operating at 400 MHz. All chemical shifts are given in ppm relative to the residual solvent resonance and coupling constants are in Hz. ^{31}P NMR spectra were obtained with a Bruker AC 250 operating at 101 MHz.

Mass spectra were recorded on a VG 7070E, operating in FAB, EI^{+} or DCI ionization modes as stated. Electrospray mass specta were recorded using a VG Platform (Fisons instruments) operating in ES^{+} mode or were performed by the SERC Mass Spectroscopy service at Swansea. Accurate mass spectroscopy was performed by the SERC Mass Spectroscopy service.

Infra-red spectra were recorded on a Perkin-Elmer 1600 FT-IR spectrometer as a thin film or KBr disc as stated. Ultra-violet spectra were recorded on a UVIKON 930 spectrometer.

Combustion analysis was performed using an Exeter Analyical Inc CE440 elemental analyser. Metal concentation was determined by atomic absorption spectroscopy using a Perkin Elmer 5000 atomic absorption spectrophotometer.

Melting points were determined on a Gallenkamp melting point apparatus and are uncorrected.

Potentiometric titrations were performed on a Molspin 1ml auto titrator using a Corning semi-micro electrode to measure the pH.

5.1.1 NMR Titrations

Two methods were employed for NMR titrations:

5.1.1.1 (A) Stock Solution method

When the ligand was available in large quantities a stock solution of the ligand and the required metal triflate (five times more concentrated than ligand) was made up

in the required NMR solvent. Using the ligand solution (0.4 ml), the appropriate amount of metal triflate solution was added and where necessary extra solvent was added so that each NMR sample was made up to a final volume of 0.8 ml. The metal/ligand ratio was varied from 0 to 5.

5.1.1.2 (B) Single NMR Sample

When there was a limited amount of ligand available, a single NMR sample was made up (0.8 ml, M/L=0). The required amount of metal triflate was weighted out into microcentrifuge polypropylene tubes and the NMR sample added into the polypropylene tube. The solution was then transferred back into the NMR tube using a Gilson pipette fitted with a polypropylene tip and the NMR recorded. This procedure of weighing out the metal triflate and adding the same NMR sample was repeated to obtain M/L ratios typically of 0.25, 0.5, 0.75, 1.0, 1.5, 2.0.

The conditions for each NMR titration experiment are given in the table below. The shift of one of the resonances of the ligand was recorded as a function of M/L ratio. Using a curve fitting program the equilibrium constant K_1 was determined[1]

Ligand	Metal	Ligand concentration (mol dm^{-3})	NMR solvent	Method
1,1'-bis(4-tert-butylbenzyl)-2,2'-bisbenzimidazole-4,4'-dicarboxylic acid	Ni Cu Zn Cd Pb	0.020	25% CD_3OD 75% $CDCl_3$	(A)
1,1-bisbenzyl-2,2'bisbenzimidazole-4,4'-dicarboxylic acid	Zn	0.016	25% CD_3OD 75% $CDCl_3$	(B)
1-(4-tert-butylbenzyl)-benzimidazole-4-carboxylic acid	Zn	0.026	25% CD_3OD 75% $CDCl_3$	(B)
1,1'-bis(4-tert-butylbenzyl)-2,2'-bisbenzimidazole-4,4'-dicarboxylic acid	Zn	0.016	25% CD_3OD 75% $CDCl_3$	(B)
O-O'-diethyl-1,1'-bis(4-tert-butylbenzyl)-2,2'-bisbenzimidazole-4,4'-thiophosphonate ester	$ZnTf_2$ $ZnCl_2$	0.006 0.026	25% CD_3OD 75% $CDCl_3$	(B)

1,10-Phenanthroline-2,9-bis(methylene(methyl-phosphinic) acid)	Zn Cu	0.019 0.021	D_2O	(B)
1,10-phenanthroline-2,9-bsis(phenyl-2-acetic acid)	Zn	0.019	CD_3OD	(B)
1,5,9-triazacyclododecane pH7 protonation state	Zn Cu(I)	0.0032 0.0024	CD_3CN	(A)
1-(2-hydroxybenzyl)-1,5,9-triazacyclododecane pH7 and pH10 protonation states	Zn Cu(I)	0.019	CD_3CN	(A)
3-(2-Hydroxy-5-bromobenzyl)-1,5,9-triazacyclododecane pH7 protonation state	Zn	0.026	CD_3CN	(B)

5.1.2 Electrospray mass spectrometry complexation analysis

Stock solutions of the ligand (10 ml, 0.3 mM) in wet methanol containing about 1-5% water (except bisbenzimidazole based ligands where dichloromethane (40%) was used to aid solubility) and the metal triflates (10 ml, 1.5 mM) in methanol were made up. To a sample of the ligand solution (1ml) the appropriate amount of metal triflate solution (in the order of 0.2 ml) was added to make a 1:1 metal/ligand ratio. Using 10µl of the test solution, mass spectra were obtained on a VG platform (II) electrospray mass spectrometer (cone voltage; 30V, sample temperature; 60°C) with positive ionization.

5.1.3 Ultra-violet and visible spectroscopic analysis

Stock solutions of the ligand (0.001M) to be tested and the metal triflates (0.01M) were disolved in the desired solvent (water or methanol, 75% dichloromethane/25% methanol with bisbenzimidazole). The samples to be tested were added into a quartz cuvette (1cm in width, $4cm^3$ in volume) and the spectra obtained on a UVIKON 930 spectrometer. For metal/ligand complexes, the appropiate amount of metal triflate solution (0.3 ml) was added to the ligand solution (3ml) to obtain a 1:1 ratio and tested as before. For aqueous samples the acidity was measured after metal addition. Dilution of the samples was performed to obtain spectra of acceptable absorbance in the 200 to 300 nm range.

Ligand	Solvent	Metal tested	pH	Dilution factor
1,1'-bis(4-tert-butylbenzyl)-2,2'-bisbenzimidazole-4,4'-dicarboxylic acid	25% MeOH 65% CH_2Cl_2	Ni Cu Zn Cd Pb Fe(III)		x12.5
1,10-phenanthroline-2,9-bis(methylene(benzyl-phosphonic acid))	MeOH	Cu Ni		x50
1,10-phenanthroline-2,9-bis(methylene(phenyl-phosphonic acid))	MeOH	Cu Ni Zn		x50
1,10-phenanthroline-2,9-bis(methylene(methyl-phosphonic acid))	H_2O	Cu Ni Zn	5.3 6.3 6	x50
1-(2-hydroxybenzyl)1,5,9-triazacyclododecane	H_2O	Cu Ni Zn Cu(I)	5.5	
1-(2-hydroxybenzyl)1,5,9-triazacyclododecane pH7 protonation state	CH_3CN	Cu(I) Zn		
3-(5-bromo-2-hydroxylbenzyl)-1,5,9-tri-azacyclododecane	H_2O	Cu Ni Zn	6 7.5 7	

For the 1-(2-hydroxylbenzyl)-1,5,9-triazacyclododecane copper complex, spectra were recorded as a function of pH (range 2 to 11.5) by adding aqueous hydrochloric acid (0.1M) or aqueous sodium hydroxide (0.1M) as required.

5.1.4 Bisbenzimidazole infra-red complexation

1,1'-Bis(4-tert-butylbenzyl)-2,2'-bisbenzimidazole-4,4'-dicarboxylic acid (5 mg, 0.0081 mmol) was dissolved in a mixed solvent system (1 ml, 25% CH_3OH, 75% $CHCl_3$) and the appropiate amount of metal triflate (0.00814 mmol) added to obtain a 1:1 metal/ligand ratio. IR measurements were performed in a CaF_2 solution cell (internal gap of 0.1 mm) on a Perkin Elmer 1600 FTIR spectrometer.

5.1.5 Bisbenzimidazole extraction tests

5.1.5.1 Zinc pH extraction test

1,1'-Bis(4-dodecylbenzyl)-2,2'-bisbenzimidazole-4,4'-dicarboxylic acid (1.28 g, 1.524 mmol) was dissolved in Analar dichloromethane (15 ml). Zinc chloride (1.863 g, 7.622 mmol) dissolved in aqueous sulphuric acid (15 ml, 0.05M, pH1) was added. The binary phase mixture was stirred vigorously for 15 minutes and then allowed to separate. The pH of the top aqueous layer was measured (Corning semi-mico pH combination electrode and Molspin program). Aliquots (0.2 ml) of the aqueous and organic layer were removed. The pH of the mixture was adjusted by adding sodium hydroxide solution (4.5M, between 0.1 to 0.3 ml) and the mixture stirred vigorously. The procedure of aliquot removal and pH adjustment was repeated to obtain 12 organic and aqueous samples in the pH range 0.71-5.15.

The aqueous samples were diluted with water (to 10 ml) and the zinc content determined by atomic absorption spectroscopy. The organic samples were diluted with chloroform (5 ml) and either decanted or filtered through a cotton wool plug to remove any residual water. The organic solution was mixed vigorously with hydrochloric acid (10 ml, 1M). The aqueous layer was carefully separated and the zinc content determined by atomic absorption spectroscopy.

5.1.5.2 Zinc and copper or ferric pH competitive extraction

Standard solutions of zinc (II) chloride (50 ml, 0.0558M), ferric chloride (50 ml, 0.0555M) and copper (II) chloride (25 ml, 0.055M) were made up in aqueous sulphuric acid (0.05M). The exact metal concentration was determined by atomic absorption spectroscopy. To a solution of 1,1'-bis(4-dodecylbenzyl)-2,2-bisbenzimidazole-4,4'-dicarboxylic acid in dichloromethane (12 ml, 0.10M) the appropiate amount of zinc solution and the competing metal solution (copper or iron) were added so that the ligand metal ratio was 4:1 for each metal. The aqueous volume was made up to 12ml with aqueous sulphuric acid (0.05M). The two phase mixture was stirred vigourously for 15 minutes and then left to separate. The pH of the aqueous layer was measured (Corning semi-micro pH combination electrode and Molspin program). Samples of the aqueous (0.2 ml) and organic (0.2 ml) layers were removed as in the zinc pH extraction experiment. The pH was adjusted using sodium hydroxide solution (4.5M) and the mixture stirred vigorously. The procedure of aliquot removal and pH adjustment was repeated to obtain 3 sets of samples in the range of pH 2 to pH 3.5. The organic and aqueous samples were treated and the metal content analysed as in the zinc extraction experiment.

5.1.6 Potentiometric Titrations

5.1.6.1 Apparatus

The titration cell was a double walled glass vessel of approximate $5cm^3$ capacity (internal dimensions of 1.2 cm in diameter by 5 cm in depth). The contents were kept at a constant temperature by passing water between the glass walls using a Grant thermostatically controlled water bath and pump. The solutions in the vessel were mixed with a cross shaped magnetic stirrer bar using an IKA-mini-MR magnetic stirrer. An IBMpc program (Molspin version 1.44 by Academic software) was used to collect and store the measured pH readings during the titration (using a Corning semi-mico pH combination electrode) and operated the 1 ml capacity autotitrator (Molspin, Newcastle-Upon-Tyne, U.K.). The titrant was delivered to the titration cell through a rigid plastic tube (internal bore size of 0.05 mm). The end of the tube was held in place so that it would always be above the surface of the solution in the titration cell and so it met the glass wall at an angle of 30^o. The volume increments, the time between additions (governed by the pH stability over the 'time delay') and final volume added were all controlled by the program and were set before each titration. The pH electrode was calibrated using 2 NBS buffer solutions (UNICAM) of pH 4.008 and 6.865 at 25^oC. The collected data (volume of titrant added and pH) were transferred to a UNIX mainframe and analysed by two non-linear least squares programs SCOGS2 and superquad.

5.1.6.2 Solution Preparation

All solutions were prepared from purite water that had been boiled for 30 minutes with nitrogen gas bubbling through it to remove carbon dioxide. Ligand solutions (25 ml or 10 ml, 0.001M) were prepared in a constant ionic strength background solution of tetramethylammonium nitrate (0.1M). Two or three equivalents of inorganic acid (HCl) were added to obtain an initial pH of between 2 and 2.5. Metal nitrate solutions (10 ml, 0.01M) in background of 0.1M TMA NO_3 were prepared and the exact metal concentration determined by atomic absorption spectroscopy prior to use.

The exact molarity of the titrant base solution, tetramethylammonium hydroxide (about 0.05M) in background of 0.1M TMA NO_3 was determined by titrating against a standard hydrochloric acid solution (3 ml, 0.01M) at 25^oC. From the titration curve a GRAMS plot was obtained (using Molspin program) which allowed the end point to be determined and hence the exact concentration. This was repeated three times until consistent results were obtained.

5.1.6.3 Measurement of pKa and metal stability constants

The ligand solution (3ml, 0.001M) was added to the titration cell and the calibrated pH electrode placed into the solution so that its frit was below the liquid surface. With the solution temperature maintained at 25°C and with efficient stirring the base solution (TMA OH, 0.05M) was titrated in (increments of 0.002 ml, time delay of 5 seconds). The pH curve was analysed as mentioned above to determine the pKa's of the ligand.

For metal stability constants the appropriate volume of metal nitrate solution (about 0.3 ml, 0.01M) was added to the ligand solution (3 ml, 0.001M) to obtain a metal/ligand ratio of one. The titration was performed as above, (increments of 0.0025 ml, time delay between 10 seconds to 45 seconds depending on the kinetics of complexation). For long time delays >25 seconds the top of the titration cell was covered with a layer of lab film which only allowed the electrode and delivery tube through, so preventing excessive solvent evaporation or carbon dioxide absorption. Knowing the pKa's of the ligand, the metal stability constants are determined by using the analysis programs and the change in the pH profile.

5.1.6.4 Titration of 1,10-Phenanthroline-2,9-bis(methylene(phenylphosphinic) acid) in a mixed solvent

As the 1,10-phenanthroline-2,9-bis(methylene(phenylphosphinic) acid) zinc complex had poor solubility in water a mixed solvent composition of 30% CH_3OH, 70 % H_2O was used. The ligand, metal and base solutions were prepared as before, in this solvent composition. The electrode was calibrated in aqueous buffer solutions of pH 4.008 and pH 6.865 at 25°C. The base was titrated against standard hydrochloric acid (0.01M in 30% MeOH, 70% H_2O) and the end point determined by a Grams plot using the Molspin software. A correction factor[2] (subtraction of 0.0314) was applied to all the measured pH values to take into account the different solvent conditions between electrode calibration and pH titration. In the analysis the autoprotolysis constant[3] was set at 14.055, the ligand pKa constant and the zinc ligand stability constants were determined as before.

5.1.7 Differential pulse voltammetry

1,5,9-Triazacyclododecane (8.5 mg, 0.050 mmol) and 1-(2-hydroxybenzyl)-1,5,9-triazacyclododecane (30.9 mg, 0.05 mmol) were individually dissolved in 'Purite' water (10 ml) and the acidity adjusted to pH7 using potassium hydroxide solution (0.1M) and hydrochloric acid (0.01M). The solutions were concentrated and vacuum dried to give the ligands in the pH7 protonation state. The ligands were dissolved in dry

acetonitrile (50 ml) containing a background electrolyte (tetraethyl ammonium perchlorate, 0.1M) to give the ligand stock solutions (0.001M). Zinc triflate (0.0182 g, 0.05 mmol) and copper triflate (0.0181 g, 0.05 mmol) were individually dissolved in dry acetonitrile (50 ml, background Et_4NClO_4, 0.1M) to give the metal stock solutions (0.001M). For the copper samples (copper and copper+ligand) the solutions had to be degassed before use. All the stock solutions were tested and the metal ligand mixtures (M/L ratio of about one).

Each test solution (5 ml) was examined at room temperature using a model 263 EG&G potentiostat (270/250 research electrochemistry software v. 4.11). A micro glassy carbon electrode was used (Bioanalytical systems Inc. model MF 2012) with a non-aqueous reference electrode (Bioanalytical systems Inc. model MW 1085). An E^o value[4] (E^o= 0.503V) for this electrode was used in the experiment. The following experimental conditions were employed; voltage range for copper (0 to -2.4 V), for zinc (-0.2 to 2.3 V); scan rate 20.0 mV/s; scan increment 2.0 mV; step/drop time 100.0 ms; pulse height 25.0 mV.

5.2 Chapter two experimental

5.2.1 Synthesis of bisbenzimidazole carboxylic acids

***2,2'-Bis-1H-benzimidazole[5]* (47)**

Anhydrous ethylene glycol (10 ml) was added to a mixture of o-phenylenediamine (8.8 g, 81.5 mmol) and oxamide (3.59 g, 40.8 mmol), heated (160°C) and stirred under nitrogen for 12 hours. The mixture was added to hot water (200 ml) and filtered to give a green coloured solid, 5.98g (63%). Crystallization from acetic acid gave yellow needle shaped crystals. Heating the crystals with ammonia solution (33 v/v, 50 ml) for 10 minutes, filtering and drying removed any residue acetic acid; m.pt > 250°C (Lit. dec 395-400°C)[7]; δ_H (DMSO-d_6) 7.29 (4H, d), 7.32 (4H, d), 7.66 (2H, bs, NH); υ_{max} (KBr disc)/cm^{-1} 1400, 1340 (C=N), 755. Found C, 70.94; H, 4.22; N 23.81%. $C_{14}H_{10}N_4$ requires: C, 71.78; H, 4.30; N, 23.92%.

***1,1'-Di(4-tert-butylbenzyl)-2,2'-bisbenzimidazole* (54)**

4-tert-Butylbenzyl bromide (1.36 ml, 7.4 mmol) was added to a slurry of 2,2'-bis-1H-benzimidazole (0.395 g, 1.69 mmol) and caesium carbonate (1.21 g, 3.71 mmol) in DMF (30 ml). The mixture was heated (80°C) under nitrogen and the course of the reaction followed by tlc on silica (1% MeOH, 99% CH_2Cl_2, R_f(product)=0.83). After 24 hours more 4-(tert-butyl)-benzyl bromide (0.681 ml, 3.71 mmol) was added and the mixture was heated for a further 6 hours. Reduced pressure distillation of DMF left a green-yellow solid. The solid was taken up into chloroform (40 ml), filtered and concentrated. Purification by column chromatography on silica (CH_2Cl_2) gave a yellow

solid, 194 mg (22%). δ_H ($CDCl_3$) 1.33 (18H, s, CH_3), 5.31 (4H, bs, CH_2), 6.52-6.7 (4H, m), 6.82 (2H, t), 7.01 (2H, t), 7.13 (2H, m), 7.28-7.38 (6H, m); δ_C ($CDCl_3$) 31.35 (CH_3), 34.68 (ArC), 45.66 (NCH_2), 104.7, 113.7, 122.5, 125.5, 125.7, 126.5, 126.8, 131.6, 133.5, 139.1, 149.9; *m/z* (DCI NH_3) 528 (M^+ +1), 527(M^+), 381 (M^+ -CH_2Ar^tBu), 235 (M^+ -2xCH_2Ar^tBu); υ_{max} (KBr disc)/cm^{-1} 2962, 1472 (C=N), 738. Found C, 82.32; H, 7.24; N, 10.16%. $C_{34}H_{34}N_4$ requires: C, 82.09; H, 7.27; N, 10.64%.

***1,1'-Di(4-tert-butylbenzyl)-2,2'-bisbenzimidazole* (54)**

Sodium hydride (0.21 g, 8.75 mmol) was added to a slurry of 2,2'-bis-1H-benzimidazole (1 g, 4.27 mmol) in DMF (30 ml) and heated (80°C) for 30 minutes. 4-tert-butylbenzyl bromide (2 g, 8.81 mmol) was added and the course of the reaction followed by tlc on silica (1% MeOH, 99% CH_2Cl_2, R_f(product)=0.83) After 24 hours reduced pressure distillation of DMF left an off-yellow solid. Taking up into dichloromethane (50 ml) filtering and concentration gave a green solid. Purification by column chromatography silica (CH_2Cl_2) gave the product, 0.70 g (27%). NMR and mass spectal data were the same as above.

***2-Acetamido-3-nitrotoluene*[6] (56)**

Concentrated sulphuric acid (1 g) was added to a stirred slurry of 2-methyl-6-nitroaniline (10 g, 65.8 mmol) and acetic anhydride (13 g, 127 mmol). Once the reaction had cooled down water (50 ml) was added, filtration gave an off-yellow solid. Recrystallization from 2:1 ethanol-water gave yellow crystals, 11.6 g (91%), m.p. 159-160°C (lit. 160-161°C)[5]; δ_H($CDCl_3$) 2.17 (3H, s, $COCH_3$), 2.26 (3H, s, $ArCH_3$), 7.21 (1H, t, Ar H5), 7.46 (1H, d, Ar H6), 7.77 (1H, d, Ar H4), 8.33 (1H, bs, NH); υ_{max} (KBr disc)/cm^{-1} 3303 (NH), 1665 (CO), 1359 (NO_2).

***2-Acetamido-3-nitrobenzoic acid*[5] (57)**

Potassium permanganate (11 g, 69.6 mmol) was slowly added to a stirred mixture of 2-acetamido-3-nitrotoluene (5 g, 25.8 mmol), magnesium sulphate (8 g, 66.7 mmol) and water (200 ml). The mixture was heated (100°C) until all the purple colour had gone (2.5 hours). Filtering through celite gave a yellow solution, acidification with sulphuric acid (50 v/v) resulted in crystallization, 3.4 g (60%), m.p. 179°C (Lit 178°C)[5]. Concentration of the mother liquor gave a further batch of less pure crystals, 1.41 g (23%); δ_H (CD_3OD) 2.15 (3H, s, CH_3), 7.46 (1H, t, Ar H5), 8.09 (1H, dd, Ar H6), 8.27 (1H, dd, Ar H4); υ_{max} (KBr disc)/cm^{-1} 3293 (NH), 3093-2900 (OH), 1716 (COOH), 1354 (NO_2).

***2-Amino-3-nitrobenzoic acid hydrochloride*[5] (58)**

Aqueous hydrochloric acid (25 v/v, 50 ml) was added to 2-acetamido-3-nitrobenzoic acid (8.4 g, 37.5 mmol) and the mixture boiled for 45 minutes. On cooling

the bright yellow solid was filtered off and dried under vacuum, 7.14 g (87%) Recrystallization from water gave a yellow solid m.p. 204-205°C (lit. 208.5-209°C)[5]; δ_H (DMSO-d_6) 6.74 (1H, t, Ar H5), 8.24 (1H, dd, Ar H6), 8.33 (1H, dd, Ar H4), 8.52 (2H, bs, NH_2), 13.51 (1H, bs, CO_2H); υ_{max} (KBr disc)/cm^{-1} 3475, 3343 (NH_2), 1690 (CO), 1356 (NO_2).

***2,3-Diaminobenzoic acid*[5] (59)**

Concentrated hydrochloric acid (80 ml) was added to a mixture of tin (II) chloride dihydrate (51.73 g, 0.23 mol) and 2-amino-3-nitrobenzoic acid hydrochloride (13.34 g, 0.061 mol) while maintaining a temperature of 60°C. Once in solution the mixture was stirred for 5 minutes and then boiled for a further 15 minutes. Adding the cooled mixture carefully to sodium hydroxide solution (59.2 g NaOH in 80 ml) and adjusting the acidity (to pH7) gave a thick off-white precipitate. Filtering and washing the residue with water (2x15 ml) followed by acidification with concentrated hydrochloric acid to pH1 of the filtrate gave white fibrous crystals. These crystals were collected by filtration and dried under vacuum, 12.2 g (89%) as the dihydrochloride salt. Sublimation (100°C, 0.05 mbar) gave the free amine, which decomposed on heating at 195°C (lit. m.p. 196-198°C)[5]; δ_H (DMSO-d_6) 6.68 (1H, t, Ar H5), 7.44 (1H, dd, Ar H4), 7.77 (1H, dd, Ar H6); υ_{max} (KBr disc)/cm^{-1} 3412, 3326 (NH_2), 2823 (OH), 1672 (CO).

***2,2'-Bis-1H-benzimidazole-4,4'-dicarboxylic acid* (60)**

Anhydrous ethylene glycol (1 ml) was added to a mixture of freshly sublimed 2,3-diaminobenzoic acid (0.39 g, 2.59 mmol) and oxamide (0.0927 g, 1.053 mmol). After heating (160°C) for 2.5 hours the mixture was added to hot water (15 ml) and filtered. An off-yellow crude product was obtained, 0.185 g (55%). Further purification proved difficult; δ_H (DMSO-d); bis-1H-benzimidazole 7.28 (2H, d), 7.32 (2H, d); bis-1H-benzimidazole-4,4'-dicarboxylic acid 7.35 (2H, d, H7), 7.45 (2H, t, H6), 7.93 (2H, d, H5); υ_{max} (KBr dics)/cm^{-1} 3442 (NH), 3064 (OH), 1690 (CO), 1347 (C=N), 743; Heating with anhydrous methanol formed the diester *m/z* (DCI, NH_3) 351 (M^+ +1), 293 (M^+ - CO_2Me +1).

***Dimethyl 2,2'-bis-1H-benzimidazole-4,4'-dicarboxylate* (61)**

Dry hydrochloric acid gas was bubbled into anhydrous methanol (15 ml) over 20 minutes. Crude 2,2'-bis-1H-benzimidazole-4,4'-dicarboxylic acid (0.503 g, 1.56 mmol) was added. The mixture was stirred and boiled under a nitrogen atmosphere. The course of the reaction was followed by tlc on alumina (2% MeOH, 98% CH_2Cl_2 R_f(product)=0.77). Afer 36 hours the remaining solid was separated by centrifugation. The green liquid was reduced in volume (to 5 ml), chloroform (10 ml) was added and more solids were formed which were separated by centrifugation. The green liquid was

washed with sodium hydrogen carbonate solution (0.1M, 2x15 ml), dried (K_2CO_3) and concentrated to give an orange yellow solid, 132 mg. Purification by column chromatography alumina (eluant 0-0.5% MeOH, 100-99.5% CH_2Cl_2) gave two main products. R_f=0.77 (10.4 mg); δ_H ($CDCl_3$) 3.97 (3H, s), 4.03 (3H, s), 7.36 (1H, t), 8.04 (2H, t), 11.0 (1H, bs); *m/z* (DCI NH_3) 351 (M^+ +1), 235 (M^+ -2x$COOCH_3$), 177. R_f=0.60 2,2'-bis-1H-benzimidazole-4-methylcarboxylate (24.9 mg); δ_H ($CDCl_3$) 4.06 (3H, s, CH_3), 7.23-7.36 (4H, m), 7.80-8.02 (3H, m); *m/z* (DCI NH_3) 294 (M^+ +2), 293 (M^+ +1), 235 (M^+ -$COOCH_3$), 177.

***Di(4-tert-butylbenzyl) 1,1'-di(4-tert-butylbenzyl)-2,2'-bisbenzimidazole-4,4'-dicarboxylate* (63)**

DMF (3 ml) was added to semi-purified 2,2'-bis-1H-benzimidazole-4,4'-dicarboxylic acid (73 mg, 0.226 mmol) and caesium carbonate (0.322 g, 1.02 mmol). The mixture was stirred under nitrogen for 5 minutes and 4-(tert-butyl)-benzyl bromide (208 ml, 1.13 mmol) was added. The mixture was heated (80°C) for 18 hours. Removal of DMF by reduced pressure distillation gave a yellow solid. Purification by column chromatography on silica (eluant 0-1% MeOH, 100-99% CH_2Cl_2 R_f(product)=0.83)) gave the product, 12.5 mg (6.1%); δ_H ($CDCl_3$) 1.32 (9H, s), 1.33 (9H, s), 5.15 (2H, s), 7.39 (11H, m); *m/z* (DCI NH_3) 907 (M^+), 761 (M^+ -R), 717 (M^+ -COOR), 571 (M^+ -COOR, -R), 425 (M^+ -COOR, -2xR), 235 (M^+ -2xCOOR, -2xR); υ_{max} ($CDCl_3$ solution)/cm^{-1} 2966 (aromatic CH), 1741 (CO), 1365 (C=N).

***2-Trichloromethyl-benzimidazole-4-carboxylic acid* (65)**

Methyl-2,2,2-trichloroacetimidate (0.29 g, 1.64 mmol) dissolved in methanol (2 ml) was added to freshly sublimed 2,3-diaminobenzoic acid (0.5 g, 3.29 mmol) in dry methanol (5 ml). The reaction was stirred at room temperature in the dark for 24 hours with nitrogen gas passing through the mixture. Water (20 ml) was added and the light yellow precipitate collected by filtration, 0.27 g (59%). Recrystallization from hydrochloric acid (0.1M) gave a light yellow solid m.p. 201-202°C; δ_H (DMSO-d_6) 7.45 (1H, t, Ar H6), 7.98 (2H, m, Ar H5 and H7); *m/z* (DCI NH_3) 283 (M^+ +1), 281, 279, 245 (M^+ -Cl); υ_{max} (KBr disc)/cm^{-1} 3391 (NH), 3084 (OH), 1694 (CO), 843, 822 (CCl). Found C, 38.81; H, 1.93; N, 9.74. $C_9H_5Cl_3N_2O_2$ requires: C, 38.66; H, 1.80; N, 10.06%.

***1-(4-tert-Butyl benzyl)-benzimidazole-4-carboxylic acid* (66)**

To a mixture of 2-trichloromethyl-benzimidazole-4-carboxylic acid (0.182 g, 0.578 mmol) and caesium carbonate (0.414 g, 1.27 mmol) in dry DMF (1.5 ml) was added 4-tert-butylbenzyl bromide (0.127 ml, 0.693 mmol). The mixture was heated (80°C) under an argon atmosphere for 35 hours. On cooling DMF was removed and the solid washed with water (20 ml), recrystallisation from chloroform gave the product as

a white solid, 100 mg (58%); m.p. 198°C; δ_H (75% $CDCl_3$ / 25% CD_3OD) 1.27 (9H, s, CH_3), 5.44 (2H, s, CH_2), 7.39 (4H, s, benzyl Ar), 7.63 (1H, t, H6), 8.05 (1H, d, H6), 8.20 (1H, d, H5), 9.48 (1H, s, H2); δ_C (CD_3OD) 31.64 (CH_3), 35.41 (CH_2), 68.3 (C2), 118.6, 120.7, 126.5, 127.6, 129.5, 131.0, 133.2, 148.8, 152.8, 154.3, 165.3 (COOH); *m/z* (DCI, NH_3) (M^+ +1) 309, (M^+ -Ar) 163; (DCI, accurate mass); found 309.1603 (M^+ +1) and calculated for $C_{19}H_{20}N_2O_2+H^+$ 309.1603; υ_{max} (KBr disc)/cm^{-1} 3425 (OH), 3100, 2961, 1706 (COOH), 1289.

1,1-Bis(methylthio)-2-nitroethene[7]

Carbon disulphide (9.34 g, 123 mmol) was added to a solution of nitromethane (5 g, 82.0 mmol) in dry ethanol (40 ml). Crushed potassium hydroxide (5.05 g, 90.2 mmol) was added and the reaction stirred under nitrogen at room temperature for 1 hour. The orange red precipitate was collected and added to a solution of methyl iodide (23.3 g, 164 mmol) in 50% aqueous methanol (50 ml). Following evaporation to dryness, the solid was dissolved in water (30 ml) and the product extracted with chloroform (3x30 ml), dried (K_2CO_3) and concentrated to give an off-yellow solid, 2.9 g (21%). Recrystallization from methanol gave yellow needle-shaped crystals m.p. 106-107°C δ_H ($CDCl_3$) 2.52 (3H, s, CH_3), 2.53 (3H, s, CH_3), 7.06 (1H, s, H); *m/z* (DCI NH_3) 183 (M^+ +18), 166 (M^+ +1), 149; υ_{max} (KBr disc)/cm^{-1} 1514, 1290 (NO_2). Found C, 29.13; H, 4.38; N, 8.42%. $C_4H_7NO_2S_2$ requires: C, 29.08; H, 4.27; N, 8.47%.

***3-Bromo-1,2-diaminobenzene* (72)**

3-Bromo-1,2-diaminobenzene was produced in four steps from 2-bromoaniline. 2-Bromo acetamide was prepared by dissolving 2-bromoaniline (25 g, 145 mmol) in acetic anhydride (30.6 g, 300 mmol) and carefully adding concentrated sulphuric acid (2.5 g). After the exothermic reaction had cooled down the mixture was poured onto warm water (100 ml) with continuous stirring. The white solid was collected by filtration, washed with water and vacuum dried, 31 g (100%). No further purification was needed; δ_H ($CDCl_3$) 2.72 (3H, s, CH_3), 6.95 (1H, t, H4), 7.28 (1H, t, H5), 7.51 (1H, d, H3), 7.64 (1H, bs, NH), 8.28 (1H, d, H6).

Nitration was carried out according to the literature[8]. A simplified purification procedure involved the recrystallization from chloroform to give the required isomer (2-bromo-6-nitroacetanilide) as white needle shaped crystals; (26%) m.p. 191-192°C (Lit. m.p. 193°C)[8]; δ_H ($CDCl_3$) 2.24 (3H, s, CH_3), 7.26 (1H, t, H4), 7.30 (1H, bs, NH), 7.98 (2H, m, H3 and H5).

2-bromo-6-nitroaniline[9] was made by the hydrolysis of the acetamide group in 78% yield; δ_H ($CDCl_3$) 6.61 (1H, m, H4), 6.6 (2H, bs, NH_2), 7.70 (1H, dd, H3), 8.14 (1H, dd, H5); υ_{max} (KBr disc)/cm^{-1} 3484, 3372 (NH_2), 1618, 1501, 1496..

Nitro group reduction using tin (II) chloride dihydrate and concentrated hydrochloric acid gave the product in 92% yield, which required no further purification; δ_H ($CDCl_3$) 3.6 (4H, s, NH_2), 6.56-6.62 (2H, m, H5 and H6), 7.02 (1H, m, H4); *m/z* (DCI, NH_3) 187, 189 (M^+ +1);υ_{max} (KBr disc)/cm^{-1} 3374, 3292 (NH_2), 1620, 1575, 1479.

***4,4'-Dibromo-2,2'-bis-1H-benzimidazole* (73)**

To a stirred solution of 3-bromo-1,2-diaminobenzene (2.98 g, 15.9 mmol) in dry methanol (25 ml), methyl-2,2,2-trichloroacetimidate (0.95 ml, 7.67 mmol) was added followed by concentrated hydrochloric acid (0.02 ml). After 3 hours fine mesh potassium carbonate (0.5 g) was added, followed by another addition (1 g) three hours later. After 18 hours water (80 ml) was added and the yellow precipitate collected by filtration and dried under vacuum. The crude product was purified by boiling the mixture in methanol to remove soluble impurities. After cooling to room temperature the mixture was filtered and dried under vacuum to give a yellow solid, 2.32 g (75%); m.p. >350°C; δ_H ($CDCl_3$, 0.5% TFA) 7.55 (2H, t, H6), 7.83 (1H, d, H7), 7.89 (1H, d, H5); δ_C ($CDCl_3$, 0.5% TFA) 107.8 (CBr), 115.0, 131.0, 133.0, 133.2 (C-C), 133.8, 134.0; *m/z* (DCI, NH_3) 391 (M^+ +1), 393 (M^+ +1), 395 (M^+ +1); υ_{max} (KBr disc)/cm^{-1} 1395, 1341, 778, 741, 732. Found C, 42.54; H, 2.01; N, 14.17%. $C_{14}H_8Br_2N_4$ requires: C, 42.89; H, 2.06; N,14.29%.

***1,1'-Bis(4-tert-butylbenzyl)-4,4'-dibromo-2,2'-bisbenzimidazole* (74)**

DMF (50 ml) was added to a mixture of 4,4'-dibromo-2,2'-bis-1H-benzimidazole (2.97 g, 7.58 mmol) and caesium carbonate (5.43 g, 16.7 mmol) and the mixture was stirred at room temperature under a nitrogen atmosphere for 15 minutes. 4-(Tert-butyl)benzyl bromide (3.78 g, 16.7 mmol) was added and the temperature raised to 80°C for 18 hours. On cooling, methanol (70 ml) was added and the precipitate collected by filtration, washed with water (40 ml) and dried to give an off-white solid. Recrystallization from methanol gave a white solid, 4.7g (90%); m.p. 316-317°C; δ_H ($CDCl_3$, 0.5% TFA) 1.21 (18H, s, CH_3), 5.53 (4H, s, CH_2), 7.10 (4H, d, H10), 7.27 (4H, d, H11), 7.67 (4H, m, H6 and H7), 7.96 (2H, dd, H5); δ_C ($CDCl_3$, 0.5% TFA) 30.82 (CH_3), 34.74 (C), 51.38 (CH_2), 109.8, 112.4, 126.8, 127.2, 127.8, 130.1, 133.8, 134.1, 134.3, 154.2; *m/z* (DCI, NH_3) 687 (M^+ +1), 685 (M^+ +1), 683 (M^+ +1), 607 (M-Br^++2), 605 (M-Br^++2), 537 (M-$CH_2C_6H_4C(CH_3)_3^+$ +2), 527 (M-2Br^+ +3), 459 (M-Br-$CH_2C_6H_4C(CH_3)_3^+$ +3); υ_{max} (KBr disc)/cm^{-1} 2964, 1410, 1334, 744. Found: C, 63.38; H, 5.26; N, 8.19% . $C_{36}H_{36}Br_2N_4$ requires: C, 63.17; H, 5.30; N, 8.18%.

***1,1'-Bis(4-tert-butylbenzyl)-2,2'-bisbenzimidazole-4,4'-dicarboxylic acid* (50)**

To a cold (-78°C) slurry of 1,1'-bis(4-tert-butylbenzyl)-4,4'-dibromo-2,2'-bis-benzimidazole (1 g, 1.46 mmol) in dry THF (30 ml) was added nbutyllithium (2.64 ml,

3.22 mmol) under a nitrogen atmosphere. After 1 hour, dry CO_2 was bubbled through the mixture for 20 minutes and allowed to warm to room temperature. Water was added (30 ml) and the solution was acidified to pH1 (HCl). The mixture was extracted with chloroform (3x20 ml), dried ($MgSO_4$), filtered and concentrated to give a light yellow solid. After recrystallizing from methanol the residue was taken up into chloroform (30 ml) and adsorbed onto silica. The starting material was recovered by washing the silica (2% MeOH, 98% CH_2Cl_2, 3x20 ml) and the product was then abstracted from the silica (40% MeOH, 60% CH_2Cl_2, 3x30 ml). The product eluate was filtered and the solution evaporated under reduced pressure. The solid was stirred with hydrochloric acid (0.01M, 40 ml) at 40°C for 10 hours, filtered, washed with water and dried in vacuum (25°C, 0.1 mmHg); 0.52 g (58%); m.p. 290°C; δ_H ($CDCl_3$) 1.26 (18H, s, CH_3), 6.06 (4H, s, CH_2), 7.01 (4H, d, bz ortho H), 7.30 (4H, d, bz meta H), 7.52 (2H, t, H6), 7.68 (2H, d, H7), 8.20 (2H, d, H5); δ_C ($CDCl_3$) 31.19 (CH_3), 34.55 (C), 49.40 (CH_2), 116.4, 120.1, 125.6, 125.9, 126.1, 127.3, 131.5, 135.5, 140.7, 141.4, 151.5, 165.2 (CO_2H); *m/z* (DCI, NH_3) 615 (M^+ +1), 469 (M^+ -$CH_2C_6H_4C(CH_3)_3$ +2); υ_{max} (KBr disc)/cm^{-1} 3211 (OH), 2955 (CH's), 1740 (C=O), 1392, 1346, 755. Found: C, 73.04; H, 6.29; N, 8.93%. $C_{38}H_{38}N_4O_4.1/2\ H_2O$ requires: C, 73.17; H, 6.30; N, 8.98%.

***1,1'-Dibenzyl-4,4'-dibromo-2,2'-bisbenzimidazole* (75)**

DMF (9 ml) was added to a mixture of 4,4'-dibromo-2,2'-bis-1H-benzimidazole (0.5 g, 1.28 mmol) and caesium carbonate (0.915 g, 2.81 mmol) and the mixture stirred at room temperature under an argon atmosphere for 10 minutes. Benzyl bromide (0.333 ml, 2.80 mmol) was rapidly added and the mixture heated at 80°C for 18 hours. After cooling, methanol (40 ml) was added and the resultant precipitate was collected by filtration, washed with water and dried under vacuum to give a white solid, 0.55 g (75%) which was recrystallized from chloroform m.pt >250°C ; δ_H ($CDCl_3$, 0.5% TFA) 5.53 (2H, s, CH_2), 6.74 (2H, d, bz ortho H), 7.08 (2H, t, bz meta H), 7.18 (1H, t,), 7.38 (2H, d,), 7.73 (1H, t, H6); δ_C ($CDCl_3$ TFA) 50.36 (CH_2), 111.2, 111.9, 126.8 (bz ortho C), 128.8, 129.3, 129.4 (bz meta C), 130.4, 132.3, 134.4, 135.8, 136.6; m/z (EI^+) 572 (M^+), 481 (M^+ -$CH_2C_6H_5$), 401 (M^+ -Br -$CH_2C_6H_5$); υ_{max} (KBr disc)/cm^{-1} 1413, 1335, 747, 715, 696. Found: C, 56.90; H, 3.49; N, 9.25%. $C_{28}H_{20}N_4Br_2.H_2O$ requires: C, 56.97; H, 3.78; N, 9.49%.

***1,1'-Dibenzyl-2,2'-bisbenzimidazole-4,4'-carboxylic acid* (76)**

To a cold slurry (-78°C) of 1,1'-dibenzyl-4,4'-dibromo-2,2'-bisbenzimidazole (0.179 g, 0.313 mmol) in dry THF (10 ml) n-butyl lithium (1.18M, 0.58 ml, 0.69 mmol) was added. The mixture was stirred under an argon atmosphere for three hours. Dry carbon dioxide was bubbled through the mixture for ten minutes and the mixture was allowed to warm to room temperature. Water (30 ml) was added and the solution acidified to pH1 (HCl). The mixture was extracted with chloroform (3x20 ml) and

concentrated to give an off white solid. Purification by column chromatography on silica (eluant 3% CH_3OH/ 97% CH_2Cl_2 to 50% CH_3OH/ 50% CH_2Cl_2) gave a white solid. Stirring with dilute hydrochloric acid (0.05M, 40 ml) for 12 hours at room temperature, vacuum drying gave the product as a white solid, 27mg (17%), m.p. > 250°C; δ_H ($CDCl_3$) 6.09 (2H, s, CH_2), 7.05 (2H, m, bz ortho H), 7.29 (3H, m, bz meta and para H), 7.54 (1H, t, H6), 7.67 (1H, dd, H7), 8.23 (1H, dd, H5); δ_C ($CDCl_3$) 49.69 (CH_2), 116.2, 120.2, 125.8, 126.0 (bz ortho C), 127.5, 128.5, 129.3 (bz meta C), 134.6, 135.6, 140.8, 141.4, 165.1 (COOH); *m/z* (DCI, NH_3) 503 (M^+ +1), 459 (M^+ -COOH +2), 415 (M^+ -2COOH +3), 369 (M^+ - CH_2Ph -COOH +3), 325 (M^+ -CH_2Ph - 2COOH +4); υ_{max} (KBr dics)/ cm^{-1} 3447 (OH), 1736 (C=O), 1407, 1396, 724. Found C, 71.00; H, 4.28; N, 10.83%. $C_{30}H_{22}N_4O_4.1/4(H_2O)$ requires C, 71.07; H, 4.47; N, 11.05%.

***4-Dodecylbenzyl bromide* (79)**

To a cooled (ice bath) mixture of paraformaldehyde (9g, 0.225 moles) in methanol (15 ml) phosphorous tribromide (15g, 0.0553 moles) was added over 30 minutes maintaining the temperature below 35°C. To this solution a mixture of concentrated sulphuric acid (44g) and highly branched dodecyl benzene[10] (50g, 0.203 moles) was added rapidly. The reaction was maintained at 65°C for 15 hours. Water (400ml) was added and the organic extracted with hexane (4x200 ml). The combined organics were washed with sodium carbonate solution (3x50 ml), dried $MgSO_4$ and concentrated to give a dark oil. Kugelrohr distillation (130°C, 0.01 mmHg) gave the product as a clear oil ; δ_H ($CDCl_3$) 0.6-0.9 (9H, m, CH_3), 0.9-1.35 (12H, m, CH_2), 1.4-1.7 (4H, m, CH), 4.50 (2H, s, CH_2Br), 7.2-7.4 (4H, m, Ar);

***1,1'-Bis-(4-dodecylbenzyl)-4,4'-dibromo-2,2'-bisbenzimidazole* (80)**

DMF (20 ml) was added to a mixture of 4,4'-dibromo-2,2'-bis-1H-benzimidazole (1 g, 2.55 mmol) and caesium carbonate (1.8 g, 5.52 mmol) and the mixture stirred at room temperature under argon for 5 minutes. 4-Dodecylbenzyl bromide (1.9 g, 5.61 mmol) was added and the temperature raised to 80°C for 36 hours. Once cooled, the mixture was poured onto methanol (100 ml), the solid collected by filtration, washed with water (40 ml) and dried under vacuum to give a light yellow solid, 1.64 g (71%). Crystallization from 40-60 petroleum ether gave a white solid m.p. 134-137°C; δ_H ($CDCl_3$) 0.65- 1.7 (50H, bm, $C_{12}H_{25}$), 6.25 (4H, s, NCH_2), 7.05-7.2 (10H, m, Ar CH's), 7.38 (2H, t, H6) 7.50 (2H, d, H5); *m/z* (DCI, NH_3) 910 (M^+ +1), 896 (M^+ -CH_2 +1), 882, 868, 854, 840; υ_{max} (KBr disc)/cm^{-1} 2980 (CH's), 1420, 1340, 770. Found: C, 67.48; H, 7.54; N, 6.35%. $C_{52}H_{68}Br_2N_4.H_2O$ requires: C, 67.38; H, 7.54; N, 6.19%.

1,1'-Bis-(4-dodecylbenzyl)-2,2'-bisbenzimidazole-4,4'-dicarboxylic acid **(81)**

To a cooled solution (-78°C) of 1,1'-bis-(4-dodecylbenzyl)-4,4'-dibromo-2,2'-bisbenzimidazole (0.8 g, 0.88 mmol) in dry THF (20 ml) was added n-butyl lithium (1.18M, 1.80 ml, 2.11 mmol). After 18 minutes of stirring under an argon atmosphere dry carbon dioxide was bubbled through the solution for 10 minutes. After warming to room temperature water (15 ml) was added and the acidity adjusted to pH1. The mixture was extracted with diethyl ether (3x15 ml), dried ($MgSO_4$) and concentrated to give a yellow solid. Crystallization from 40-60 petroleum ether gave the product as a light yellow solid, 0.5g (68%); m.p. 198-203°C; δ_H ($CDCl_3$) 0.4-1.6 (25H, m, $C_{12}H_{25}$), 6.04 (2H, s, CH_2), 6.99 (2H, d, bz ortho H), 7.19 (2H, d, bz meta H), 7.52 (1H, t, H6), 7.68 (1H, d, H7), 8.21 (1H, d, H5); *m/z* (DCI, NH_3) 839 (M^+ +1), 825 (M^+ -CH_2 +2), 811, 795; υ_{max} (KBr disc)/cm^{-1} 3182 (OH), 2956, 2928, 2867 (CH), 1736 (C=O), 1403, 1361, 758. Found C, 77.33; H, 8.42; N, 6.66%. $C_{54}H_{70}N_4O_4$ requires: C, 77.29; H, 8.41; N, 6.68%.

5.2.2 Synthesis of bisbenzimidazole phosphorus (V) esters

1,1'-Di(4-tert-butylbenzyl) 2,2'-bisbenzimidazole-4,4'-bis(O-ethyl-benzyl-phosphate ester) **(85)**

n-Butyl lithium (1.22 M, 1.53 ml, 1.86 mmol) was added to a cold (-78°C) slurry of 4,4'-dibromo-1,1'-di(4-tert-butyl)benzyl-2,2'-bisbenzimidazole (0.51 g, 0.745 mmol) in dry THF (10 ml) under a nitrogen atmosphere. After 45 minutes diethylchlorophosphonite (0.26 ml, 1.79 mmol) was added and the reaction allowed to warm to room temperature. The solvent was removed under vacuum and dry acetonitrile (10 ml) was added followed by benzyl chloride (1.5 g, 11.8 mmol). The reaction was heated (60°C) and followed by ^{31}P NMR (starting material δ_P = 153 ppm, product δ_P = 41 ppm). Concentration gave a light yellow solid, purification by column chromatography, alumina (eluant CH_2Cl_2, going to 1% MeOH/99% CH_2Cl_2, R_f(product)= 0.24) gave a white solid 170 mg (26%), δ_P ($CDCl_3$) 37.6, 37.1; δ_H ($CDCl_3$) 1.17 (6H, t, CH_2CH_3), 1.19, 1.20 (18H, s, CCH_3), 3.6 (2H, quint, CH_2), 4.01 (2H, quint, OCH_2), 6.50 (4H, s, NCH_2), 6.93 (4H, m, Pbenzyl ortho H), 7.11 (6H, m, Pbenzyl meta and para H), 7.21 (4H, d, ^{t}butylbenzyl ortho H), 7.28 (4H, d, ^{t}butylbenzyl meta H), 7.37 (2H, td, H6), 7.74 (2H, d, H7), 7.88 (2H, dd, H5); δ_C ($CDCl_3$) 16.33 (d, ^3J=6.3 Hz, OCH_2CH_3), 31.06 (CCH_3), 34.29 (C), 37.1 (d, ^1J=50 Hz, PCH_2), 49.0 (NCH_2), 60.71 (d, ^2J=6.7 Hz), 115.3, 123.9 (d, J=12 Hz), 122.4 (d), 125.6, 126.1, 126.2, 128.1, 130.0 (d, J=6Hz), 131.4 (d, J=8.2), 133.2, 135.8 (d), 142.2 (d), 142.9 (s), 150.6 (s); *m/z* (DCI, NH_3) 890 (M^+ +1), 708 (M^+ -P(O)OEtBz +2), 527 (M^+ -2P(O)OEtBz +3), 381 (M^+ -2P(O)OEtBz -tBuAr +4).

***1,1'-Di(4-tert-butylbenzyl)-2,2'-bisbenzimidazole-4,4'-bis(O-ethyl phenyl thiophosphinate ester)* (89)**

To a cold (-78°C) slurry of 1,1'-di(4-tert-butylbenzyl)-2,2'-bisbenzimidazole (0.3 g, 0.438 mmol) in dry THF (15 ml), n-butyl lithium (1.18M, 0.82 ml, 0.97 mmol) was added, and the reaction stirred under argon for one hour. Freshly made chloroethylphenylphosphine (0.198 g, 1.05 mmol) (made by the equal molar addition of dichlorophenylphosphine and diethylphenylphosphine at 0°C under an argon atmosphere) was added and the reaction allowed to warm to room temperature. Dried sulphur (0.3 g, 1.17 mmol) was added and the mixture stirred at room temperature for 4 hours. THF was removed under vacuum and the organics extracted with hot chloroform (3x20 ml), concentration gave an off-white solid. Partial purification by column chromatography silica (eluant CH_2Cl_2, R_f(product)=0.25), gave the product 50% pure by ^1H NMR with the major impurity being the starting bisbenzimidazole. δ_P ($CDCl_3$) 79.14, 79.50; *m/z* (DCI, NH_3) 895 (M^++1), 750 (M^+ -$CH_2ArC(CH_3)_3$ +2).

***1,1'-Di(4-tert-butylbenzyl)-2,2'-bisbenzimidazole-4,4'-bis(O,O-diethyl thiophosphinate ester)* (91)**

To a cold (-78°C) slurry of 1,1'-di(4-tert-butylbenzyl)-2,2'-bisbenzimidazole (0.5 g, 0.73 mmol) in dry THF (20 ml), n-butyl lithium (1.18M, 1.6 ml, 1.83 mmol) was added and the mixture stirred under an argon atmosphere for 2 hours. Diethyl chlorophosphite (0.16 ml, 0.94 mmol) was added and the mixture allowed to warm to room temperature. Dry sulphur (0.5 g, 1.95 mmol) was added and the mixture stirred for a further 4 hours. Concentration gave a light yellow solid. Initial purification by column chromatography on silica (eluant CH_2Cl_2) gave the product as a 50/50 mixture with the starting bisbenzimidazole. Further purification by column chromatography alumina (eluant chlorobenzene) increased the purity (75% product/25% starting material). Final purification by preparative tlc on alumina (eluant xylene) gave the product as a white solid, 80 mg (13%); m.p. 253°C; δ_P ($CDCl_3$) 83.02; δ_H ($CDCl_3$) 1.30 (6H, t, CH_2CH_3), 1.35 (18H, s, CCH_3), 4.24 (8H, quint, OCH_2), 6.56 (4H, s, NCH_2), 7. 28 (4H, d, ortho bz H), 7. 35 (4H, d, meta bz H), 7.46 (2H, td, J =3.2 Hz, H6), 7. 70 (2H, d, H7), 8.05 (2H, dd, J =17 Hz, J =7 Hz , H5); δ_C ($CDCl_3$) 16.12 (d, J =7.6 Hz, OCH_2CH3) 31.24 (CCH_3), 34.40 (C), 48.75 (NCH_2), 62.75 (d, J =5.6 Hz, OCH_2), 115.4 (d, J =3 Hz), 123.4 (d, J =16.1 Hz), 124.3 (d, J =152 Hz, C4), 125.4 (ortho bz C), 126.8 (meta bz C), 128.3 (d, J =11.5 Hz), 133.6, 136.1 (d, J = 13.3 Hz), 142.0 (d, J =7.6 Hz), 143.1, 150.3; *m/z* (DCI NH_3); υ_{max} (KBr disc)/cm^{-1} 2961 (CH's), 1055, 1023, 960. (DCI, accurate mass), found 831.330 (M^+ +1) and calculated for $C_{44}H_{56}N_4P_2S_2O_4$+H^+ 831.3297.

5.3 Chapter three experimental

5.3.1 Synthesis of phenanthroline 2,9-bis(methylene phosphinic acids)

***2,9-Bis(bromomethyl)-1,10-phenanthroline[11]* (104)**

A modification to the Chandler method[11] was made. A solution of HBr in acetic acid (48% v/v, 130 ml) was added to 2,9-bis(hydroxymethyl)-1,10-phenanthroline (3.71 g, 15.6 mmol) and the mixture stirred at 45°C for 15 hours. After cooling, the solution was poured into diethyl ether (1 L) and the yellow precipitate collected by filtration and dried under vacuum, 8.0 g. After neutralizing the solid with aqueous potassium carbonate solution (200 ml), the product was extracted with chloroform (3x150 ml), dried (K_2CO_3), filtered and concentrated to give a yellow solid, 3.93 g (69%), m.p. 109°C (Lit. m.p. 110-111°C)[11]; δ_H ($CDCl_3$) 4.97 (4H, s, CH_2), 7.80 (2H, s, H5 and H6), 7.91 (2H, d, H3 and H8), 8.30 (2H, d, H4 and H7); *m/z* (CI) 365, 367, 369 (M^+ +1).

Reaction of 2,9-bis(bromomethyl)-1,10-phenanthroline with diethylmethyl phosphonite.

Using 2,9-bis(bromomethyl)-1,10-phenanthroline (0.37 g, 2.13 mmol), diethylmethyl phosphonite (1.16 g, mmol) and dry acetonitrile (15 ml) the procedure of E. Cole[12] was followed. Purification by column chromatography (alumina, eluant CH_2Cl_2 going to 2% CH_3OH/98% CH_2Cl_2, Tlc conditions alumina, 5% CH_3OH/95% CH_2Cl_2) revealed a number of components:-

R_f=0.85 2,9-dimethyl-1,10-phenanthroline, 97 mg (22%); δ_H ($CDCl_3$) 2.94 (6H, s, CH_3), 7.48 (2H, d, H3 and H8), 7.69 (2H, s, H5 and H6), 8.11 (2H, d, H4 and H7), identical to an authentic sample.

R_f=0.47 Ethyl 9-methyl-1,10-phenanthroline-2-methylene(methylphosphinate) 54 mg (9%); δ_P ($CDCl_3$) 50.97; δ_H ($CDCl_3$) 1.29 (3H, t, OCH_2CH_2), 1.63 (3H, d, ^1J=14 Hz, PCH_3), 2.89 (3H, s, phenCH_3), 3.80 (2H, d, ^1J=18 Hz, PCH_2), 4.17 (2H, quint, OCH_2), 7.48 (1H, d, H8), 7.69 (1H, dd, H3), 7.71 (2H, s, H5 and H6), 8.11 (1H, d, H7), 8.18 (1H, d, H4); δ_C ($CDCl_3$) 14.10 (d, J=95 Hz, PCH_3), 14.48 (d, J=6 Hz, OCH_2CH_3), 25.63 (s, phenCH_3), 41.18 (d, J=84 Hz, PCH_2), 60.70 (d, J=6.5 Hz, OCH_2), 123.6 (s; C8), 123.7 (d, J=5 Hz, C3), 125.2 (C6), 126.1 (C5), 126.8 (C7c), 127.3 (d, J=2 Hz, C4b), 136.2 (C7), 136.7 (d, J=2 Hz, C4), 145.4 (C10d), 146.1 (d, C1a), 153.4 (d, J=6 Hz, C2), 159.3 (C9); *m/z* (DCI, NH_3) 315 (M^+ +1), 209 (M^+ - $P(O)OEtCH_3$ +2).

R_f=0.36 Diethyl 1,10-phenanthroline-2,9-bis(methylene(methylphosphinate)) 22.3 mg (2.5%) same data as literature[10].

***Diethyl 1,10-phenanthroline-2,9-bis(methylene(benzylphosphinate))* (105)**

To a slurry of 2,9-bis(bromomethyl)-1,10-phenanthroline (0.5 g, 1.37 mmol) in dry acetonitrile (10 ml) was added diethyl-benzyl phosphonite (1 ml). The mixture was stirred at room temperature for 15 minutes and then heated at 60°C for 4 hours. The reaction was followed by ^{31}P NMR (starting material δ_P = 175ppm). Concentration gave a light brown oil. Purification by column chromatography on neutral alumina (100% CH_2Cl_2 to 99.5% CH_2Cl_2 / 0.5% MeOH R_f(Product)=0.2) gave a clear glass, 0.28 g (36%); δ_P ($CDCl_3$) 47.62; δ_H ($CDCl_3$) 1.12 (6H, t, CH_3), 3.30 (4H, d, $PhCH_2$ ^2J=8.4Hz), 3.71 (4H, d, $PhenCH_2$ ^2J=8.6Hz), 3.95 (4H, quint, OCH_2), 7.24 (6H, m, phenyl ortho and para H), 7.47 (4H, d, phenyl meta H), 7.73 (2H, dd, H3 and H8), 7.77 (2H, s, H5 and H6), 8.21 (2H, d, H4 and H7); δ_C ($CDCl_3$) 16.36 (d, ^3J=5.8Hz CH_3), 35.84 (d, ^1J=88.2Hz, $PhCH_2$), 39.54 (d, ^1J=87.7Hz $PhenCH_2$), 61.00 (d, ^2J=7.03Hz, OCH2), 124.2 (d, ^3J=3.37Hz, C3 and C8), 125.9 (s, C5 and C6), 126.6 (d, ^5J=3.37, Ph para C), 127.2 (s, C4a), 128.4 (d, ^4J=2.82Hz, Ph meta C), 130.1 (d, ^3J=5.78Hz, Ph ortho C), 131.5 (d, ^2J=8.25Hz, Ph*C* CH_2), 136.5 (s, C4 and C7), 145.5 (s, C10b), 153.5 (d, ^2J=6.79Hz, C2 and C9); *m/z* (DCI, NH_3) 573 (M^+ +1), 482 (M^+ -Bz), 454 (M^+ -Bz-Et +1), 391 (M^+ - P(O)EtBz), 271 (M^+ -2Bz-2Et +2), 208 (M^+ -2P(O)EtBz); υ_{max} (thin film)/cm-^{1} 1496, 1227, 1033, 726.

***1,10-Phenanthroline-2,9-bis(methylene(benzylphosphinic) acid)* (107)**

To diethyl-1,10-phenanthroline-2,9-bis(methylene(benzylphosphinate)) (0.165 g, 0.288 mmol) hydrochloric acid was added (6M, 10 ml) and the solution heated at 105°C for 18 hours. The reaction was followed by ^{31}P NMR (product δ_P = 45.07 ppm). Concentration and vacuum drying gave a light yellow glass. Recrystallization from methanol gave a colourless solid, m.p. 145-146°C; δ_P (CD_3OD) 43.2; δ_H (CD_3OD) 3.44 (4H, d, ^1J=19.6Hz, CH_2Ph), 4.04 (4H, d, ^1J=16.4Hz, $PhenCH_2$), 7.08 (6H, m, phenyl ortho and para H), 7.30 (4H, d, phenyl meta H), 7.98 (2H, d, H3 and H8), 8.08 (2H, s, H5 and H6), 8.75 (2H, d, H4 and H7); δ_C (CD_3OD) 38.0 (bm, $PhenCH_2$), 38.29 (d, ^1J=90.2Hz, CH_2Ph), 127.9 (d, ^3J=3.42Hz, C3), 128.1 (s, C5), 128.4 (d, ^5J=3.92Hz, Ph para C), 129.6 (d, ^4J=2.46Hz, Ph meta C), 131.1 (d, ^3J=5.98Hz, Ph ortho C), 132.2 (d, ^2J=8.30Hz, $PhCCH_2$), 138.0 (d, ^4J=1.36Hz, C10b), 142.8 (s, C4), 154.7 (d, ^2J=8.55Hz, C2); *m/z* (DCI, NH_3) 518 (M^+ +2), 363 (M^+ -P(O)OHBz), 209 (M^+ -2P(O)OHBz); υ_{max} (KBr dics)/cm-1 2710, 1603, 1216, 1185, 934, 698. Found C, 58.38; H, 5.30; N, 4.56%. $C_{28}H_{26}N_2O_4P_2.HCl.3/2H_2O$ requires: C, 57.99; H, 5.21; N, 4.83%.

***Diethyl 1,10-phenanthroline-2,9-bis(methylene(phenylphosphinate))* (106)**

To a stirred slurry of 2,9-dibromo-1,10-phenanthroline (2.0 g, 5.46 mmol) in dry acetonitrile at room temperature, diethyl phenylphosphonite (3.25 g, 16.4 mmol) was added. Under a nitrogen atmosphere the mixture was allowed to stir for 30 minutes and

then heated at 60°C for 3 hours. Concentration gave an orange-brown viscous oil. Purification by column chromatography on neutral alumina (100% CH_2Cl_2 to 99.5% CH_2Cl_2/ 0.5% MeOH), tlc alumina (99% CH_2Cl_2 1% MeOH) R_f(product)=0.15, gave a light yellow glass, 0.93 g (31%); δ_P ($CDCl_3$) 38.73; δ_H ($CDCl_3$) 1.24 (6H, t, CH3), 3.98 (4H, d, ^2J=17.0Hz, CH_2P), 3.98 (1H, qd, OCH_2), 4.15 (1H, qd, OCH_2), 7.46 (6H, m, benzyl ortho and para H), 7.62-7.89 (8H, m, benzyl meta H, H5, H6, H3 and H8), 8.10 (2H, d, H4 and H7); δ_C ($CDCl_3$) 16.38 (d, ^3J=6.43 Hz, CH_3), 41.44 (d, ^1J=91.5 Hz, CH_2P), 61.24 (d, ^2J=6.43 Hz, OCH_2), 124.0 (d, ^3J=2.92 Hz, C3), 125.9 (s, C5), 127.3 (d, ^5J=1.86 Hz, C4a), 128.4 (d, ^2J=12.9 Hz, Ph ortho C), 130.6 (d, ^1J=126.2 Hz, Ph C-P), 131.7 (d, ^3J=10.0 Hz, Ph meta C), 132.3 (d, ^4J=2.77 Hz, Ph para C), 136.2 (s, C4), 145.4 (s, C10b), 153.1 (d, ^2J=6.64 Hz, C2); *m/z* (DCI, NH_3) 544 (M^+ +1), 376 (M^+ -P(O)OEtPh), 208 (M^+ -2P(O)OEtPh); υ_{max} (neat)/cm-1 1591, 1224, 1122, 954.

1,10-Phenanthroline-2,9-bis(methylene(phenylphosphinic) acid) **(108)**

To the ester diethyl 1,10-phenanthroline-2,9-bis(methylene(phenyl-phosphinate)) (52.3 mg, 0.096 mmol) was added potassium hydroxide solution (1 ml, 50% v/v MeOH/H_2O) and the solution stirred at room temperature. The reaction was followed by ^{31}P NMR monitoring the disappearance of starting material (δ_P = 43.3 ppm). After 48 hours the solution was neutralised with hydrochloric acid to pH6.5 and pumped dry. The product was extracted with ethanol (3x10 ml) and concentrated to give a white solid. δ_P (CD_3OD) 25.3; δ_H (CD_3OD) 3.61 (4H, d, ^2J=16.8 Hz, CH_2), 7.21 (2H, dd, benzyl para H), 7.37 (6H, m, Ar), 7.72 (6H, m, Ar), 8.09 (2H, d, H4 and H7); δ_C (CD_3OD) 45.0 (bd, CH_2), 126.1 (d, ^3J=3.27Hz, C3), 126.8 (s, C5), 128.5 (d, ^5J=2.01Hz, C4a), 128.9 (d, ^2J=12.1Hz, Ph ortho C), 131.5 (d, ^4J=2.5Hz, Ph para C), 132.5 (d, ^3J=9.1Hz, Ph meta C), 137.7 (s, C4), 139.3 (d, ^1J=128.1Hz, PhC-P), 146.1 (d, ^4J=2.16Hz, C10b), 158.3 (d, ^2J=8.05Hz, C2); m/z (ESMS) 554.9, 555.9 (MNa_3^+); υ_{max} (KBr disc)/cm^{-1} 3385, 1589, 1174, 1129, 1043. Refer to page 97 for micro analysis of cadmium and zinc complexes.

4-Dodecoxybromobenzene **(119)**

4-Bromophenol (20 g, 0.1156 mol) was added to sodium ethoxide (0.117 mol) in dry ethanol (150 ml) under a nitrogen atmosphere. After 30 minutes dodecyl bromide (23.05 g, 0.0925 mol) was added and the reaction boiled for 48 hours. Water (100 ml) was added and the pH adjusted to pH 12 (K_2CO_3) and the organics extracted with diethyl ether (3x150 ml). The combined organic layers were washed with sodium hydroxide solution (50 ml pH 13), dried ($MgSO_4$) and concentrated to give a low melting point solid. Recrystallization from 40-60 petroleum ether gave colourless crystals m.p. 27°C; δ_H ($CDCl_3$) 0.90 (3H, t, CH_3), 1.25-1.50 (18H, m, CH_2's), 1.78 (2H, quint, OCH_2CH_2), 3.92 (2H, t, OCH_2), 6.78 (2H, d, ArH2), 7.36 (2H, d, ArH3); δ_C ($CDCl_3$) 14.12 (CH_3), 22.69, 25.98, 29.16, 29.36, 29.56, 29.59, 29.64, 31.9

(OCH_2CH_2), 68.22 (OCH_2), 112.5 (ArC4), 116.3, 132.1, 158.2 (ArC1); *m/z* (DCI, NH_3) 340, 342 (M^+ +1), 172,174 (M^+ -$C_{12}H_{25}$); υ_{max} (KBr dics)cm^{-1} 2918, 2849 (CH), 1490, 1475, 1240, 821. Found C, 63.47; H, 8.65%. $C_{18}H_{29}BrO$ requires: C, 63.34; H, 8.56%.

***Diethyl dodecylphosphonite* (116)**

To a cold (-10°C) diethyl ether solution of dodecylmagnesium bromide (1M, 50 ml, 50 mmol) was added diethyl chlorophosphonite (9.3 ml, 65 mmol) while maintaining a temperature of 0-5°C. The mixture was stirred for 30 minutes and allowed to warm to room temperature. Filtering through a sinter (No. 3) under a nitrogen atmosphere and concentration gave a wax. The product was not purified further. A standard solution in benzene was made (0.323 mmol/1 ml). δ_P (C_6H_6) 182.5; δ_H ($CDCl_3$) 0.84 (6H, t, CH_2CH_3), 1.17-1.35 (23H, m, CH_2 and CH_3), 3.83 (4H, quint, OCH_2), 4.21 (2H, quint of d, CH_2P); δ_C ($CDCl_3$) 14.00 (s, CH_3), 17.17 (d, ^3J = 5.3 Hz, OCH_2CH_3), 22.08 (d, J = 16.6 Hz, CH_2), 22.60 (s), 29.29 (d, J = 1.87 Hz, CH_2), 29.42 (s), 29.56 (bs, CH_2's), 30.95 (d J = 11.7 Hz), 31.84 (s), 34.18 (d, J = 16 Hz), 62.79 (d, ^2J = 12.9 Hz, OCH_2); *m/z* (DCI, NH_3) 307 (M^+ +17), 291 (M^+ +1), 263 (M^+ -Et); υ_{max} (solution, benzene)/cm^{-1} 2927, 2855 (CH's), 1467, 1035 (POC).

***Diethyl 4-dodecoxyphenylphosphonite* (120)**

4-Dodecoxybromobenzene (16 g, 46.9 mmol) was added to magnesium turnings (4.5 g, 188 mmol) and an iodine crystal in dry THF (100 ml) over 45 minutes. After heating (60°C) initiation occurred and the reaction gave a light brown solution. Excess magnesium was filtered off using a sinter under a nitrogen atmosphere. To the solution diethyl chlorophosphosphonite (8.7 ml, 61 mmol) was added slowly while maintaining a temperature of 0-5°C. After allowing to warm to room temperature and stirring for 47 minutes, the solution was pumped dry. Dry benzene (60 ml) was added and the insoluble magnesium salts were removed by filtering through a sinter (No. 3) under a nitrogen atmosphere. The resultant solution was concentrated and a standard solution made in dry benzene (0.695 mmol/1ml). No further purification was attempted, ^{31}P NMR indicated only one phosphorus containing compound and ^1H NMR analysis indicated the compound was about 80% pure; δ_P (C_6H_6) 155.3; δ_H ($CDCl_3$) 0.89 (6H, t, CH_2CH_3), 1.23-1.35 (21H, m, CH_2 and CH_3), 1.78 (2H, quint, $ArOCH_2CH_2$), 3.90 (2H, t, $ArOCH_2$), 3.95 (4H, quint, $POCH_2$), 6.93 (2H, d, ArH3), 7.52 (2H, dd, ArH2).

5.3.2 Synthesis of 2,9-diphenyl phenanthrolines

***2,9-Bis(2-methoxymethylphenyl)-1,10-phenanthroline*[13] (139)**

2,9-Dichloro-1,10-phenanthroline[14] (2.04 g, 8.19 mmol) was added to a mixture of toluene (55 ml), water (28 ml), sodium carbonate (5.87 g, 0.055 mol) and

tetrakis(triphenylphosphine)palladium (0) (97 mg, 0.083 mmol). The vessel was purged with nitrogen and 2-methoxymethylphenylboronic acid[15] (3.029 g, 18.25 mmol) in ethanol (15 ml) was added. The mixture was boiled under a nitrogen atmosphere. After 18 hours the reaction was cooled and then filtered through a celite bed. The filtrate was added to water (60 ml) and extracted with dichloromethane (3x50 ml). The combined organic extracts were dried ($NaSO_3$), filtered and concentrated, purification by column chromatography (silica, eluant 100% CH_2Cl_2 going to 99% CH_2Cl_2/1% CH_3OH), gave the product as a light yellow solid, 2.8g (81%), m.p. 85°C; δ_H ($CDCl_3$) 3.37 (6H, s, CH_3), 5.00 (4H, s, CH_2), 7.46 (4H, m, phenyl Ar), 7.71 (4H, m, phenyl Ar), 7.79 (2H, s, phen H5 and H6), 7.91 (2H, d, phen H4 and H7), 8.29 (2H, d, phen H3 and H8); δ_C ($CDCl_3$) 85.14 (CH_3), 72.72 (CH_2), 123.5, 126.1, 127.2, 127.3, 128.5, 128.6, 130.4, 136.3, 137.1, 139.9, 145.5, 160.0; *m/z* (DCI, NH_3) 421 (M^++1); υ_{max} (KBr disc)/cm^{-1} 2918, 2868, 2820 (CH), 1477, 1089, 850, 771, 745. Found C, 77.63; H, 5.64; N, 6.76%. $C_{28}H_{24}N_2O_2.2/3(H_2O)$ requires C, 77.76; H, 5.90; N, 6.86%.

***2,9-Bis(2-bromomethylphenyl)-1,10-phenanthroline hydrobromide* (141)**

A solution of HBr in acetic acid (48 v/v, 20 ml) was added to 2,9-bis(2-methoxymethylphenyl)-1,10-phenanthroline (1.4 g, 3.3 mmol) and the mixture stirred at room temperature for 18 hours. The mixture was added to ether (70 ml), the precipitate was collected by filtration, washed with diethyl ether (40 ml) and dried under vacuum to give a yellow solid which started to decompose at about 190°C; δ_H ($CDCl_3$, 0.5% TFA) 4.57 (4H, s, CH_2Br), 7.50-7.75 (8H, m, phenyl Ar), 8.54 (2H, s, phen H5 and H6), 8.541 (4H, d, phen H4 and H7), 9. 29 (4H, d, phen H3 and H8); δ_C ($CDCl_3$, 0.5% TFA) 30.80 (CH_2), 128.3, 129.6, 130.6, 131.6, 131.9, 130.0, 136.6, 146.1, 157.5; υ_{max} (KBr disc)/cm^{-1} 3000 (broad), 1620, 1602, 1585, 1516, 1226, 882, 771, 740, 607.

***12-(2-Bromomethylphenyl)-1H-Indeno-[1,2-b]-phenanthrolin-14-ium bromide* (140)**

A solution of HBr in acetic acid (48 v/v, 2ml) was added to 2,9-bis(2-methoxymethylphenyl)-1,10-phenanthroline (50 mg, 0.012 mmol) and heated (100°C) for 36 hours. The mixture was pumped dry to give a light brown solid; δ_H ($CDCl_3$, 0.5% TFA) 4.62 (2H, s, CH_2Br), 7.03 (2H, s, CH_2N^+), 7.61-7.88 (7H, m, phenyl), 8.18 (1H, d), 8.32 (1H, s H5), 8.34 (1H, s, H6), 8.42 (1H, d), 8.71 (1H, d), 8.87 (1H, d), 9.34 (1H, d)

***Ethyl 2-bromophenylmethylene(phenylphosphinate)* (144)**

Diethyl phenylphosphonite (2.94 g, 14.9 mmol) was added to 2-bromobenzyl bromide (3.38 g, 13.5 mmol) in dry THF (20 ml). The mixture was stirred at 60 °C under a nitrogen atmosphere for 22 hours. The reaction was followed by ^{31}P NMR

(starting material δ_P = 154 ppm). Concentration gave a light yellow oil which was purified by column chromatography, (silica 100% CH_2Cl_2 going to 3% MeOH/97% CH_2Cl_2, R_f (product)= 0.4) to give a clear light yellow oil, 4.07g (89%); δ_P ($CDCl_3$) 38.9; δ_H ($CDCl_3$) 1.287 (3H, t, CH_3), (2H, m, benzylic CH_2), 3.81 (1H, quint, OCH_2), 4.06 (1H, quint, OCH_2), 7.06 (1H, tt, Ar), 7.23 (1H, t, Ar), 7.38-7.70 (7H, m, Ar); δ_C ($CDCl_3$) 16.30 (d, ^3J= 6.5 Hz, CH_3), 37.5 (d, ^1J=94.6 Hz, benzylic CH_2), 60.88 (d, ^2J= 6.5 Hz, OCH_2), 127.2 (d, J=3.1 Hz), 128.1 (s), 128.2 (d, J=3.4 Hz), 128.4 (s), 131.6 (s), 131.7 (d, J=2.4 Hz), 131.9 (s), 132.2 (d, J=2.8 Hz), 132.6 (d, J=2.8 Hz); *m/z* (DCI, NH_3) 339 and 341 (M^+ +1), 259, 215; υ_{max} (thin film)/cm^{-1} 2980 (CH), 1231, 1034, 1024, 954. Found C, 53.10; H, 4.91%. $C_{15}H_{16}BrO_2P$ requires: C, 53.12; H, 4.75%.

(2-Bromophenyl)methylene(phenylphosphinic) acid

Hydrochloric acid (6M, 15 ml) was added to ethyl(2-bromophenyl)methylene (phenylphosphinate) (0.51 g, 1.504 mmol) in isopropyl alcohol (2 ml). The reaction mixture was heated at 105 °C for four days and followed by ^{31}P NMR (product δ_P = 40.0 ppm). On cooling a white solid developed which was separated by centrifugation, washed (H_2O) and dried, 0.37 g (79%), m.p. 141-142°C; δ_P ($CDCl_3$) 40.05; δ_H ($CDCl_3$) 3.41 (2H, d, ^1J=18.5 Hz, CH_2), 6.98 (1H, tt, Ar), 7.14 (1H, t, Ar), 7.26-7.57 (7H, m, Ar), 11.2 (1H, s, OH); δ_C ($CDCl_3$) 38.20 (d, ^1J=92.9 Hz, CH_2), 125.2 (d, J=7.5 Hz), 127.2 (d, J=1.6 Hz), 128.1 (d, ^2J=13.6 Hz, P-Ar ortho C), 128.2 (d, J=3.8 Hz), 129.6 (s), 131.5 (d, J=10.1 Hz), 131.9 (d, J=4.9 Hz), 132.0 (d, ^1J=29.4 Hz, P-Ar), 132.1 (d, J=2.8 Hz), 132.6 (d, J=2.9 Hz); *m/z* (DCI, NH_3) 311, 313 (M^+ +1); υ_{max} (KBr disc)/cm^{-1} 2958, 2912 (CH's), 1672, 1251, 997 . Found: C, 50.14; H, 3.78%. $C_{13}H_{11}BrO_2P$ requires: C, 50.19; H, 3.89%.

***N,N-Dimethyl-(2-bromophenyl)ethanamide* (147)**

Oxalyl chloride (8.9 g, 69.8 mmol) was added to 2-bromophenyl acetic acid (3 g, 14.0 mmol) followed by DMF (0.1 ml) and the reaction left at room temperature for 90 minutes. The mixture was concentrated and pumped dry under vacuum for 30 minutes. After dissolving in dichloromethane (20 ml) dimethylamine (40% aqueous solution, 4 ml, 34.9 mmol) was added and the 2 phase mixture stirred vigorously for 45 minutes. The reaction mixture was washed with sodium hydroxide solution (2x30 ml, pH 13), then aqueous hydrochloric acid (1M, 2x30 ml). The organic phase were dried ($MgSO_4$), filtered and concentrated to give a white solid, 3.22 g (96%); m.p. 47°C; δ_H ($CDCl_3$) 2.98 (3H, s, CH_3), 3.01 (3H, s, CH_3), 3.79 (2H, s, CH_2), 7.10 (1H, m, H5), 7.26 (2H, dd, H3 and H4), 7.53 (1H, d, H3); δ_C ($CDCl_3$) 35.54 (CH_3), 37.46 (CH_3), 40.69 (CH_2), 124.6 (Ar C1), 127.5, 128.4, 130.6, 132.5, 135.2 (Ar C2), 169.9 (CO); *m/z* (DCI, NH_3) 242, 244 (M^+ +1); υ_{max} (KBr disc)/cm^{-1} . Found C, 49.52; H, 4.86; N, 5.23%. $C_{10}H_{12}BrNO$, requires; C, 49.61; H, 5.00; N, 5.79%.

***2-(2-Bromophenyl)ethylbenzyl ether* (148)**

To a solution of 2-(2-bromophenyl)ethanol (2.54 g, 12.67 mmol) in dry THF (30 ml) sodium hydride (0.37 g, 15.4 mmol) was carefully added under an argon atmosphere. After stirring for 10 minutes at room temperature benzyl bromide (2.60 g, 15.2 mmol) was added. The reaction was heated (70°C) for 12 hours and monitored by tlc for the disappearance of the alcohol (silica, CH_2Cl_2, R_f(alcohol)=0.33). Water (30 ml) was added and the organics were extracted with diethyl ether (3x40 ml), dried ($MgSO_4$), filtered and concentrated. Purification by Kugelrohr distillation (120°C, 0.005 mmHg), gave a clear oil, 2.58 g (70%); δ_H ($CDCl_3$) 3.20 (2H, t, Ar*CH*$_2$ CH_3), 3.83 (2H, t, $ArCH_2$*CH*$_3$), 4.66 (2H, s, $ArCH_2O$), 7.21 (1H, td, Ar), 7.4 (7H, m, Ar), 7.64 (1H, d, 2-Br phenyl H3); δ_C ($CDCl_3$) 36.5 (Ar*CH*$_2$$CH_3$), 69.4, 72.9, 124.7, 127.4, 127.6, 128.0, 128.4, 131.2, 132.8, 138.2, 138.4; *m/z* (DCI, NH_3) 290, 292 (M^+ +1), 108; υ_{max} (neat)/cm^{-1} 3029, 2931, 2858 (CH), 1099 (C-O-C).

***O-Ethyl (2-bromophenyl)-methyl-methylene(phenylphosphinate)* (149)**

To a cold (-78°C) solution of O-ethyl (2-bromophenyl)methylene (phenylphosphinate) (0.33 g, 0.98 mmol) in dry THF (3 ml) n-butyl lithium (1.18M, 0.96 ml, 1.08 mmol) was added under an argon atmosphere. After 15 minutes methyl iodide (0.154 g, 1.08 mmol) was added and the solution allowed to warm up to room temperature. The solution was re-cooled (-78°C) and the addition of n-butyl lithium (1.18M, 0.96 ml, 1.08 mmol) and methyl iodide (0.154 g, 1.08 mmol) was repeated. Once the reaction was completed (2 hours) the mixture was concentrated, taken up into diethyl ether (20 ml), filtered and concentrated to give a yellow oil. Purification by column chromatography (silica, eluant CH_2Cl_2 going to 1% MeOH/99% CH_2Cl_2) gave a colourless oil which was homogeneous single by tlc (silica 5% MeOH/95% CH_2Cl_2 R_f(product)=0.42), but consisting of 2 distereoisomers 0.15 g (42%) ; δ_P ($CDCl_3$) 42.43, 43.69; δ_H ($CDCl_3$) 1.10 and 1.30 (3H, t, OCH_2*CH*$_3$), 1.43 and 1.57 (3H, dd, J=16Hz and J=7.2Hz $CHCH_3$) 3.70 to 4.20 (4H, m, CH and OCH_2), 6.93 and 7.05 (1H, t, Ar); 7.15 to 7.70 (8H, m, Ar); *m/z* (DCI, NH_3) 353, 355 (M^+ +1).

***2-(Trimethylstannyl)-benzeneacetonitrile* (151)**

Dry degassed toluene (4 ml) was transferred by steel cannula to a mixture of 2-iodophenylacetonitrile (0.84 g, 3.44 mmol), hexamethylditin (2.25 g, 6.87 mmol) and tetrakis(triphenylphosphine)palladium (0) (70 mg, 0.0606 mmol) under an argon atmosphere. The reaction was heated at 110 °C for 18 hours, cooled, filtered and concentrated to give an oil. Purification by column chromatrography (silica, 100 % hexane to 70 % hexane / 30 % dichloromethane) gave the product as a colourless oil, 0.83 g (86%); GC analysis (50-250°C) showed the material to be greater than 95% pure ; δ_H ($CDCl_3$) 0.39 (9H, t, CH_3, J = 27.4 Hz), 3.74 (2H, s, CH_2), (7.36-7.48 (4H, m, Ar);

δ_C ($CDCl_3$) -8.39 (CH_3), 26.23 (CH_2), 118.0 (CN), 127.4, 128.1, 129.3, 136.8, 141.8; *m/z* (EI^+) 266 (M^++1-CH_3), 236; υ_{max} (neat)/cm^{-1} 3055, 2980, 2913 (CH), 2249 (CN), 1416, 773, 752, 529.

Reaction of 2,9-dichloro-1,10-phenanthroline with 2-(trimethylstannyl)-benzeneacetonitrile

Under an argon atmosphere dry degassed toluene (5 ml) was added to a mixture of 2,9-dichloro-1,10-phenanthroline (0.299 g, 1.202 mmol), 2-(trimethylstannyl)-benzeneacetonitrile (0.808 g, 2.89 mmol) and tetrakis(triphenylphosphine)palladium (0) (70 mg, 0.0606 mmol). The reaction was heated at 106 °C for 5 days. Filtering and concentration gave a light brown solid. Purification by column chromatography on silica (100% CH_2Cl_2 to 0.25% MeOH/99.75% CH_2Cl_2) gave the following compounds:

2-(2-(cyanomethyl)phenyl)-9-chloro-1,10-phenanthroline (152) as a white solid 0.14 g (35%) tlc on silica (99.5% CH_2Cl_2, 0.5% MeOH) R_f(product)=0.35, recrystallized from dichloromethane m.p.= 241°C; δ_H ($CDCl_3$) 4.60 (2H, s, CH_2), 7.49 (2H, m, phenyl-H), 7.67 (3H, m, H4 and phenyl-H), 7.82 (1H, d, H5), 7.88 (1H, d, H6), 7.96 (1H, d, H8), 8.22 (1H, d, H4), 8.39 (1H, d, H7); δ_C ($CDCl_3$), 23.0 (CH_2), 118.6 (CN), 123.5, 124.3, 125.8, 126.4, 127.3, 127.4, 128.2, 129.3, 129.8, 130.1, 130.4, 137.1, 138.5, 138.8, 144.0, 145.8, 151.4, 158.3; *m/z* (DCI, NH_3) (M^+ +1) 330, 332; υ_{max} (KBr dics)/cm^{-1} 2888, 2238 (CN), 1476, 1133, 849, 733; (DCI, accurate mass); found 330.0798 (M^+ +1), calculated for $C_{20}H_{12}ClN_3$+1 330.0798.

2,9-bis(2-(cyanomethyl)phenyl)-1,10-phenanthroline (153) as a white solid 0.10 g (20%) tlc on silica (99.5% CH_2Cl_2, 0.5% MeOH) R_f(product)=0.30. Further purification by plc (silica, 1% MeOH/ 99% CH_2Cl_2) did not improve the purity (about 85%); δ_H ($CDCl_3$) 4.54 (4H, s, CH_2), 7.26-7.50 (8H, m, phenyl-H), 7.90 (2H, s, phen H5 and H6), 7.91 (2H, d, phen H3 and H8), 8.42 (2H, d, phen H4 and H7); *m/z* (DCI, NH_3) 411 (M^+ +1); υ_{max} (KBr disc)/cm^{-1} 3051, 2925 (CH), 2239 (CN), 1478, 1433, 857, 745; (DCI, accurate mass); found 411.1610 (M^+ +1) and calculated for $C_{28}H_{18}N_4$+H^+ 411.1610.

2-(2-(cyanomethyl)phenyl)-9-methyl-1,10-phenanthroline (154) as a white solid which was recrystallized from dichloromethane, 0.037g (10%); δ_H ($CDCl_3$) 2.91 (3H, s, CH_3), 4.64 (2H, s, CH2), 7.48 (3H, m, phen H8, benzene H's), 7.67 (2H, m, benzene H's), 7.71 (2H, s, phen H5 and H6), 7.78 (1H, d, phen H3), 8.15 (1H, d, phen H7), 8.36 (1H, d, phen H4); *m/z* (DCI, NH_3) 310 (M^+ +1); υ_{max} (KBr disc)/cm^{-1} 2871 (CH), 2237 (CN), 1498, 1481, 846, 731. (DCI, accurate mass); found 309.1266 (M^+ +1) and calculated for $C_{21}H_{15}N_3$+H^+ 309.1266.

***2-(9-Hydroxy-1, 10-phenanthroline)-phenylacetic acid* (155)**

Hydrochloric acid (6M, 3 ml) was added to 2-(2-(cyanomethyl)phenyl)-9-chloro-1,10-phenanthroline (30 mg, 0.091 mmol). The mixture was heated at 110 °C for four days. Concentration gave a yellow solid, which was recrystallized from methanol to give white needle-shaped crystals, 10 mg (35%) m.p. 172°C; δ_H (CD_3OD), 3.97 (2H, s, CH_2), 6.83 (1H, d, H4), 7.45 (3H, m, Ar), 7.64 (1H, m, Ar), 7.73 (1H, s, H5), 7.75 (1H, s, H6), 7.87 (1H, d, H7), 8.15 (1H, d, H3), 8.45 (1H, d, H8); δ_C (CD_3OD) 40.59 (CH_2), 120.3, 123.2, 124.0, 126.1, 127.2, 129.1, 129.2, 130.7, 131.9, 132.8, 133.6, 134.8, 137.0, 137.7, 139.0, 141.6, 143.3, 161.0 (COOH); *m/z* (DCI, NH_3) 348 (M^+ +1); υ_{max} (KBr disc)/cm^{-1} 3444 (OH), 1716 (C=O), 1655, 1611; (DCI, accurate mass); found 348.144, and calculated for $C_{20}H_{14}N_2O_3 + NH_4^+$, 348.1348.

***1,10-Phenanthroline-2,9-bis(phenyl-2-acetic acid)* (157)**

2,9-Bis(2-(cyanomethyl)phenyl)-1,10-phenanthroline triphenylphosphine complex (0.049g , 0.097 mmol) was dried under vacuum (40°C, 0.1 mmHg) for 24 hours. To the solid, dry benzene (5 ml) and dry ethanol (1 ml) were added and the mixture cooled to 5°C. Dry hydrogen chloride (generated from concentrated sulphuric acid and sodium chloride) was bubbled through the mixture for 10 minutes. The flask was sealed and allowed to warm to room temperature with stirring. Reaction of the nitrile was monitored by ESMS (nitrile *m/z* = 411). After 48 hours concentration gave a yellow solid, which was heated (100°C) in acetic acid/6M HCl (1/1, 8 ml) for 36 hours. Filtering and concentration gave the crude product as a yellow glass. Attempted purification by prepatative HPLC (reverse phase conditions) did not remove all the triphenylphosphine oxide (1:3 triphenylphosphine oxide:product); 17.1mg (34%); δ_H (CD_3OD) 3.94 (4H, s, CH2), 7.54-7.64 (8H, m, phenyl-H), 8.24 (2H, d, H4 and H7), 8.31 (2H, s, H5 and H6), 8.95 (2H, d, H3 and H8); *m/z* (ESMS) 449 (M^+ +1); υ_{max} (KBr disc)/cm^{-1} 3422 (OH), 1718 (CO), 1186, 1120.

***O-Ethyl (2-(trimethylstannyl)phenyl)methylene(phenylphosphinate)* (158)**

O-Ethyl(2-bromophenyl)methylene(phenylphosphinate) (0.43 g, 1.79 mmol), hexamethylditin (1.17 g, 3.578 mmol) and tetrakis(triphenylphosphine)palladium (0) (30 mg, 0.026 mmol) were placed in a Schlenk tube and degassed 3 times. Dry degassed toluene (3 ml) was added under an argon atmosphere and the mixture heated (100 °C) for 6 hours. More catalyst (30 mg, 0.026 mmol)was added and the reaction heated for a further 12 hours. Filtering and concentration gave a light yellow oil. G.C.-M.S. (EI^+, 50-270 °C) indicated the presence of the product (retention time 1394 seconds) *m/z* (EI^+) 405, 407, 409, 410 (M^+ +1-CH_3).

5.4 Chapter four experimental

5.4.1 Synthesis of N-substituted $12N_3$

9-(2-Methoxylbenzyl)-1,5,9-triazacyclododecane-2,4-dione **(174)**

To a stirred slurry of 1,5,9-triazacyclododecane-2,4-dione[16] (2.06 g, 10.35 mmol) and fine-mesh potassium carbonate (1.57 g, 11.38 mmol) in anhydrous acetonitrile (40 ml), 2-methoxybenzyl chloride[17] (2.13 g, 13.6 mmol) in anhydrous acetonitrile (10 ml) was added. The mixture was boiled under nitrogen and followed by tlc silica (1% NH_3OH, 59% MeOH, 40% CH_2Cl_2, Rf(1,5,9-tricyclododecane-2,4-dione)=0.37). After 48 hours concentration gave the crude product. Washing with water (15 ml), dissolving in chloroform (20 ml) drying (K_2CO_3) and concentration gave an off-white solid, 3.14 (95%). Recrystallization from methanol gave rectangular white crystals m.p. 180-181°C. δ_H ($CDCl_3$) 1.74 (4H, quint, CH_2CH_2 CH_2), 2.54 (4H, t, CH_2 NHCO), 3.07 (2H, s, CH_2CO), 3.22 (4H, q, CH_2 NH), 3.47 (2H, s, $ArCH_2$), 3.90 (3H, s, OMe), 6.98 (2H, m, Ar), 7.21-7.35 (2H, m, Ar), 7.41 (2H, bt, NH); δ_C ($CDCl_3$) 24.6 (CH_2CH_2 CH_2), 40.6 (CH_2 NHCO), 46.3 ($ArCH_2$), 53.6 (CH_3), 55.0 (CH_2N), 55.8 (CH_2 CO), 111.5 (Ar C3), 121.0 (Ar C5), 126.3 (Ar C1), 129.1 (Ar C4), 132.0 (Ar C6), 157.7 (Ar C2), 166.8 (CO); *m/z* (DCI, NH_3) 320 (M^+ +1); υ_{max} (KBr disc)/cm^{-1} 3309 (NH), 3067, 3007 (Ar CH), 1683, 1643 (CO), 1242 (COC). Found C, 63.93; H, 7.89; N, 13.06%. $C_{17}H_{25}N_3O_3$ requires C, 63.93; H, 7.89; N, 13.16%.

1-(2-Methoxybenzyl)-1,5,9-triazacyclododecane **(175)**

To a cold slurry of 9-(2-methoxybenzyl)-1,5,9-triazacyclododecane-2,4-dione (0.5 g, 1.57 mmol) in anhydrous THF (15 ml) BH_3.THF (1M, 40 ml) was added slowly under a nitrogen atmosphere. The reaction was boiled and followed by IR spectroscopy for the disapperance of the carbonyl (1643 cm^{-1}). After 48 hours the mixture was cooled and methanol (20 ml) was carefully added followed by concentration. Two further additions of methanol (20 ml) followed by concentration were performed.

The resultant solid was boiled with hydrochloic acid (6M, 20 ml) for 3 hours. Following the removal of the acid, the solid was washed with methanol (3x25 ml). The white solid was taken up into aqueous sodium hydroxide solution (pH13, 50 ml). Extraction with chloroform (4x50 ml), drying (K_2CO_3), filtering and concentration gave a clear oil in quantitative yield. Slow recrystallization from toluene gave white crystals m.p. 118-119°C. δ_H ($CDCl_3$) 1.83 (4H, quint, NCH_2CH_2), 1.95 (2H, quint, $NHCH_2CH_2CH_2NH$), 2.53 (4H, t, $HNCH_2CH_2CH_2NH$), 2.78 (4H, t, $HNCH_2CH_2CH_2N$), 2.97 (4H, t, NCH_2), 3.55 (2H, s, $ArCH_2$), 3.80 (3H, s, CH_3), 6.90 (2H, t, Ar), 7.23 (2H, s, Ar); δ_C ($CDCl_3$) 23.56 ($NHCH_2CH_2CH_2NH$), 23.93 (NCH_2CH_2), 46.70 ($HNCH_2CH_2CH_2NH$), 49.36 ($HNCH_2$ CH_2CH_2N), 52.55 (CH_2N), 55.19 (CH_3), 110.7(Ar C3), 120.0 (Ar C5), 125.4 (Ar C1), 128.5 (Ar C4), 130.8 (Ar

C6), 157.9 (Ar C2); *m/z* (DCI, NH_3) 292 (M^+ +1), 170 (M^+ -$CH_2C_6H_4OCH_3$); υ_{max} (KBr disc)cm^{-1} 1597, 1584 (Ar CC), 1242 (COC). (DCI, accurate mass), found 292.2389 (M^+ +1) and calculated for $C_{17}H_{29}N_3O+H^+$ 292.2389

***1-(2-Hydroxybenzyl)-1,5,9-triazacyclododecane* (166)**

A solution of HBr in acetic acid (48% v/v, 6 ml) was added to 1-(2-methoxybenzyl)-1,5,9-triazacyclododecane (0.98 g, 3.18 mmol), p-hydroxyphenol (18.6 mg, 0.17 mmol) and heated to 110°C with stirring for 15 hours. After concentration of the mixture the material was taken up into aqueous sodium hydroxide solution (30 ml) and adjusted to pH12. Extraction with chloroform (3x30 ml), drying (K_2CO_3), filtering and concentration gave a dark coloured glass 0.72 g, (82%) purification by HPLC: R_t = 9.8 min. observed at λ = 254nm (Dynamax, reverse phase) with gradient elution $10cm^3min^{-1}$; A = H_2O/0.1% TFA, B = CH_3CN/0.1% TFA from t = 0 min.; A=90%, B=10% to t = 20min.; A=75%, B=25% and finally to t = 25 min.; A=100%, B=0% gave the product; δ_H ($CDCl_3$) 1.71 (6H, m, CH_2CH_2 CH_2), 2.54 (4H, t, $HNCH_2$ CH_2CH_2 NH), 2.64 (4H, t, $HNCH_2$ CH_2CH_2N), 2.80 (4H, t, CH_2N), 3.51 (2H, s, $ArCH_2$), 6.35 (3H, bs, NH and OH), 6.66 (1H, td, Ar H5), 6.79 (1H, dd, Ar H3), 6.94 (1H, dd, Ar H6), 7.08 (1H, td, Ar H4); δ_C ($CDCl_3$) 24.82 ($HNCH_2CH_2$ CH_2N), 25.13 ($HNCH_2CH_2$ CH_2NH), 46.18 ($HNCH_2$ CH_2CH_2 NH), 48.94 ($HNCH_2$ CH_2CHN), 52.79 (CH_2N), 56.50 ($ArCH_2$), 116.7 (Ar C3), 117.4 (Ar C5), 123.9 (Ar C1), 128.3 (Ar C6), 129.8 (Ar C4), 158.6 (Ar C2); *m/z* (DCI, NH_3) 278 (M^+ +1), 172 (M^+ -CH_2ArOH), 124 (M^+ -$H_2ArOH+NH_3$), 107 (M^+ -CH_2ArOH); υ_{max} (KBr disc)/cm^{-1} 3401 (OH), 1585. (DCI, accurate mass), found 278.2232 (M^+ +1) and calculated for $C_{16}H_{29}N_3O+H^+$ 278.2232.

5.4.2 Synthesis of C-substituted $12N_3$

***Diethyl 2-methoxylbenzylmalonate* (176)**

A solution of diethylmalonate (8.37 g, 52.3 mmol) in dry ethanol (20 ml) was added dropwise to a solution of sodium ethoxide (27 mmol) in dry ethanol (50 ml). After stirring for 30 minutes under a nitrogen atmosphere a solution of 2-methoxybenzyl chloride[15] (4.02 g, 25.7 mmol) in dry DMF (25 ml) was added dropwise over 30 minutes. The mixture was brought to reflux for 24 hours. Water (70 ml) was added to the cooled reaction and the solution filtered to remove any precipitated diethyl-bis(2-methoxybenzyl)malonate. Reduction in the solvent volume, extraction with diethyl ether (5x50 ml), drying the extract (K_2CO_3) and concentration gave a light yellow liquid. Purification by vacuum distillation (0.05 mmHg, 125-127°C)

gave the product as a colourless oil, 5.19 g (72%); δ_H ($CDCl_3$) 1.19 (6N, t, CH_3), 3.20 (2H, d, $ArCH_2$), 3.82 (3H, s, OCH_3), 3.82 (1H, t, CH), 4.13 (4H, q, CO_2CH_2), 6.85 (2H, m, Ar), 7.20 (2H, m, Ar); δ_C ($CDCl_3$) 14.50 (CH_3), 30.76 ($ArCH_2$), 51.95 (CH), 5.66 (OCH_3), 61.68 (OCH_2), 110.6 (Ar C3), 120.8 (Ar C5), 126.4 (Ar C1), 128.6 (Ar C4), 131.4 (Ar C6), 159.1 (Ar C1), 169.7 (C=O); *m/z* (EI^+) 280 (M^+), 206, 133, 115; υ_{max} (neat)/cm^{-1} 1730 (C=O). Found C, 63.78; H, 7.20%. $C_{15}H_{20}O_5$, requires; C, 64.27; H, 7.19%.

3-(2-Methoxybenzyl)-1,5,9-triazacyclododecane-2,4-dione **(177)**

1,5,9-Triazanonane (4.67 g, 35.6 mmol) was added to a stirred solution of diethyl-(2-methoxybenzyl)-malonate (10 g, 35.7 mmol) in ethanol (1.2 dm^3). The mixture was boiled under reflux for 40 days followed by concentration to give a clear yellow oil. Purification by column chromatography on silica (eluant 0-10% NH_3OH, 60-50% MeOH, 40% CH_2Cl_2) gave a white solid, 250 mg (2.2%) as the minor product and a viscous oil 2.53 g (19%) as the major half-cyclized intermediate. Attempted further cyclization of this material in dry acetonitrile (100 ml) did not give any more product. For 3-(2-methoxybenzyl)-1,5,9-triazacyclododecane-2,4-dione; δ_H (CD_3OD) 1.56 (2H, m, $CH_2\mathit{CH_2}$ CH_2), 1.69 (2H, m, $CH_2\mathit{CH_2}$ CH_2), 2.12 (1H, t, CH), 2.53 (2H, td, CH_2N), 2.84 (2H, td, CH_2N), 3.07 (2H, m, CH_2N), 3.10 (2H, d, $ArCH_2$), 3.51 (2H, td, CH_2N), 3.81 (3H, s, OCH_3), 6.79 (1H, t, Ar H5), 6.88 (1H, d, Ar H3), 7.08 (1H, d, Ar H6), 7.17 (1H, t, Ar H4); δ_C (CD_3OD) 28.02 ($CH_2\mathit{CH_2}CH_2$), 29.18 ($ArCH_2$), 41.56 (CH_2NHCO), 49.88 (CH_2NH), 54.68 (CH), 55.6 (OCH_3), 111.3 (Ar C3), 121.3 (Ar C5), 128.5 (Ar C1), 128.8 (Ar C4), 131.8 (Ar C6), 158.9 (Ar C2), 171.9 (CO); *m/z* (DCI, NH_3) 320 (M^+ +1); υ_{max} (KBr disc)/cm^{-1} 3309 (NH), 1669 (CO).

For half-cyclized material; δ_H ($CDCl_3$) 1.08 (2H, t, $CH_2\mathit{CH_3}$), 1.54 (4H, quint, $CH_2\mathit{CH_2}$ CH_2), 2.51 (2H, m, CH_2NHCO), 2.70 (2H, t, CH_2NH_2), 3.13 (4H, m, CH_2NH), 3.51 (2H, t, $ArCH_2$), 3.67 (1H, d, CH), 3.74 (3H, s, OCH_3), 4.01 (2H, q, OCH_2), 6.73 (2H, m, Ar), 7.07 (2H, m, Ar), 7.71 (1H, bs, NHCO); δ_C ($CDCl_3$) 13.78, 28.58, 30.83, 32.51, 38.11, 40.01, 47.44, .51.96, 52.59, 55.01, 60.89, 109.9, 120.1, 126.0, 127.8, 130.7, 157.2, 168.0, 170.7; *m/z* (DCI, NH_3,) 366 (M^+ +1), 352 (M^+ -CH_3), 294; υ_{max} (neat)/cm^{-1} 1730 (COO), 1650 (HNCO).

2-(2-Methoxybenzyl)propan-1,3-diol **(181)**

Lithium aluminium hydride (5 g, 131.6 mmol) was carefully added to cooled dry ether (300 ml) while stirring. The ester diethyl (2-methoxybenzyl)-malonate (12.3 g, 43.9 mmol) dissolved in dry ether (50 ml) was added dropwise to the cold solution while under nitrogen. The mixture was brought to reflux and stirred for 18 hours. Once cooled excess $LiAlH_4$ was quenched with water (5 ml), followed by sodium hydroxide solution (15%, 10 ml) and finally with water (5 ml). Filtering through celite, washing the residue with chloroform (50 ml) and concentration gave a clear viscous oil, 7.47 g

(87%). δ_H ($CDCl_3$) 1.99 (1H, m, CH), 2.66 (2H, d, $ArCH_2$), 3.02 (2H, bs, OH), 3.68 (4H, dd, CH_2O), 3.83 (3H, s, CH_3), 6.78 (1H, d, Ar H3), 6.90 (1H, td, Ar H5), 7.51 (1H, d, Ar H6), 7.20 (1H, td, Ar H4); δ_C ($CDCl_3$) 27.82 (CH), 43.28 ($ArCH_2$), 55.43 (OCH_3), 64.80 (CH_2 OH), 110.4 (Ar C5), 120.8 (Ar C3), 127.4 (Ar C4), 128.1 (Ar C1), 131.0 (Ar C6), 157.3 (Ar C2); *m/z* (DCI, NH_3) 214 (M^+ +18), 197 (M^+ +1), 179 (M^+ -OH); υ_{max} (neat)/cm^{-1} 3906 (OH), 3068, 3009 (Ar CH), 1601, 1588(Ar). Found C, 65.95; H, 8.50; N, 0.0%. $C_{11}H_{16}O_3.1/4(H_2O)$ requires C, 65.81; H8.28; N, 0.0%.

***2-(2-Methoxybenzyl)-propan-1,3-ditoluenesulfonate* (182)**

The alcohol 2-(2-methoxybenzyl)-propan-1,3-diol (1.50 g, 7.65 mmol) was dissolved in dry pyridine (10 ml) and stirred at -20°C. Recrystallized tosyl chloride (4.39 g, 23 mmol) dissolved in dry pyridine (10 ml) was slowly dripped into the solution while under nitrogen and maintaining the temperature (-20°C). After addition the flask was sealed and placed in a fridge (-18°C) for 3 days. Pouring onto crushed ice (25 cm^3) with stirring caused a white precipitate to form. Filtering, washing with dilute hydrochloric acid (2x10 ml, 0.01M) and vacuum drying gave a white solid, 3.38 g (87%). Recrystallizing from toluene gave needle shaped crystals m.p. 87-88°C; δ_H ($CDCl_3$) 2.35 (1H, septet, CH), 2.46 (6H, s, $ArCH_3$), 2.55(2H, d, $ArCH_2$), 3.74 (3H, s, OCH_3), 3.94 (4H, dd, CH_2O), 6.70-6.85 (3H, m, Ar), 7.18 (1H, td, Ar), 7.33 (4H, d, tosyl Ar H3), 7.72 (4H, d, tosyl Ar H2); δ_C ($CDCl_3$) 21.60 ($ArCH_3$), 28.34 (CH), 38.00 ($ArCH_2$), 55.01 (OCH_3), 68.56 (CH_2O), 110.2 (Ar C3), 120.3 (Ar C2), 125.6 (Ar C1), 127.8 (TsAr C3), 128.0 (Ar C4), 129.9 (TsAr C2), 130.8 (Ar C6), 132.4 (TsAr C4), 144.9 (TsAr C1), 157.3 (Ar C2); *m/z* (DCI, NH_3) 522 (M^+ +18), 504 (M^+), 333 (M^+ -OTs); υ_{max} (KBr disc)/cm^{-1} 3025, 2978 (Ar CH), 1359, 1178 ($S(=O)_2$). Found: C, 59.64; H, 5.56%. $C_{25}H_{28}O_7S_2$ requires: C, 59.51; H, 5.59%.

***1,5,9-Tris(p-tolylsulfonyl) 1,5,9-triazanonane* (183)**

1,5,9-Triazanonane (13.1 g, 0.1 mol) was added to a stirred solution of potassium carbonate (55.2 g, 0.4 mol) in water (150 ml). Tosyl chloride (76.4 g, 0.4 mol) in THF (350 ml) was slowly added over 1 hour. The two phase system was vigorously stirred and heated to 50°C for 12 hours. On cooling the upper THF layer was poured onto crushed ice, no crystals resulted. Evaporation of the THF, followed by extraction of the aqueous solution with dichloromethane (5x75 ml), drying (K_2CO_3) the extract, filtering and concentration gave a yellow oil. Dilution of the oil with hot ethanol (100 ml), resulted on crystallization on cooling. Collecting the crystals by filtration and drying by vacuum gave colourless crystals, 40.68 g (68%); m.p. 112°C; δ_H ($CDCl_3$) 1.70 (4H, quint, CH_2CH_2 CH_2), 2.41 (9H, s, CH_3), 2.94 (4H, q, $NHCH_2$), 3.09 (4H, t, NCH_2), 5.32 (2H, t, NH), 7.29 (6H, d, Ar H2), 7.62 (2H, d, Ar H3), 7.73 (2H, d, Ar H3); δ_C ($CDCl_3$) 21.40 (CH_3), 28.97 (CH_2CH_2 CH_2), 40.03 (CH_2NH), 46.57 (CH_2N), 126.9 (C4), 127.0 (C10), 129.6 (C3), 129.8 (C11), 135.3 (C12), 136.6

(C2), 143.3 (C5), 143.6 (C9); *m/z* (DCI, NH_3) 594 $(M)^+$, 440 $(M^+ -Ts)$; υ_{max} (KBr disc)/cm^{-1} 1337, 1161 ($S(=O)_2$). Found: C, 54.69; H, 6.10; N, 6.76%. $C_{27}H_{35}N_3O_6S_3$ requires: C, 54.62; H, 5.94; N, 7.08%.

***1,5,9-Tri(p-toylsulfonyl)-3-(2-methoxybenzyl)-1,5,9-triazacyclododecane* (184)**

1,5,9-Tri(p-tolylsulfonyl) 1,5,9-triazanonane (11.8 g, 19.8 mmol) was dissolved in dry DMF (250 ml) with fine potassium carbonate (5.7 g, 41.2 mmol). 2-(2-Methoxybenzyl)-propan-1,3-ditosylate (9.98 g, 19.8 mmol) dissolved in dry DMF (50 ml) was added dropwise over 2.5 hours at room temperature with stirring. The temperature was raised to 50°C for 18 hours and then to 70°C for 4 days. The reaction was followed by tlc silica (2% MeOH, 98% CH_2Cl_2, R_f(product)=0.69). DMF was distilled off under reduced pressure and the solids taken up into water (80 ml) and dichloromethane (80 ml). The organic layer was collected and the water layer extracted with dichloromethane (2x30 ml). Combining of the organic layers, drying (K_2CO_3), filtering and concentration gave a viscous oil. Crystallization from toluene gave colourless crystals, 4.03 g (27%) m.p. 238-239 °C; δ_H ($CDCl_3$) 1.64 (2H, bm, CH_2CH_2 CH_2), 1.94 (2H, bm, CH_2CH_2 CH_2), 2.41 (9H, s, CH_3), 2.54 (1H, m, CH), 2.65 (4H, m, CH_2N), 2.90 (1H, d, $ArCH_2$), 2.94 (1H, d, $ArCH_2$), 3.09 (4H, m, CH_2N), 3.42 (4H, m, CH_2N), 6.81 (2H, t, H3 and H4), 7.02 (1H, dd, H6), 7.69 (1H, td, H4), 7.28 (4H, d, H12), 7.29 (2H, d, H20), 8.09 (2H, d, H19), 7.65 (2H, d, H11); δ_C ($CDCl_3$) 21.45 (CH_2CH_2 CH_2), 25.53 ($ArCH_3$), 32.59 (CH), 33.88 ($ArCH_2$), 44.13, 46.58, 49.84 (unassigned), 55.53 (OCH_3), 110.2 (C3), 120.1 (C5), 126.9 (C1), 127.1 (C11), 127.5 (C19), 127.7 (C4), 129.7 (C12 and C20), 131.0 (C6), 135.9 (C13), 143.3 (C18), 143.7 (C10), 157.4 (C2); *m/z* (DCI, NH_3) 754 $(M)^+$, 598 $(M^+ -Ts)$, 444 $(M^+ -2xTs)$, 288 $(M^+ -3xTs)$; υ_{max} (KBr disc)/cm^{-1} 1335, 1159 ($S(=O)_2$). Found: C, 60.86; H, 6.34; N, 5.40%. $C_{38}H_{47}O_7S_3$ requires: C, 60.54; H, 6.28; N, 5.57%.

***3-(2-Hydroxy-5-bromobenzyl)-1,5,9-triazacyclododecane* (167)**

A solution of HBr in acetic acid (48% v/v, 80 ml) was added to a mixture of 1,5,9-tri(p-tolylsulfonyl)-3-(2-methoxybenzyl)-1,5,9-triazacyclododecane (4.03 g, 5.34 mmol) and phenol (3 g, 31.9 mmol). The mixture was heated at 110°C for 5 hours. More HBr/acetic acid solution (48% v/v, 15 ml) was added and the mixture boiled for 12 hours. On cooling a pink precipitate formed which was collected by filtration and dried, 1.48 g (53%). Initial purification by column chromatography silica (eluant 0.5% NH_3OH, 15% MeOH, 84.5% CH_2Cl_2) and further purification by HPLC: R_t = 11.8 min. observed at λ = 254nm (Dynamax, reverse phase) with gradient elution 10cm^3min^{-1}; A = H_2O/0.1% TFA, B = CH_3CN/0.1% TFA from t = 0 min.; A=90%, B=10% to t = 20min.; A=75%, B=25% and finally to t = 25 min.; A=100%, B=0% gave the product; δ_H (CD_3OD) 1.68 (4H, quint, $CH_2CH_2CH_2$), 2.05 (1H, m, CH), 2.59 (2H, d, $ArCH_2$), 2.74-2.92 (12H, m, CH_2N), 6.66 (1H, d, Ar H3), 7.10 (2H, m, Ar H6 and

H4); δ_C ($CDCl_3$) 26.37 ($HNCH_2\mathit{CH_2}CH_2NH$), 31.02 (CH), 38.23 (Ar CH_2), 48.80 ($HN\mathit{CH_2}$ CH), 49.15 ($\mathit{CH_2}$ $NHCH_2CH$), 52.34 ($\mathit{CH_2}$ $CH_2CH_2NHCH_2CH$), 107.8 (Ar C5), 118.9 (Ar C3), 129 (Ar C1), 130 (Ar C4), 132.6 (Ar C6), 159.5 (Ar C2); *m/z* (DCI, NH_3) 356, 358 (M^+ +1); υ_{max} (KBr dics)/cm^{-1} 3422 (OH), 1590, 755 (CBr). (DCI, accurate mass), found 356.1337 (M^+ +1) and calculated for $C_{16}H_{26}BrN_3O+H^+$ 356.1337.

5.5 References

1) L. Collie, J.E. Denness, D. Parker, F. O'Carroll, C. Tachon *J. Chem. Soc., Perkin Trans. 2* , 1993, 1747; using a routine in 'Kaleidagraph'.

2) O. Popovych, R.P.T. Tomkins; 'Nonaqueous solution chemistry' ; John Wiley and Sons, Chichester, 1981, p221.

3) S. Rondinini, P. Longhi, P.R. Mussini, T. Mussini; *Pure and Appl. Chem.*, 1987, **59**, 1693.

4) A.K. Covington, T. Dickinson; 'Physical Chemistry of Organic Solvent Systems', Plenum Press, London; 1973 p168 and p196.

5) E.S. Lane; *J. Chem. Soc,* 1953, 2238.

6) C.W. James, J. Kenner, W.V. Stubbings; *J. Chem. Soc.* 1920, **117**, 775.

7) Y. Chen, L. Zhoa; *Yiyao Gongye,* 1987, **18(7)**, 318. Chem. Abstract 108: 221257q.

8) Franzen, Engel; *J. Pr. Chem,* 1921, **102**, 188. Chem Abstract 1921, 15:3633.

9) S.H. Dandegaonker, G.R. Revanker; *J. Karnatak Univ.,* 1961, **6**, 25; Chem Abstract 1963, 59:10023f.

10) Supplied from ZENECA specialities as a mixture of isomers.

11) C.J. Chandler, L.W. Deady, J.A. Reiss; *J. Heterocyclic Chem.,* 1981, **18**, 599.

12) E.J. Cole; PhD. Thesis, University of Durham, 1993.

13) M.H. Delton, H.C. Warren; Patent, Eastmann Kodak Co, EP339.973 ClC07D471/04.

14) J. Lewis, T.D. O'Donoghue; *J. Chem. Soc., Dalton Trans.*, 1980, 736.

15) M.E. Bos, W.D. Wulf, R.A. Miller, S. Chamberlin, T.A. Brandvold; *Tetrahedron,* 1991, **47**, 4739.

16) I.M. Helps, D. Parker, K.J. Jankowski, J. Chapman, P.E. Nicholson; *J. Chem. Soc., Perkin Trans. 1,* 1989, 2079.

17) R. Grice, L.N. Owen; *J. Chem. Soc*, 1963, 1947.

Appendices

Appendix 1 Derivation of $[ML_2]$ binding equation

Derivation of a 1:2 binding model assuming only one complexation step :-

$$2L + M \underset{}{\overset{K_1}{\rightleftharpoons}} ML_2 \qquad K_1 = \frac{[ML_2]_{eq}}{[L]_{eq}[M]_{eq}}$$

$$\delta_H = \frac{\delta_0[L]_{eq} + \delta_1 2[ML_2]_{eq}}{[L]_{eq} + 2[ML_2]_{eq}} \qquad \text{at equilibrium}$$

where $\delta_0 = {}^1H$ chemical shift in the absence of added metal and $\delta_1 = {}^1H$ chemical shift of the 1:2 complex. At equilibrium $[L]_{eq} + 2[ML_2]_{eq} = [L]_{int}$ where $[L]_{int}$ is the initial concentration of ligand.

$$\Rightarrow \quad \delta_H = \frac{\delta_0[L]_{eq} + \delta_1 2[ML_2]_{eq}}{[L]_{int}}$$

$$= \frac{\delta_0([L]_{int} - 2[ML_2]_{eq}) + \delta_1 2[ML_2]_{eq}}{[L]_{int}}$$

$$= \frac{2[ML_2]_{eq}(\delta_1 - \delta_0) + \delta_0[L]_{int}}{[L]_{int}}$$

$$= \frac{2[ML_2]_{eq}(\delta_1 - \delta_0)}{[L]_{int}} + \delta_0$$

$$\Rightarrow \quad \Delta\delta_H = \frac{2[ML_2]_{eq}(\delta_1 - \delta_0)}{[L]_{int}}$$

expressing $[ML_2]$ in terms of known quantities

$$K_1 = \frac{[ML_2]_{eq}}{[L]_{eq}[M]_{eq}} \qquad \text{and} \qquad 2L + M \underset{}{\overset{K_1}{\rightleftharpoons}} ML_2$$

initially $2L = [L]int$
$M = [M]int$
$ML_2 = 0$

at equilibrium $2L = [L]_{int} - 2[ML_2]_{eq}$

$M = X[L]_{int} - [ML_2]_{eq}$

$ML_2 = [ML_2]_{eq}$

where $X = [M]_{int}/[L]_{int}$ = quanitity measured

$$\Longrightarrow \quad K_1 = \frac{[ML_2]_{eq}}{([L]_{int} - 2[ML_2]_{eq})\,(X[L]_{int} - [ML_2]_{eq})}$$

$$K_1\{X[L]^2_{int} - [L]_{int}[ML_2]_{eq} - 2X[L]_{int}[ML_2]_{eq} + 2[ML_2]^2_{eq}\} = [ML_2]_{eq}$$

$$K_1[ML_2]^2_{eq} - (1 + K[L]_{int} + 2K_1X[L]^2_{int})[ML_2]_{eq} + K_1X[L]^2_{int} = 0$$

solving for a quadratic in $[ML_2]$

$$[ML_2]_{eq} = \left(\frac{1 + K_1[L]_{int} + 2K_1X\,[L]_{int}}{4K_1}\right) \pm \sqrt{\frac{(1 + K_1[L]_{int} + 2K_1X[L]_{int})^2 - 8K_1{}^2X[L]^2_{int}}{4K_1}}$$

$$\Delta\delta_H = \frac{(\delta_1 - \delta_0)}{2K_1[L]_{int}}\left[(1 + K_1[L]_{int} + 2K_1X\,[L]_{int}) \pm \sqrt{(1 + K_1[L]_{int} + 2K_1X[L]_{int})^2 - 8K_1{}^2X[L]^2_{int}}\right]$$

Points on the graph are experimental values ($\Delta\delta_H$ versus X) and curves are those calculated by a general curve fitting procedure to the above equation, giving values of the equilibrium constant, K_1 and ^1H chemical shift of the 1:2 complex.

Appendix 2

First year courses

Ionic and Molecular Recognition
Organometallics in Synthesis
Polymer Synthesis

Research colloquia, seminars and lectures

Organized by the Department of Chemistry (October 1992- July 1995)

1992

October 15th	Dr M. Glazer & Dr. S. Tarling, Oxford University & Birbeck College, London. It Pays to be British! - The Chemist's Role as an Expert Witness in Patent Litigation.
October 20th	Dr. H. E. Bryndza, Du Pont Central Research. Synthesis, Reactions and Thermochemistry of Metal (Alkyl) Cyanide Complexes and their Impact on Olefin Hydrocyanation Catalysis.
October 22th	Prof. A. Davies, University College London. *The Ingold-Albert Lecture* The Behaviour of Hydrogen as a Pseudometal.
October 28th	Dr. J. K . Cockcroft, University of Durham. Recent Developments in Powder Diffraction.
October 29th	Dr. J. Emsley, Imperial College, London. The Shocking History of Phosphorus.
November 4th	Dr. T. P. Kee, University of Leeds. Synthesis and Co-ordination Chemistry of Silylated Phosphites.
November 5th	Dr. C. J. Ludman *, University of Durham. Explosions, A Demonstration Lecture.
November 11th	Prof. D. Robins †*, Glasgow University. Pyrrolizidine Alkaloids : Biological Activity, Biosynthesis and Benefits.
November 12th	Prof. M. R. Truter *, University College, London. Luck and Logic in Host - Guest Chemistry.
November 18th	Dr. R. Nix†, Queen Mary College, London. Characterisation of Heterogeneous Catalysts.
November 25th	Prof. Y. Vallee. University of Caen.

Reactive Thiocarbonyl Compounds.

November 25th Prof. L. D. Quin †, University of Massachusetts, Amherst.
Fragmentation of Phosphorous Heterocycles as a Route to Phosphoryl Species with Uncommon Bonding.

November 26th Dr. D. Humber, Glaxo, Greenford.
AIDS - The Development of a Novel Series of Inhibitors of HIV.

December 2th Prof. A. F. Hegarty *, University College, Dublin.
Highly Reactive Enols Stabilised by Steric Protection.

December 2th Dr. R. A. Aitken †*, University of St. Andrews.
The Versatile Cycloaddition Chemistry of $Bu_3P.CS_2$.

December 3th Prof. P. Edwards, Birmingham University.
The SCI Lecture - What is Metal?

December 9th Dr. A. N. Burgess †, ICI Runcorn.
The Structure of Perfluorinated Ionomer Membranes.

1993

January 20th Dr. D. C. Clary †, University of Cambridge.
Energy Flow in Chemical Reactions.

January 21th Prof. L. Hall *, Cambridge.
NMR - Window to the Human Body.

January 27th Dr. W. Kerr *, University of Strathclyde.
Development of the Pauson-Khand Annulation Reaction : Organocobalt Mediated Synthesis of Natural and Unnatural Products.

January 28th Prof. J. Mann *, University of Reading.
Murder, Magic and Medicine.

February 3th Prof. S. M. Roberts *, University of Exeter.
Enzymes in Organic Synthesis.

February 10th Dr. D. Gillies †, University of Surrey.
NMR and Molecular Motion in Solution.

February 11th Prof. S. Knox *, Bristol University.
The Tilden Lecture Organic Chemistry at Polynuclear Metal Centres.

February 17th Dr. R. W. Kemmitt †, University of Leicester.
Oxatrimethylenemethane Metal Complexes.

February 18th Dr. I. Fraser, ICI Wilton.
Reactive Processing of Composite Materials.

February 22th Prof. D. M. Grant, University of Utah.
Single Crystals, Molecular Structure, and Chemical-Shift Anisotropy.

February 24th Prof. C. J. M. Stirling †*, University of Sheffield.

Chemistry on the Flat-Reactivity of Ordered Systems.

March 10th — Dr. P. K. Baker, University College of North Wales, Bangor.
'Chemistry of Highly Versatile 7-Coordinate Complexes'.

March 11th — Dr. R. A. Y. Jones, University of East Anglia.
The Chemistry of Wine Making.

March 17th — Dr. R. J. K. Taylor †*, University of East Anglia.
Adventures in Natural Product Synthesis.

March 24th — Prof. I. O. Sutherland †*, University of Liverpool.
Chromogenic Reagents for Cations.

May 13th — Prof. J. A. Pople, Carnegie-Mellon University, Pittsburgh, USA.
The Boys-Rahman Lecture Applications of Molecular Orbital Theory.

May 21th — Prof. L. Weber, University of Bielefeld.
Metallo-phospha Alkenes as Synthons in Organometallic Chemistry.

June 1th — Prof. J. P. Konopelski, University of California, Santa Cruz.
Synthetic Adventures with Enantiomerically Pure Acetals.

June 2th — Prof. F. Ciardelli, University of Pisa.
Chiral Discrimination in the Stereospecific Polymerisation of Alpha Olefins.

June 7th — Prof. R. S. Stein *, University of Massachusetts.
Scattering Studies of Crystalline and Liquid Crystalline Polymers.

June 16th — Prof. A. K. Covington, University of Newcastle.
Use of Ion Selective Electrodes as Detectors in Ion Chromatography.

June 17th — Prof. O. F. Nielsen, H. C. Ørsted Institute, University of Copenhagen.
Low-Frequency IR - and Raman Studies of Hydrogen Bonded Liquids.

September 13th — Prof. Dr. A.D. Schlüter *, Freie Universität Berlin, Germany.
Synthesis and Characterisation of Molecular Rods and Ribbons.

September 13th — Dr. K.J. Wynne, Office of Naval Research, Washington, USA.
Polymer Surface Design for Minimal Adhesion.

September 14th — Prof. J.M. DeSimone, University of North Carolina, Chapel Hill, USA.
Homogeneous and Heterogeneous Polymerisations in Environmentally Responsible Carbon Dioxide.

September 28th — Prof. H. Ila *, North Eastern Hill University, India.
Synthetic Strategies for Cyclopentanoids via Oxoketene Dithioacetals.

October 4th — Prof. F.J. Feher †, University of California, Irvine, USA.
Bridging the Gap between Surfaces and Solution with Sessilquioxanes.

October 14th — Dr. P. Hubberstey, University of Nottingham.
Alkali Metals: Alchemist's Nightmare, Biochemist's Puzzle and Technologist's Dream.

October 20th Dr. P. Quayle†, University of Manchester.
Aspects of Aqueous ROMP Chemistry.

October 21th Prof. R. Adams†, University of South Carolina, USA.
Chemistry of Metal Carbonyl Cluster Complexes : Development of Cluster Based Alkyne Hydrogenation Catalysts.

October 27th Dr. R.A.L. Jones†, Cavendish Laboratory, Cambridge.
Perambulating Polymers.

November 10th Prof. M.N.R. Ashfold†, University of Bristol.
High Resolution Photofragment Translational Spectroscopy : A New Way to Watch Photodissociation.

November 17th Dr. A. Parker†, Rutherford Appleton Laboratory, Didcot.
Applications of Time Resolved Resonance Raman Spectroscopy to Chemical and Biochemical Problems.

November 24th Dr. P.G. Bruce†*, University of St. Andrews.
Structure and Properties of Inorganic Solids and Polymers.

November 25th Dr. R.P. Wayne, University of Oxford.
The Origin and Evolution of the Atmosphere.

December 1th Prof. M.A. McKervey †*, Queen's University, Belfast.
Synthesis and Applications of Chemically Modified Calixarenes.

December 8th Prof. O. Meth-Cohn †*, University of Sunderland.
Friedel's Folly Revisited - A Super Way to Fused Pyridines.

December 16th Prof. R.F. Hudson, University of Kent.
Close Encounters of the Second Kind.

1994

January 26th Prof. J. Evans †, University of Southampton.
Shining Light on Catalysts.

February 2th Dr. A. Masters †, University of Manchester.
Modelling Water Without Using Pair Potentials.

February 9th Prof. D. Young †, University of Sussex.
Chemical and Biological Studies on the Coenzyme Tetrahydrofolic Acid.

February 16th Prof. K.H. Theopold, University of Delaware, USA.
Paramagnetic Chromium Alkyls : Synthesis and Reactivity.

February 23th Prof. P.M. Maitlis †, University of Sheffield.
Across the Border : From Homogeneous to Heterogeneous Catalysis.

March 2th Dr. C. Hunter †*, University of Sheffield.
Noncovalent Interactions between Aromatic Molecules.

March 9th Prof. F. Wilkinson, Loughborough University of Technology.
Nanosecond and Picosecond Laser Flash Photolysis.

March 10th — Prof. S.V. Ley *, University of Cambridge.
New Methods for Organic Synthesis.

March 25th — Dr. J. Dilworth *, University of Essex.
Technetium and Rhenium Compounds with Applications as Imaging Agents.

April 28th — Prof. R. J. Gillespie, McMaster University, Canada.
The Molecular Structure of some Metal Fluorides and Oxofluorides: Apparent Exceptions to the VSEPR Model.

May 12th — Prof. D. A. Humphreys, McMaster University, Canada.
Bringing Knowledge to Life.

October 5th — Prof. N. L. Owen, Brigham Young University, Utah, USA.
Determining Molecular Structure - the INADEQUATE NMR way.

October 19th — Prof. N. Bartlett, University of California.
Some Aspects of Ag(II) and Ag(III) Chemistry.

November 2th — Dr P. G. Edwards, University of Wales, Cardiff.
The Manipulation of Electronic and Structural Diversity in Metal Complexes - New Ligands.

November 3th — Prof. B. F. G. Johnson, Edinburgh University.
Arene - Metal Clusters.

November 9th — Dr J. P. S. Badyal, University of Durham.
Chemistry at Surfaces, A Demonstration Lecture.

November 9th — Dr G Hogarth, University College, London.
New Vistas in Metal Imido Chemistry.

November 10th — Dr M Block, Zeneca Pharmaceuticals, Macclesfield.
Large Scale Manufacture of the Thromboxane Antagonist Synthase Inhibitor ZD 1542.

November 16th — Prof. M. Page *, University of Huddersfield.
Four Membered Rings and β-Lactamase.

November 23th — Dr J. M. J. Williams *, University of Loughborough.
New Approaches to Asymmetric Catalysis.

December 7th — Prof. D Briggs, ICI and University of Durham.
Surface Mass Spectrometry.

1995

January 11th — Prof. P. Parsons *, University of Reading.
Applications of Tandem Reactions in Organic Synthesis.

January 18th — Dr G. Rumbles, Imperial College, London.
Real or Imaginary 3rd Order non-Linear Optical Materials.

January 25th — Dr D. A. Roberts *, Zeneca Pharmaceuticals.
The Design and Synthesis of Inhibitors of the Renin-Angiotensin System.

February 1th — Dr T Cosgrove, Bristol University.
Polymers do it at Interfaces.

February 8th — Dr D. O'Hare, Oxford University.
Synthesis and Solid State Properties of Poly-, Oligo- and Multidecker Metallocenes.

February 22th — Prof. E Schaumann, University of Clausthal.
Silicon and Sulphur Mediated Ring-opening Reactions of Epoxide.

March 1th — Dr M. Rosseinsky *, Oxford University.
Fullerene Intercalation Chemistry.

March 8th — Nikki Chesters, Wayne Devonport & Penelope Herbertson*, University of Durham.
1995 Graduate Seminar Series.

March 15th — Janet Hopkins, Brian Rochford & Graham Rivers*, University of Durham.
1995 Graduate Seminar Series.

March 22th — Dr M. Taylor, University of Auckland, New Zealand.
Structural Methods in Main Group Chemistry.

April 26th — Dr M. Schroder *, University of Edinburgh.
Redox Active Macrocyclic Complexes : Rings, Stacks and Liquid Crystals.

May 3th — Prof. E. W. Randall, Queen Mary and Westfield College.
New Perspectives in NMR Imaging.

May 4th — Prof. A. J. Kresge *, University of Toronto.
The Ingold Lecture Reactive Intermediates : Carboxylic Acid Enols and Other Unstable Species.

May 10th — George Bates, Steve Carss, Martyn Coles *, University of Durham
1995 Graduate Seminar Series.

May 17th — Graham McKelvey, Richard Towns & Tim Thompson *, University of Durham.
1995 Graduate Seminar Series.

May 31th — Rob Spink, Ian Reynolds & Nick Haylett *, University of Durham.
1995 Graduate Seminar Series.

June 7th — Abdulla Ahmed, Mike Chan & Alex Eberlin *, University of Durham.
1995 Graduate Seminar Series.

June 14th — Iain May, Leela Sequeira & Gareth Williams *, University of Durham.
1995 Graduate Seminar Series.

June 21th — Oliver Greenwood, Mike Chalton & Alex Roche *, University of Durham.
1995 Graduate Seminar Series.

July 5th — Alan Gilbert, Emma Rivers & Simon Lord *, Univeristy of Durham.
1995 Graduate Seminar Series.

July 12th — M Ryan, Steven Dunn & R Samadi, Univeristy of Durham.
1995 Graduate Seminar Series.

† Invited specially for the graduate training programme.
* Indicates that the author attended.

Conferences Attended

1)	Stereochemistry at Sheffield, University of Sheffield.	December 15th 1993
2)	R.S.C. U.K. Marrocycles Group, University of Warwick.	Janurary 5-6th 1994
3)	R.S.C. U.K. Macrocycles Group, University of Newcastle.	Janurary 4-5th 1995
4)	S.C.I. Novel Extractants, London.	March 15th 1995
5)	North East Graduate Symposium, University of Durham *.	April 6th 1995

* Indicates author spoke

Publications

1) G.B. Bates, D. Parker, P.A. Tasker; 'Synthesis and solution complexation behaviour of dimeric zinc-selective bisbenzimidazole derivatives', submitted 1995.

2) G.B. Bates, D. Parker; 'Synthesis of a Ligand Imposing Tetrahedral Coordination Based on 1,10-Phenanthroline', submitted 1995.

3) G.B. Bates, D. Parker; 'Complexation Behaviour of C and N-Functionalised Tetradentate Ligands Based on 1,5,9-Triazacyclododecane', submitted 1995.